SEDIMENTOLOGICAL EFFECTS OF AEOLIAN PROCESSES ACTIVE IN THE TENTSMUIR AREA, FIFE, SCOTLAND

Abhilasha Wal

A Thesis Submitted for the Degree of PhD
at the
University of St Andrews

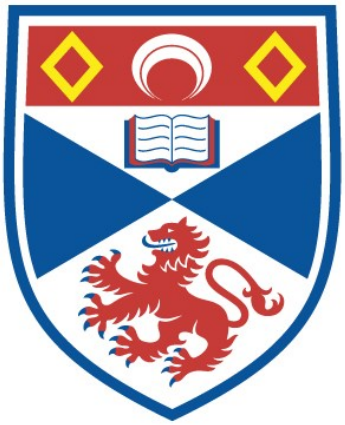

1993

SEDIMENTOLOGICAL EFFECTS OF AEOLIAN PROCESSES ACTIVE IN THE TENTSMUIR AREA, FIFE, SCOTLAND

by

Abhilasha Wal

B.Sc(Hons), M.Sc(spl)

A thesis submitted for the award of

Doctor of Philosophy

University of St Andrews

November 1992

ProQuest LLC.
789 East Eisenhower Parkway
P.O. Box 1346
Ann Arbor, MI 48106 – 1346

DECLARATION FOR THE DEGREE OF Ph.D.

I **Abhilasha Wal** hereby certify that this thesis has been composed by myself, that it is a record of my own work, and that it has not been accepted in partial or complete fulfillment of any other degree of professional qualification.

Signed.

Dated.....19.11.92.....

I **Abhilasha Wal** was admitted to the faculty of Science of the University of St Andrews under Ordinance General No 12 on ...JULY, 1989... and as a candidate for the degree of Ph.D. on JULY 1990

Signed.

Dated...19.11.92.....

I hereby certify that **Abhilasha Wal** has fulfilled the conditions of the Resolution and Regulations appropriate to the Degree of Ph.D.

Signature of Supervisor....

Dated.....19 11 1992.....

THESIS COPYRIGHT DECLARATION

In submitting this thesis to the University of St Andrews I understand that I am giving permission for it to be made available for use in accordance with the regulations of the University Library for the time being in force, subject to any copyright vested in the work not being affected thereby. I also understand that the title and abstract will be published, and that a copy of work may be made and supplied to any bona fide library or research worker.

Signed

Dated 19.11.92

Frontispiece Barchan dunes forming at Tentsmuir point

.....For as long as they are fed with a supply of grains, and as long as a motive power is available from the wind- just as true life requires food and motive and power from the sun's rays to keep it alive - dunes can move from place to place, can grow in size, can maintain their own particular shape, repair any damage done to them , and lastly, in the case of Barchan dunes there is some evidence that they are capable of a sort of reproduction whereby baby dunes are formed in the open a hundred yards or so down-wind of the horn of a fully grown parent. .....these dunes appear to ape most of the attributes we think essential for a definition of life...Excerpt from Libyan Sands- Travel in a dead world by R.A.S. Bagnold, 1935.

ABSTRACT

SEDIMENTOLOGICAL EFFECTS OF AEOLIAN PROCESSES ACTIVE IN THE TENTSMUIR AREA, FIFE, SCOTLAND

Abhilasha Wal

University of St Andrews

Present day coastal accretion at Tentsmuir is manifest in the form of hummocky dune accumulations along the shoreline. The mode and variability of the distribution of surface sediments by the wind and the magnitude of accumulation of wind laid deposits in the Tentsmuir beach-dune complex is a measure of aeolian activity in the area.

In the Tentsmuir area fine to medium grained well sorted beach sands are entrained by high to moderate energy, seasonal, directionally unimodal to bimodal winds of low variability. During the winter season the dominant winds are from the south west (blowing towards the sea) whereas, generally during the spring the more effective winds are derived from the east (blowing towards land). The bimodal winds are composed of contrasting unimodally directional winds blowing for shorter durations. Daily sea breezes are observed during the summer.

Field measurements of sand transport rates, with the aid of sand traps during anemometer determined wind speeds ranging from 4 m s^{-1} to 20 m s^{-1}, in the study area show that while the onshore transport vector results in rapid foredune development, the longshore and offshore component contributes to a positive beach sediment budget. However, the net beach sediment budget is a complex interplay of aeolian, wave and tidal processes.

Shear velocities on the Tentsmuir beaches ranged from 18.5 cm s^{-1} to 52 cm s^{-1} and the focal point, u' and z' values were 1.75 m s^{-1} and 0.03 cm respectively.

In general, the variability of the short-term aeolian sand transport rates in the Tentsmuir beach-dune subenvironments is controlled by (i) variation in wind velocity, (ii) presence or absence of vegetation, (iii) ground surface moisture, and (iv) the sand size and source limitation.

The potential sand input by the onshore winds during the last eleven years is estimated to have been approximately 28,532 m^3. During the same period the potential amount of sand blown towards the sea was 109,570 m^3. The amount of predicted onshore sediment input (28,532 m^3) compares well with the 33,000 m^3 of sand estimated to have accumulated in the lee of the beach at Tentsmuir Point. The close agreement of the measured and predicted values of aeolian transport suggests that the White (1979) expression, used in the present study to predict transport rates on the beach, provides fairly reliable estimates.

Very high velocity offshore winds (>9 ms^{-1}) produce a shelly deflation surface along the backshore, surface parallel sand sheets and sand strips on the foreshore; adhesion plane bed and adhesion structures along the moist/wet tidal margin and pyramidal dunes (offshore transport across a dune ridge >2.5m high.). Onshore high velocity winds result in the formation of surface parallel sand strips on the foreshore and a high volume of aeolian sediment accumulation in the backshore and foredune area. Prolonged days of high velocity unidirectional winds result in the formation of barchans.

Medium to high wind velocities (~6-9 ms^{-1}) produce ballistically rippled foreshore sand lobes, lee dunes downwind of tidal debris, adhesion structures (offshore/longshore transport) and some sand accumulation in the foredune area (onshore transport).

Abundant parallel laminated sand, pinchout laminae, sand lenses, precipitation deposits, trough crossbeds, plant remains at places overlying beach shell layers constitute a prograding coastal dune facies at Tentsmuir.

ACKNOWLEDGEMENTS

This project could not have been carried out and completed without the assistance and cooperation of numerous people, to whom I am greatly indebted.

I would particularly like to thank Dr John McManus, as my supervisor of studies, for his stimulating supervision, encouragement and support during this work and critical review of the manuscript. His experience, guidance and insight were nothing short of outstanding.

A special word of thanks is extended to Dr Ken Glennie for his sincere advice, helpful discussions and for welcoming me on my trips to his highland home in Ballater.

To Mr Pete Kinnear, Senior Warden, Nature Conservancy Council, I am more deeply indebted than can be adequately expressed, for supplying me with earlier records (manuscripts and photographs), areal photographs of the Tentsmuir National Nature Reserve and field assistance during the course of my study. Permission for access to the field site by the Forestry Commission, Kelty is grately acknowledged.

This thesis was produced at University of St Andrews, where I am indebted to a many individuals in the Department of Geography & Geology. Financial support provided by the Committee of Vice-Chancellors and Principals of the Universities in U.K. in form of an Overseas Research Award, and FCO maintenance grant through British Council is gratefully acknowledged. Thanks are also extended to Dr G W Whittington, Chairman of the Department, for his support in organization of some of the financial resources.

Support from the Director and staff of Tay Estuary Research Centre, for the construction of traps, field assistance and financial support is grately acknowledged.

I am especially thankful to Dr Jack Jarvis for the construction of the data logger, Jim Allen for his photographic skills, Mr C B Bremner of Reprographic services for helping me with presentation diagrams, Angus Calder and Andy Mackie for the day to day technical assistance. It is a pleasure to acknowledge the help of Mrs Jean Galloway, Mrs Ramona McCormack and Mr. Stuart Harvey for administrative assistance. The project has without doubt benefited from the friendly and

communicative attitude of majority of staff and students with special thanks to Robin, Phillipa, Justin, Rod and Gopal.

I would also like to thank Professor Ken Walton, University of St. Andrews and Dr Kenneth Pye, Postgraduate Research Institute of Sedimentology, Reading for many helpful periods of discussion. Sincere gratitude is extended to Richard Batchelor, Parthasarthy Joerdar and the Computing Lab for providing the invaluable assistance in computing.

A great deal of invaluable cooperation was provided by Dr Brian Willetts and Dr Ann Rice of Aberdeen University for loaning me the Cassella Cup Rotation Anemometers.

Constant motivation and enlightening discussions with Mohit have undoubtedly benefitted this work.

It is my pleasure to record sincere appreciation for my parents, brother and other family members for their constant encouragement and dedication throughout my studies.

Contents

Chapter 3

PRINCIPLES OF AEOLIAN SEDIMENT TRANSPORT: THEORY AND MEASUREMENT

List of Plates

List of figures

List of Tables

Chapter 1

(with 12 figures and 1 table)

Chapter 1

Introduction

The 8 km long Tentsmuir beach-dune complex is a coastal unit extending from the rocky cliffs at St Andrews to the southern shore of the Tay estuary (Fig. 1.1). In the context of the Earth's 4.5 billion year history 'Tentsmuir' is a geological newcomer. Ice sheets originating in the Perthshire Highlands moved across the area during the Pleistocene. The glacial retreat left behind deposits of loose sand and gravels and these have been reworked into raised beaches which Sissons *et al* (1966) recognise as forming a suite of levels, the most prominent of which is at 22 m above the present sea level at St Andrews (Late Glacial Raised Beach). The sea began to rise due to glacial melting allowing the waves and currents to sculpt the bay into its distinctive outline during the last 7,000 years. The dynamic forces of nature - winds, waves and tides, are continuously at work changing the coastal silhouette not only of Tentsmuir, but worldwide.

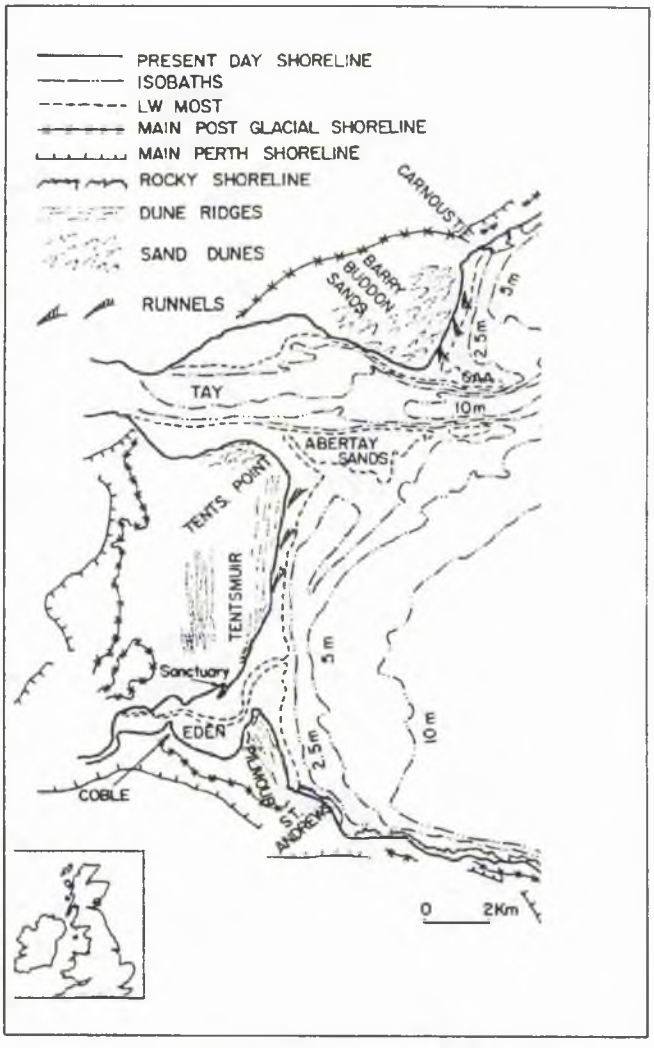

Fig. 1.1 Location of the study area, indicating the Late Glacial (Main Perth) and Post Glacial (Flandrian) shorelines, and present day features referred to in the text (after Rice, 1962; Cullingford, 1972; Chislom, 1966, 1971; Ferentinos & McManus, 1981).

The area of the Tentsmuir dunes is one of the largest in Scotland, situated on the macro-tidal (tidal range 4-6 m) coast of North

East Fife, which has been categorised as a 'dune coast' associated with a 'big beach foredune' system (Olson & Maarel, 1989). Occupying an area of 1781 ha (Doody, 1989), it is a site of long term net accretion (Ferentinos & McManus, 1981) created through marine sediment transport coupled with aeolian activity.

1.1 SELECTION OF THE STUDY SITE AND THE NATURE OF THE PROBLEM

Many studies have been completed in the estuarine and littoral environments of the Tay estuary and extending to the Tayport - Tentsmuir area. However, prior to this study little was known of aeolian processes active at Tentsmuir. Since the area was known to be subject to shoreline accretion commonly taking the form of wind blown accumulations, an urgent need was recognised for systematic investigation of the aeolian movement of sand with a view to carrying out sand transport rate measurements and making sand budget estimations within a continuous monitoring programme. There was a need to develop a clear understanding of the types of winds, the mechanisms of sediment entrainment, transport and deposition. Information was also needed to explain the sediment transport pathways, mobilisation and accumulation resulting from these winds.

The number of studies relating to actual aeolian sand transport rate measurements in the field is small. Most previous studies of coastal dunes have been limited to descriptive accounts of dune form and succession (Cooper, 1958; Jennings 1957; Olson, 1958; Smith & Messenger, 1959), their ecological importance (Ranwell, 1972; Woodhouse, 1978) and their development in relation to nearshore processes. A growing concern has arisen in recent years that there is a need for a universal methodology to be developed to permit a more widespread understanding and quantification of the various factors controlling coastal aeolian activity and dune development.

The study of wind regimes and the accurate prediction of aeolian sedimentary processes is fundamental to the development of potential beach-dune sand transport models (Bauer *et al*, 1990). The principal thrust of the project has been to examine the

characteristic wind regimes of a temperate coast and the routing and volumes of the resultant aeolian sand transport in the beach and foredune subenvironments.

1.2 THE COASTAL ZONE

The coastal zone and the associated coastal processes do not have the same sort of regionalisation or restriction that accompany other divisions of landform analysis such as arid land geomorphology. The coast is a periphery that has no latitudinal or zonal limitation. It exists in the polar regions as well as the mid latitudes and the tropics, so that the coast is quite distinct from that of any grouping of climatic variables. The coastal zone is a broad area that extends from some location in the aqueous environment to the beach and further inland to some position beyond the influence of subaquatic system (Psuty & Miller, 1989). Studies of the classification of coasts (Shepherd, 1963; McGill, 1958) and their description have shown that the coastal zone is a mix of environments, of processes and of landforms (Bird & Schwartz, 1985; Snead, 1982).

Wind, vegetation, sediment quality and quantity, near-shore wave energy, tidal range, beach width, and local weather conditions are components of the complex of variables that combine to establish a spatial and temporal sequence of foredune form and development. Coastal foredunes are the product of dune - beach interaction and exchange which are related to the ambient processes active in the beach dune realm and to the sediment budget (Fig. 1.2).

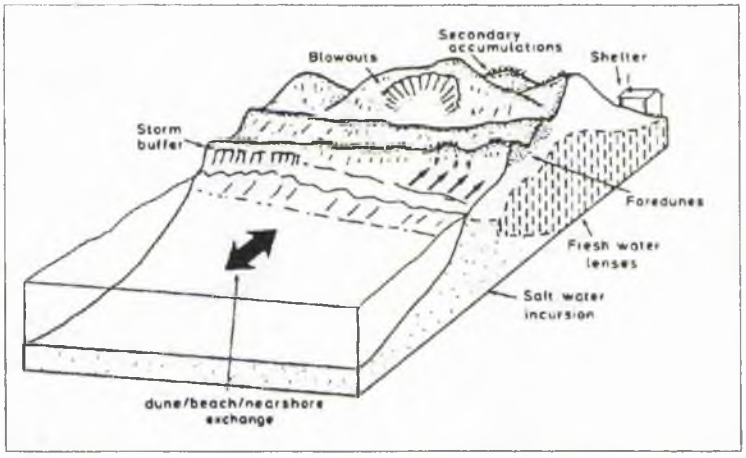

Fig. 1.2 Diagrammatic representation of the functions of coastal foredunes which act as buffer to storm waves and receive, store and release excess beach sand (after, Carter, 1988).

As a consequence of changes in the controlling variables, dunes respond by either retreating as a result of a series of erosional events,

supply continues to be available, wave conditions become more constructive, or sea levels fall. The later is described as progradation and is characterised by the formation of a series of parallel dune ridges.

After the initial formation, dunes should reach and remain in a state of balance, in that the sand added to the beach zone just replaces the quantities that are lost by the wind carrying sand beyond the links and on to the surrounding landforms. For the sediments to pass through all the stages of near-shore sand banks, beaches, dunes or links takes a long period, wherein short term fluctuations inevitably occur, especially in the crucial zone at the junction of the upper beach and the face of the frontal dune. This sensitive zone - the foredune (defined later) is normally the best indicator of contemporary dune forming processes. Aeolian sand transport in the coastal environment is one of the most important mechanisms by which sediment transfer, exchange between the beach and foredune, and accumulation takes place.

The unconsolidated and fragile nature of coastal dune systems at the interface of three environments- the sea, the atmosphere, and the land- gives this concept added significance and makes the beach and dune environment particularly vulnerable to relatively rapid and extensive change.

1.3 TERMINOLOGY

The plethora of descriptive terms used in coastal studies is varied and imprecise. The following section is an attempt to define certain basic terms and concepts in order to clarify the meaning of the terms used in this thesis.

1.3.1 'Aeolian' processes

'Aeolian' is defined as pertaining to the wind (Gary *et al*, 1972). It is a term applied to rocks, soils and deposits (such as loess, dune sand, and some volcanic tuffs) whose constituents were transported (blown) and laid down by air currents, to landforms produced or eroded by the agency of wind, to sedimentary structures (such as ripples) made by the wind, or to geological processes (such as erosion and deposition) accomplished by the wind (Fig. 1.3). Thus, any planet or satellite having a dynamic atmosphere and a solid surface is subject to aeolian processes.

Aeolian processes basically involve the interaction of the atmosphere - the external gaseous parts of some planets - with the lithosphere, or the solid surfaces of the planets. The zone where this interaction occurs constitutes the aeolian environment. Aeolian processes are capable of redistributing enormous quantities of sediments over planetary surfaces, resulting in the formation of large scale and small scale landforms and in the deposition of sediments hundreds of metres thick.

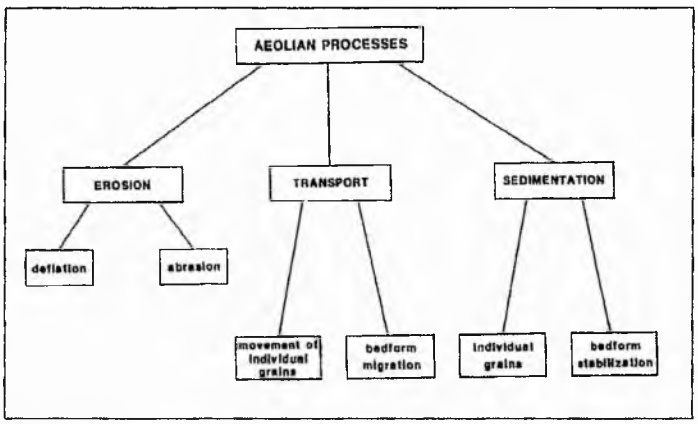

Fig. 1.3 The nature of Aeolian processes (after Pye & Tsoar, 1990).

Aeolian processes can both mix as well as sort sediments. Deposits consisting of a wide range of particle sizes, such as river and glacial deposits, when subjected to wind may become depleted in fine particles, leaving the coarser particles behind, ultimately giving rise to rock strewn or desert pavement surfaces. Conversely, wind blown dust derived from a range of rocks may become compositionally homogenised in dust storms and settle on widespread surfaces. Because aeolian activity involves the interaction of the atmosphere with the surface, the analysis of various wind related features can provide clues to the nature of the atmosphere (Greely & Iversen, 1985).

1.3.2 Concept of sediment budget

The dynamic aeolian parameters, entrainment, transportation and deposition, combine to determine the sand budget. The definition of the idea of sand budget has been demonstrated by means of the principle of load substitution for large systems (Brookfield, 1970; Mainguet & Callot, 1978; Wilson, 1973), using the Grand Erg de Fachi Bilna as an example. Mainguet & Chemin (1983) have defined the sand budget as follows;

" When the input of sand is greater than the output, sand budget is positive and the sand sea thickens; its surface is moulded into dunes of deposition - coalescing

barchans, barchan chains or transverse chains. The sand budget is positive, even though there are locally conspicuous deflation streaks indicating the beginning of a net loss of sand.

When the output of sand is greater than the input, the sand budget is negative and the sand sea thins; deflation corridors with level surfaces appear, which are dunes of erosion, or sand seas of the sand ridge type".

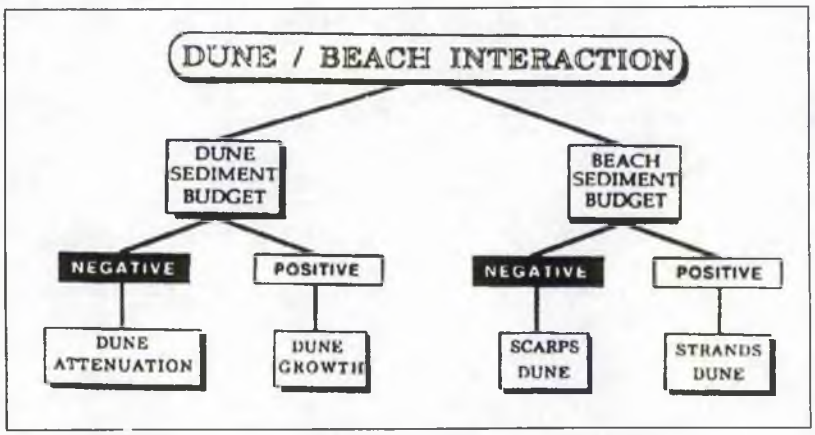

Fig. 1.4 Relationship of dune growth to beach and dune sediment budgets (after Psuty, 1988).

The concept of sediment budgets has been used by Psuty (1986, 1988) to create a model for coastal dune development that ascribes current day fore-dune accumulation to a slightly negative sediment budget at the shoreline (Fig. 1.4). In an alongshore continuum the sediment budget concept has been shown to have some aspects of zonality within it (Psuty & Millar, 1989).

1.3.3 Coastal dune types

The classification of coastal dunes has been attempted by Davies (1980), Goldsmith (1985), Pye (1983), Short & Hesp (1982), Short (1988) and Hesp (1988). The first three sources indicate a basic separation into primary and secondary dunes. Short & Hesp (1982) classified all the dunes in a single grouping but within a sequence which is driven by the relative wave energy reaching the shoreline and creating an assemblage of beach and dune types.

The terminology of the dune form in the coastal dune context has been presented by Psuty & Millar (1989) (Table 1.1). The essential component of the classification is the relationship of the dune form to the active beach and to the exchange of sediment in the sand-sharing system of the dune-beach profile. While elaborating on the terminology problem of foredunes, Hesp (1988) has suggested to

divide the foredunes into two basic sub-types, namely incipient foredunes and established foredunes. He stated -"Incipient foredunes are the initial foredune formed by sand deposition within pioneer vegetation species growing along the backshore of beaches". These dunes as they grow are eventually colonised by a woody vegetation (e.g. mat tufted plants and shrubs) and are then termed established foredunes.

Table 1.1: Coastal foredune categorisation: related to beach-dune interaction, foredune form and sand sharing (after Psuty & Millar, 1989).

Primary Dune
- Foredune, in active exchange of sediment between foredune and beach; coherent foredune ridge form; may be amassing or losing sand, or in an equilibrium sediment balance.
Secondary Dune
- Transgressive dune forms, sediment is being transferred inland through blow outs and deflation hollows; ridge planform is crenulate as the form is being dissected; sediment is being lost from the dune beach profile to inland positions.
- Paleodune forms, has foredune features but is stranded inland by the progradation of the shoreline; form may be either coherent linear ridge or a crenulated planform; dune form is no longer active in exchange of sediment with the beach.

The terminology of the dunes used in the later chapters is based on the coastal dune categorisation of Psuty & Millar (1989) and Hesp (1988) foredune classification. The term 'Incipient foredune' has been used for the widely spaced initial foredunes, which form as shadow structures, up to 25 - 50 cm high, in the lee of pioneer dune grass, along the backshore of beaches. The incipient foredunes grow and coalesce partly to form foredunes (1-2 m high). 'Foredune' is the *Ammophila sp.* dominated dune form undergoing active sediment exchange between itself and the beach. The foredune shows rapid accretion concomitant with vegetation growth. The term 'primary dune ridge' is referred here to a coherent ridge-like form, 3-4 m high, experiencing intermittent episodes (e.g. a storm) of sediment exchange. Being cut-off

from a regular sand supply the primary dune ridge is covered by *Ammophila sp* in various stages of decay.

1.3.4 Beach and shoreface environments

Beaches, dunes and links may be regarded as a unified system whereby sand is transferred by wave action from nearshore sediment banks to the beach. Under certain conditions the wind carries sand landward and, if conditions are suitable dunes may form in time and become stabilised by vegetation. A generalised profile and terminology of the beach and shoreface environments is shown in Fig. 1.5.

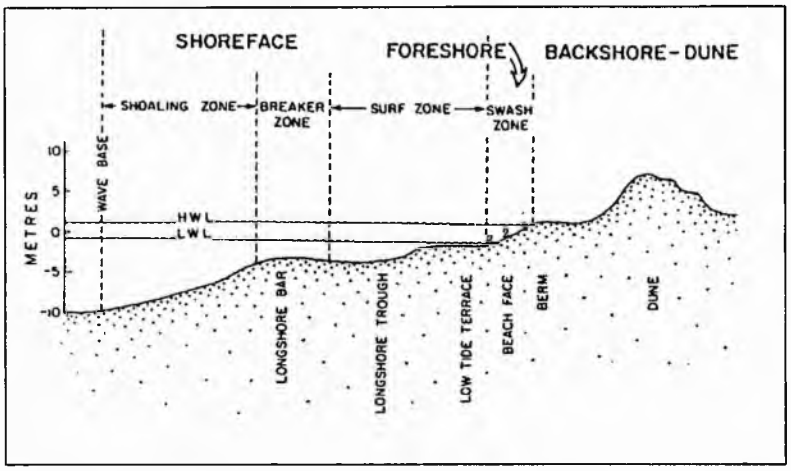

Fig. 1.5 Generalised profile of the beach and shore face environments. 1- Upper Beach Face, 2- Middle Beach Face, 3-Lower Beach Face (modified from Walker, 1980).

The foreshore/beach face environment is of special interest as most of the observations have been limited to this swash zone. Experiments have also been conducted in the backshore/incipient foredune environment. The foreshore has been further sub-divided into three subenvironments. The lower beach face (L.B.F.) subenvironment is the area bordering the low water level at a given time. The middle beach face (M.B.F.) subenvironment is the area in between the lower beach face and the upper beach face. The upper beach face (U.B.F.) is the area which marks the limit of the beach environment from the incipient foredune zone along the backshore. If there is no development of incipient foredune the upper beach face is the beach/dune cliff. The incipient foredune/backshore zone has been referred to as F.D. in the following chapters. Whilst the position of the upper beach face remains constant over a period of time, the position of the lower beach face is a dynamic zone and may well extend up to the middle of the beach depending on the state of the tide. In this case the width of the middle beach face is reduced. In general, for example, across a 100 m

wide beach-foredune profile, the L.B.F. zone may extend from 10 to 15 m, the M.B.F. zone from 40 to 50 m, U.B.F. zone from 15 to 20 m and the foredune zone from 10 to 15 m.

1.4 PREVIOUS WORK

The oldest geological reference to the field study area is found in the works of Chambers (1843) who noted raised beaches marking the Post-Glacial high sea level at Tentsmuir. Later descriptions of Tentsmuir relate to the problem of soil blowing and coastal changes (Grove, 1950). Ecological studies of the rapidly evolving dune succession involving detailed description of the plant communities were made by Gimmingham (1964), Crawford & Wishart (1966), Deshmukh (1974) and Garcia (1976).

The Holocene evolution of Tentsmuir has been described by Chisholm (1971) and the Late-Glacial shorelines traced by Cullingford & Smith (1966). Paleoenvironmental reconstructions of the Holocene deposits at some of the sites in Tentsmuir have been attempted by Haggart (1978).

Sedimentological and morphological characteristics of the Tay estuary region and the inter-tidal sedimentation processes, produced by wave and tide activity, have been addressed by Green (1974a, 1974b), McManus *et al* (1980), Ferentinos and McManus (1981), Cracknell *et al* (1982), Al-Mansi (1986), Sarrikostis (1986), Jarvis and Riley (1987) and Boalch (1988).

Reports on the natural resource utilization of the Tentsmuir beach-dune complex and its land use management have been compiled as a part of the surveys for the Countryside Commission for Scotland by Ritchie (1979) and Mather & Ritchie (1977, 1984).

1.5 GEOLOGICAL SETTING

The solid geology of the area is dominated by Devonian formations (Lower and Upper Old Red Sandstones) and Carboniferous strata over which rests the Glacial and Post-Glacial sands and gravels. The Post-Glacial/Modern deposits are about 18 m thick (Morton Lochs) with their thickness increasing towards Tentsmuir Point (Green,

1974). The maximum thickness of the sand is not known, as none of the boreholes along the eastern margin of the Tentsmuir sands have reached bedrock.

1.6 GEOMORPHOLOGICAL CHARACTERISTICS

St Andrews Bay is a semi-circular embayment 27 km wide on the east coast of Scotland (Fig. 1.1). The modern and Post-Glacial deposits at the head of the bay are divided into three units: the Pilmour-Coble Spits; Tentsmuir Platform and the Barry-Buddon cuspate Foreland. Of these only the first and second are of significance to this study.

The Tentsmuir Platform is a straight 8 km long beach which faces the open sea. The foreshore is dominated by ridge and runnel topography with the runnel openings facing the northeast. The backshore is dominated by foredunes parallel to the present shoreline.

To the west of the of the sequence of links, dunes, beaches and sand spits, is a series of prominent raised beaches varying in height up to 22 m above O.D. The sedimentary deposits consist of material ranging from silts and clays interlayered with shelly sands, to rounded cobbles and pebbles.

At Tentsmuir the links and dunes east of the raised beaches have been forested, being first planted in 1922 by the Forestry Commission. High forested dunes up to 11 m above O.D. are present around the Tentsmuir Point area. The mature dunes are heath covered wheres the younger dunes have *Ammophila sp.* flourishing upon them.

The inter-tidal zone ranges in width from one hundred to several hundred metres. The beach gradients vary from 0.5^0 in the south to 3^0 in the north (Sarrikostis, 1986).

The immediate offshore bathymetry is characterised by a relatively smooth bottom topography except at the estuary mouths where the ebb-delta deposits extend out from the coast (Ferentinos & McManus, 1981).

1.7 GENERAL CLIMATE AND VEGETATION AROUND TENTSMUIR

Beach and dune evolution is ultimately controlled by weather conditions. On a smaller scale, dune systems have their own local climates whereby frontal dunes

modify the wind flow that impinges on more landward features and blowouts, and other erosional hollows often have wind speed considerably above those produced by regional and local winds. Tidal ranges are also important in that they determine the length of time for which specific beach widths are exposed for drying and therefore become potential source areas for aeolian transport further onshore. Apart from the waves and tides the weather parameters of Tentsmuir, Fife, recorded at the Leuchars meteorological site, will be discussed briefly to provide a general background.

1.7.1 Waves

Three main directional components of the waves were identified by Green (1974). Waves from the south westerly component with an approximate fetch of 16 kms were considered the most frequent in the seaward reaches of the Tay estuary, followed closely by the easterly (fetch of about 700 kms) and south easterly (fetch of 750 kms) waves. Subsequent study of wave height and period in St Andrews Bay by Boalch (1988) indicated that the most frequent waves occurred between a height of 0.3 and 1.0 m and a period of 3 - 7 seconds while storm waves ranged in period from 4 to 8 seconds and in height from 1 to 3 m.

The onshore wave power has been found to be significantly higher, often by a factor of 4, than the longshore wave power and thus it follows that the onshore/ offshore sediment exchange exerts the greatest influence on coastal geomorphology (Boalch, 1988). The pronounced bathymetric profile above Abertay and Gaa sands act as a magnet causing all immediate waves to bend towards the central spine of the banks. Further these sand banks act as an effective wave energy buffer as the incident wave energy becomes concentrated on the banks, little energy remains to be propagated westwards (Boalch, 1988). Although of considerable consequence to coastal stability within the lower reaches of the Tay estuary the major sand bars exert little direct influence on the Tentsmuir beach in its general sense. Wave refraction and energy loss is very important in the north but non-existent in the south.

1.7.2 Tides

The mean neap and spring tidal ranges in the Tay estuary average 3.5 m and 5.0 m respectively. In conclusion Green(1974) stated that west of Tentsmuir Point the main channel of the Tay experienced a reversing two directional flow system with an ebb residual, a large recirculatory eddy flow system existed east Tentsmuir point. Water is carried by a clockwise rotating eddy during flood tide and in an anti-clockwise moving eddy during an ebb tide (Fig. 1.7).

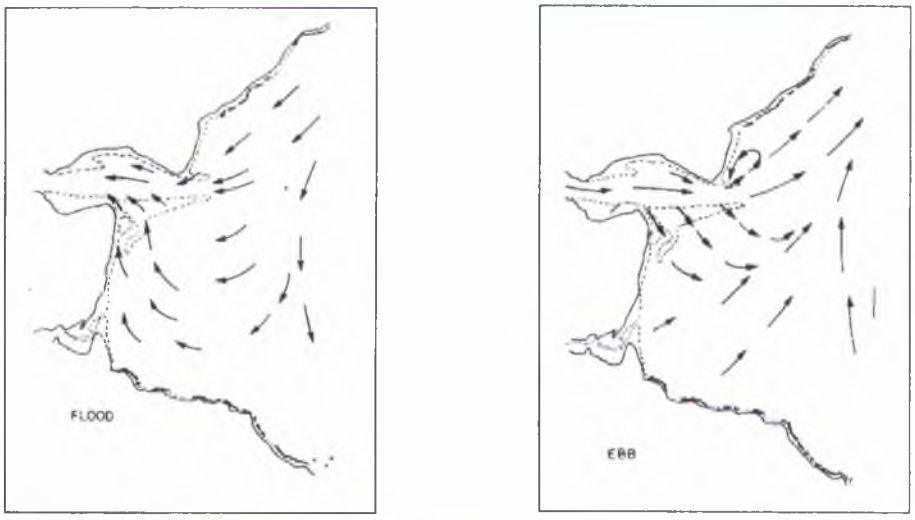

Fig. 1.7 Mid-flood and mid-ebb tidal current patterns in St Andrews Bay (after Ferentinos & McManus, 1981).

1.7.3 Winds

The average wind data for the last ten years show that most of the winds are derived from the south west sector (Fig. 1.8). The next in relative abundance are the winds from the east and north east.

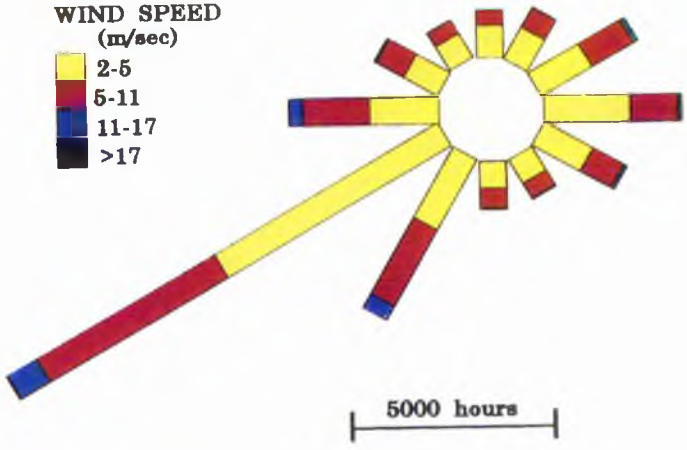

Fig. 1.8 Average wind rose for ten years (1980-1990),

1.7.4 Temperature

Tentsmuir lies within the dry belt (average rainfall for 1980 - 1990 is 670 mm) which extends along most of the east coast of Scotland. Air temperatures recorded

from the Leuchars meteorological station are shown in the form of monthly averages for 1980 - 1990 in Fig. 1.9. The minimum and maximum winter temperatures are 1 °C and 6 °C respectively. During summer the average temperature in the area vary between 10 °C and 19 °C.

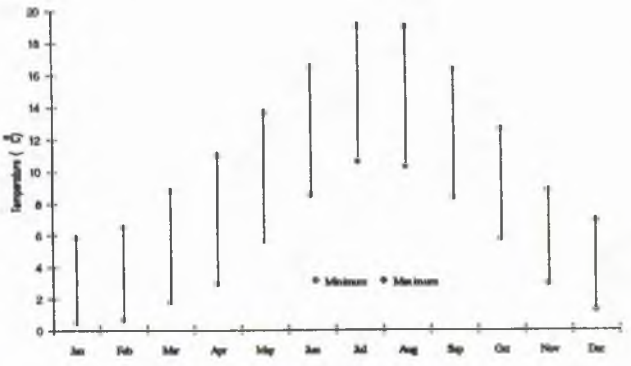

Fig. 1.9 Monthly Maximum and Minimum Temperature distribution.

1.7.5 Rainfall

During the period 1980- 1990 the average monthly rainfall in the last ten years has ranged from 40mm in April to 80 mm in October (Fig. 1.10). The winter season is the wet period (60-80 mm mean monthly rainfall) while the spring and summer season are the drier periods of the year (40-60 mm mean monthly rainfall).

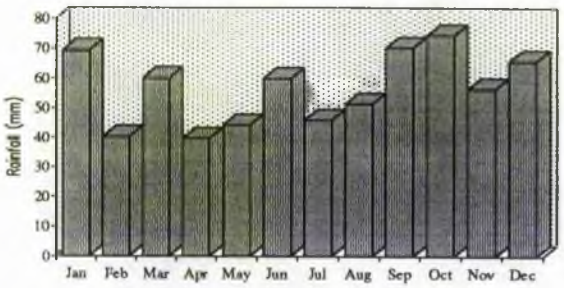

Fig. 1.10 Monthly rainfall distribution for 1980 - 1990.

1.7.6 Sunshine

On average the duration of sunshine varies from 5-7 hours daily from April to August; 2-4 hours of daily sunshine are experienced from October to March (Fig. 1.11).

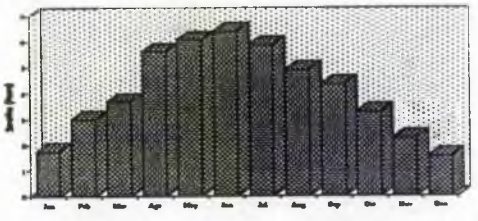

Fig. 1.11 Monthly sunshine hours (daily) distribution for 1980 - 1990.

1.7.7 Air masses

The atmospheric pressure system of the U.K. mainland is dominated by the maritime air masses (Fig. 1.12) from the west. During the winter these comprise the: polar maritime air mass (cold) from Greenland and the tropical maritime air mass (warm) from the Azores. The maritime air masses are frequently present during the summer, leading to reduced air temperatures during that season but occasionally the effect of the tropical continental air mass travelling north from the Sahara results in hot, dry and sunny weather.

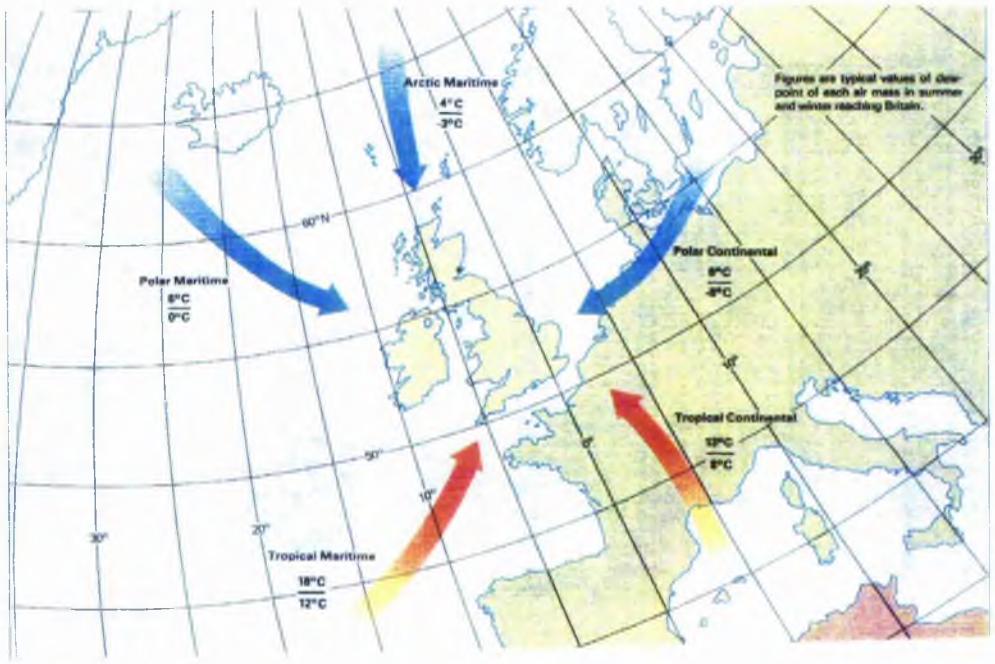

Fig. 1.12 Air masses observed over the mainland of U.K. (from Bartholomew Weather Map, 1980).

1.7.8 Vegetation

Vegetation is the best single index of stability and contemporary processes. The density, vigour and dominance of the tall dune grasses [such as: Marram grass (*Ammophila sp.*), Sea Lyme (*Leymus arenaria* formerly termed *Elymus arenaria*) and Sea Couch Grass (*Elymus farctus* formerly termed *Agropyron sp.*) found at Tentsmuir serve as excellent indicators of sand deposition and redeposition, and to some extent of soil and drainage conditions (Crawford, *pers comm.* 1992).

Cakile maritima and *Elymus farctus* are the pioneer dune colonisers. Further inland *Ammophila arenaria* flourishes along with *Epilobium augustifolium*, and *Carex sp.*

1.8 OBJECTIVES OF STUDY

The main objectives of this study are listed as follows.

1. Study of wind regimes and drift potential in the area.

2. Actual short term (minutes) sand transport rate measurements in the beach and dune environments.

3. Testing the validity of established transport rate expressions against measurements made on the beach.

4. Usage of standard long term (years) meteorological data to predict long-term sediment transfers along the coast.

5. Description of wind-induced bedforms and to propose a conceptual facies model.

Chapter 2 encompasses the present-day shoreline changes, beach-foredune development stages and grain size characteristics. A review of literature dealing with the fundamental principles of aeolian transport is the main aim of Chapter 3. The ambient wind regimes and drift potentials prevalent in the area have been described in Chapter 4. Chapter 5 deals with the methodology and measurements of short term aeolian sand transport rate in the beach and dune subenvironments. Prediction of long-term potential aeolian sand input using wind velocity data from a weather station has been attempted in Chapter 6.

Chapter 7 is devoted to the description of wind-induced aeolian bedforms along the coastline and a proposed facies model for the area.

Finally, discussion and conclusions are presented in Chapter 8.

Chapter 2

SHORELINE CHANGES AND BEACH-DUNE MORPHOLOGY

(with 17 figures, 15 plates and 2 tables)

Chapter 2
Shoreline changes and beach-dune morphology

2.1 INTRODUCTION

The Tentsmuir area has undergone buildup since the retreat of the ice. This accretionary process continues today and as a first step to understanding the process active in the area an attempt has been made here to describe the shoreline changes which have been observed in the study area during the last 150 years in general and the past 10 years in particular. This has been done by analysing sequential maps, ground photographs and successive aerial photographs (Courtesy: Nature Conservancy Council, now Scottish National Heritage, Scotland, Cupar).

The Tentsmuir coast is a macro-tidal coast (tidal range 4-6 m, Davies, 1964 classification) on which a range of beach types, and foredune morphologies occur along the 8 km long area under study. Beach width varies from 85 m to 400 m.. The beaches are wider towards the northern and southern extremities of the Tentsmuir platform where the mouths of the Tay and Eden estuaries respectively are situated (Fig. 2.1). Dune accumulations in the lee of the beaches are found at Tentsmuir Point (2 - 4 m high), Kinshaldy (1 - 2 m high) and West Sands (4 m high).

2.2 SHORELINE CHANGES

The present day shoreline is mainly an admixture of areas of foredune development and cliff erosion (Plate 2.1). Aerial photographs, from 1948 to 1990 shown in Plate 2.2 reveal that the area marked 'A' (northern extremity of the Tentsmuir platform- Tentsmuir Point) in the 1948 photo is a beach platform almost 500 m wide. By 1972 hummocky aeolian accumulations had developed on the seaward margin of the 1948 HWMOST line. At present almost the entire inter-tidal area (area A) of 1948 has changed into an area of 2 to 4 m high vegetated sand hummocks.

Tentsmuir Point has been reported to be accreting since 1812 in the NE direction (Deshmukh, 1974; Grove, 1950). During the last decade coastal growth has been at a discontinuous rate of 3 m a^{-1} (rate calculated from 1978-1990). Detailed

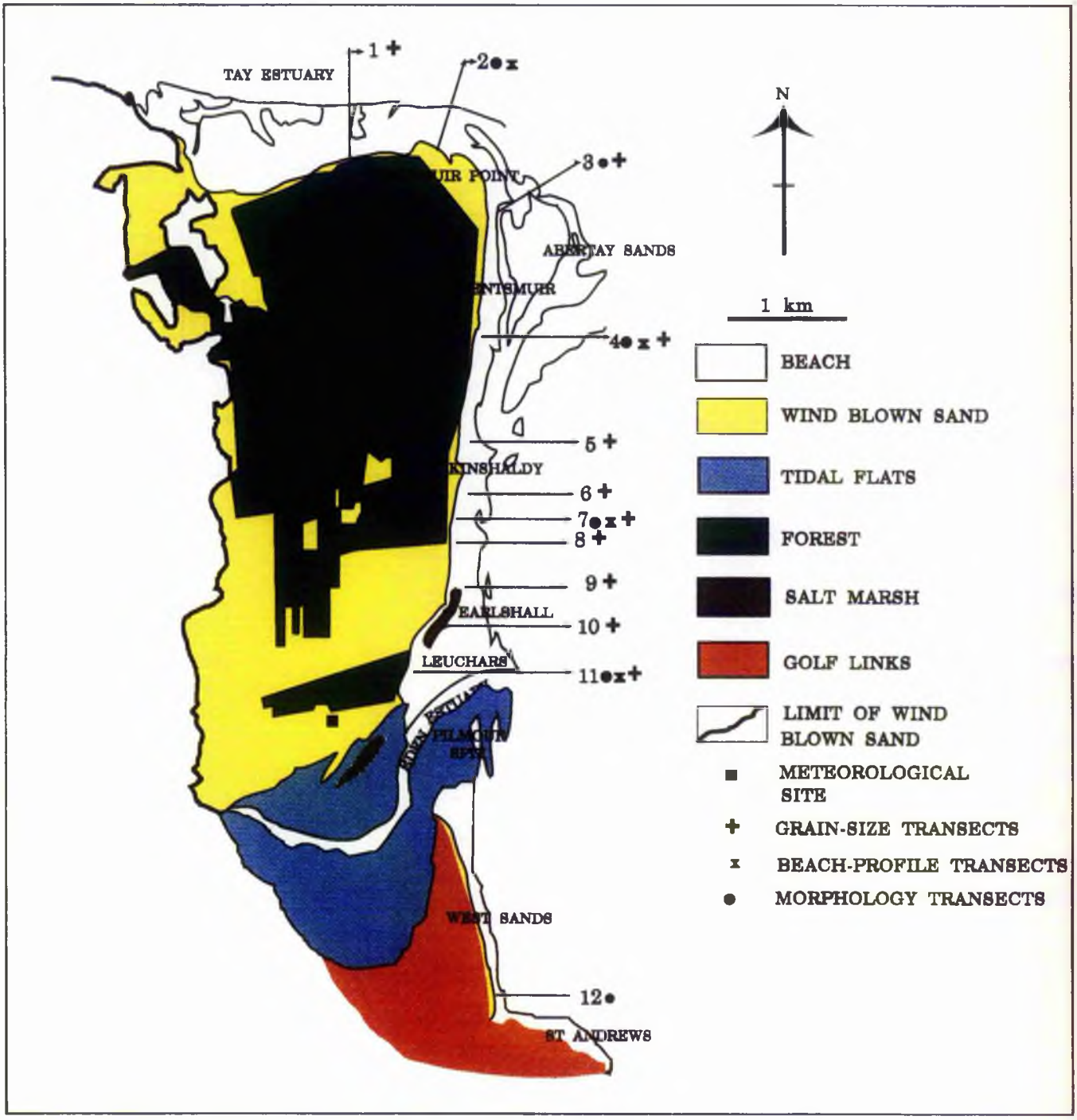

Fig. 2.1 Location map of study area showing transects of beach profiles, grain size studies and beach-dune morphology. Leuchars meteorological station has provided the wind data.

development of the shoreline changes have been shown in Fig. 2.2. The 1941 anti-tank blocks (concrete blocks of 1 m side length 1.5 m high and placed 0.5 m apart, seen in Plate2.1) originally placed along the shoreline at H.W.M. now lie approximately 580 m away from the present day beach (Fig. 2.2). An artificial ridge like structure appears to

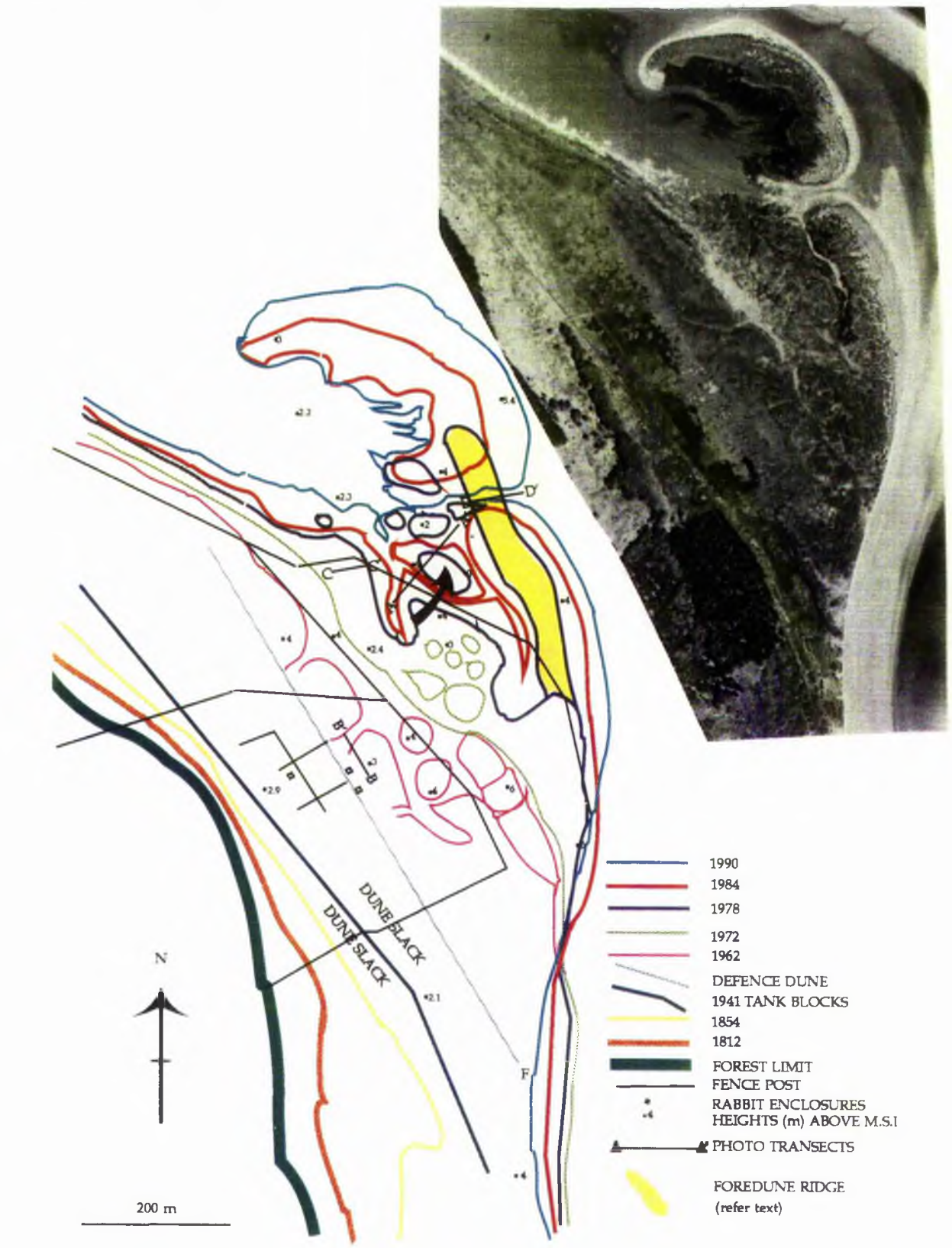

Fig. 2.2 Sketch showing shoreline changes at Tentsmuir Point from 1812 to present day. Inset shows 1990 aerial photograph (courtesy: Nature Conservancy Council, Cupar) (Source: Aerial photographs for 1962 - 1990; Deshmukh (1974) for 1812 - 1854).

been formed as part of the military defence construction (Plate 2.3 also marked on Plate 2.1). This defence dune (Fig. 2.2) remains at the core of an existing linear feature. Accretion at Tentsmuir Point in relation to the anti - tank blocks and the defence structure can be seen in Plate 2.1.

The rest of the area shows hummocky aeolian sand accumulations along the exposed backshore areas which are stabilised by pioneer vegetation (*Elymus farctus*, *Cakile maritima*). These aeolian accumulations generally form as wind shadow structures and continue to accrete concomitant with vegetation growth. The lower ground between the hummocks is occasionally inundated by spring tidal waters through minor tidal channels (1-2 m wide). Several such tidal inlets active in 1962 have been identified by ground survey (photo transects in Fig. 2.2). Photo transects AA' (Plate 2.4) and BB' (Plate 2.5) show such paleo-tidal channels active up to 1984 and 1962 respectively. Comparison of the 1984 photograph of transect AA' with that from 1991 shows the complete absence of any sand accumulation east of the coastal fence (Plate 2.4). The 1984 photograph shows the development of the triangular aeolian accumulation (shown by an arrow in Fig. 2.2) which has later been stabilised by vegetation. CC' (Plate 2.6) shows the tidal flooding in a dune slack channel active in 1984.

A blowout (transect DD', Plate 2.7) has breached the longshore foredune ridge which was formed in 1978 (foredune ridge area shown as yellow coloured area in Fig. 2.2). The detached portion of the breached ridge north of the blowout served as a locus for the formation of the kidney plan deposit seen today. Another blowout 1.8 m deep developed, in the course of a few days of windstorm in May 1992, amongst the stabilised dune hummocks at Tentsmuir (Fig. 2.8). The wind formed a deflation trough, scoured the sand out of the blowout and deposited it onto the adjacent topography. Exposure and instability of the blowout slope caused the mobile sand to slide down in the form of sand tongues (grainflow process).

Sequential longshore changes in the shoreline since 1972 are shown in Fig. 2.3. Although the extent of the area photographed during different years does not coincide with entire area under study, the figure has been drawn from the available photographs. The coastline has been grouped into three sections: Tentsmuir Point

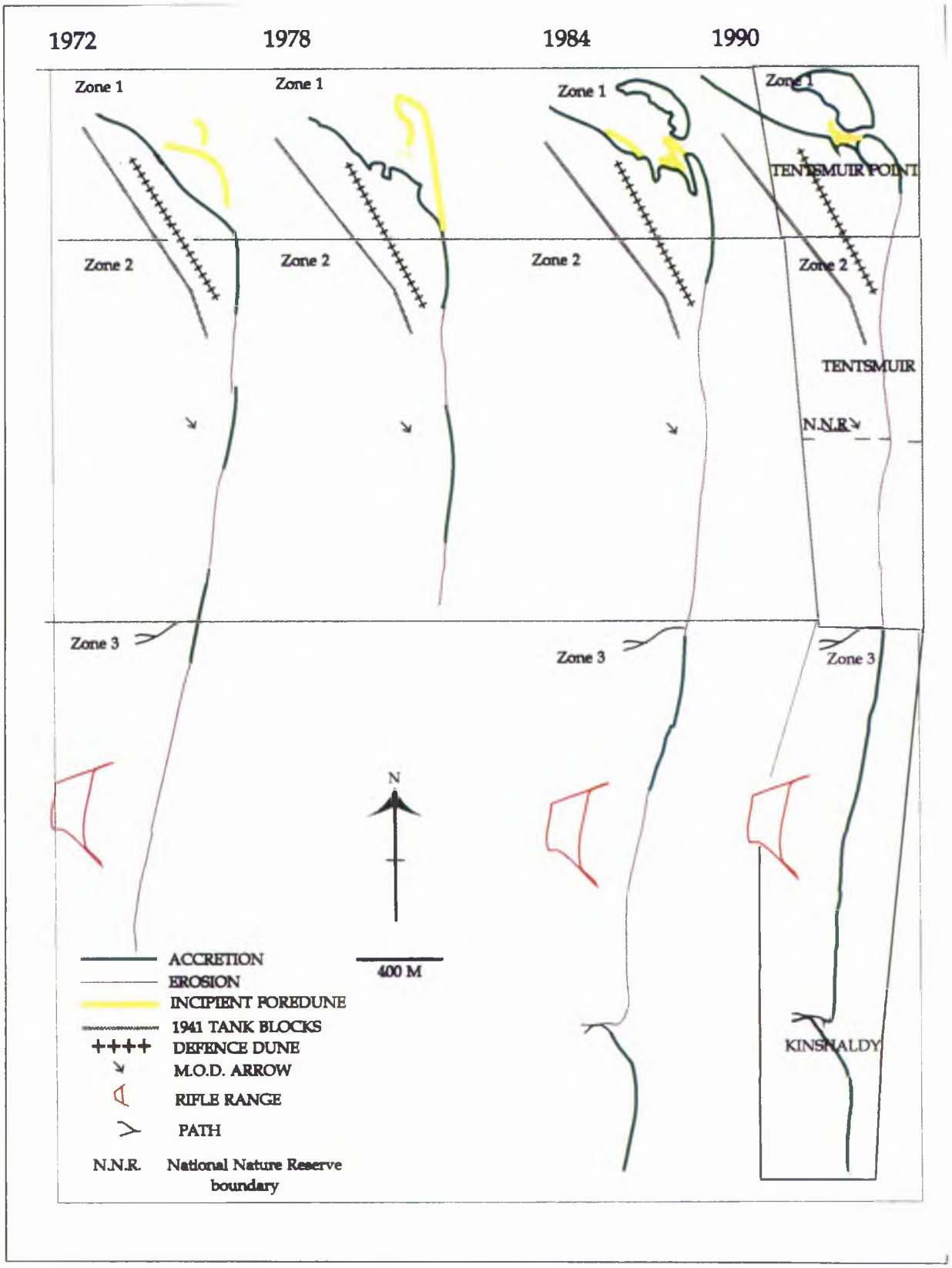

Fig. 2.3 Sequential longshore coastline changes from 1972 to 1990 in zone 1 - Tentsmuir Point, zone 2 - Tentsmuir, and zone 3 - Kinshaldy area (Source: Aerial photographs).

(Zone 1), the area south of the point has been referred to as Tentsmuir (Zone 2) and Kinshaldy (Zone 3). Between 1972 and 1990 net foredune accretion, as observed earlier, has occurred in zone 1 (Plate 2.2). The northern part of Zone 2 of Tentsmuir (Opposite Anti tank blocks; Fig. 2.3) accreted until 1972 after which it suffered erosion and this part of the shoreline is backed by a 5 m high steep dune cliff. The central portion of Zone 2 opposite the M.OD. arrow (Fig. 2.3) started to erode after 1978 and at present the shoreline in the area has moved approximately 180 m inland exposing the older N-S trending, 5-6 m high, dune ridges (Plate 2.9). Zone 3, which was, erosional up to 1984 and is accreting at present.

2.2.1 Volume estimates of shoreline changes

The volume estimates of shoreline changes were made by measuring the area of change (accretion or erosion), by square counting, from successive scale-corrected aerial photographs. The area estimates have then been multiplied by the height of the accumulations, read off from contour lines drawn on the 1987 Tentsmuir survey map of the Nature Conservancy Council, Cupar (Enclosure 1). The magnitude of erosion/accretion has been calculated by observing the change in area in relation to a fixed landmark further inland e.g.the anti-tank blocks at Tentsmuir Point (Zone 1), the concrete arrow mark at Tentsmuir (Zone 2) or the rifle range at Kinshaldy (Zone 3) (Fig. 2.3).

At Tentsmuir Point estimates of the volume of foredune accretion during the last 10 years is approximately 33 x 10^3 m^3 (Fig. 2.3, Zone 1). During the same period 46 x 10^4 m^3 of sand was eroded away from the adjacent Tentsmuir shoreline (Fig. 2.3, Zone 2), immediately south of Tentsmuir Point. The elongate ridge-like NW trending successive foredune growth at Tentsmuir Point (Fig. 2.3, Zone 1) and the development of an increasingly narrow and erosional profile at Tentsmuir (Fig. 2.3, Zone 2), immediately south of the accreting area, is very conspicuous also shown as yellow coloured area in Fig. 2.2). The erosion of the shoreline and the release of sediments along the Tentsmuir coast (Zone 2, Fig. 2.3) are probably responsible for the accretion at Tentsmuir Point (Zone 1, Fig. 2.3). The nearness of the estimates of the volumetric exchanges involved in the Tentsmuir dune development between 1978 and 1990,

confirm that the shoreline is in a state of quasi equilibrium, where net erosion roughly equals net accretion.

Prior to 1984, the Kinshaldy area (Zone 3; Fig. 2.3) was eroding, the lines of 1941 anti-tank blocks being excavated from beneath the retreating line of dunes. The shoreline was being eroded by wave and tidal attack. Between 1984 and 1990, welding of the off shore bar to the beach increased the beach width and reduced the vulnerability of the shoreline to further wave and tidal attack (Plate 2.10). This led to the widening of the beach and increase in the stored beach sediment volume. Approximately three ridges of foredunes developed in the area which in 1984 was devoid of any foredune development.

The change from an erosional to an accretional shoreline at Kinshaldy is probably related to the position of the offshore sand bars (Plate 2.10). As a consequence of change in the nearshore morphology, due to the welding of the bar, which reduces the severity of wave and tidal attack; conditions (wide beach, dissipation of wave and tidal energy, increase in beach sediment volume) conducive to the formation of foredunes developed along the backshore. The shore parallel bar systems that lie off the coast of Tentsmuir are thought to have been formed in response to the direct onshore/offshore sediment exchange, their position marking a dynamic equilibrium between the opposing onshore and offshore forces (Boalch, 1988).

Out of the 500 m wide inter-tidal beach area of 1948, approximately 330 m has been covered by vegetated sand hummocks (3-4 m high) between 1948 and the present (area A on Plate 2.2). The 500 m wide beach (of 1948) in the area 'A' has in turn been reduced to a present-day width of 170 m. Foredune development in area 'A' has led to the development of an increasingly narrow beach since 1948 (Plate 2.1, Plate 2.2). Hence, foredune accretion at Tentsmuir Point, under the influence of the prevalent wind regimes and the resultant aeolian sand transport, is one of dune encroachment over the beach. In the sediment budget concept it is proposed that dune development is fostered and enhanced under conditions of net negative sediment budget whereby the dune is positive while the beach is negative (Psuty, 1988).

2.3 BEACH-DUNE MORPHOLOGY

Beaches and dunes occur in shore parallel marine-aeolian depositional settings where sand supply and beach form are controlled by surf-zone beach processes, and where dune morphology is controlled partly by wind and partly by vegetation (Hesp, 1988).

The beach at Tentsmuir Point (170 m wide) continues northwards then curves northwestwards (Fig. 2.1). The average surface elevation of the dune ridges is 2 - 4 m O.D. (Fig. 2.4). The inland area is covered by mosses, *Epilobium sp.* and *Carex sp.* The primary dune ridge is covered by *Ammophila arenaria.*

The Tentsmuir beach (transect 4 in Fig. 2.1; 2.4) is a narrow beach approximately 65 m in width, with steep erosive beach-dune interface of 5 m height. The scarped shoreline of the beach is prone to severe undercutting by wave and tide activity.

At Kinshaldy, a 160 m wide beach with a well developed ridge and runnel topography is present (transect 7 in Fig. 2.1; 2.4). It has a 10 m wide berm where widely spaced clumps of incipient foredunes flourish in the lee of pioneer dune grass (*Elymus farctus*). Further inland a primary dune ridge dominated by *Ammophila sp.* is present to the east of the forest edge.

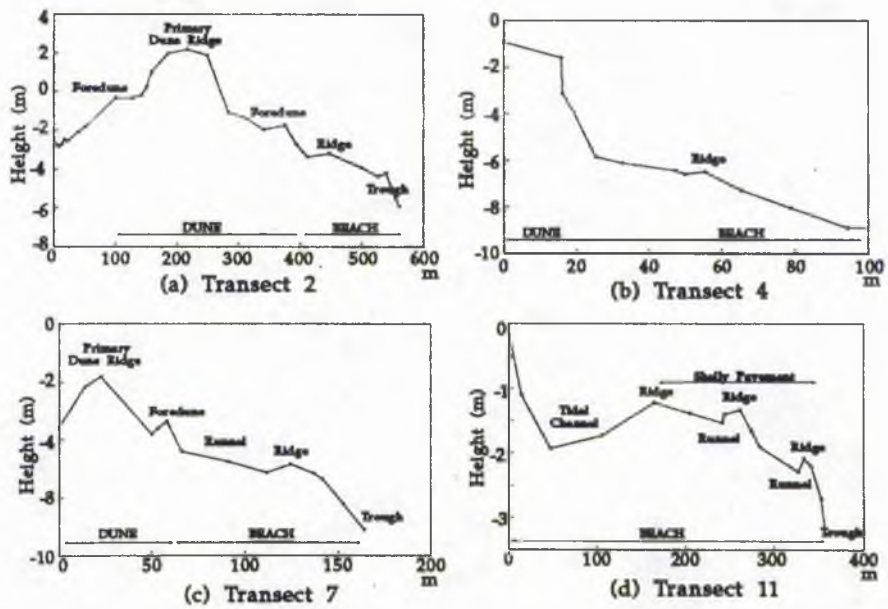

Fig. 2.4 Representative beach-dune profiles of (a) Tentsmuir Point, (b) Tentsmuir, (c) Kinshaldy, and (d) Leuchars. For transect locations see Fig. 2.1.

In alignment with the Leuchars airfield is a very wide beach (400 m) where the anti-tank blocks lie exposed along the shoreline (Fig. 2.1). This beach has been referred to as an offshore sand bar in earlier descriptions (Ritchie, 1979). It is notably rich in shells and is dissected by a tidal channel along the western beach edge. Both to the north (southern edge of Earlshall) and south of this wide beach an active salt marsh has developed landward of the sand bar. North of this area the Earlshall beach locally exhibits foredune accretion.

The West Sands northward broadening beach is quite wide (250 m) (Fig. 2.1). At the southern limit of the beach the Swilken Burn flows across the beach beside a low sea wall before discharging across a low sandstone rock platform. Dunes at the back of the beach are 15 - 30 m wide about 2 - 5 m high with abundant blowouts. The shoreline appears as fragmented coastal line of tussocky dunes.

2.3.1 Beach Profiles

The beach is not only the most dynamic coastal environment, it is probably also the most studied (Shephard, 1950; Zeigler & Tuttle, 1961; Aubrey, 1979; Carr *et al*, 1982). One of the first generalisations that was made about beach dynamics is that the beach represents a cyclic process-response system often in phase with the seasons (erosional during winter storms and accretional during summer swells), essentially universal although the scale and rate of change may differ (Davis, 1983). Since storms are likely to occur throughout the year the 'winter' and 'summer' profiles have been replaced by 'storm' and 'swell' profiles (Komar, 1976). The beach cycle is a function of several morpho-dynamic processes, operating in conjunction, which cause the system to alternate between transgressive and regressive phases of development. The beach profile is a system which, at any given time, accommodates a specific amount of material within a specific linear sub-aerial boundary which varies with changes in the wave-climatic regimes (Du Bois, 1988).

The exchange of beach sediments between different portions of the beach profile (sub-, inter- and supra-tidal) is accomplished by onshore-offshore transport, mainly by waves, but sometimes aided by wind (Aibulatov, 1961).

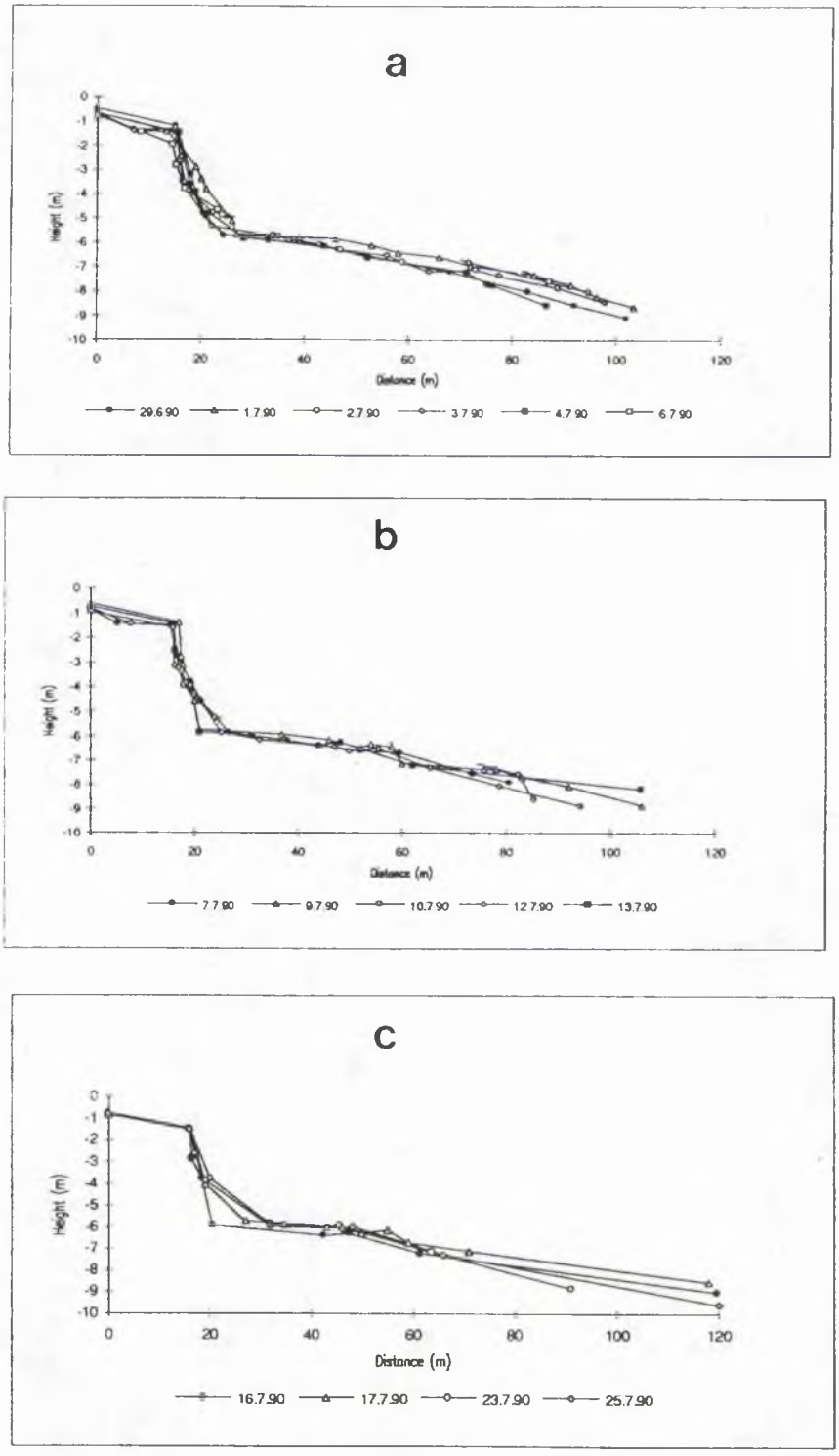

Fig. 2.5 Beach profile surveys between June 29 and July 25, 1990 along Transect 4. The arrow (Fig. 2.5 a) points to the beach face berm crest.

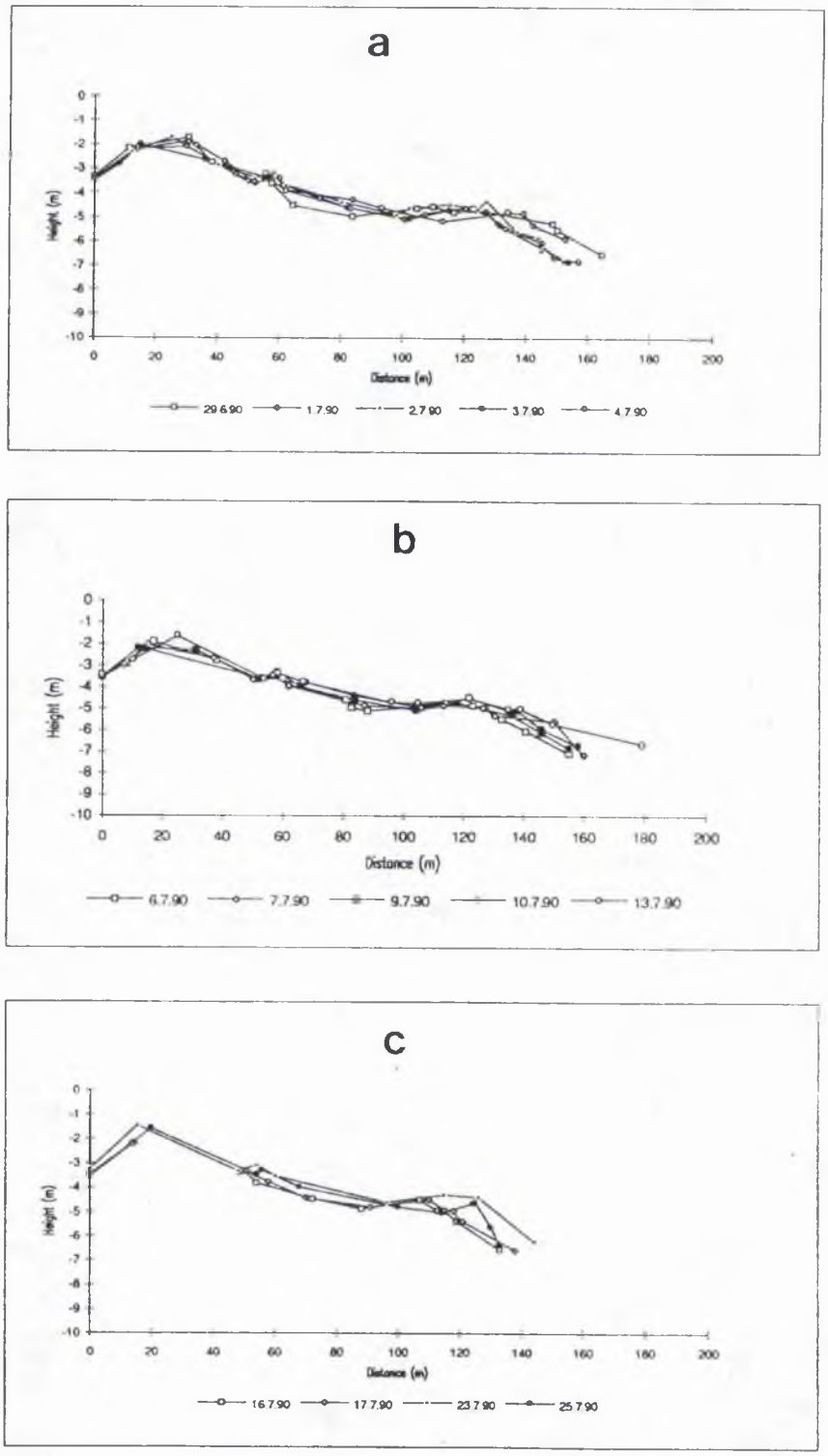

Fig. 2.6 Beach profile surveys between June 29 and July 25, 1990 along Transect 7. Lateral migration of beach face levels can be seen in (b). (c) shows the rise and fall of the beach surface.

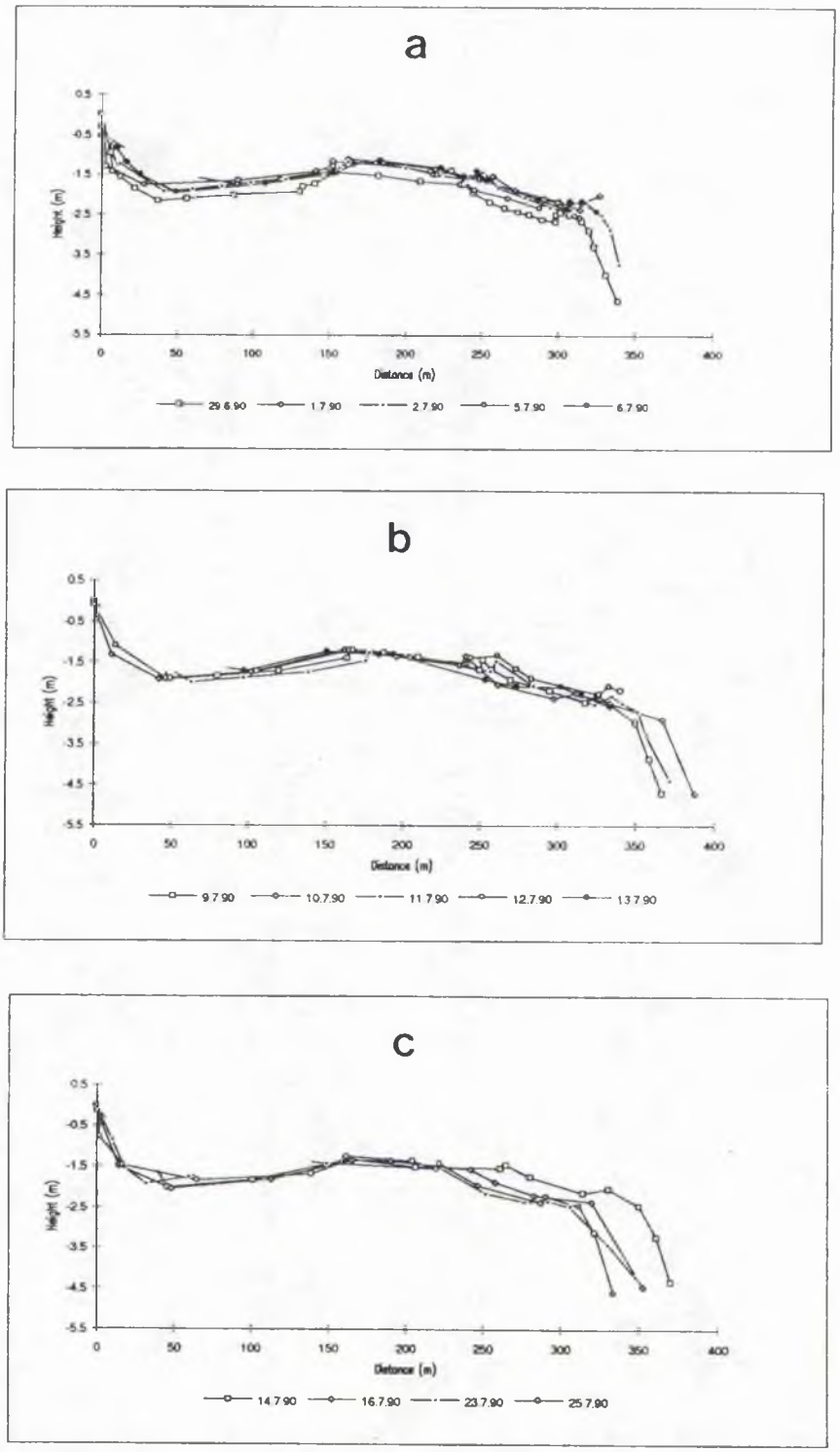

Fig. 2.7 Beach profile surveys between June 29 and July29, 1990 along Transect 11 showing systematic seaward and landward migration with time.

Profile surveys were conducted to generate first hand information on the temporal and spatial variability of beach profiles on a day to day basis in the study area. Three survey transects were chosen; Tentsmuir, Kinshaldy and Leuchars (transect 4, 7 and 11 in Fig. 2.1, 2.4, 2.5, 2.6, 2.7). Access was easy to all three beaches which were surveyed between June 29, 1990 and July 25, 1990.

The profiles were surveyed with a 'Kern' GKO-A automatic construction level and levelling rod to the nearest 3.0 cm adjusted to the Nature Conservancy Council stile gate square wooden posts at Tentsmuir (transect 4) and Kinshaldy (transect 7) and to the 1941 anti-tank blocks at Leuchars (transect 11). Along a profile, elevational readings were taken at intervals ranging from 15 m on wide beaches (Leuchars) to 5 m on narrower ones (Tentsmuir and Kinshaldy), on the open beach during low water. Tidal stages ranged from 4.2 m (neap tides) to 5.4 m (spring tide) during the study period (Appendix I-A). Meteorological wind information has also been collected from the Leuchars meteorological site throughout the survey period (Appendix I-B). The winds during the period were generally sea breezes ranging in speed from 2 - 8 ms^{-1}.

Along transect 4 (Tentsmuir) between 29.6.90 and 6.7.90 (Fig. 2.5a) the beach profile shows no significant change. However, between 7.7.90 and 13.7.90 (as the high tide levels rose from 4.5 - 5.1 m) the development of a middle beach face crest is observed (arrow in Fig. 2.5b). Later this crest disappears and is not visible on 25.7.90 (Fig.2.5c). Another beach ridge crest developed on 10.7.90 at ~82 m which was later planed off on 12.7.90 (Fig. 2.5b).

Beach profile surveys along the Kinshaldy transect (transect 7) between June 29 and July 25 are shown in Fig. 2.6. The Kinshaldy beach surveys (transect 7) began with a profile showing an upper beach face swale (29.6.90), a middle beach face ridge (50 cm vertical difference in height) and a long lower beach face profile (Fig. 2.6, 2.8). By 1.7.90 the upper beach face swale had become partly filled and the landward side of the middle beach face ridge had been eroded as had the lower beach face (2.6a). Onshore winds (8 ms^{-1}) during the period are probably responsible for the change via wave activity. The profile of 3rd July showed the swale to have become largely filled whereas the beach ridge had migrated seawards by 30 m during a period of six days (Fig. 2.6a, 2.8). Migration of beach face levels is conspicuous along the lower

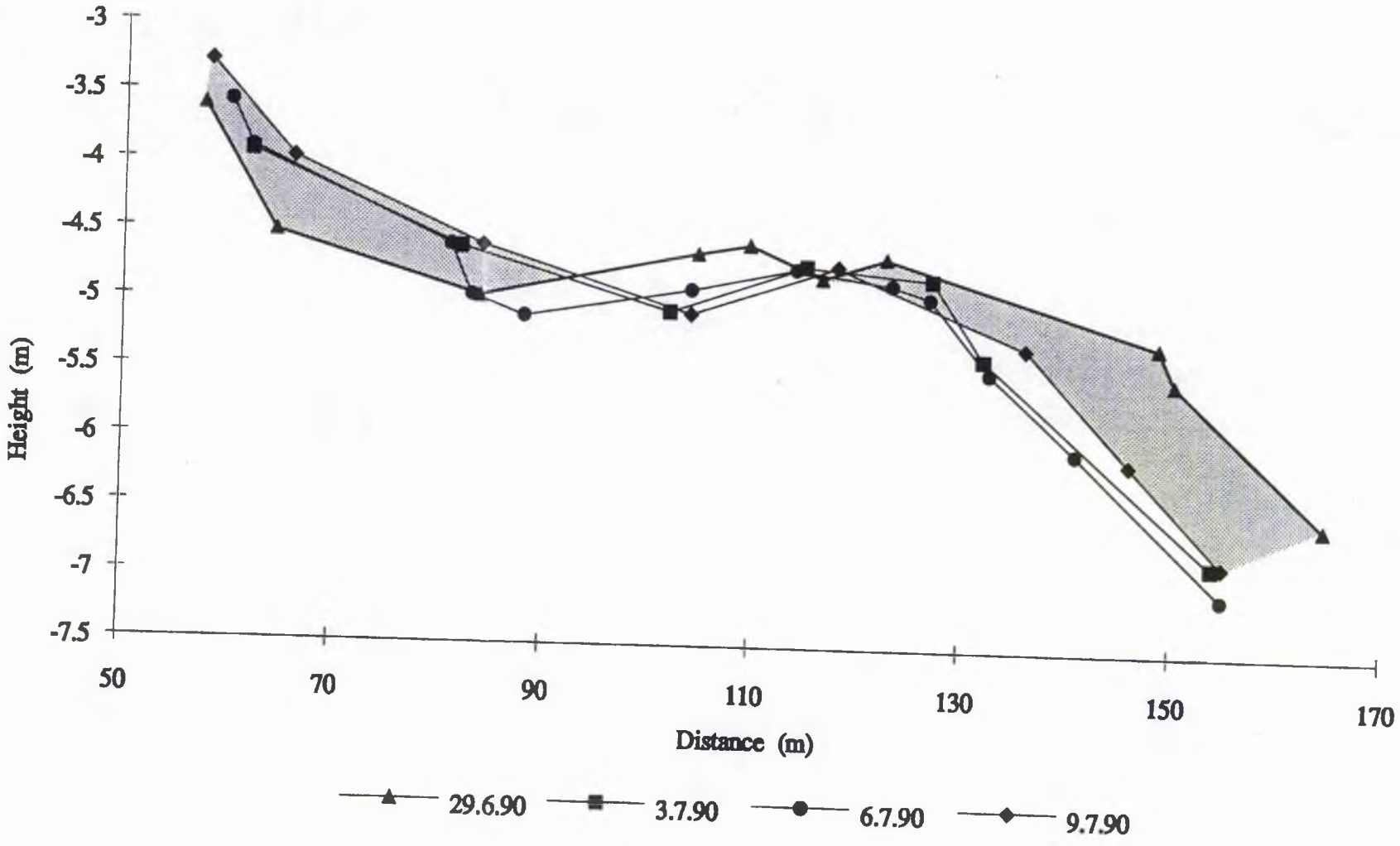

Fig. 2.8 Changes in beach profile along transect 7. Stippled area shows net vertical aggradation.

beach face profile (between 120 and 160 m in Fig. 2.6b). Although the upper and middle beach face profiles show no significant change between 3.7.90 and 9.7.90 the lower beach face (between 125 and 160 m) shows vertical accretion (Fig. 2.8). Lateral migration of the lower beach face ridge crest by 20 m occurred on 23.7.90 (2.6c), as the profile was acted upon by increasingly higher levels of the tidal cycle (from 4 - 5 m, Appendix I-B)

Due to the presence of the tidal channel flowing along the edge of the Leuchars beach, the profile along the edge is very steep (Fig. 2.4d). Beach profile surveys between 29 June and 25 July are shown in Fig. 2.7. The 29.6.90 Leuchars profile began with two swales (h_1 & h_2 in Fig. 2.9) separated by a small beach ridge (r_1 Fig. 2.9) followed by another ridge (r_2 Fig. 2.7, 2.9). The swales continued to accrete vertically for about 1 m from 29.6.90 to 6.7.90, but were subsequently eroded on 10.7.90 by about 50 cm resulting in a net accretion of 50 cm till 25.7.90 (Fig. 2.9). This erosional event can be related to the occurrence of the spring tide levels of 5.1 m on 10.7.90 (Appendix I-A). During the observation r_1 shifted seawards by about 25 m (Fig. 2.9). However, ridge r_2 accreted vertically by about a metre but started to erode from 13.7.90 leading to its complete disappearance by 25.7.90 (Fig. 2.8b, 2.9). Since, the Leuchars beach is very wide only the beach profile 150 m from the landward edge is acted upon by the tides and most of the changes are most likely to occur in this area. In general, the period before and after 10.7.90 is coherent with the two phases of beach profile change i.e. accretion and erosion respectively. Net vertical aggradation of the swales and lateral migration of the intervening ridges during summer swells (high tidal levels accompanying onshore winds) by overtopping processes was the probable explanation for the day to day variation along the beach profiles in the study area.

2.3.2 Description of beach-foredune morphology

Six transects were selected (transect 2, 3, 4, 7, 11, and 12 in Fig. 2.1) to describe the longshore variations of the beach-foredune morphology presented in Table 2.1 and described as follows.

Transect 2 (Fig.2.1) in the extreme north is an area of rapid foredune accretion since the turn of the century (Ritchie, 1979). It is characterised by a 167 m wide beach

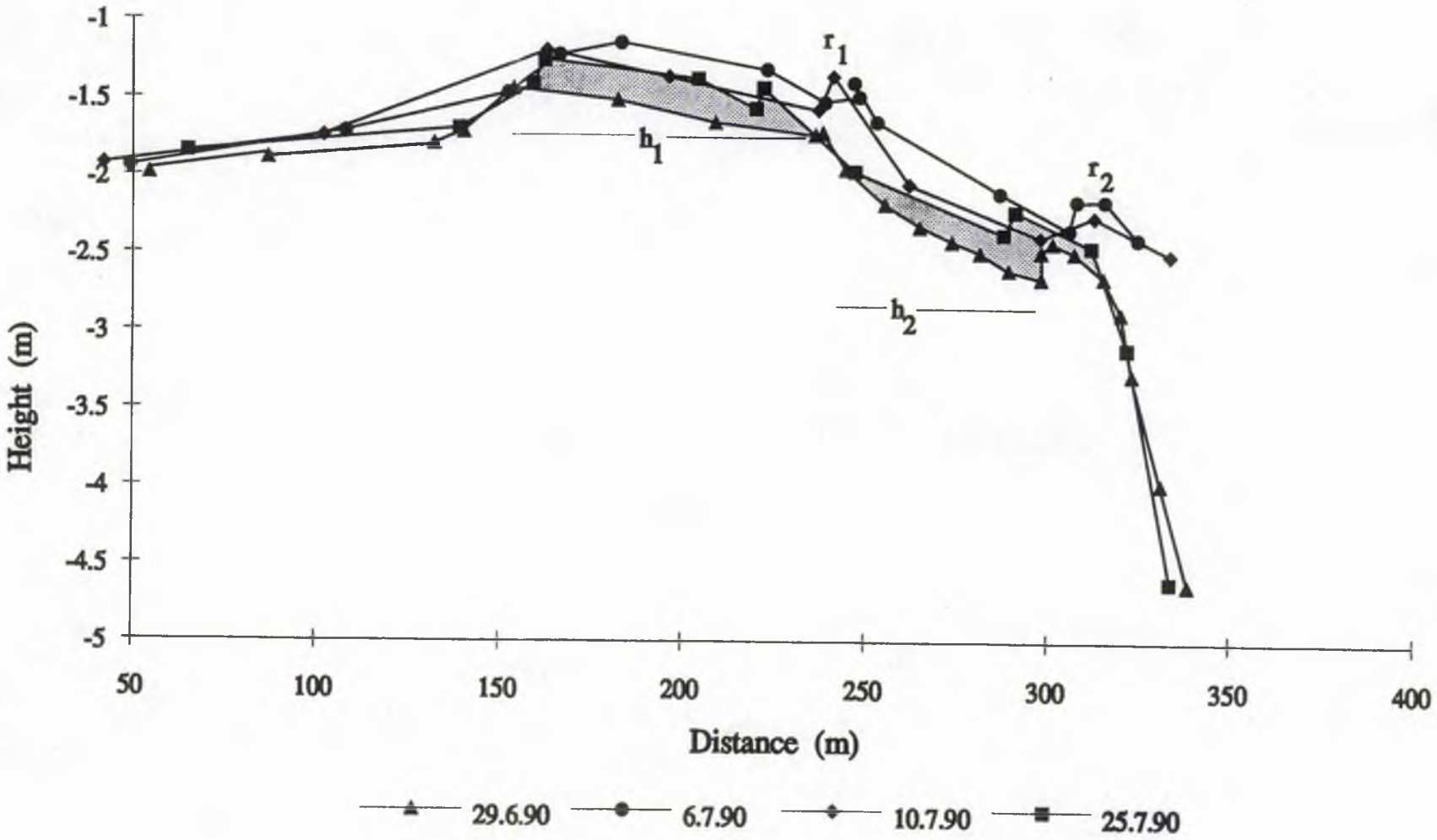

Fig. 2.9 Changes in beach profile along transect 11. h_1, h_2, and r_1, r_2 are the swales and ridges respectively. Stippled area shows net vertical aggradation.

with 1.3 m high foredune, a vegetation cover of 45-75% (*Ammophila arenaria*), moderate size blowouts and occasional breaching by storm wave attack (Plate 2.11).

The foredunes along transect 3 (Fig.2.1) are topographically continuous and well vegetated. Highly stable aeolian accumulations are formed in the lee of a 190 m wide beach. The beach in turn is sheltered by the giant offshore Abertay sands. This foredune type is present for a 400 m long stretch south of transect 2. The vegetation varies from *Elymus farctus* along the incipient foredune area to *Ammophila sp.* in the primary dune ridge. Further inland in the mature dune area mosses, *Epilobium sp.* and *Carex sp.* flourish.

At transect 4 (2 km south of transect 2) the shoreline is erosional, where a 2.5 - 5 m high erosional dune cliff is present in the lee of a relatively narrow 85 m wide beach (Plate 2.12). There is no foredune development in this area. Scarce vegetation cover develops when the erosional ridge receives fresh sand input during a storm. Occasional very small embryo dunes (0.25 m wide) are seen to flourish at the toe of an erosional dune ridge (2 m high).

At Kinshaldy (transect 7) the 1.5 m high foredune is backed by a 4 m high primary dune ridge, colonised by *Ammophila sp.* (Plate 2.13). The beach is 160 m wide and exhibits well developed ridge and runnel topography. The incipient dune

Table 2.1 Beach-dune morphology and stages of foredune development in the study area. WTH - width, HGT - height, GRAD - gradient, VEG - vegetation, TYPE* - see Fig. 2.8

LOCATION	BEACH WTH.	BEACH GRAD	PRIMARY DUNE HGT.	PRIMARY DUNE WTH.	PRIMARY DUNE VEG	FORE DUNE HGT.	FORE DUNE WTH.	FORE DUNE TYPE*	FORE DUNE STABILITY	REMARKS
Tentsmuir Transect 2 0 km	167 m	Mod	3 m	60 m	45-75 %	1.3 m	6 m	Stage 3	Mod	Small-mod blowouts
Transect 3 1.25 km	189 m	Mod	3 m	80 m	90-100 %	2 m	19 m	Stage 1	High	
Transect 4 2 km	85 m	High	No foredune development							Scarped shoreline
Kinshaldy Transect 7 4.25 km	160 m	Mod	4 m	40 m	70 %	1.5 m	10 m	Stage 2	High	
Leuchars Transect 11 6.5 km	400 m	Low	No foredune development							Shell pavement
West Sands Transect 12 10 km	250 m	Low	5 m	30 m	25-45 %	–	–	Stage 4	Mod	Large blowouts, shadow dunes

consists of sand accumulation in the lee of pioneer dune grass *Elymus farctus* (75 - 90%) with small scale unvegetated troughs. This part of the shoreline was erosional until 1984 but in the past seven years it has changed into an area of stable foredune development due to the widening of the beach as a consequence of the welding of an offshore bar to the earlier (1984) narrow beach.

Further south at the mouth of the Eden estuary, the southern limit of the Tentsmuir beach-dune complex, is present a very wide coarse shelly beach of Leuchars (transect 11; Plate 2.14). The Leuchars beach has silty sand deposits on the landward side due to the presence of a tidal channel opening into the Eden estuary. This channel is believed to be a precursor of the present day Eden estuary channel (*pers. comm.* Jarvis, 1992). The floor of this channel is composed of silty sand. The channel runs close to the land and thus the lower beach face profile is steep (Fig. 2.4d). The channel has now been infilled and a modern bar now transects the channel. Reworking of the bar sediments by waves and tides has produced a wide coarse shell-dominated beach of Leuchars. The beach has the development of a ridge and runnel profile (Fig. 2.4d). Immediately north and south of the beach is a well developed salt marsh. No dune development is present in this area.

Further south beyond the influence of the Eden estuary, are present the West-Sand dunes (transect 12; Plate 2.15). The 5 m high primary dune ridge appear as remnant knobs and have large sand blowouts. These dunes are present behind a 250 m wide beach. Vegetation is scarce (*Ammophila sp.*), approximately 30% on the windward dune edge whereas the leeward dune blowouts are literally devoid of any vegetation cover. The overall structure of the dune is avalanche and slump dominated and there is no definite vegetation succession.

2.4 AEOLIAN SEDIMENT TRANSPORT FROM MODAL BEACH-TYPES

A classification of foredunes into five morpho-ecological stages has been presented by Hesp (1988). This provides linkages between surf zone - beach dynamics, aeolian transport on beaches and foredune morphology and ecology (Fig. 2.10). Initially (Short and Hesp, 1982) related the offshore zone and the beach face to the spectral distribution of energy modes reaching the shoreline. The Short and Hesp

(1982) classification is based on the percentage of vegetation cover and relates the integrity of the coastal foredune ridge to the proportion of the cover.

The five morpho-ecological stages of foredunes switches from stage 1 foredune, one being dominated by vegetation (fixed shore parallel ridges) to stage 5 characterised by remnant knobs large-scale deflation blowouts and sheets.

Variation in foredune morphology along the Irish coastline has been attributed to the local rate of sediment input (Carter, 1990). Three sediment supply systems: low intermediate and high: have been identified to be associated with erosional, mixed and accretional dune morphology respectively.

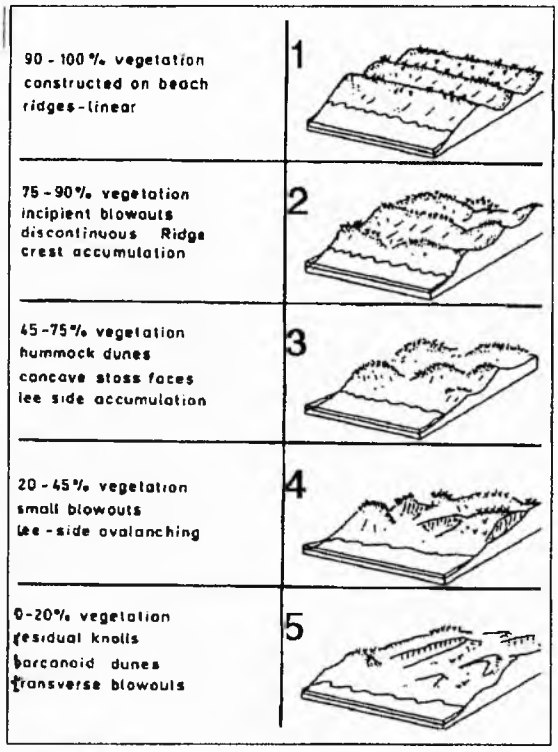

Fig. 2.10 Classification of foredunes based on the proportion of vegetation cover (after Hesp. 1988).

The foredune assemblage at transect 2 comprises a 45-75 % vegetation cover, which has incipient blowouts and the landward face of the dune often becomes rejuvenated by inland sand transfers. It corresponds to stage 3 foredune of Fig. 2.10 and has an intermediate to high sediment budget.

Along transect 4 is present a progradational sequence of topographically continuous *Ammophila sp.* and *Elymus sp.* dominated foredune accumulations. These are similar to the stage 1 foredunes of Hesp (1988). These accumulations appear to prograde due to the presence of abundant sediment supply.

Small sediment budget and low sediment supply will lead to the development of an erosional dune face as described along transect 5.

Along transect 7 the accretional foredune sequence is comparable to stage 1 foredune of Fig. 2.10 and high sediment supply system of Carter (1989). Whereas along transect 12, which is the southern limit of the West Sands dunes, the seaward face of the dunes comprise large quantities of mobile sand which are avalanche- or

slump- dominated and are covered by a very scarce vegetation cover. These are the stage 4 foredunes of Hesp (1988) and belong to the intermediate supply system of Carter, (1988).

The dune systems of the Tentsmuir coast do not fall within a single group of the Hesp (1988) classification and appear to span the intermediate to abundant supply grouping recognised by Carter (1988).

The foredune zone is the only active coastal dune form. All other forms are secondary dunes in the sequence which involve inland transfers of sediment and form. If there is abundant sand on the upper beach, the frontal dune is usually vegetated; the dunes show signs of recent growth in height and are possibly advancing seawards. Dune vegetation is vigorous and may contain pioneer species. Erosion forms are rare and slope angles tend to be low. In contrast, if sand supply is deficient or there is a change in the nature of wind or wave attack, the coastal edge becomes a steep dune cliff.

2.4.1 Beach-dune sediment characteristics

Sediment samples have been collected from the top 2 cm of the beach-dune surface across seven transects in the study area (Fig. 2.1). Representative samples (moist sand weighing approximately 250 gm) from the lower, middle and upper beach face and foredune areas were subjected to grain size analysis achieved by seiving the samples, following the procedure outlined by Folk (1974) and McManus (1989).

Sub - samples of 150 gm obtained by coning and quartering, were passed through a nest of seives at quarter phi intervals over a range of 2 to 0.16 mm. In all cases sieves were shaken mechanically for 20 minutes using a mechanical shaker. The results of the grain size distribution for the different transects are shown in Figs. 2.11-2.13. An example of the grain size analysis worksheet is shown in Appendix I-C. All recorded dry weights per sample were utilised to derive statistical measures (sorting, skewness and kurtosis) using the Folk & Ward (1957) and Trask (1939) formulae (Appendix I-D). The samples were further treated separately with hydrochloric acid (in excess of 20% by volume) and left overnight for the removal of calcium carbonate. The samples were then washed with distilled water, oven dried at 110^{0}C for 15 hours. The carbonate percentages have been included in Appendix I-E.

The beach-foredune sediment characteristics are shown in Table 2.2. The results for each of the transects are tabulated in Appendix I-E. Example of grain size frequency distributions are shown in Fig. 2.11, 2.12 and 2.13. In all cases the sediments are fine to medium grained sands.

Along transect 1 (Fig. 2.11), the lower beach face sediment size distribution is symmetrical to negatively skewed while the upper beach face sediments are positively skewed showing an abundance of finer sediments. Sediments of the upper beach face and foredune subenvironment are finer (2 ϕ) than those of the lower and middle beach face (1.6 ϕ and 1.9 ϕ) along transect 3 and 4 (Fig. 2.11).

Along transect 5 (Fig. 2.12), the middle beach face sediments are distinctly negatively skewed and leptokurtic in contrast to the lower beach face sediments which

Table 2.2 Average beach-dune sediment characteristics. (WS - well sorted; MS - moderately sorted; VWS - very well sorted; VNS - very negatively skewed; NS - negatively skewed; SYM - symmetrical; L - leptokurtic; VL - very leptokurtic; M - mesokutic; Coarse sand < 1ϕ, Medium sand 1 - 2ϕ., Fine sand > 2ϕ).

Location (Fig. 2.1)	Median ϕ	Mean ϕ	Dispersion		Skewness		Kurtosis	
Tayport								
Transect 1	1.89	1.86	0.38	WS	-0.08	NS	1.22	L
Tentsmuir Point								
Transect 3	2.1	1.9	0.39	WS	-0.12	NS	1.11	L
Transect 4	1.8	1.85	0.37	WS	-0.11	NS	1.07	M
Kinshaldy								
Transect 5	1.69	1.72	0.57	MWS	-0.21	NS	1.16	L
Transect 6	1.8	1.79	0.54	MWS	-0.3	NS	1.37	L
Transect 7	2.02	1.96	0.5	WS	-0.33	VNS	1.13	L
Transect 8	2.04	2.03	0.37	WS	-0.24	NS	1.54	VL
Earlshall								
Transect 9	2.06	2.04	0.28	VWS	-0.04	SYM	1.03	M
Transect 10	2.1	2.09	0.25	VWS	-0.11	NS	1.09	M
Leuchars								
Transect 11	2.04	2.05	0.42	WS	-0.3	NS	1.94	VL
Foredune Sediments	2.1	2.03	0.25	VWS	0.03	SYM	1.56	VL

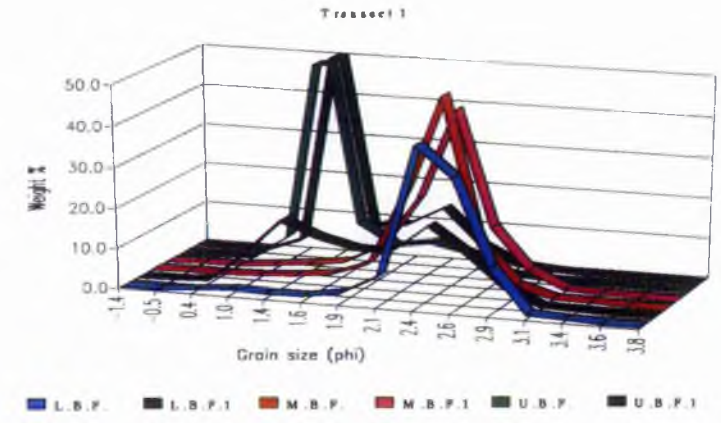

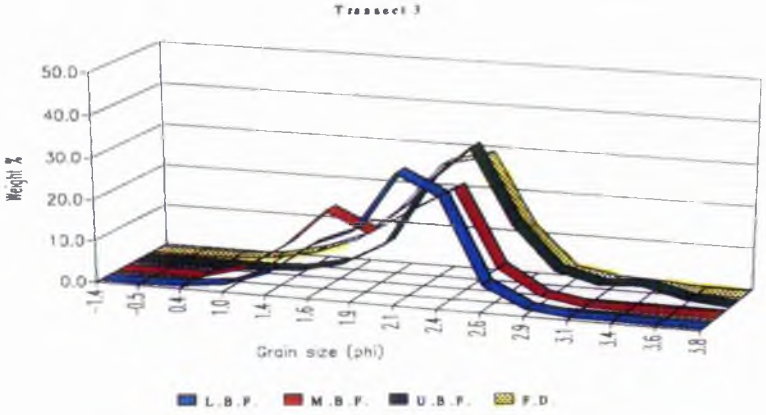

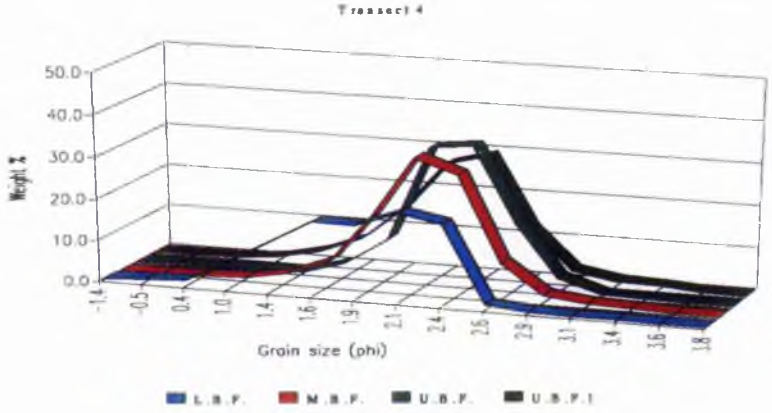

Fig. 2.11 Sediment size frequency distribution curves of Transect 1, 3 and 4. Transect 1: Lower beach face sediments are fine grained (2.2ϕ), while the upper beach face sediments are coarser (1.2ϕ). Sediments show a bimodal distribution in the lower and upper beach face. Transect 3 and 4: Sediments from upper beach face and fore dune are finer (2ϕ) than the lower and middle beach face (1.6ϕ & 1.9ϕ). M.B.F. sediment distribution show a distinct bimodality. (L.B.F - lower beach face; M.B.F. - middle beach face; U.B.F. - upper beach face; F.D. - fore dune.

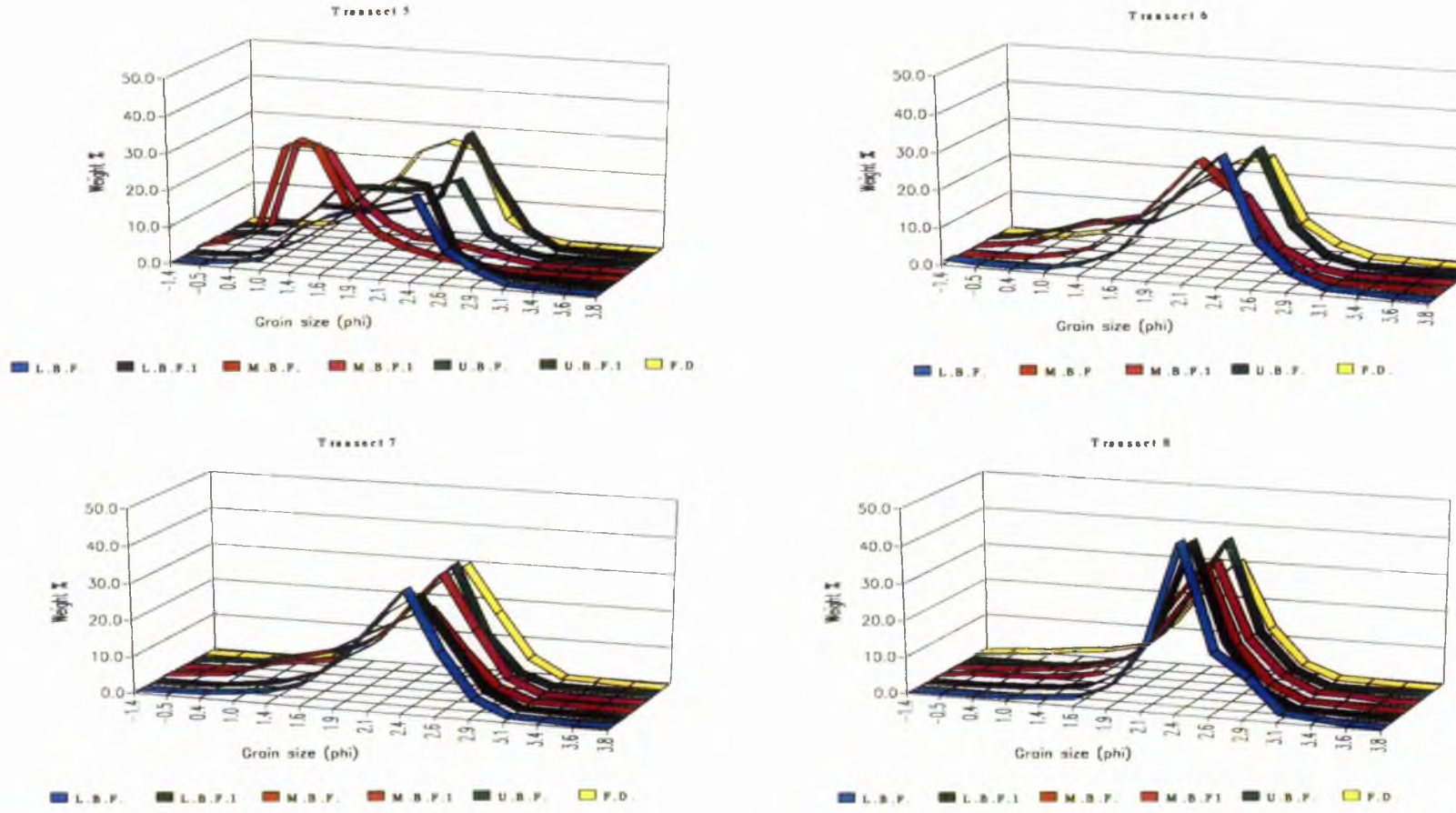

Fig. 2.12 Sediment size frequency distribution curves of Transect 5, 6, 7 and 8. Transect 5: Middle beach face sediments are distinctly negatively skewed and leptokurtic in contrast to the lower beach face sediments which are mesokurtic and symmetrically skewed. The upper beach face sediments are platykurtic and bimodal in distribution. The fore dune sediments are very negatively skewed and show mesokurtic curves. Transect 6: Middle beach face sediments have a wider grain size distribution. Sediment distribution curves of the lower and middle beach face are mesokurtic, while those of upper beach face and fore dune are leptokurtic. Transect 7: The sediment distribution curves have a wider distribution and are mesokurtic. Transect 8: Fine grained and very well sorted sediments showing leptokurtic frequency distribution curve. M.B.F. sediment distribution show a distinct bimodality. (L.B.F - lower beach face; M.B.F. - middle beach face; U.B.F. - upper beach face; F.D. - fore dune.

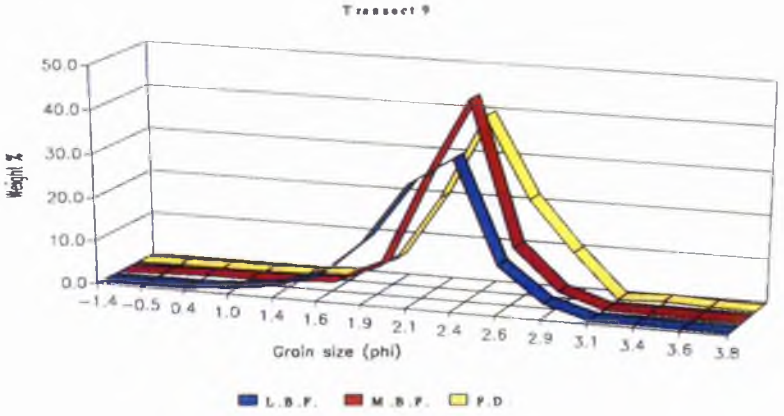

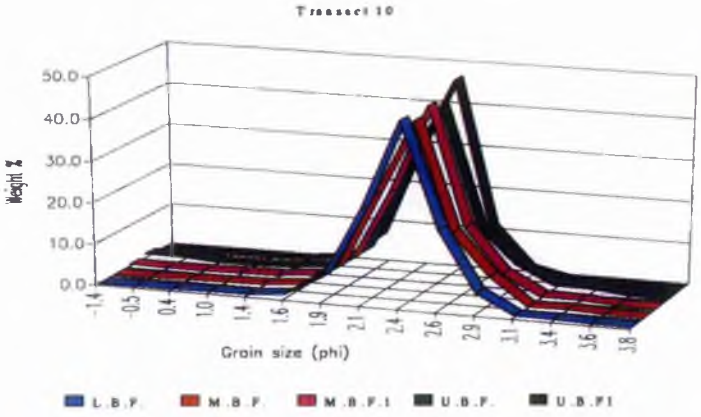

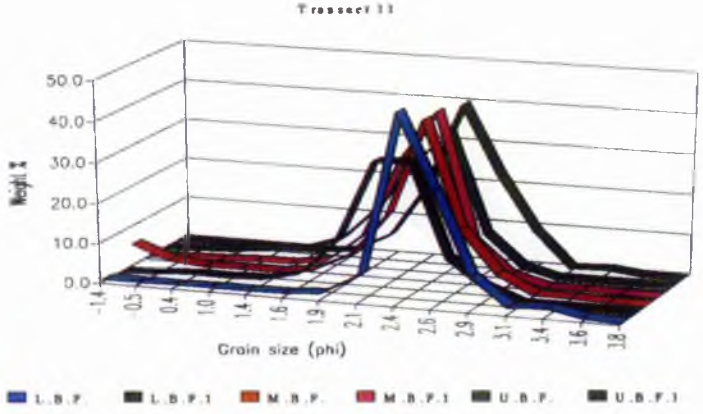

Fig. 2.13 Sediment size frequency distribution curves of Transect 9, 10 and 11. Transect 9: The L.B.F. sediment curve show mesokurtic distribution, flatter curve and has a wider grain size distribution in contrast to the M.B.F and F.D. Transect 10: Sediments from all the sites are fine to medium in size, very well sorted and leptokurtic. Transect 11: Sediments from L.B.F.1 are poorly sorted and the distribution shows a flat curve. The L.B.F. curve is tailing towards the right showing the abundance of finer sediments, while the sediments from U.B.F.1 has a wider distribution of grain size. (L.B.F - lower beach face; M.B.F. - middle beach face; U.B.F. - upper beach face; F.D. - fore dune.

are mesokurtic and symmetrically skewed. The upper beach face sediments are bimodal and platykurtic peaking at 1.2 ϕ and 2.2 ϕ respectively. The foredune sediments are negatively skewed (abundance of coarse sediments) and have a wider grain size distribution resulting in a mesokurtic curve.

Symmetrically to negatively skewed mesokurtic sediments are present along the lower beach face subenvironments along transect 6 (Fig. 2.12). The lower beach face sediments tend to have a wider spread of grain size distribution than the sediments of the middle and upper beach face, which are leptokurtic and negatively skewed. Along transect 7 (Fig. 2.12), except for the upper beach face and foredune sediments which are leptokurtic, the rest of the sediments (lower and middle beach face) have a mesokurtic distribution, although all the sediments are negatively skewed. Transect 8 (Fig. 2.12), comprises fine grained leptokurtic and very well sorted sediments.

The tendency towards a bimodal distribution decreases from transect 5 to transect 7 disappearing completely along transect 8 where the sediments are very well sorted and have a leptokurtic distribution.

The lower beach face sediments along transect 9 (Fig. 2.13) are mesokurtic while the middle beach face and foredune sediments are leptokurtic. The foredune sediments along most of the transects are very well sorted and are symmetrical to negatively skewed. In most cases the foredune sediment characteristics mimic the sediment characteristics of the source deposits i.e., the beach sands.

The beach sediments became coarser from Leuchars (median 2.1 ϕ) towards Tentsmuir (1.68 ϕ). The sediments generally are negatively to symmetrically skewed, leptokurtic and well sorted in the study area. This is due to the reworking of the sediments by waves and tides followed by aeolian activity during periods of beach exposure. The winnowing action of the waves and tides results in the formation of well sorted beach sediments. Negative skewness can be partly attributed to the deflationary activity of the wind during periods of beach exposure which removes the finer fractions.

2.4.2 Bivariate analysis

There have been numerous attempts to relate statistical parameters calculated from grain-size distribution to different environments of deposition (Stewart, 1958; Sly, 1977, 1978; Passega, 1957, 1964; Buller & McManus, 1972). The main idea is to enable recognition of environments in ancient sediments.

Skewness-kurtosis interrelationship has been used by Sly (1977, 1978) to distinguish mainly fine sediments from low (A,B,C,D) and high (E,F,G,H) energy environments (Fig. 2.14). The Tentsmuir sediments when plotted on the Sly (1977) diagrams, virtually all fall within the fields H and E (sediments of most active area) confirming the appropriateness of the method, for the beaches and dunes are certainly high energy environments.

In order to distinguish sediments from rivers, the wave dominant zone and quiet water environments, Stewart (1958) plotted median diameter (ϕ) against standard deviation. The sediments of the study area dominantly fall within the river and wave dominant envelopes suggested by Stewart (1958) (Fig. 2.15). However as beach samples plot in the river dominant envelope as well in the wave dominant area and the method does not appear very sensitive in depositional environment recognition.

The C.M. plot of Passega (1957, 1964), which uses the median diameter against the ratio of the coarsest one percentile (from cumulative frequency curves) of the sediment plot, showed that most of the sediments from the study area lie in the beach envelope (Fig. 2.16). The upper beach face sediments lay scattered across the beach envelope unlike the lower and middle beach face sediments which were mainly concentrated in the central portion of the beach envelope and bedload zone of fluvial transport, suggesting the role played by swash and backwash currents in their formation.

Trask's arithmetic measure of quartile deviation (QDa, in mm) against median diameter (mm) has been plotted by Buller and McManus (1972) on a double log paper. They found that plots of sediments from different environments vary in a linear fashion (Fig. 2.17). All the sediments (L.B.F., M.B.F.,U.B.F. & foredune) plot in the aeolian and wave dominant envelopes. Only 12% of the total sediments fall beyond any of the recognised limits of the plot (which were based on only 68% of all the samples

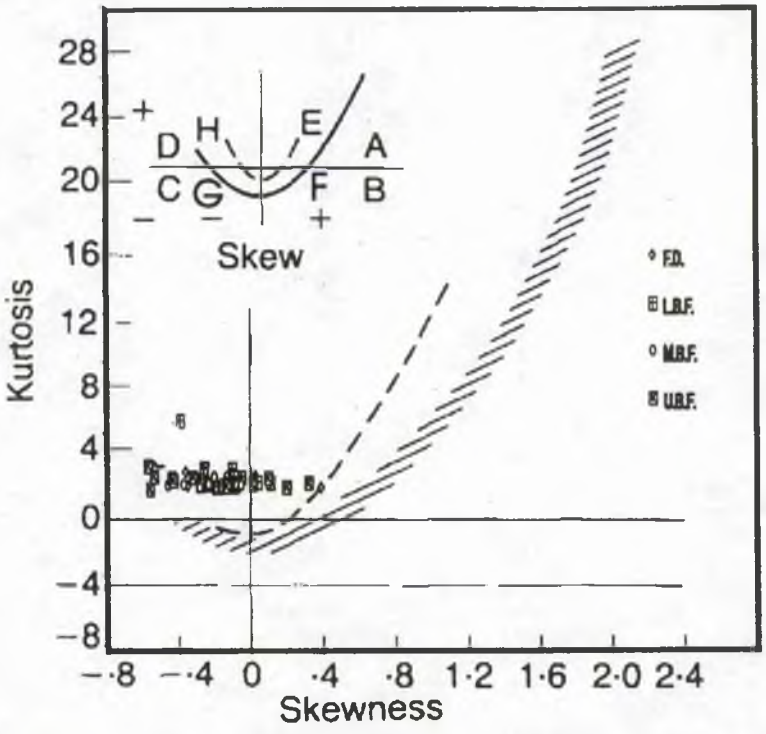

Fig. 2.14 Kurtosis - skewness Sly (1977) plot of sediments of beach-foredune samples from Tentsmuir platform. F.D. - foredune (incipient); U.B.F. - upper beach face; M.B.F. - middle beach face; L.B.F. - lower beach face. A,B,C,D - low energy environment; E,F,G,H - active environment.

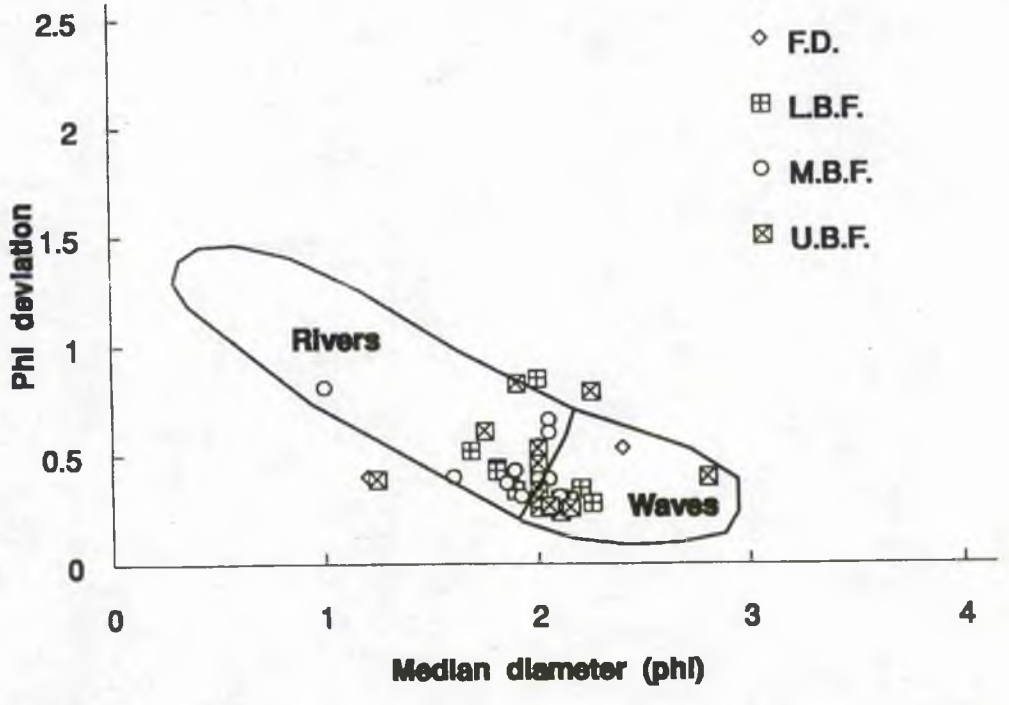

Fig. 2.15 Standard deviation - median diameter Stewart (1958) plot of sediments of beach - foredune surface samples from Tentsmuir platform. F.D. - foredune (incipient); U.B.F. - upper beach face; M.B.F. - middle beach face; L.B.F. - lower beach face. Since none of the samples plotted in the quiet water envelope it has not been drawn here.

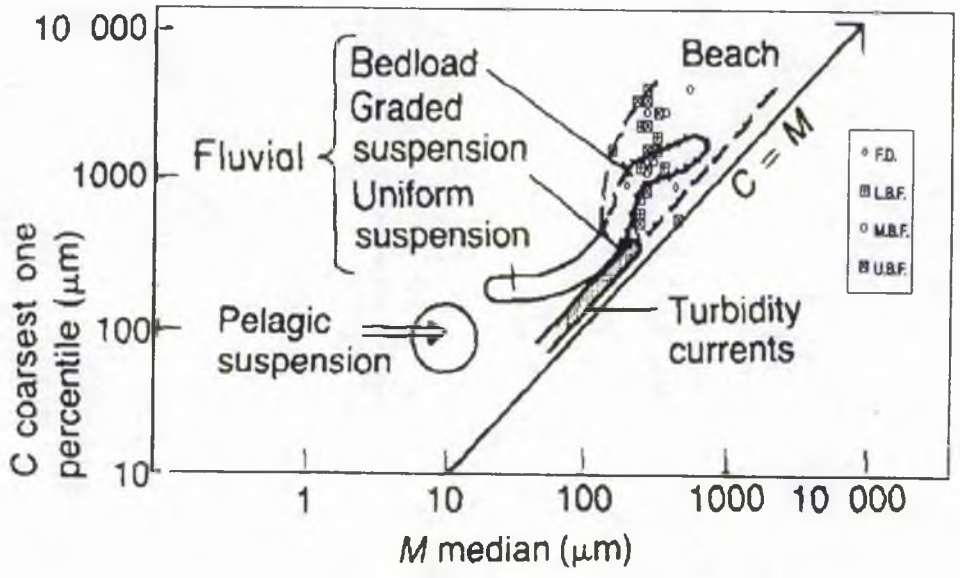

Fig. 2.16 Coarsest percentile - median diameter Passega (1964) plot of sediments of beach-foredune samples from Tentsmuir platform. F.D. - foredune (incipient); U.B.F. - upper beach face; M.B.F. - middle beach face; L.B.F. - lower beach face. Dashed curve represents the beach envelope.

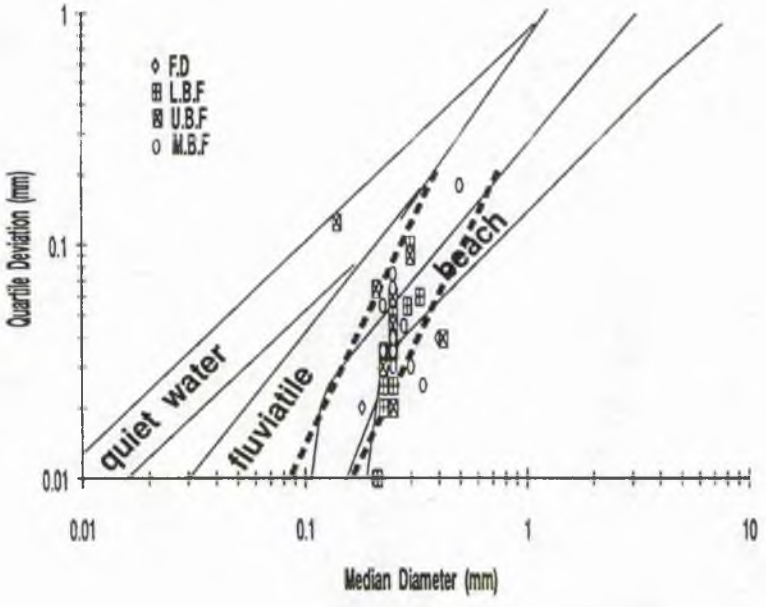

Fig. 2.17 Metric quartile-deviation - median diameter plot (Buller & McManus, 1972) of Tentsmuir sediments. F.D. - foredune (incipient); U.B.F. - upper beach face; M.B.F. - middle beach face; L.B.F. - lower beach face. Dashed line represents aeolian envelope.

analysed).

This suggests that the aeolian and wave processes dominate sediment deposition along the Tentsmuir coastline, and adds to the validity of the plot. The foredune sediments have been derived from the adjacent wave dominated environment. Since, the distance of transport is very small (av. 200 m) these sediments show similar sediment characteristics to those of the source area. However, where there is little variation in average grain size multiple discriminant analysis does not clearly discriminate between sedimentary environments (e.g. Thomas, 1987). This may be due to local reworking and mixing of sediments and in other instances the source sediment characteristics exert a strong influence on the properties of other sediments derived from them (Pye & Tsoar, 1990).

2.5 DISCUSSION & CONCLUSIONS

The shoreline of the Tentsmuir platform is an admixture of areas of foredune progradation (Tentsmuir Point, Kinshaldy & Earlshall) and cliff erosion (Tentsmuir). The West-Sands beach is neither prograding nor retreating but is in the recovery stage from an earlier erosional cycle. At Leuchars, foredune development is retarded due to the influence of the Eden estuary tidal waters through a small tidal inlet running northwards along the backshore. The presence of a shell pavement further reduces the inland transfer of sand for the development of foredunes in the area. A salt marsh is present north of Leuchars airfield along the southern limit of Earlshall. The Leuchars shelly sand banks-spit-salt marsh complex has many characteristics of a juvenile chenier plain.

Blowout activity is common along the northern edge of Tentsmuir Point, further south at Tentsmuir and West Sands. Blowouts often give a good indication of the direction and possible severity of wind erosion. Initial gaps in the foredune line often remain as wind corridors, and in time as the dune grows to either side of them, assume the characteristics of blowouts (Carter, 1988). As observed by Carter (*op. cit.*) at Magilligan Point in Ireland, these gaps allow small volumes of blown sand to pass inland. During offshore winds sediments are blown back to the beach and the exchange is quite rapid, as the sediments form a loose veneer of dry sand which can

be returned quickly to the foredunes. However, that the magnitude of sand volumes blown offshore is unknown.

Study of aerial photographs suggest that shoreline progradation at Tentsmuir Point during the last ten years has been continuing at a discontinuous rate of 3 ma^{-1}. A similar condition exists at Magilligan Point in Ireland, where the average growth rate of the foredunes varies between 6 and 9 $m^3m^{-1}a^{-1}$ (Carter, 1990).

The foredune progradation can be attributed to the presence of the giant offshore sand bars which encompass a large sediment volume and provide a sheltering effect to the wave and tidal attack on the shoreline. The net annual potential sediment transport pathways studied by Sarrikostis (1986) and Boalch (1988) predict a northward sediment transport along the Fife coastline from Fife Ness, with deposition occurring at the Pilmour Spit (Fig. 2.1). Further transport of sediments occurs along Tentsmuir beach, with deposition taking place on the leeward face of Abertay Sands. This results in abundance of sediments in the nearshore sand banks which are later transported on to the beach by waves and tides. Longshore marine sediment transport and further redistribution of the beach sediments by wind is the mechanism of foredune accretion at Tentsmuir Point.

Of the transects studied, Tentsmuir Point and Kinshaldy are undergoing rapid foredune accretion and exhibit stage 1 foredunes of Short (1988). The dunes at West Sands have a low vegetation cover and numerous blowouts and confirm to a higher order of foredune maturity i.e. stage 4 of the Short (1988) foredune classification.

The Leuchars juvenile 'chenier' is formed as a result of episodic wave reworking of the Eden estuary tidal flats, leading to erosion of the upper position of the flats which causes winnowing and shoreward reworking and deposition of the coarser shell material. Characteristically 'cheniers' are wave deposited linear shelly sand ridges, deposited on top of and separated by swales composed of finer sediments (Short, 1987). The 'cheniers' occur in areas removed from direct ocean wave attack, where fine sediments have prograded as inter-tidal flats, vegetated by mangroves (Short, 1987).

Vegetation is the best single index of dune stability and growth. Incipient foredune accumulation along the backshore is initiated by deposition of sand in the

lee of the tufts of pioneer vegetation species e.g. *Elymus farctus* and *Cakile maritima.* Subsequent vertical and lateral accretion of the foredune ridge takes place due to the stabilising effect of *Ammophila arenaria* growth.

Surveys along the three transects of Tentsmuir, Kinshaldy and Leuchars during July, 1990 show that the beach profiles are steeper in the north but have lower gradients as we move southwards. Net vertical aggradation in the swales and lateral migration of the intervening ridges constitute the daily variations along the beach profiles. These profiles are a result of summer swells and overtopping processes prevalent during the period.

The sediments are fine to medium grained sand and become progressively coarser from south (Leuchars) to north (Tentsmuir Point). The sediments are very well sorted and mostly leptokurtic. However, bimodal platy-mesokurtic medium grained well sorted sediments are found at Tentsmuir and in the Tentsmuir Point area. Bivariate analysis of the grain size variables was unsuccessful in delineating upper, middle, lower beach face and foredune subenvironments. Eighty eight percent of the sediment sample distribution from the study area plotted in the wave and aeolian environment envelopes of the Buller & McManus (1972) plot.

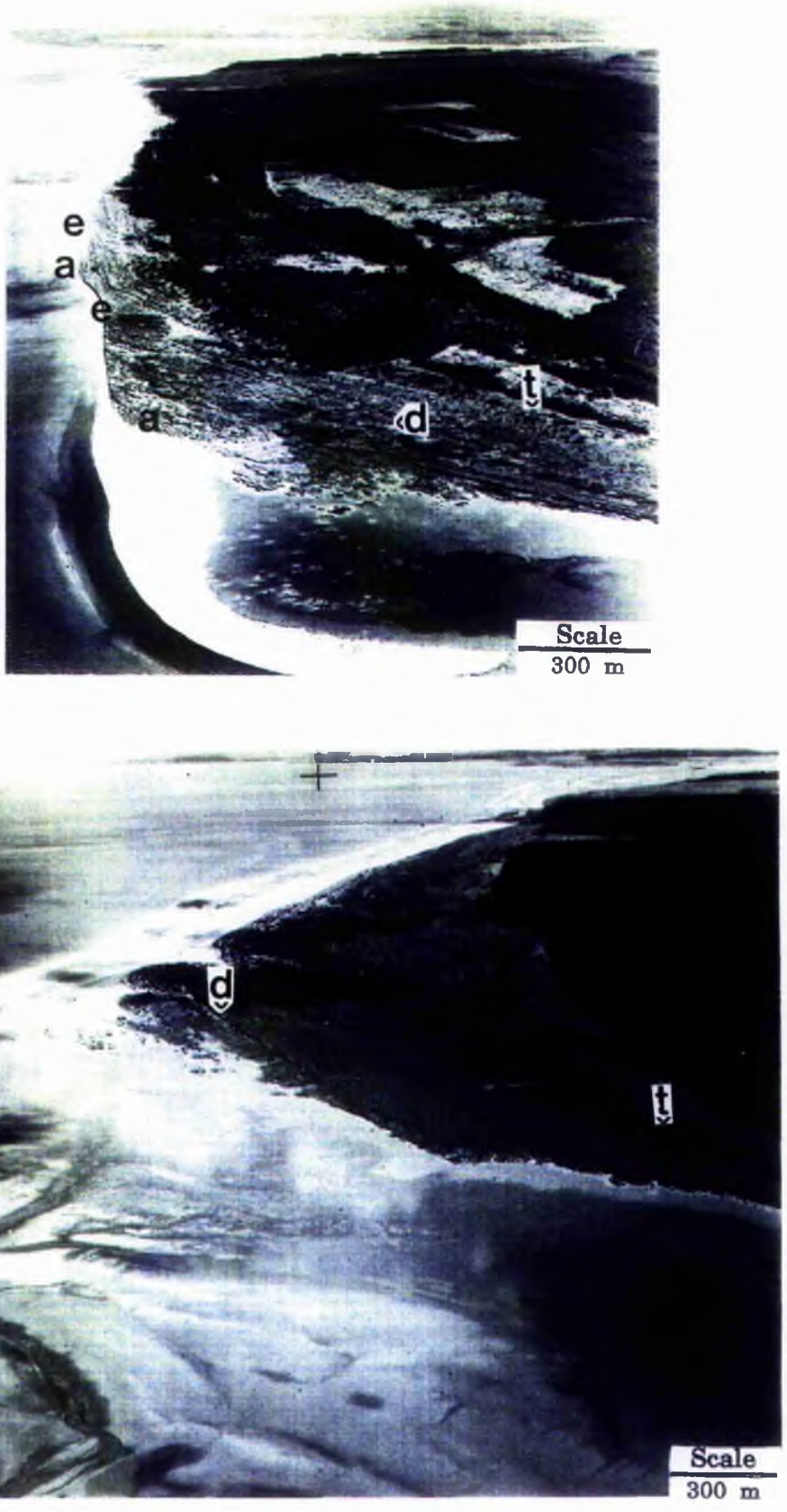

Plate 2.1 Oblique aerial photos of 1972 (above) showing areas of accretion (a) and erosion (e) along the Tentsmuir shoreline. Comparison of the 1950 oblique aerial photo (below) with the 1972 (above) shows the magnitude of accretion at Tentsmuir Point. The line of anti-tank blocks (t) and the defence dune (d) have been shown to facilitate comparison. Zone 1 and Zone 2 of Fig. 2.3 are also marked.

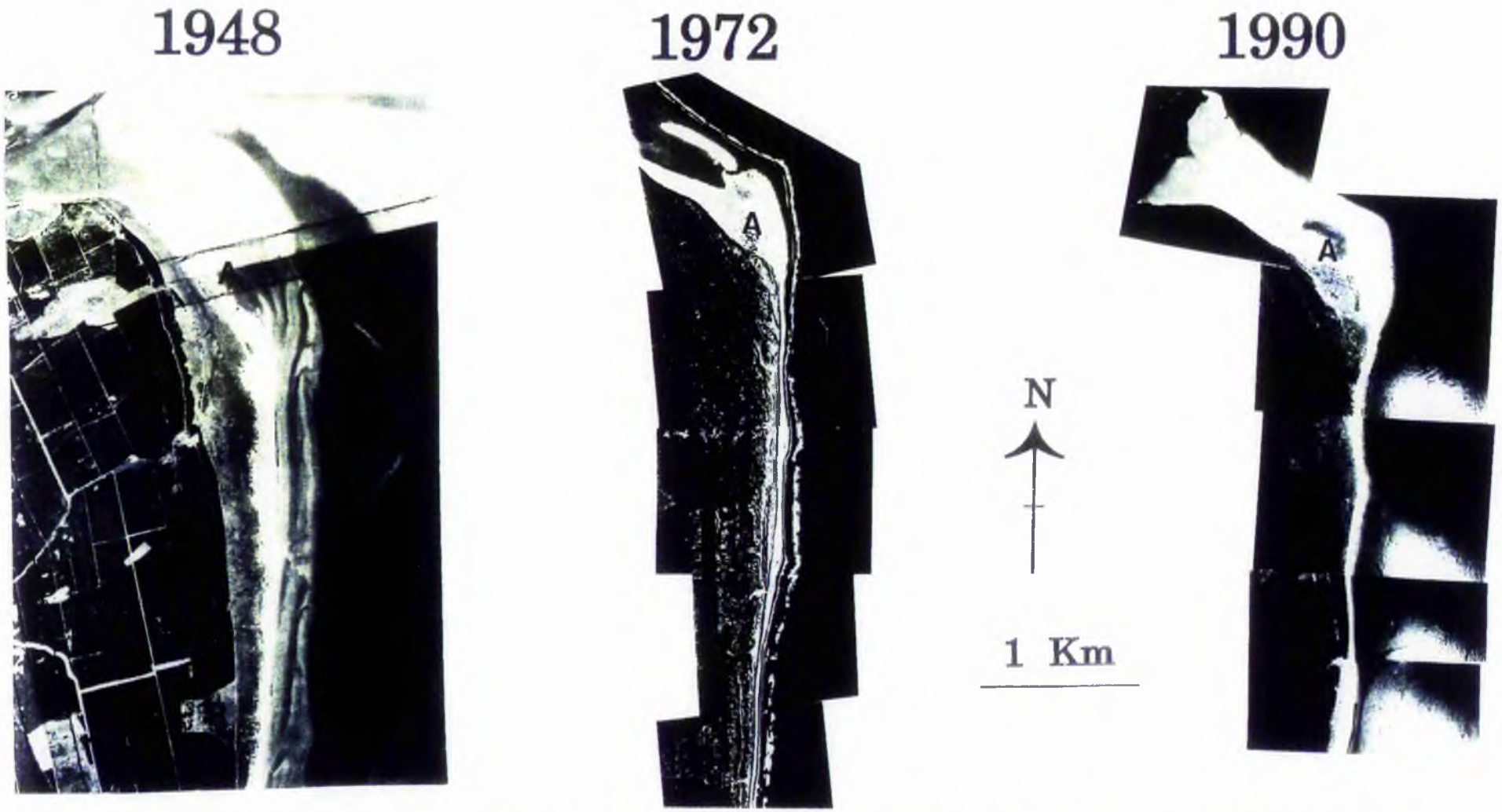

Plate 2.2 Successive shoreline changes 1948 - 1990 along part of Tentsmuir shoreline (up to Kinshaldy). Area marked 'A' (1948 aerial) has been a site of spectacular shoreline change. Kidney-plan aeolian deposit seen in area A of the 1990 aerial. A portion of the Abertay offshore sand bar complex is seen in the top right corner of the 1948 aerial. r - rifle range at Kinshaldy. Photo courtesy: Nature, Conservancy Council, Cupar.

Plate 2.3 End of an artificial dune ridge formation on an antecedent linear defence structure showing part of a cork mooring buoy. (site F on Fig. 2.2). *Epilobium sp.* and *Ammophila sp.* are seen flourishing in this area.

Plate 2.4 Transect AA' - A 1978 triangular plan deposit (vertical arrow mark) dissected by present day inactive tidal channels (curved arrow). Inset shows the same view in 1984 when the channels became active during high tide.

Plate 2.5 BB' - Tidal channel 1962 is seen in the form of a curved depression indicated by an arrow. To the left of the channel are seen the rectangular remnants of the rabbit enclosures. The forest edge and the anti tank blocks (1941) are also seen.

Plate 2.6 CC' - View of a dune slack which is dry at present. Inset shows the same view in 1984 when the slack was flooded. Arrow mark shows the dune ridge profile in the background.

Plate 2.7 Transect DD' - Post 1978 blowout (arrow) leading to the separation of the NW-SE trending 1978 dune accumulation (south of the blowout) from the 1990 isolated 500 m long *Ammophila arenaria* covered kidney-plan aeolian accumulation (north of the blowout). During the last two years (1990-1992) the blowout has been partially colonised by incipient shadow dune accumulations growing in the lee of *Elymus farctus*.

Plate 2.8 Photograph showing a 1.8 m deep blowout within the Tentsmuir dunes formed as a result of a heavy storm during May 1992. Arrow shows the scouring action of the wind exposing the internal bedding. Also seen are the sand flow structures along the instable slope. The sand scoured from the trough has been deposited on the adjacent topography.

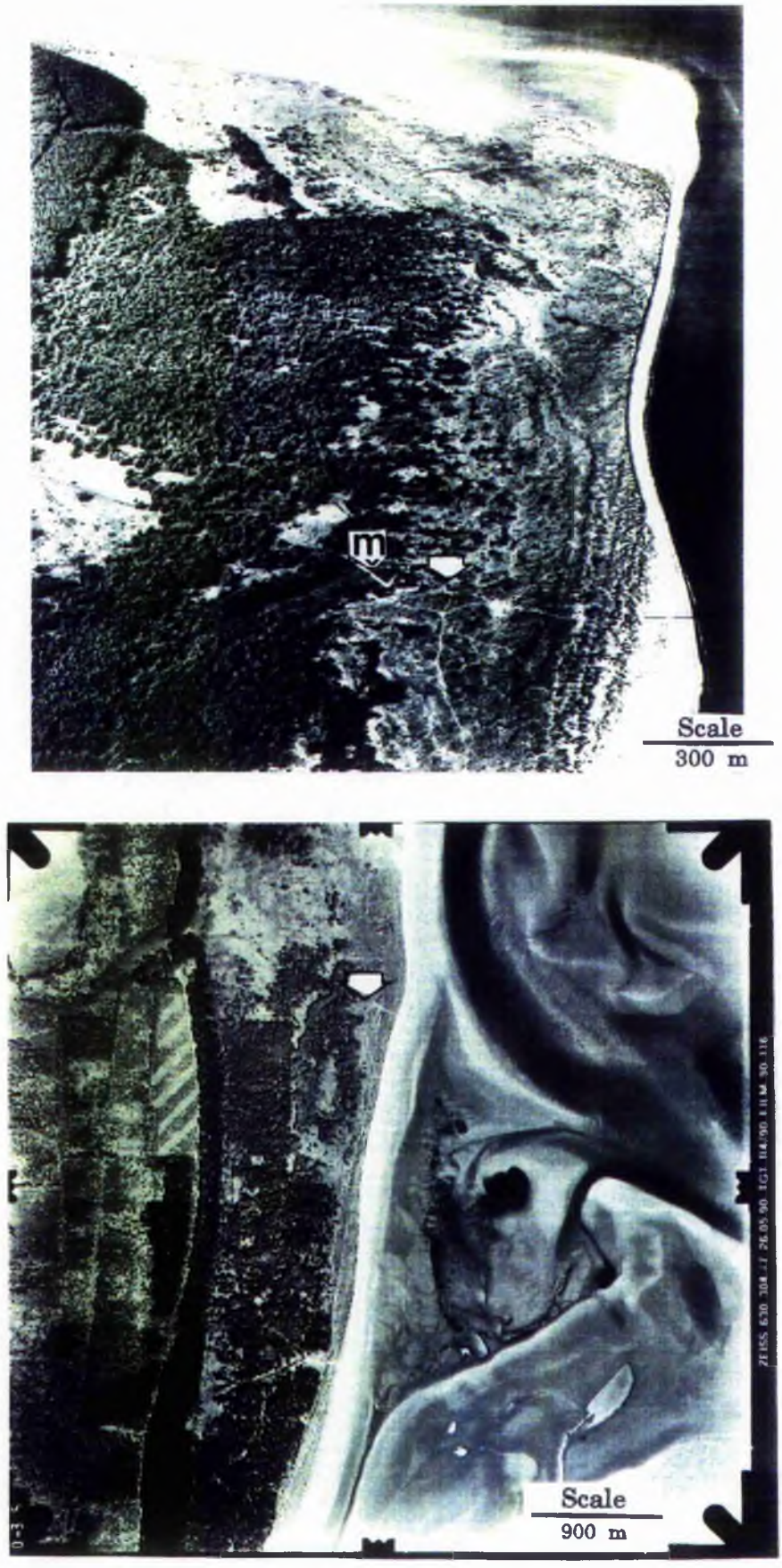

Plate 2.9 Comparison of the 1972 oblique aerial photograph with the 1990 aerial photo to show the magnitude of erosion opposite the M.O.D. arrow mark in Zone 2 (Fig. 2.3) along the Tentsmuir shoreline. Arrow mark shows the position of the observation tower. 'm' is the M.O.D. arrow mark in 1972 aerial and is not visible on the 1990 aerial photograph due to the dense vegetation canopy.

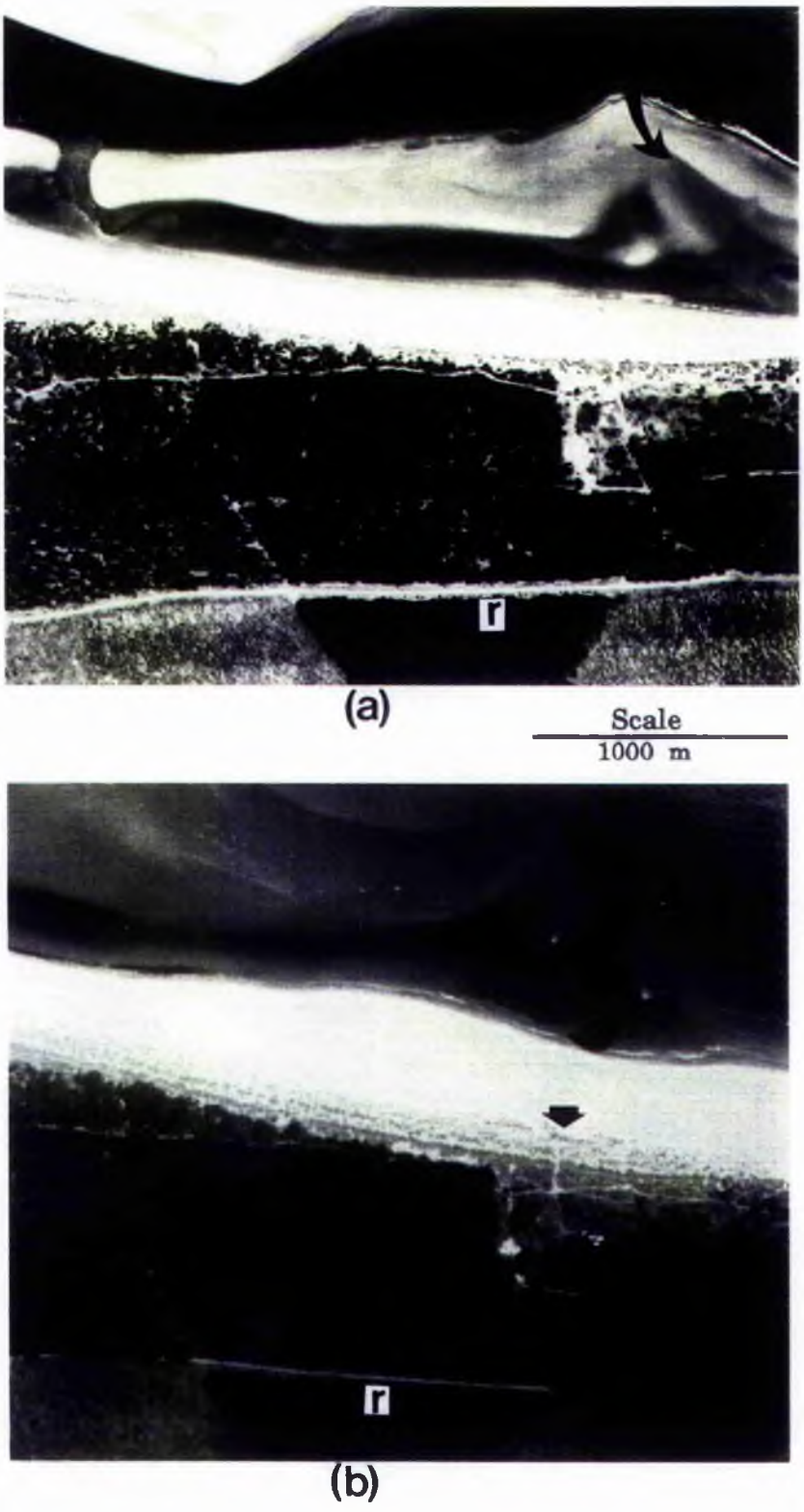

Plate 2.10 (a) 1984 Aerial photograph of the rifle range area (r). Note the prominent offshore sand bar lying detached from the eroding shoreline with a narrow beach (no foredune development). (b) 1990 Aerial of the same as above. The offshore bar has now welded onto the beach thereby increasing the beach width. Approximately three ridges of foredunes are now seen in the lee of the beach.

Plate 2.11 Tentsmuir Point beach-foredune morphology. 19 m wide rapidly accreting *Ammophila arenaria* dominated foredune in the lee of 189 m wide beach

Plate 2.12 Scarped shoreline with a narrow beach and no foredune development at Tentsmuir.

Plate 2.13 Moderate gradient Kinshaldy beach with a 10 m wide foredune

Plate 2.14 Very wide 400m wide shelly beach at Leuchars with no foredune development

Plate 2.15 West Sands beach-dune morphology. 250 m wide beach with blowouts (mobile sand, arrow mark) in the lee of a primary erosional dune ridge.

Chapter 3

PRINCIPLES OF AEOLIAN SEDIMENT TRANSPORT: THEORY AND MEASUREMENT

(with 7 figures)

Chapter 3

Principles Of Aeolian Sediment Transport: Theory And Measurement

3.1 INTRODUCTION

The aim of this chapter is to review literature dealing with the fundamental principles of aeolian sand transport, including many publications which have made significant contributions to our understanding of aeolian sand movement. The review is intended to provide a background of theory upon which both the experimental field programme for the calculation of aeolian sand transport rates on the beach and the subsequent development of an aeolian sand transport model are based.

Although, the research surrounding the phenomena of aeolian sand transport has been varied and extensive during the past decade, we still continue to derive our fundamental knowledge of wind blown sand from the pioneer work of Brigadier R.A.S. Bagnold, 'The physics of blown sand and desert dunes' (Bagnold, 1941). From the 'dust bowl' years of the 1930s, when Chepil and his associates explained the mechanics of soil erosion by wind in the United States, the *modus operandi* of aeolian sand transport research has been one of modification and refinement of the Bagnold concept.

3.2 THE SURFACE WIND

Wind is the motion of the atmosphere relative to the earth's surface, it is caused by variations in solar heating from one point to another and by variation in the reflection and absorption of the solar radiation. In contrast to the general circulation of the atmosphere, as being relatively independent of the surface, except for very large features as mountain ranges and oceans, winds close to the surface can be greatly effected by small scale features such as trees or boulders. The part of the atmosphere

which is significantly affected by the direct influence of the surface is called the **atmospheric boundary layer**. The boundary layer is of the order of 1 km in thickness, and it is the characteristics of this layer which govern sand transport by wind (Greely, 1985).

Wind blowing across a planetary surface has the potential for directly eroding material and redistributing it to other areas. However most aeolian erosion occurs through abrasion caused by wind borne particles of sand size or smaller. The most important factor of aeolian processes is the threshold wind speed or the minimum speed required to mobilise particles of different sizes, densities and shapes. The ability of wind to attain threshold is a function of atmospheric density, viscosity, composition, and temperature (Iversen *et. al*, 1976a)

3.3 ATMOSPHERIC FLOW IN THE BOUNDARY LAYER

Without going into the detail of derivation of the equations stated for flow in the atmospheric boundary layer an attempt is made to define the various parameters and basic equations relating to natural flows involved in aeolian processes. The movement of sand by wind results from momentum transfer from the air to the sediment. The shear stress (τ)[1] imparted to the surface by the air flow resulting in a net downward flow of momentum is given by:

$$\tau = \rho u_*^2 \qquad 3.1$$

where ρ is the air density (1.22×10^{-6} kg m^{-3}), and u_* is shear velocity. For turbulent flow, momentum transfer depends on the aerodynamic roughness of the surface, and is proportional to the change in velocity with height.

3.3.1 Variation of wind velocity with height

According to the Von Karman - Prandtl logarithmic velocity profile law, valid in the lowest zone of the boundary layer, over an aerodynamically rough surface, the logarithmic velocity profile (Fig. 3.1) is given by

$$u = (u_* / k) \ln [(z - h)/z_o] \qquad 3.2$$

[1]list of symbols shown in Appendix II.

where u is the time averaged wind speed, u_* is the shear velocity which is a measure of shear stress, k is the von Karman universal constant for turbulent flow and has an empirically determined value ranging from 0.33 to 0.41. z is the distance above the surface, z_o is the surface roughness height and h is the displacement height (the aerodynamic boundary, usually assumed to be at the sand surface). For unvegetated surfaces the displacement height is small relative to the surface roughness length. In areas where tall vegetation of height h_v covers the surface, the datum surface of zero height h cannot be taken at ground level. The value of h depends on h_v and the spacing of the canopy. Generally, it is between $0.6h_v$ and $0.8h_v$ (Pye & Tsoar, 1990). Empirical determination of u_* (shear velocity, otherwise known as friction velocity or wind shear) (Horikawa, 1987) is achieved by plotting the vertical distribution of wind speed data against height on semi-log arithmetic paper and drawing straight lines through them. From the straight line, the wind speeds at the heights of 10 cm (u_{10}) and 1 cm (u_1) are read. The shear velocity can be calculated using the expression (Horikawa, 1987):

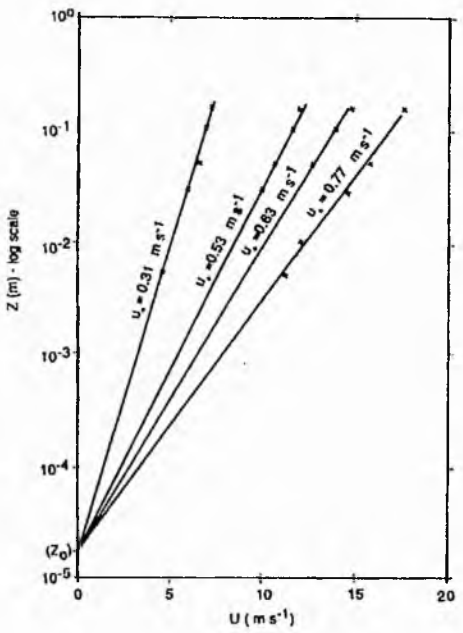

Fig. 3.1 Wind velocity profiles measured over a fixed surface (from Bagnold, 1941).

$$u_* = (u_{10} - u_1)/5.75 \qquad 3.3$$

The parameter z_o is calculated by plotting the measured wind velocity profile (when there is no sand movement) above the ground surface on a semi-logarithmic paper and obtaining the intercept of the profile with the height (z) ordinate at zero wind velocity.

The threshold shear velocity i.e. the shear velocity at the threshold of sand movement, according to Bagnold (1941) is a function of the shear stress measured in terms of the change in velocity with height above the bed surface. Bagnold (1941)

defined the threshold shear velocity (u_{*t}) in a form derived from the Sheild's (1936) threshold criterion, where the threshold velocity is a function of grain size and the immersed weight of the grains:

$$u_{*t} \quad A[(\rho_s' \rho)gd]^{1/2} \qquad 3.4$$

where A is a dimensionless coefficient, ρ_s' is the density of sand and d the grain diameter. On simplification, the threshold friction velocity for quartz sand grains larger than 0.25 mm in air can be written as (Pye & Tsoar, 1990):

$$u_{*t} = 146\, d^{1/2} \qquad 3.5$$

3.3.2 Wind profile modification during sand movement

Experiments conducted both in the field and wind tunnel (Chepil & Milne, 1941; Horikawa & Shen, 1960; Belly, 1964; Hsu, 1973; Ungar & Haff, 1987) have revealed that whereas wind velocity gradients over a stable sand surface converge at a point (z_0) just above the ground surface (Fig. 3.1), those measured during active sand movement converge at a higher focal point z' above the surface (Fig. 3.2). As a result of the drag on the wind caused by moving grains there is a shift in the wind velocity profile. Hence Bagnold (1936) rewrote the logarithmic wind velocity equation for wind shears over stable surfaces for a saltating flow as

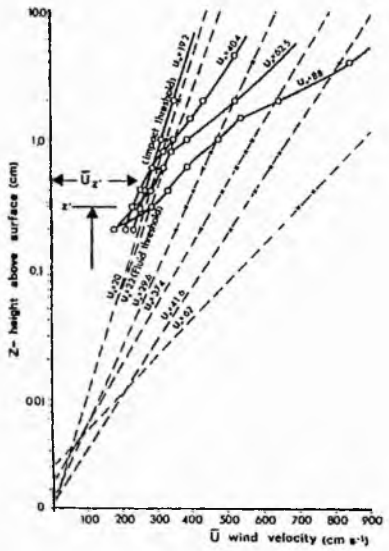

Fig. 3.2 Wind velocity profiles measured by Bagnold (1936) over a bed of 0.25 mm uniform sand with (solid lines) and without (dashed lines) sand movement.

$$u \quad 5.75\, u_*' \ln (z z') \cdot u_z' \qquad 3.6$$

where u_*' is the shear velocity for saltating flows, and z is height. Bagnold (1941) considered that the height z' was related to the ripple height, while Zingg (1953) and White & Schultz (1977) suggest that it is a function of the grain diameter. Evidence suggests that the ripple wavelength and height are related to grain size, through the

characteristic length and height of the saltation jump (Sharp, 1963; Ellwood, *et al*, 1975) it seems likely that both the hypotheses are correct.

Empirical determination of z' and u_z' is specifically important as these are the critical parameters which govern the calculation of u_*' from the velocity at any one given height above the surface. The determination of the focal point (u_z', z') has immense practical use as it links the shear velocity to the wind speed at an arbitrary height. This is one of the most fundamental relationships in understanding sediment transport (Sherman & Hotta, 1990). Considerable scatter, and the problem of the inability to quantify surface roughness height and focal point data exists among various workers (Svasek & Terwindt, 1974; Letteau & Letteau, 1978; Sarre, 1988, Gerety & Slingerland, 1983). On analysing this problem, Horikawa *et al*, (1986) concluded that Zingg's formulas (Zingg, 1953) to calculate the roughness height and focal point are acceptable for engineering purposes, although further study is needed requiring more accurate measurement instruments for the determination of wind speed and sand transport.

3.3.3 Initiation of sediment movement

The fluid forces of lift and drag operate to move the grain upward and downwind. Various forces acting on a grain are shown in Fig. 3.3. The forces opposing the motion are due to gravity and partially due to cohesive agents (e.g. surface moisture). The total drag force acting on the grain is the product of the surface shear stress, the grain's projected area and the friction velocity. The pressure drag results from positive pressure on the upwind side and negative pressure on the particle's downwind side. The drag force results from the force of the air against the exposed

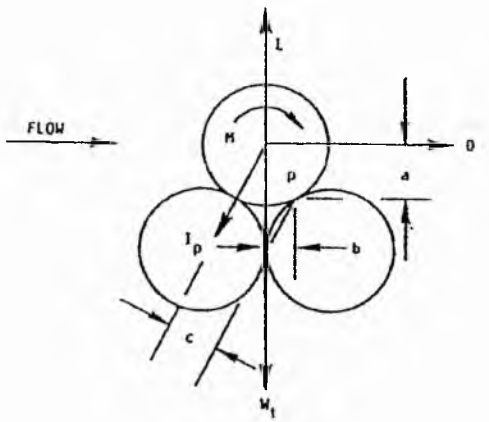

Fig. 3.3. Schematic diagram of an erodible spherical particle resting on other light particles. Forces include aerodynamic drag, D, lift, L, moment, M, interparticle force, I_p, and weight, W.

areas of the grain, and is a function of wind speed and aerodynamic roughness. In addition to drag force, another force tending to dislodge the grain is the lift force. The lift force arises as a consequence of the high wind velocity gradient near the bed which creates a high static pressure under the grain and a lower pressure on top. This Bernoulli effect and the consequent aerodynamic thrust causes a lift on the grain (Jefferys, 1929, Chepil, 1959). Wind flowing over a sand grain thus exerts a horizontal drag force D, a vertical lift force L and opposing these aerodynamic forces are inertial forces such as the grain's weight W, and moment M, in addition to the cohesive forces I_c acting in between neighboring grains, and the adhesive forces I_a acting in between the grains and a surface. At threshold the particle forces are assumed to be in equilibrium at point p. The grain will be entrained if the drag and lift forces, resulting from static pressure difference, exceed the inertial forces acting on the grain.

3.3.4 Initial particle motion

The wind speed at which sand movement starts, due to the direct pressure of the fluid was called fluid threshold (Fig. 3.4) by Bagnold (1941). These moving sand grains initiate movement of other grains on the bed which can be sustained at a wind velocity below the fluid threshold velocity. This lower threshold velocity was termed the impact threshold velocity by Bagnold (1941). He recognised that the initial motion of surface grains, previously at rest as occurring when the friction velocity u_* ranged from 20-44 cm s^{-1} (Lylles & Krauss 1971; Chepil 1959; Zingg 1953; Bagnold 1943). This corresponds to a surface drag of 0.48 to 1.94 dynes cm^{-2}. The wind speed observed during initial

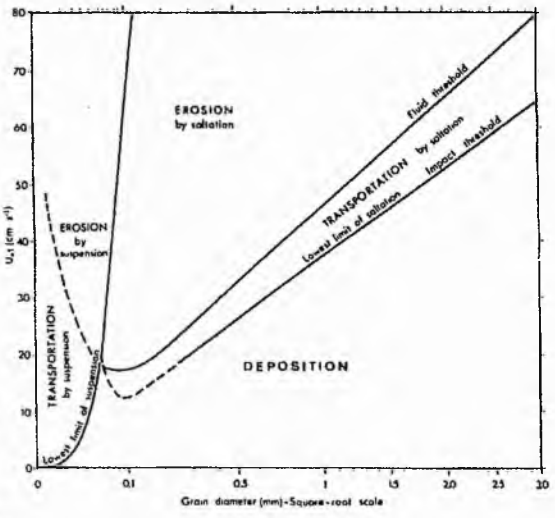

Fig. 3.4 Variation of fluid threshold velocity and the impact threshold velocity with grain size (data from Bagnold, 1941; Chepil, 1945b).

particle movement is from 4.0 to 5.8 ms^{-1} at 30cm (Chepil 1945, Malina 1941). Bagnold recorded that in the initial motion surface grains, previously at rest began to be rolled along the surface by the direct pressure of the wind "...A foot or so downwind of the point at which the rolling began, the grains could be seen to have gathered sufficient speed to start bouncing off the ground." Direct observation at a limited range of wind speeds of grain behaviour near the upwind edge of a sand deposit in a wind tunnel using high speed films show that disturbed grains usually, but not always, roll before taking off into reptation or saltation (Willetts *et al*, 1991). Others observed that as the fluid threshold was approached, some particles began to vibrate, or rock back and forth (Bisal & Neilsen, 1962; Lyles & Krauss, 1971). The erosive particles vibrated with increasing intensity as wind speed increased and then left the surface instantaneously as if ejected. Evidence supported the hypothesis that particle vibration frequency is related to the frequency band containing the maximum energy of the turbulent motion.

3.4 MODES OF AEOLIAN SAND TRANSPORT

Three distinct, nevertheless inter-related modes of particle transport are identified- saltation, creep and suspension. Grains moving very close to the surface i.e. by saltation or creep constitute the bed load. The different modes are defined by wind velocity and grain size (Fig. 3.5).

3.4.1 Creep

The rolling or sliding of larger particles (0.5 to 1.0 mm) with energy derived from the saltating particles is

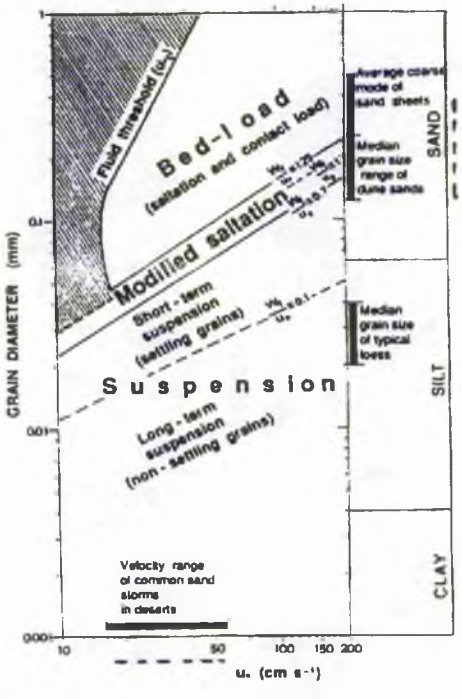

Fig. 3.5 Modes of transport of quartz spheres at different wind shear velocities (after Tsoar & Pye, 1987). Data from the study area is indicated by a dashed line.

called creep (Fig. 3.6a and b). Individual grains are knocked onward and are displaced laterally without loosing contact with the surface, by the blow they receive from behind. The term reptation includes the various small scale transitional movements of such grains (Pye & Tsoar, 1990). Bagnold (1941) observed that at low wind speeds the grains move in jerks a few mm at each time, but as wind speed increases, the distance moved lengthens and more grains are set in continuous motion until in high winds the whole surface appears to be creeping forward.

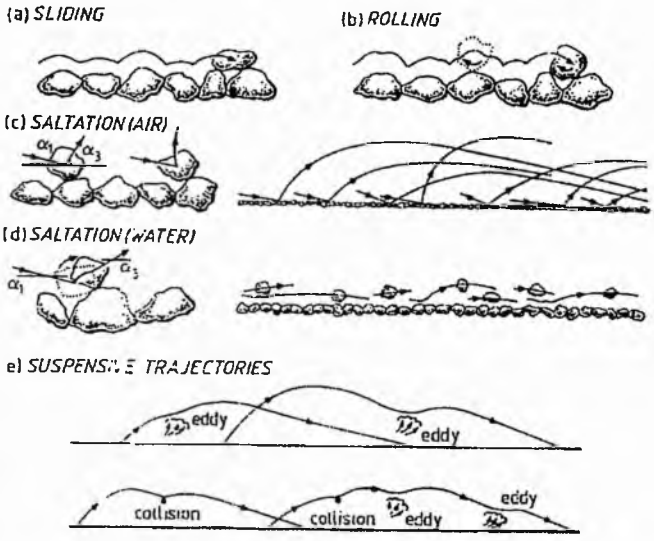

Fig. 3.6 Modes of sediment transport (after Allen, 1984).

The difference in the rate of movement between grains in saltation and grains in surface creep are of the order of 200-400 times (Pye & Tsoar, 1990). Nevertheless field and wind tunnel measurements indicate that surface creep represents about one quarter of the total transport (Bagnold, 1938 ; Willetts & Rice, 1985).

3.4.2 Saltation

The bouncing or ejection of an eroding particle off the bed surface into the air stream and its subsequent forward movement is referred to as saltation (Latin, *saltare*, to dance) (Fig. 3.6c). Between 50% and 75% of the movement of soil particles takes place through saltation (Chepil 1945a). Inter - saltation collisions are the most important mechanism needed to sustain transport of sand grains once the transport process is established (Bagnold, 1941; Rumpel, 1985; Mitha *et. al,* 1986; Willetts & Rice, 1986). During saltation the particles rise almost vertically, rotating from 20 to 1000 revolutions per second, travel 10-15 times the height of rise, and return to the surface with an angle of descent of about 6-12 degrees from the horizontal (Chepil &

Woodruff 1963). On striking the surface they either rebound and continue their movement in saltation or impart most of their energy by striking other grains, causing these to rise upward or roll along the surface. Most of the saltating particles range in size from 0.1 - 0.5 mm.

3.4.2.1 The saltation trajectory- the characteristic path

Bagnold tried to quantify saltation more effectively by developing the concept of a characteristic grain path (Fig. 3.7). The characteristic ballistic trajectory of saltating grains in air was demonstrated photographically by Bagnold (1936) and subsequently by Chepil (1945b) and Zingg (1953). Bagnold concluded that the ripples are a physical manifestation of the characteristic path length, just as the wind profile irregularities are a manifestation of the characteristic height. Theoretical calculations by Owen (1980) indicate the mean saltation height is given by 0.82 u_*/g and the mean saltation path length by 10.3 u_*^2/g. He found that the horizontal distance travelled during saltation was approximately 12 times the mean maximum jump height. However, Gerety and Slingerland (1983) concluded that Bagnold's 'characteristic path' concept though applicable to homogeneous sands is an unrealistic approximation of grain behavior in heterogeneous size-density sands.

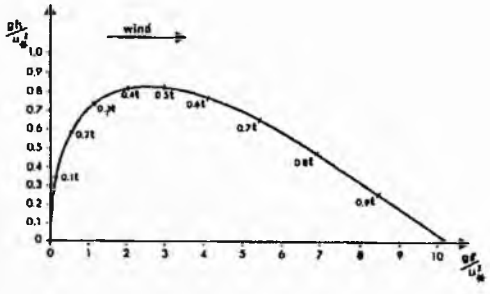

Fig. 3.7 Depiction of the mean saltation trajectory after Owen (1983). h - maximum jump height; l - distance between lift off point and impact point, and t - time taken to complete the trajectory. Coordinates non-dimensional; ordinate scale exaggerated by a factor of 5.

The height and length of the saltation trajectory are dependent on grain shape and also on grain size and friction velocity (u_*). Studies of the dynamics of the saltating grains in terms of the mean ascent angles of the saltating grains (White & Schulz, 1977; Naplanis, 1985; Willetts & Rice, 1985; Anderson & Hallet, 1986) spinning rates (Chepil, 1945a; White & Schulz, 1977; White, 1982) variation of size and shape of saltating grains with height (Gerety & Slingerland, 1983; Williams, 1964; De Ploey, 1980; Draga, 1983), the mean forward velocity (Willetts & Rice, 1985) and the

influence of grain shape on the nature of the saltation trajectory (Rice, 1991) has been accomplished.

In general the trajectory of a saltating grain in air depends on whether the grain is entrained by lift/drag or by impact of other saltating grains, or whether the grain is already saltating and rebounds off the bed in a series of jumps known as successive saltation. The saltating grains extract momentum from the wind, thereby modifying the wind velocity profile near the bed and reducing the friction velocity below threshold. Sand transport is then maintained wholly by the impact of the saltating grains. Finally in equilibrium condition, a steady-state saltation is attained between the near surface wind velocities and the saltating grains. Decreasing grain size of saltating grains denotes low impact angle, low grain forward velocities are a function of low friction velocities. Less spherical grains are entrained more easily during low wind speeds and also have longer and flatter trajectories. However increase in grain sphericity is accompanied with higher bed activity. A decrease in grain size with height of a saltating cloud is observed, although large numbers of coarse grains are seen to bounce more than 50 cm above the surface. The influence of the various grain/bed characteristics influence the collision, aerodynamic entrainment and saltation trajectories which in turn determine the aeolian sand transport rate.

3.4.3 Suspension

Particles smaller than about 0.1 mm may enter suspension and be carried to great heights by the eddies of the erosive winds (Fig. 3.6e). Movement of these fine particles is usually initiated by the impact of particles in saltation. Turbulent airflow is able to keep a grain in suspension, when the vertical fluctuating velocity component of the flow exceeds the settling velocity of the grain. The greatest amount of sand is moved by saltation and surface creep but that moved by suspension is the most spectacular and easily recognised from a distance.

3.5 TRANSPORT RATE EXPRESSIONS

3.5.1 Introduction

The formation of all aeolian bedforms from ripples to dunes is related to the rate of sand transport (of the saltating grains) 'q' which is the mass passing a unit width of bed in unit time. The relationship between sand transport rate and wind velocity has been an important aspect of study among aeolian researchers during the last four decades. The estimation of sand transport rates is largely based on the fundamental approaches established by Bagnold (1941), Kawamura (1951) and Kadib (1965). Bagnold's approach derives an expression from the loss of momentum from the air to saltating grains while Kawamura proposed that the shear stress exerted by the wind on the surface, consists of two components viz. (i) caused directly by the wind, and (ii) the other by the impact of falling grains. Kadib (1965) incorporated the lift generated by turbulent fluctuations and the relationship between the flow intensity and the intensity of sand transported. A brief review of the fundamental mathematical models of Bagnold (1941), Kawamura (1951) and Kadib (1965) will be followed by an appraisal of sand transport equations by other researchers, most of which are deviations from the above mentioned basic transport models of wind blown sand.

3.5.2 Bagnold equation

The most frequently cited equation is that derived by Bagnold (1941). It is based on a sand grain of mass m lifted from the surface with a horizontal velocity of u_1 striking the ground after a distance l with a horizontal velocity u_2. The loss of momentum of the wind per unit length due to the drag of the grain is:

$$m(u_2-u_1)/l \qquad 3.7$$

Since u_1 is very small relative to u_2, it can be neglected. Bagnold also substituted q_s, the mass of grains in saltation moving per unit width in unit time, in place of m resulting in a rate of loss of momentum expressed as:

$$q_s u_2/l \qquad 3.8$$

This equation measures the resisting force per unit area, which is the surface shear stress drag force and can be equated as:

$$q_s u_2/l = \tau = \rho u^2_* \quad 3.9$$

The ratio l/u_2 was found to approximate closely with the time taken for the grain's ascent, which is w_1/g, where w_1 is the initial velocity of rise, when no drag is present. It was then assumed that,

$$w_1 = B u_* \quad 3.10$$

w_1 is proportional to the shear velocity, u_*; the initial velocity of rise w_1 is determined by the descending grains impacting the surface and B is an impact coefficient.

The total sand transport q consists of the saltation transport q_s plus the creep transport. Bagnold assumed that the latter comprises 1/4 of the total transport load, hence the rate of sand movement becomes:

$$q = (4/3)B(p/g)u^3_* \quad 3.11$$

B = 0.8 for uniform sand with average diameter of 0.25 mm and increases with increasing grain size as calculated from wind tunnel experiments giving

$$q_s = 3/4q \text{ with } B \text{ as } 0.8 \quad 3.12$$

Taking into account the variation of grain size during sand transport Bagnold found that q varies approximately as the square root of the grain diameters. As equation 5 is valid only for uniform sand with average diameter of 0.25mm, the total sand transport within a grain size range of 0.1 - 1.0 mm can be given by the expression:

$$q = C_B(d/D)^{1/2}(\rho/g)u_*^3 \quad 3.13$$

where d mean grain diameter, D is 0.025 cm and C_B is a constant (related to B) with values: 1.5 for nearly uniform sand, 1.8 for naturally graded sand, 2.8 for poorly sorted sand, and 3.5 for a pebbly surface.

The variation in C_B results from the greater impact coefficient obtained because of (a) increased w_1 velocities as smaller grains bounce off larger grains with little loss of momentum, and (b) an increase in the splashing effect as larger grains impact the surface ejecting more grains into the fluid.

3.5.3 Kawamura equation

According to Kawamura (1951) the total shear stress τ_o exerted by the wind is the sum of shear stress exerted due to the impact of the sand grains τ_s and the shear stress τ_w caused by the wind directly. Under equilibrium flow conditions:

$$\tau_w = \tau_t \qquad 3.14$$

where τ_t is the threshold shear stress thereby giving:

$$\tau_o - \tau_t = \tau_s \qquad 3.15$$

The shear stress τ_s caused due to the impact of the sand grains can be expressed in terms of loss of momentum of the grains when they hit the surface. This relationship takes the form:

$$\tau_s = G_o(u_2 - u_1) \qquad 3.16$$

where G_o is the mass of sand falling in unit time per unit area.

Substituting the final and initial velocities of rise w_2 and w_1 respectively in place of the horizontal velocities u_2 and u_1 we get:

$$\tau_s \quad G_o(w_2 - w_1) \qquad 3.17$$

Averaging the final and initial velocities of rise to $-2w_1$ the equation becomes:

$$\tau_s = 2 G_o w_1 \qquad 3.18$$

Thus:

$$2 G_o w_1 \quad \tau_o - \tau_t \quad \rho(u_*^2 - u_{*t}^2) \qquad 3.19$$

Therefore:

$$\tau_s = \rho u_*^2 \qquad 3.20$$

From experimental results it was found that :

$$G_o = K_1 \rho(u_* - u_t) \qquad 3.21$$

From equation 14 and 15 it follows that:

$$w_1 = K_1(u_* - u_t) \qquad 3.22$$

Since,

$$q = G_o l \qquad 3.23$$

where l is the average grain path length, it follows that:

$$Q = K_k \frac{\rho}{g}(u_* - u_t)(u_* + u_t)^2 \qquad 3.24$$

where K_k is a constant, based on wind tunnel studies and has a value of 2.78.

3.5.4 Kadib equation

The Kadib's (1965) sediment load equation is based on the findings of Einstien (1950) for a water grain system. He derived the sand transport rate equation in terms of the intensity of sand transport (ϕ) through the expression:

$$q = I\phi(\rho_s' g)\{(\rho_s' - \rho)\rho\}^{1/2}(gd^3)^{1/2}\} \times 10^{-5} \qquad 3.25$$

The intensity of sediment transport (ϕ) is related to the flow intensity by:

$$A^*\phi(1 + A^*\phi) = F(\psi^* B^* - I\eta_o) \quad 3.26$$

where A^* and B^* are constants with values of 43.5 and 0.143, respectively, $F(x)$ is the normal distribution integral between the limits of infinity and $(\psi^* B^* - I\eta_o)$. The flow intensity ψ^* is a function of the disturbance of the bed caused by the falling grains (I) and degree of sheltering in the laminar sublayer ξ through the following expression $\psi^* = \psi\xi/I$. The dimensionless parameter ψ is given by:

$$\psi = \{(\rho_s - \rho)gd\,\rho u_*^2\} \times 10^{-3} \quad 3.27$$

where ρ_s' is the density of the sand grain. Kadib (1965) graphically related the parameters ψ and ξ/I and gave the relation $\xi/I = 5.765\psi^{0.68}$.

3.5.5 Other equations

It is clear from the above basic four derivations that both the Bagnold and Kawamura approaches (the two benchmark equations) are similar in that both rely on the assumption of a characteristic grain path and both relate the transport rate as a function of wind shear to the power three, although the inclusion of the threshold velocity term should provide more realistic values for the transport rate at wind speeds near to the threshold velocity. Numerical modelling of the saltation cloud in a wind tunnel by McEwan and Willetts (1991) has shown that the response of the total mass flux to shear velocity is approximately cubic.

Subsequent research on the applicability of the various transport rate expressions has been in the form of modification and diversification of the fundamental equations subject to field measurements and wind tunnel studies.

Chepil (1945) used the Bagnold equation to study soil movement in agricultural settings. On comparing actual and theoretical values he found the value of C_C to vary between 1.0 and 3.1 depending upon the degree of erosiveness of the soil. However Chepil excluded the grain diameter term from his equation and contested that the rate of sand movement varies as the cube of the drag velocity of the wind, density of the air and degree of gustiness of the wind:

$$q = C_C \rho / g\, u_*^3 \qquad 3.28$$

The sand transport expression proposed by **Zingg (1953)** was similar to that of Bagnold except that the value of the constant C_Z was 0.83 and his power function for the diameter of the sand in question was 3/4 instead of 1/2 as described by Bagnold (1941). Zingg's equation can be written as:

$$q = C_Z(d/D)^{3/4}(\rho / g)u_*^3 \qquad 3.29$$

Owen (1964) supported Zingg's modification and concluded that the 3/4 function is more appropriate for larger grain sizes whereas 1/2 function of the grain diameter was appropriate for finer sands.

Hsu (1971), while estimating sand transport rates on Eucadorian beaches, showed that the rate of sand transport is a function of the particle Froude number (F_r) which expresses the interrelationship of wind stress, grain acceleration, and mean grain size of sand particles:

$$q = KFr^3 \qquad 3.30$$

The Froude number is found to be a function of grain size. Thus the final equation is:

$$q = K\{(u_*/(gd)^{1/2}\}^3 \qquad 3.31$$

where K = -0.47 + 4.97D (same D as in equation 3.11)

Williams (1964) generated an average relationship for a wide range of grain sizes, with a mean of 0.033 cm. The formula for sand transport that he obtained was:

$$q = a'\rho / g u_*^{b'} \qquad 3.32$$

where a' = 0.1702 and b' = 3.4222

A refinement of the Kawamura equation was suggested by **Letteau & Letteau (1978)** which incorporated a single threshold term to give:

$$q = C_L(d/D)^{1/2}(\rho/g)u_*^2(u_*-u_t) \quad 3.33$$

the value of C_L being 4.2.

Another equation incorporating a threshold term was proposed by **White (1979)** based on wind tunnel studies simulating both Martian and earth conditions:

$$q = 2.61\, u_*^3\,(1-u_{*t}/u_*)\,(1+u_{*t}^2/u_*^2)\,\rho/g \quad 3.34$$

Since sand transport rates are often influenced by vegetation the Bagnold equation was modified by Wasson & Nanninga, (1986) and Buckley (1987). The **Buckley (1987)** equation is:

$$q = B'(u(1-k_pC_p)-u_z')^3 \quad 3.35$$

where B' is a function of the plant cover percentage C_p, u is the average wind velocity measured at 0.5m u_z' is the threshold velocity at height z and k_p is a constant dependent on plant shape. It is estimated that sand movement can take place with plant covers up to 40%.

As the earlier Bagnold (1941) equation suffered from a limitation that it predicted unrealistic transport rates when u_* is below the threshold (Belly, 1964), **Bagnold (1954, 1956)** corrected this and included a threshold term:

$$q = C_B(d/D)^{1/2}(\rho/g)u\,(u-u_z)^3 \quad 3.36$$

in which u is the mean wind velocity and u_z is the threshold velocity at height z' and is a constant equal to (0.174/lnz/z').

O'Brien & Rindaulb (1936) used the mean wind speed at a height of 3 feet to compute the transport rate by the equation which when converted in cgs units is:

$$q = 9.96*10^{-7}(u_*-10.8)^3 \quad 3.37$$

Howard *et al*, (1978) expressed the Bagnold (1956) equation over a flat surface in a modified form to include the slope effect:

$$q_s = q\cos\theta\,(\tan\alpha - \tan\theta) \quad 3.38$$

Where θ is the slope of the surface in the direction of transport, α is the angle of repose of sand and q_s is the rate of sand transport on a sloping surface.

For application of wind velocity data from meteorological stations Hsu (1971) proposed the value friction velocity to be calculated by:

$$u_* (cm\ s^{-1}) = 4.0\ u(ms^{-1}) \qquad 3.39$$

and the sand transport rate q to be:

$$q = 1.16 \times 10^{-4} u^3 \qquad 3.40$$

3.6 FIELD EVALUATION OF SAND TRANSPORT MODELS

Most studies that attempt to measure aeolian sediment transport in the laboratory or in the field use several of the above models for purposes of comparison, usually with mixed to poor results (Svasek & Terwindt, 1974; Berg, 1983; Sarre, 1987; Hotta *et. al,* 1985; McCluskey, 1987; Bauer *et. al.* 1990) There are several general criticisms to these approaches. The dependence of the equation on the grain size is much more with the Bagnold (1941) formula than the Kawamura as the latter only incorporates it in the term for the threshold velocity. Svasek and Terwindt (1974) used both the Kawamura (1951) and Bagnold (1941) expressions to measure the sand transport rate on a beach (d = 0.25 mm). The best correlation of their data with the Bagnold (1941) and Kawamura (1951) equations at shear velocities of 0.4 ms^{-1} was reported to be with empirical coefficients of 2.0 and 1.8 respectively. Horikawa et al. (1983) found that both the Bagnold (1941) and Kawamura (1951) expressions underestimated the transport rate for sand with a wide range of grain diameter under high shear velocities and that the empirical coefficient in the Kawamura expression should be 2.3. Berg (1983) compared his results with Bagnold (1941), Kadib (1965) and Hsu (1971) and concluded that the Kadib equation gave the closest prediction, except for coarse grained sediments for which the estimates were less than those observed.

The Kadib expression appears to be more complicated though it does not rely on variables which are difficult to quantify or are subjective in their measurement in the field. His derivation is also more sophisticated as it includes the influence of turbulence in generating the lift forces. In spite of being a bit troublesome as Kadib's expression relies on graphical solutions both Berg (1983) and Sarre (1988) report that the Kadib

model worked best in their field applications. However, Sarre (1988) later found that the White (1979) expression gave the best fit to his data. The O'Brien & Rindaulb/Horikawa-Shen approach is too general and ignores several fundamental transport parameters such as grain size.

3.7 FACTORS INFLUENCING AEOLIAN SAND TRANSPORT

The rate of sand transport and the threshold of sand movement are purely a function of wind shear and grain size factors. However, certain additional factors e.g. grain characteristics, inter - particle cohesion forces and vegetation also influence the threshold of sand entrainment and transport.

3.7.1 Grain characteristics

There are four ways in which the grain characteristics can influence the threshold velocity for motion and rate of transport.

3.7.1.1 Mean Grain Size

Bagnold (1941) comments that the rate of sand transport increases as the grain size widens, probably due to the continual supply of grains of a size capable of being moved. The influence of the grain size parameter during sand transport has been discussed earlier.

3.7.1.2 Availability of grains

Availability of grains of a size capable of motion either by saltation or creep is also important. A possibility exists that either all grains fine enough to be moved by the wind may be removed or there may be a development of a surface layer of grains too large to be moved, sheltering finer grains below. Carter (1976) observed that this kind of a coarse grain layer was represented by a shelly layer. This phenomenon is of utmost importance to beaches where large grain sizes make up a significant proportion, which may become enhanced further over a storm event as surface lowering exposes more large grains and the surface becomes increasingly protected. Investigation on a coarse

sand beach of the Channel Islands by Sarre (1984, Unpublished dissertation) indicated the increase in grain size from 0.045 cm. to 0.062 cm. over a 48 hour period occurred with a corresponding decrease in the transport rate for the same wind velocity.

3.7.1.3 Grain shape

Low wind shears coupled with decreasing sphericity causes an increase of sand transport whereas at high wind shears the rate of movement increased with grain sphericity. Williams (1964) and Willetts *et. al,* (1982) concurred with these findings on the basis of a series of wind tunnel experiments, i.e. a higher rate of transport is observed for an increase in the general sphericity for a given wind velocity.

3.7.1.4 Sorting

An eroding wind has been said to act on the soil as a fanning mill on grain, removing the fines and more porous particles and leaving coarser and denser sediments behind. (Chepil, 1957; Daniel, 1936). The coarser eroded material usually ends up in a soil drift whereas the finer grains enter suspension and are transported often for great distances before deposition. Chepil (1957) observed that the most distinct feature in the sorting process was that the particles of greatest diameter tend to remain in the wind eroded fields, and particles smaller than this diameter tend to be carried far through the atmosphere in suspension.

3.7.1.5 Particle Cohesion

Iversen *et al* (1976) observed that the major cohesive forces acting within sediments are Van der Waals forces, electrostatic charges, and forces between absorbed films on the grains. Cohesive forces between the much larger particles on the beach generally result from high moisture and soluble salts. Increase in inter - particle attraction tends to raise the surface stability thereby increasing the shear stress needed to initiate movement. Smalley (1970) attributed this inter - particle attraction to fractional packing density, inter - particle bond strength and the inverse cube of the grain diameter.

3.7.2 Moisture Content

The fact that moisture has a limiting effect on sand movement was indicated by Crofts (1971), who found that moisture content was more instrumental than wind velocity as regards sand movement. Although this parameter has been more often neglected the observations of Belly (1962) are important. Belly (1964) found that the relationship between threshold velocity and moisture content was logarithmic as indicated by the equation.

$$u_{*_{tw}} = u_{*_t}(1.8 + 0.6\ log_{10}w) \qquad 3.41$$

w = moisture content of the sand in %

At higher moisture content (>4%) the threshold velocity increases disproportionately probably due to the filling up of the grain interstices with water. Hence the relationship established above cannot be extrapolated beyond 4% moisture content. Later Svasek and Terwindt (1974) while using a neutron moisture probe found that a precise relationship was difficult to establish and observed that threshold velocities were higher than those given by Belly (1962) for a given moisture content. They also indicated that once grains became mobile in the downwind areas, moisture content had a limited role to play. According to them a minimum fetch of about 10-20 m. is required for the wind to become saturated with sand. Chepil (1959) stated that the maximum rate of movement on highly erodible soils was achieved with about a 60m fetch.

From analysis of existing literature Hotta *et. al,* (1985) found that the standard threshold equation to assess the influence of water content on sand movement should be:

$$u_{*_{tw}} = u_{*_t} + 7.5w \qquad 3.42$$

where w is the percent water content of the upper 5 mm of sand. Equation 3.41 is valid for w up to 8% and a grain diameter between 0.2 mm and 0.8 mm. However, it is interesting to note that Sarre (1988, 1990) believes that moisture level up to 14% in the top 1-2 mm of the damp/wet beach has no discernible effect on the transport rate.

3.7.3 Salt Encrustations

Salt encrustations, a common phenomenon of tropical beaches, are of local importance in temperate beaches, reducing transport rates especially during the summer months when evaporation rates are high enough to allow crusts to form. Svasek & Terwindt (1974) considered that on temperate beaches crusts can easily be broken by the saltating grains whereas Boughey (1957), Morton (1957) and Pye (1980) while studying salcretes on tropical beaches observed that the phenomenon is of immense importance in limiting dune growth. Nickling & Ecclestone (1981), through extensive wind tunnel studies, found that a correlation existed between different concentrations of NaCl and KCl and the threshold velocity. However the effect was indirect, as can be deduced by the following modified Bagnold equation

$$u_{*_t} = A(0.97 \exp 0.103\, s/c)[(\rho\ '_s/\rho\ gd]^{1/2} \qquad 3.43$$

where s/c is the salt content in mg sal g^{-1} soil. Yasso (1966) attributed the formation of 'Salcrete' or salt encrustations on the beach, to be dependent on local factors as potential evaporation rate, beach morphology, tidal range and grain characteristics.

The role of biological agents such as algae in crust formation is described in Fletcher and Martin (1948), Campbell (1979) and Forster & Nicholson (1981). Ancker *et al.* (1985) found that transport over a well developed crust was less than 1% of that over an unprotected surface.

3.7.4 Vegetation

The primary influence of vegetation is to modify the near surface shear velocity field in a manner that reduces the bed shear stress (Hesp, 1981). Olson (1958) reports a thirty fold increase in the roughness length z' after planting *Ammophila sp.*. Bressolier and Thomas (1977) show that the roughness length increases with both vegetation height and density, especially with the latter. The displacement height h (eq. 3.2), is the average elevation of the surface roughness elements (Sherman & Hotta, 1990) and it is also the elevation at which the average surface shear stress acts (Jackson, 1981). For dense vegetation, h is about two thirds mean plant height. (Oke,

1978; Jackson, 1981). The role of vegetation is, therefore to increase the elevation where the mean shear stress occurs. If this statistical elevation is lifted above the highest elements of the sediment surface, then the transport can be sporadic at best (Sherman & Hotta, 1990).

3.7.5 State of the tide

On the beach the sand transport is limited by the state of the tide and the relation of the sand height to the sea-level. According to Sarre (1987) the moisture content (5-35% in inter-tidal areas and 1-10% in backshore areas) of the surface has three limiting factors (Sarre, 1987). It causes a reduction of sand transport by allowing only the extreme topmost grains to become mobile and by causing the saltating grains to stick together on impact with the surface. The tidal margin acts as the seaward limit of aeolian sand transport, where adhesion structures form.

3.7.6 Atmospheric parameters

The important atmospheric variables influencing sediment transport are wind speed and direction, temperature, precipitation, surface moisture, humidity and fluid density (Sherman & Hotta, 1990). As the role of wind velocity has been accounted for,in all the transport rate expressions and the importance of surface moisture has already been discussed, the effect of temperature, humidity, fluid density and precipitation will be dealt here briefly.

3.7.6.1 Atmospheric density, temperature and humidity

It is generally assumed that air density (ρ) is constant (1.22 kg m^{-3} x 10^{-6}). However, the density of air decreases with rising temperature and increasing humidity. Chepil dismisses this variation (3%) as insignificant. Since density enters linearly into transport rate expressions, variation in incorrect density values can lead to an error as large as 20% (Sherman & Hotta, 1990). This error can be corrected by referring to Monteith (1973). Berg (1983) suggests that errors in the estimation of u_* resulting from ignoring the thermal gradient seldom exceed 10%. Although quantitative linkages

between relative humidity and transport rate have not been established, high and low relative humidities are thought to retard and increase the transport rates respectively (Belly, 1962, Johnson, 1965) .

3.7.6.2 Precipitation

The occurrence of precipitation can cause (i) intense wind driven rain to transport sand by splash processes; (ii) the residual moisture to greatly reduce aeolian sand transport by increasing the threshold shear stress (Sherman & Hotta, 1990). De Ploey (1980) concurs with these conclusions while working on a Belgian beach.

The sand transport rate expressions are primarily a function of the wind speed and the grain size of the surface sand. However, an analysis has also been done on the importance of various climatological factors, vegetation, moisture, beach exposure etc. in modifying (reducing/accelerating) the transport potential in natural conditions.

Since the wind speed is one of the primary factors governing sand transport, in the next chapter a detailed discussion of the wind regimes, present in the study area, will be presented. The role of other important variables as moisture, vegetation etc will be dealt with in chapter 5.

Chapter 4

WIND DISTRIBUTION AND POTENTIAL AEOLIAN DRIFT REGIMES

(with 16 figures and 2 tables)

Chapter 4

Wind Distribution And Potential Aeolian Drift Regimes

4.1. INTRODUCTION

The worldwide distribution of coastal dunes at every latitude (both tropical and temperate) indicates that the morphogenesis and dynamics of coastal dune development is independent of climatic data and of aridity and is thus primarily governed by the wind regime (Mainguet, 1986). The wind regime is characterised by velocity distribution and directional variability (Pye & Tsoar, 1990), which in turn determine the direction and rate of aeolian sand transport. It is therefore important that the nature of the winds prevalent at Tentsmuir should be examined to enable one to understand the aeolian dynamics active in the area. The analysis of the wind data has been carried out to explain the variations in the wind regime during both long term (monthly variation) and short term (hourly variation) periods. The principal reason for analysing meteorological wind velocity data in this chapter is to enable the quantification of both the magnitudinal and directional variability of the winds in relation to their sand transporting capability.

4.2. DATA COLLECTION AND ANALYTICAL MODES

At R.A.F. Leuchars, 9 km south of Tentsmuir point is a long established first class weather station with records extending for more than 70 years (Fig. 2.1). The measurements by cup anemometer at 10m above mean sea level recorded hourly are available at the meteorological office in Edinburgh. Wind velocity data for the site have been collected for an eleven year period - 1980-1990.

The number of hours that the wind of given direction and strength blew during each month have been extracted from tables produced by the meteorological office. An example of the data table is given in Appendix III - A. Wind speed is measured in knots (1knot = 0.52 ms^{-1}) and wind direction in degrees from true north. The 12

azimuth categories shown in the meteorological table have been represented by their mid point values, for e.g. the mid point of the 350°-10° azimuth category is 360° and is denoted by N. The unit of wind speed used in the standard meteorological data is knots which has been converted to ms^{-1} for the sake of consistency. Since the Tentsmuir coastline is north aligned the onshore and offshore components of the wind velocity range from 20° to 160° and 200° to 340° respectively. The longshore component comprises of northerly (350° - 10°) and southerly components (170° - 190°) respectively.

Meteorological data has been analysed in two different ways:

a) Frequency analysis of the total number of hours of a particular wind velocity both on a long term (years - monthly variations) and short term basis (daily - hourly variations).

b) Vectorial representation of wind velocity data, using the Fryberger & Dean (1979) method (discussed later), for a given compass direction and computation of the offshore and onshore vector resultants in order to describe the types of wind regime prevalent around Tentsmuir over a monthly period.

4.3 HOURLY WIND VELOCITY FREQUENCY ANALYSIS BY MONTH

4.3.1 Wind Direction

A rose diagram showing average wind velocity distribution for the period 1980-1990 has been shown in Fig. 1.8 (p. 1.12). The south-westerlies are the dominant winds of the British Isles and the east coast of Fife is no exception. The most prominent offshore winds, at Tentsmuir, originate from the WSW sector, the next in relative abundance being those blowing from SSW sector.

The south westerlies (SSW-WSW sector) are the characteristic winds of the winter months of December, January, February (Fig. 4.1, 4.3c, 4.4a, 4.4b, 4.5c, 4.6b). The frequency of these winds decreases during the summer months. The north westerlies (NNW - WNW sector) are exclusively abundant during the months of March and April (Fig. 4.1, 4.3a, 4.3b, 4.3c, 4.4c, 4.5b and 4.5c). The onshore winds blow approximately 25% of the time at Tentsmuir in contrast to the offshore

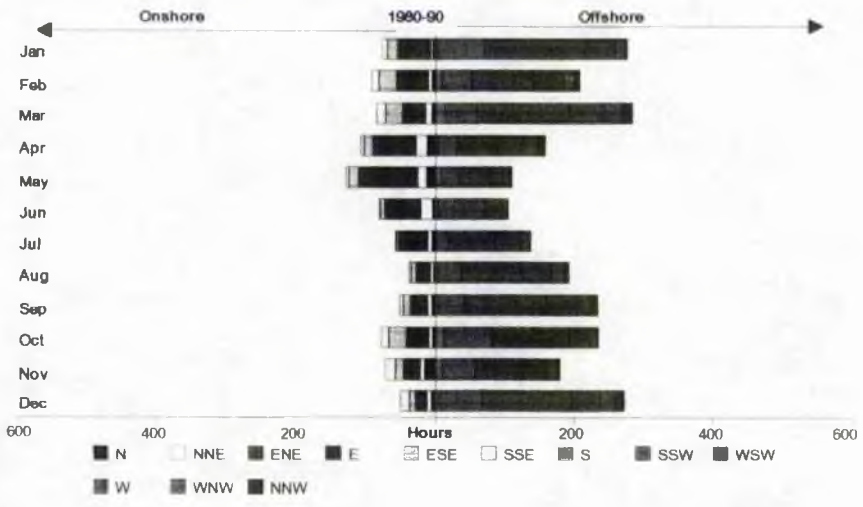

Fig. 4.1 Eleven year average (1980-90) of the monthly azimuth frequency. Winds blow from the direction indicated.

component which blows for about 70% of the year. The onshore winds comprise of the easterlies (ENE-NNE sector) and the south easterlies (ESE-SSE sector), generally the former predominate over the latter. The onshore winds are prominent during the spring and autumn season (Fig. 4.3a, 4.3b, 4.4b, 4.4c, 4.5a). Thus on an average the winds at Tentsmuir are distinctly bimodal though with a predominant offshore component.

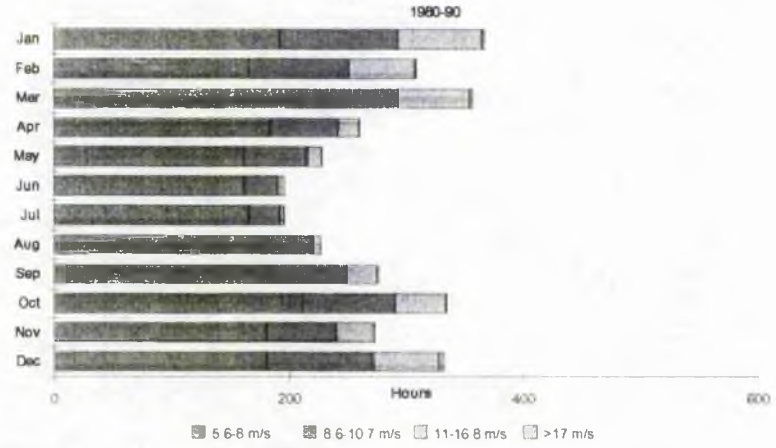

Fig. 4.2 Average wind speed frequency for 1980-90.

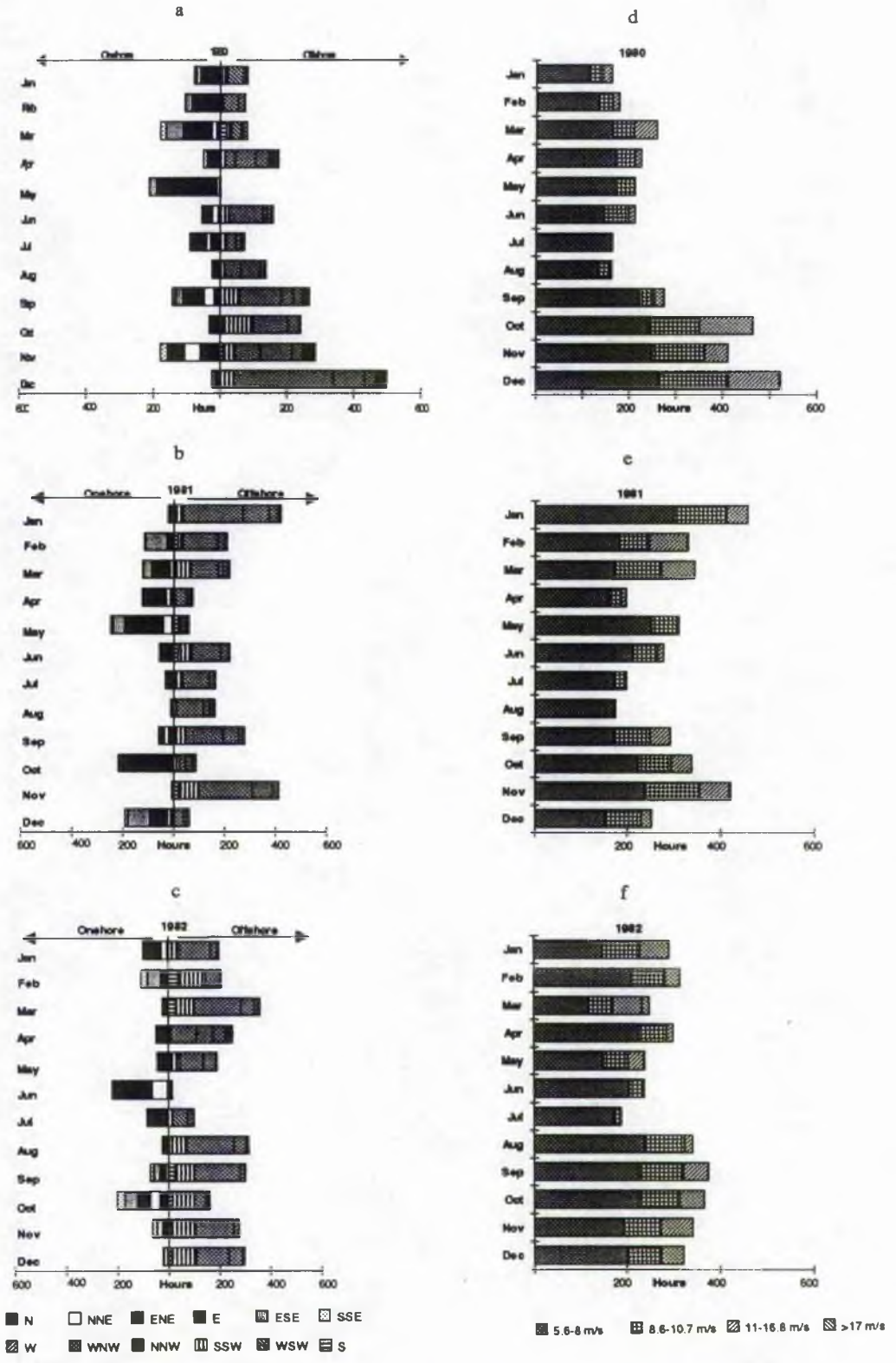

Fig. 4.3 Monthly wind velocity distribution for 1980-82. a, b & c - monthly offshore-onshore wind distribution. d, e & f- Monthly wind speed class duration distribution.

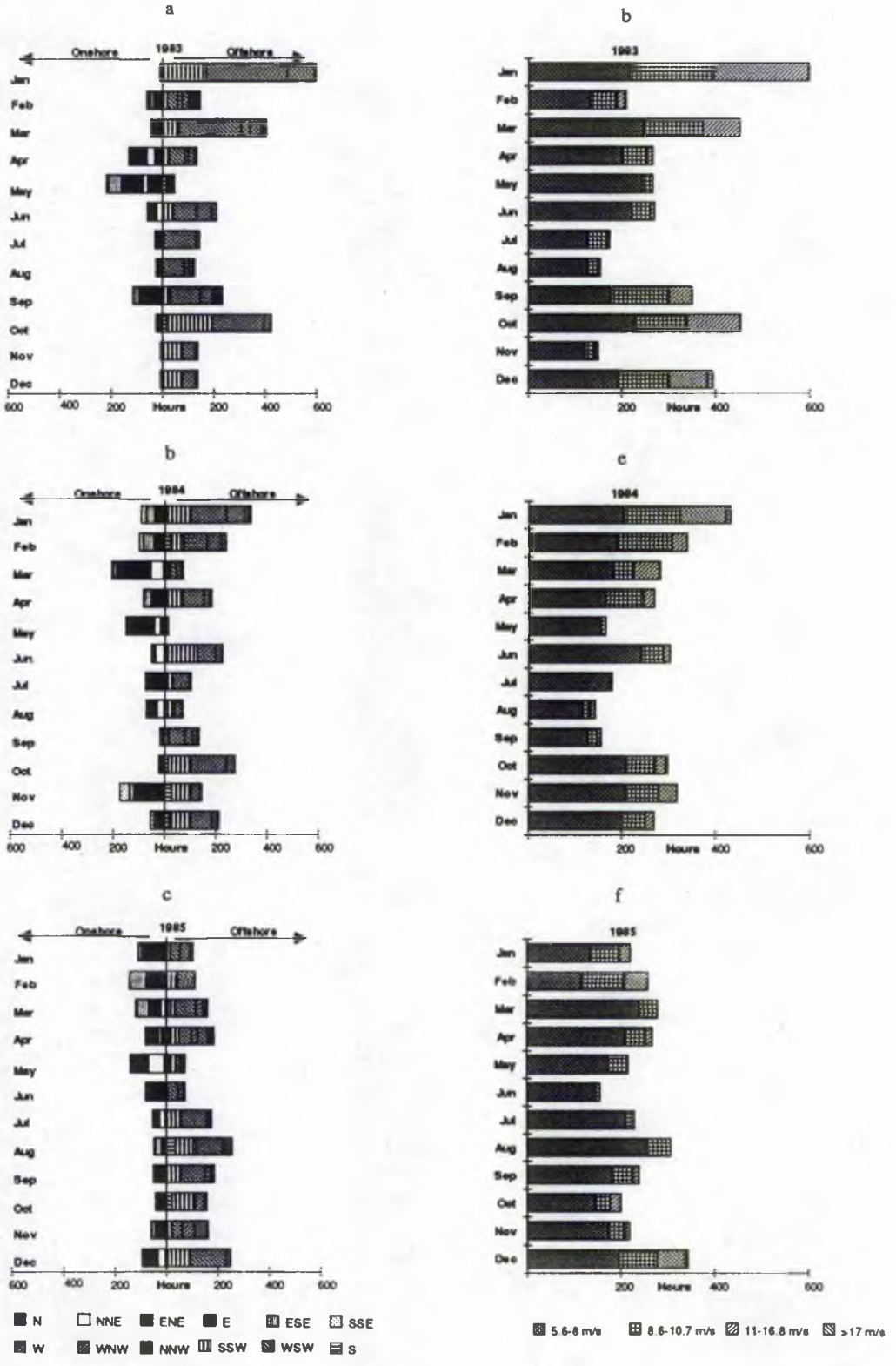

Fig. 4.4 Monthly wind velocity distribution for 1983-85. a, b & c - monthly offshore-onshore wind distribution. d, e & f- Monthly wind speed class duration distribution.

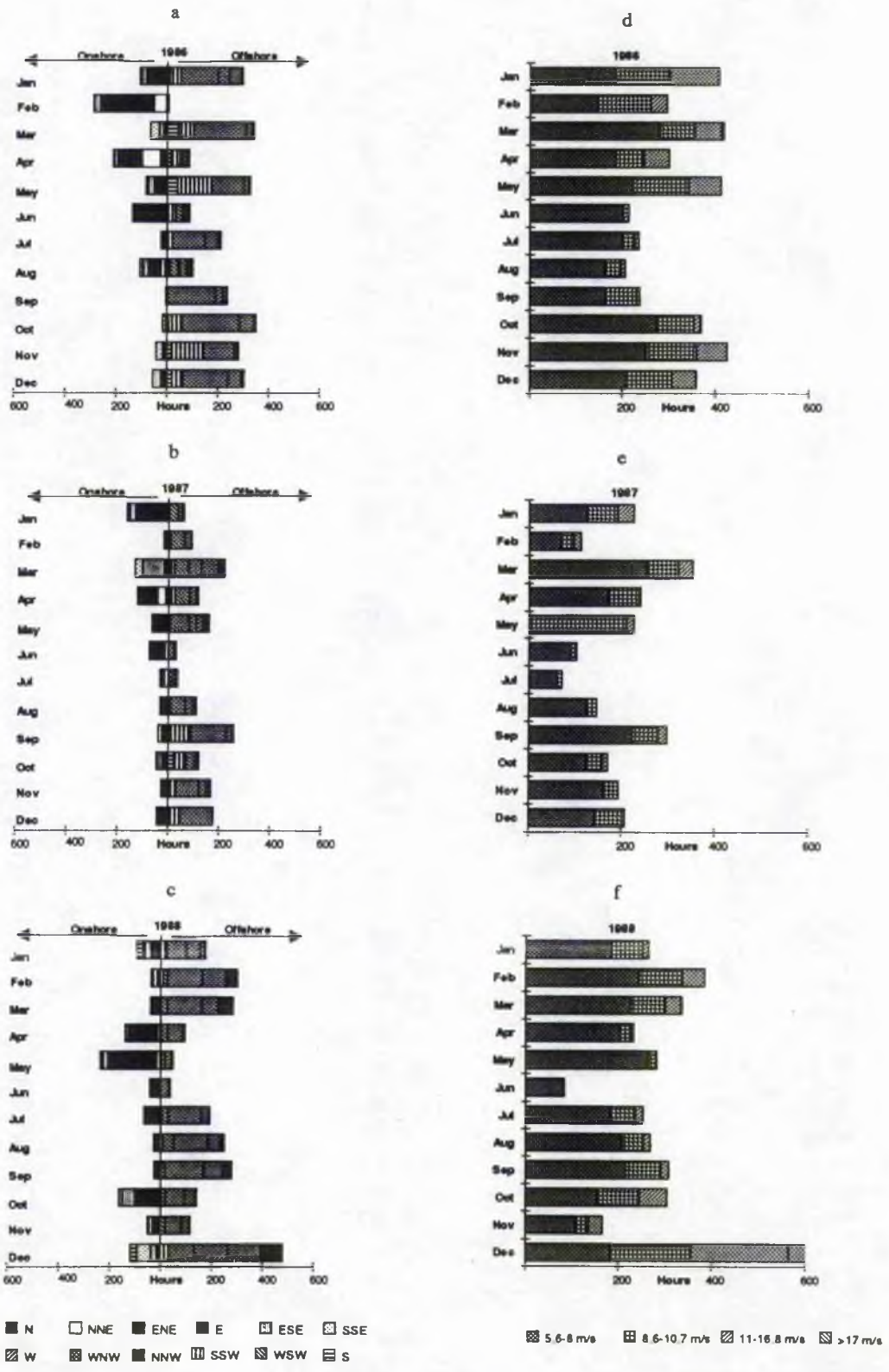

Fig. 4.5 Monthly wind velocity distribution for 1986-88. a, b & c - monthly offshore-onshore wind distribution. d, e & f - Monthly wind speed class duration distribution.

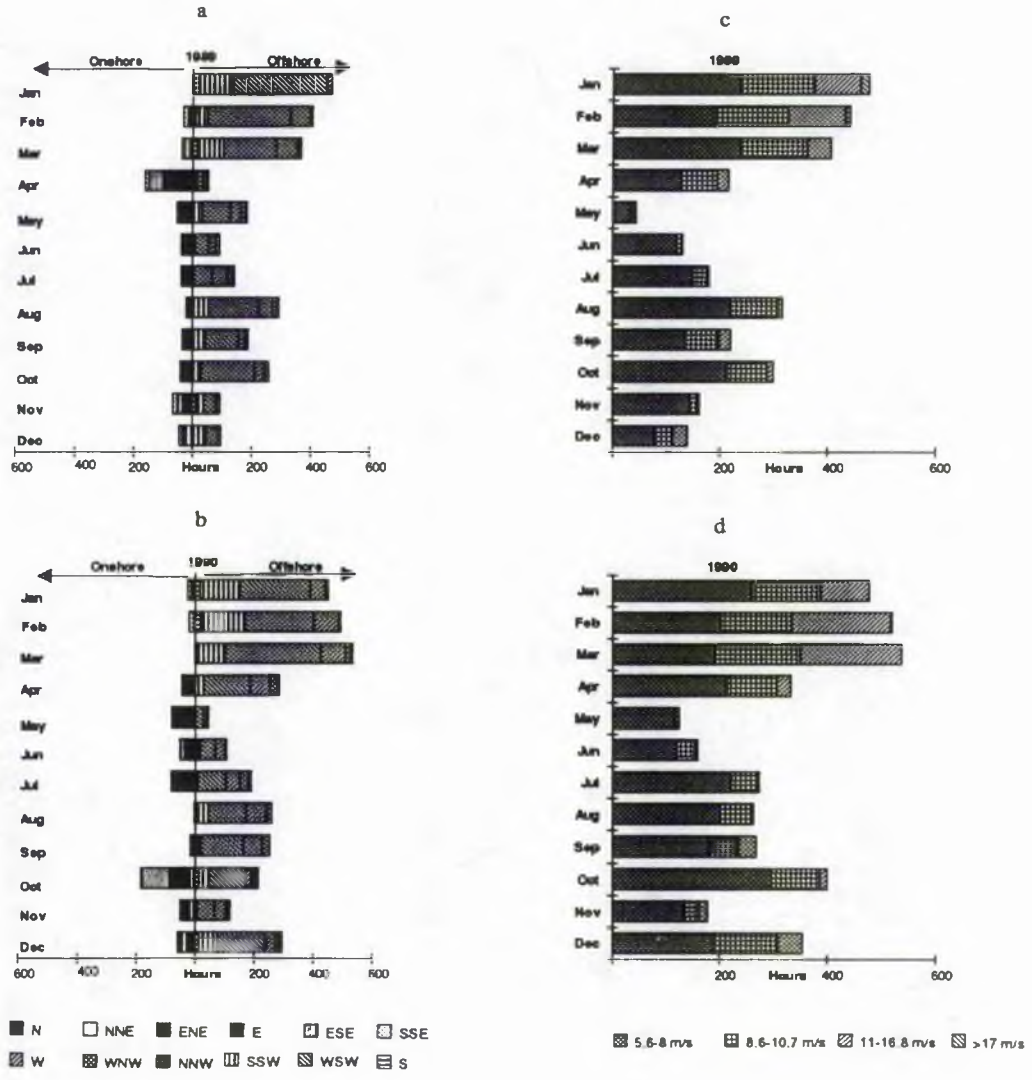

Fig. 4.6 Monthly wind velocity distribution for 1989-90. a & b - monthly offshore-onshore wind distribution. c & d - Monthly wind speed class duration distribution.

4.3.2 Wind Speed

All months during the year (Fig. 4.2) experienced a long term average of 160-200 hours of winds with speeds of 5.6 - 8 ms^{-1}, approximately 90 hours of 8.6 - 10.7 ms^{-1} winds during winter, 54 hours during spring and 26 hours during June and July whereas the months of August, September and October experience averages of 42, 64 and 77 hours respectively. The 11 - 16.8 ms^{-1} winds were well represented from September (30 hrs.) to March (61 hrs.), being greatest during January (71 hrs.), with much shorter durations (3-18hrs) from April to August. Wind speeds above 17 ms^{-1} were experienced generally in the winter months of December (Fig. 4.4d, 4.4f, 4.5f), January (Fig. 4.6c) and March (Fig. 4.3f).

4.3.3 The Offshore-Onshore Distribution

The monthly off-shore wind frequency (~200 hours) was nearly constant through an annual cycle (Fig. 4.3a, 4.4a, 4.6a, 4.6b) although these winds were less common during the spring and summer months (100-145 hours from April to July). The onshore winds reached their acme generally in the months of April (av. 145 hours, Fig. 4.5a, 4.5b, 4.6a) and May (~140 hours, Fig. 4.3a, 4.3b, 4.4a, 4.4c, 4.5e), but were of importance in October (~89 hours, Fig. 4.5c, 4.6b) and February (av. 92 hours, Fig. 4.3a, 4.3b, 4.3c, 4.5a). The onshore winds were least common in magnitude during July, August (Fig. 4.3a, 4.3b, 4.4a, 4.4b, 4.4c, 4.5c). The offshore - onshore frequency ratio is generally high (4 - 5) during August, September, January and March (Fig 4a, 4.5e, 4.6a, 4.6b) moderate (2-3) in November, December, February and July and nearly equal in October (Fig. 4.3c, 4.4b, 4.5c, 4.6b) April, May and June (Fig. 4.3b, 4.4c, 4.5b).

4.4. HOURLY VARIATIONS OF WIND REGIME

4.4.1. Sea Breeze

On plotting the hourly wind data for the month of July 1990 daily cycles of sea breezes have been identified commencing on 13 July, and becoming very prominently developed after 20 July (Fig. 4.7). Sea breezes are mesoscale circulations due to

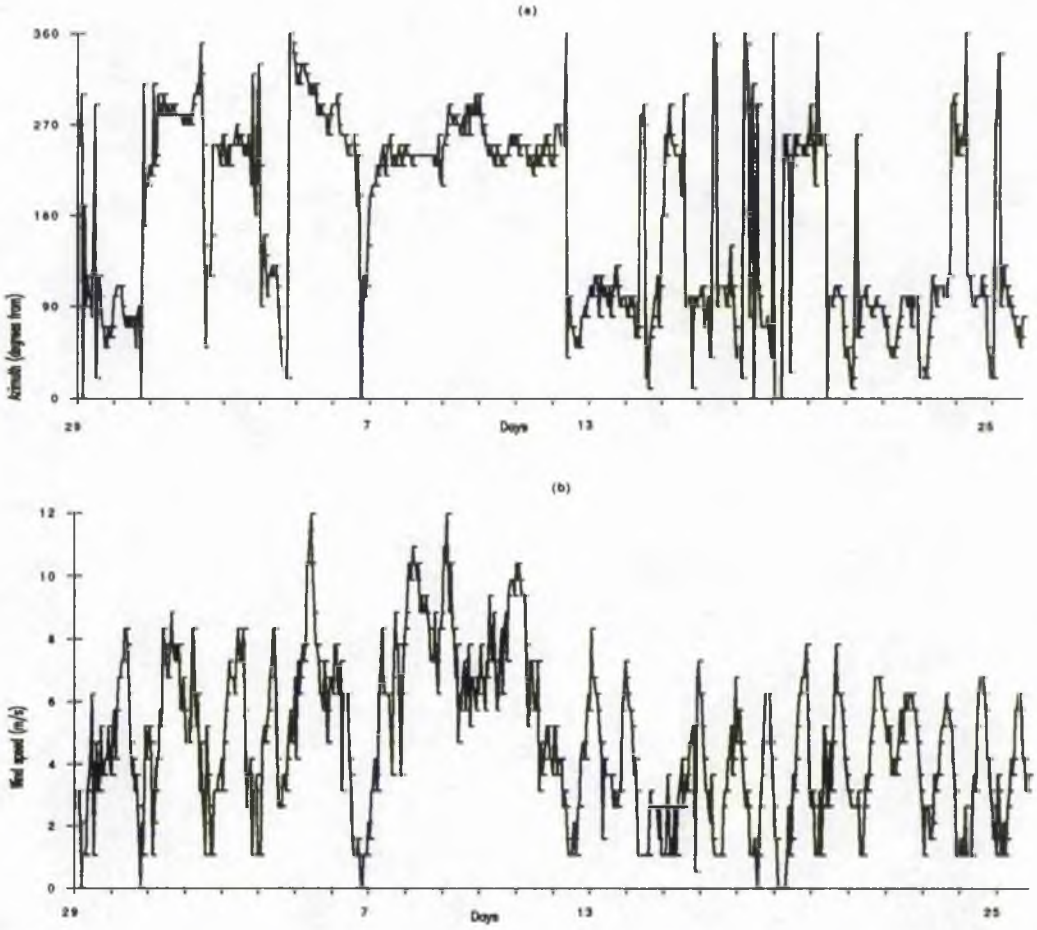

Fig. 4.7 Example of daily cyclic sea breeze - July 1990. Note the regular sea breeze after July 13, in contrast to a dominantly SW - offshore wind prior to July 13. (a) Azimuth, (b) Wind speed (m/s).

land/sea temperature differences. The sea breeze ranges in speed from 2.04 - 8.16 ms^{-1}, the maximum speed occurring in the late afternoon from 2-8 p.m. The other part of the daily cycle is formed by land breezes which characteristically have low speed (never exceeding 1.02 ms^{-1}) (Fig. 4.7). The sea breeze is very steady in duration and direction for most of the summer.

4.4.2 Offshore, Onshore And Longshore Winds

Study of the daily hourly variation of winds at Tentsmuir revealed that the bimodal distribution found in a particular month is in fact composed of distinct unimodal winds (either offshore, onshore or longshore) spread over a period of days.

Hourly wind velocity distribution for February, 1991 has been shown here as a case example. Unimodal onshore winds from the east are shown in Fig. 4.8a. The wind speed ranged from 10 - 12 ms^{-1} between 7 and 9 February. Examples of offshore winds are shown in Fig. 4.8b. The winds are blowing from the SW quadrant ranging in speed from 2 to 10 ms^{-1}. Longshore winds blowing from the north (360^0 - 10^0 azimuth) are shown in Fig. 4.8c. Their wind speed is seen to vary from 2 to 7 ms^{-1}. It is thus important to bear in mind that apart from the summer cyclic land and sea breezes, the winds in the area in general are steady in direction and are characteristically unimodal over moderate time periods (days).

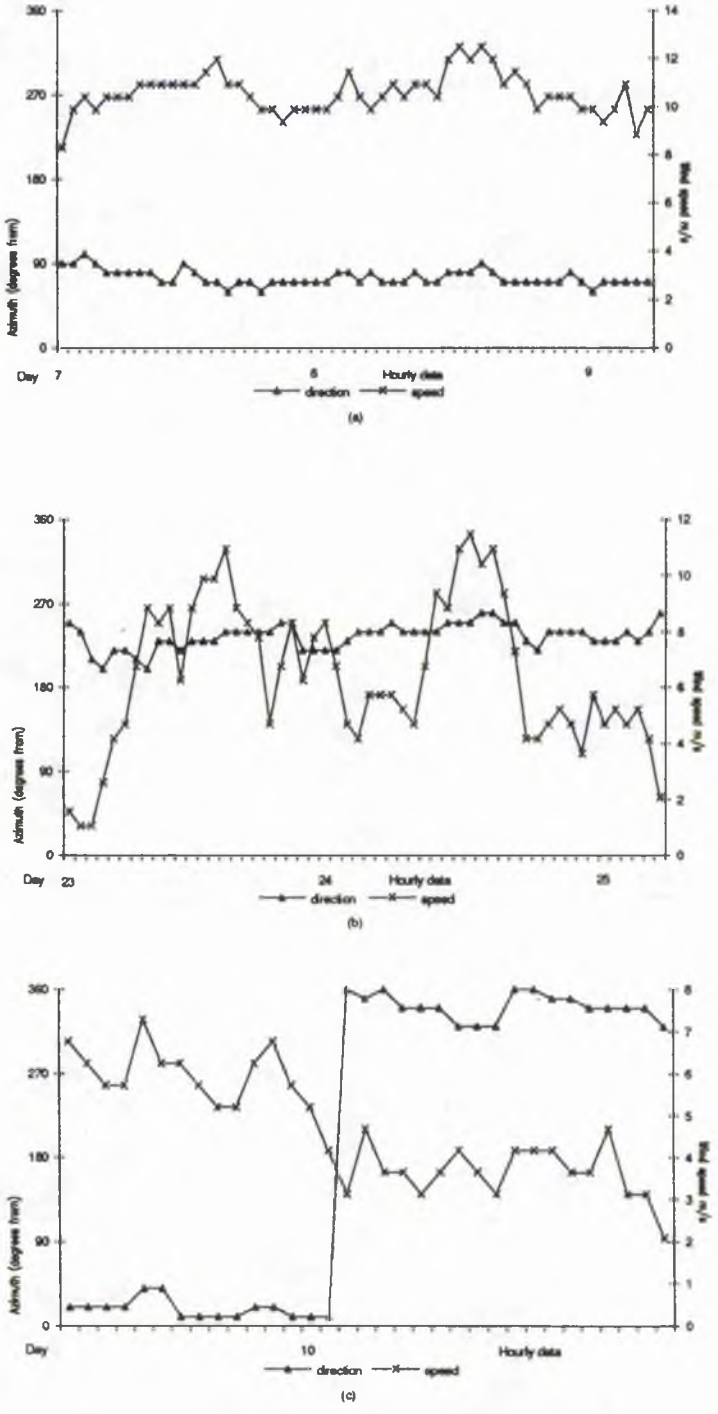

Fig. 4.8 Examples of daily unimodal winds during February 1991. (a) Onshore winds, (b) Offshore winds, and (c) Longshore winds.

4.5 VECTOR ANALYSIS OF WIND VELOCITY & SAND DRIFT POTENTIALS

4.5.1 Methodology

Wind velocity data has been used to analyse the variation of wind vectors within the 12 azimuth direction groupings over a period of time (1980-1990). Sand drift potential of these vectors have been calculated using the method of Fryberger & Dean (1979), while analysing wind information from the deserts of Libya, China and Mauritania.

The Letteau & Letteau (1978) sand transport equation (eq. 3.33, chapter 3) was generalised by Fryberger & Dean (1979) as Eq. 4.1 below. This generalisation was based on two assumptions: (1) the surface consists of loose quartz grains with an average diameter of 0.25-0.35 mm and (2) the wind blows over an unvegetated dry surface without bedforms larger than ripples. They estimated the potential sand drift (Q), expressed numerically in vector units (V.U.), as being proportional to the product of a weighting factor and the percentage of total wind recorded in time (t), as:

$$Q \quad \alpha \quad \underbrace{[V^2 (V-V_t)]^1}_{[\text{weighting factor}]^1} \quad x \quad t \qquad 4.1$$

where, V is the wind velocity at 10m height for the time period t and V_t, is the threshold velocity (10m height) at which the sand moves (5.9 ms^{-1}) (Fryberger & Dean, 1979).

The value of V in the weighting factor has been derived from the average wind speed of a velocity category as grouped in the meteorological data sheets, for example the average wind velocity for the 11-16 knot wind speed category is 13.5. The weighting factor is then calculated by substituting the value of V in Equation 4.1. However, this value has been divided by 100 to reduce the weighting factors to smaller values for convenience in plotting the sand roses (Table 4.1).

The weighting factor represents a number which expresses the relative amount of sand potentially moved during the time it is presumed to blow. The product of the

weighting factor and the time factor, 't', results in a number referred to as the *drift potential (DP)*, which is a measure of the relative amount of potential sand drift at a given location for a stated period of time.

Table 4.1 Calculation of weighting factor for different wind speed classes. V_t is the threshold wind velocity (10 m height) for sand movement.

Wind speed category (knots)	Mean	$V-V_t$ V_t = 11.6 knots	Weighting factor $v^2(V-V_t)$
11-16	13.5	1.9	2.7
17-21	19	7.4	25.3
22-27	24.5	12.9	75
28-33	30.5	18.9	172.1
34-40	37	25.4	342.8

Vector units (V.U.) are the units of drift potential since wind velocities are treated as vectors. 't' is the time during which the wind of a given wind speed class blew. This is extracted from the meteorological data sheets, and expressed as a percentage of the total wind record in a month. To evaluate the relative directional and magnitudinal variability of the amount of sand drift at a particular location, each velocity category is multiplied by the percentage occurrence of wind in that category for all 12 directions and the results summed. An example of the worksheet is shown in Appendix III - B.

4.5.2 Description Of The Sand-Rose

The variations are plotted in the form of a 'sand' rather than the conventional 'wind' rose as the arms of the sand rose represent the drift potential (in vector units) of the winds from that particular azimuth for a given month. Sand roses (Fig. 4.9) represent the potential sand drift from twelve compass directions, the arm lengths of which are proportional to the potential sand drift from a given direction computed in vector units. Vector unit totals from the different directions have been vectorially resolved to three single

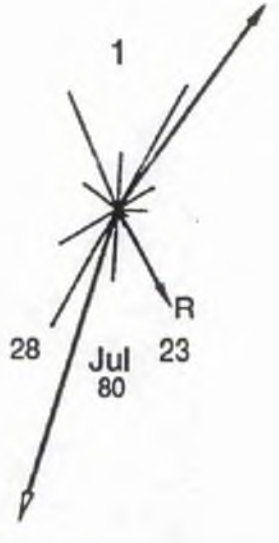

Fig. 4.9 Example of a sand rose. The arm length is proportional to vector unit totals. Numbers on the left, and right are onshore (open arrow) and offshore (solid arrow) resultant drift potentials. Effective drift resultants are shown as a solid arrow with the letter 'R'. Number at the top is the reduction factor.

resultants: an onshore resultant drift potential vector (vector resultant for 0^0-150^0 azimuth), an offshore resultant drift potential vector (vector resultant for 180^0-330^0 azimuth) and the effective resultant drift potential vector (0^0-360^0). The reason for computing the two additional resultants (offshore and onshore), along with the effective resultant (0^0-360^0) which is the only one used in desert dunefields, is to be able to quantify the differential role of seaward or landward potential aeolian drift and sand movement in the coastal environment. The vector resultant arms point towards the direction in which the wind blows unlike the arms of the sand rose which represent the direction from which the wind is derived.

The sand roses have been plotted using the UNIRAS software on a SUN workstation The resultant offshore, onshore and effective drift potentials were calculated using a Fortran program. The listing of the program used to plot the roses is given in the Appendix III - C .

The *geometric variations of the monthly sand roses are used as surrogates to describe the wind regimes,* the drift potential and the sand transporting capability of the winds will be examined later while elaborating on the long term (months/years) sand transport rate and foredune growth at Tentsmuir.

4.6.3 Wind Regime Classification

Analysis of monthly sand roses for 1980-90 has permitted the classification of wind regimes in terms of the offshore, longshore and onshore components (drift potentials) of wind velocity.

Wind regimes are classed *'Unimodal'* (Fig. 4.10a & b) when either offshore or onshore component is the dominant wind resultant i.e. the ratio of the resultant drift potentials (RDP) of the two components is >9 and *'Bimodal'* (Fig. 4.9) when both the offshore and onshore resultants are present in significant magnitudes (ratio of RDP of the two components is between 2 and 9). *'Bimodal offshore'* and *'Bimodal onshore'* respectively can be considered as types of the bimodal regime occurring when winds to one or other direction are more significant. When the offshore and onshore components are nearly equal (ratio of the RDP is between 1 and 1.9) the wind regime

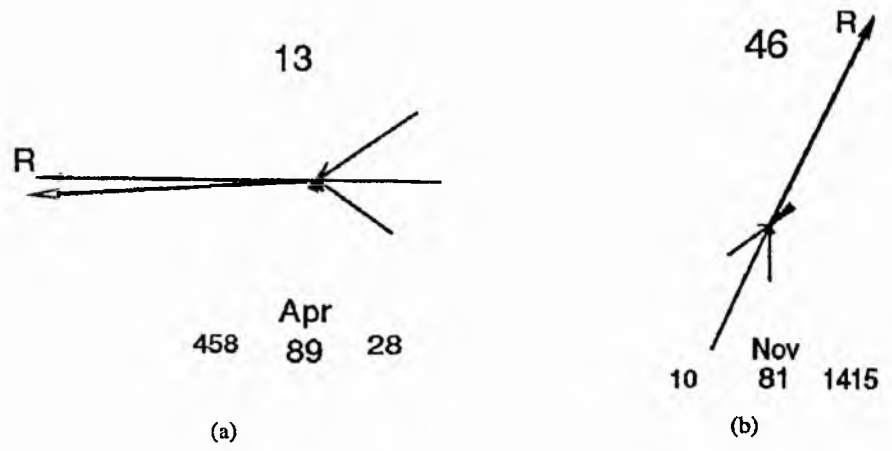

Fig. 4.10 Sand rose classification based on the ratio of the offshore and onshore drift resultants. (a) unimodal onshore, and (b) unimodal offshore.

is classed as *'Bimodal equal'*. *'Longshore'* wind regimes both northward and southward are essentially parallel to the coastline.

4.5.4. Description Of Potential Drift Regimes

The winter months from October to January are dominated by the unimodal offshore winds which are the south westerlies. Extremely high sand drift potentials (700 V.U. - 3959 V.U.) are recorded during this season. The month of March is also, at times, prone to these wind conditions. Some examples of the unimodal offshore wind regime are shown in Fig. 4.11.

Unimodal onshore (north easterly to easterly) wind regime is characteristic of the months of February to June (Fig. 4.12). The onshore sand drift potentials are not as high as the offshore ones ranging from 197 V.U. in June - 855 V.U. in March. At times anomalously high values of onshore drift potentials (1158 V.U.) are identified as for example during May 1988.

Dominantly offshore bimodal winds (Fig. 4.13) are much more abundant than the bimodal onshore wind regimes and are experienced throughout the year, particularly from September to December, occasionally in March and rarely in April. During some months the onshore component of the bimodal offshore wind regime has significant values (e.g. February 1981, January 1984, October 1980 and December 1983).

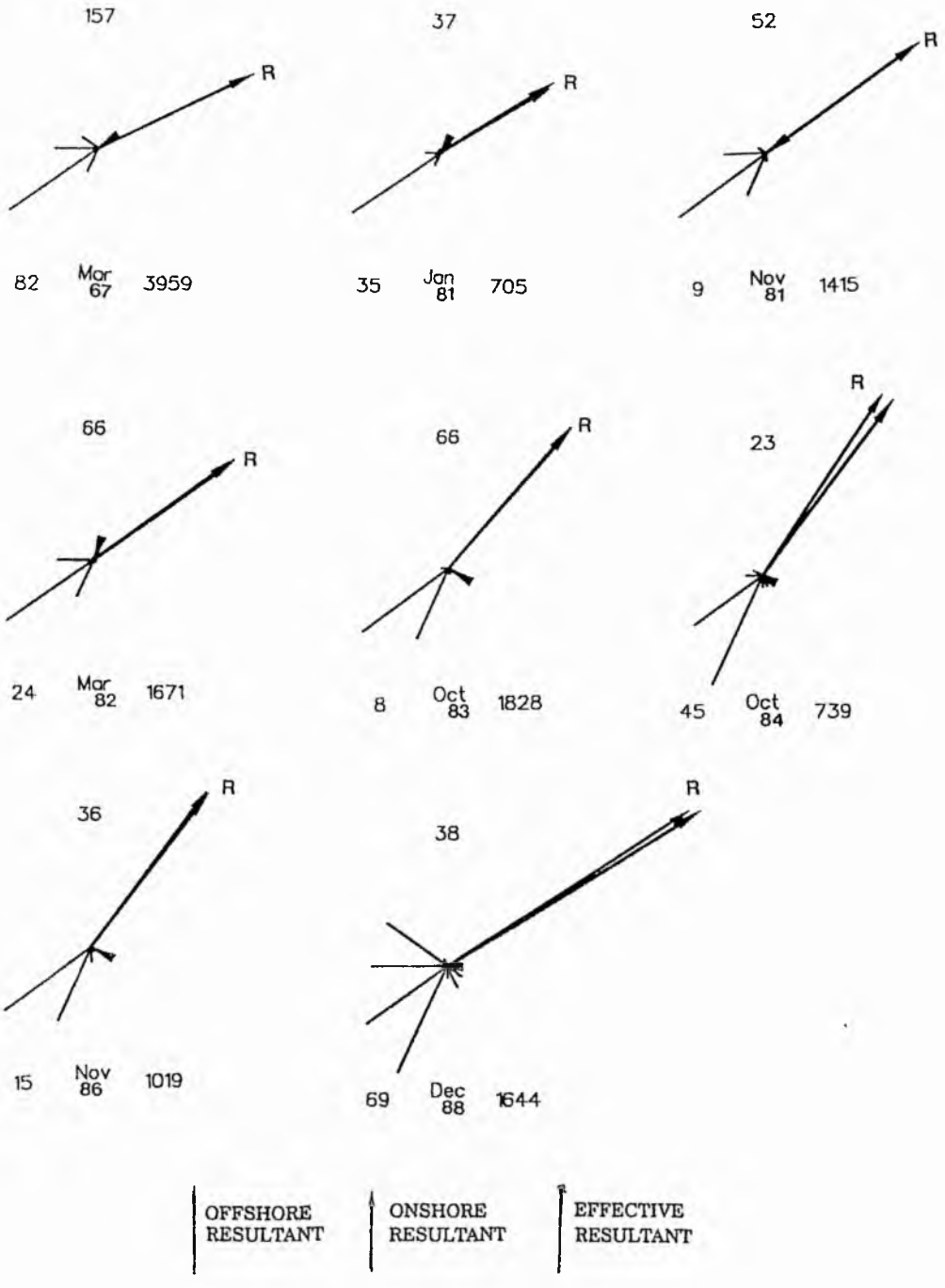

Fig. 4.11 Examples of monthly sand roses showing unimodal offshore wind regimes. Lines represent the sand drift potential from that particular azimuth and arrows point in the direction of the resultant drift potential. Numbers on the left, right and top centre of each sand rose are the onshore drift potential, offshore drift potential and reduction factor respectively.

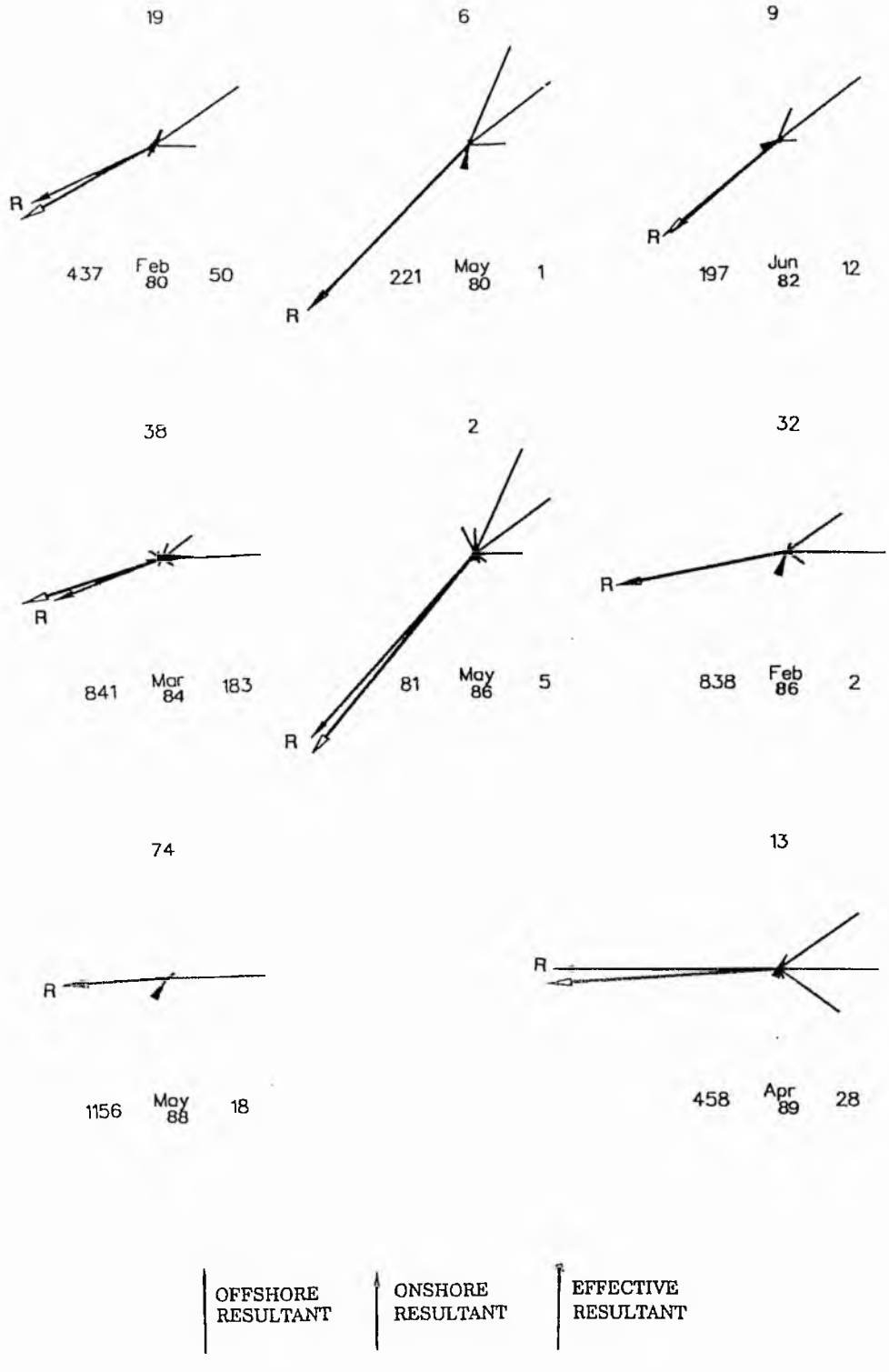

Fig. 4.12 Examples of monthly sand roses showing unimodal onshore wind regimes. Lines represent the sand drift potential from that particular azimuth and arrows point in the direction of the resultant drift potential. Numbers on the left, right and top centre of each sand rose are the onshore drift potential, offshore drift potential and reduction factor respectively.

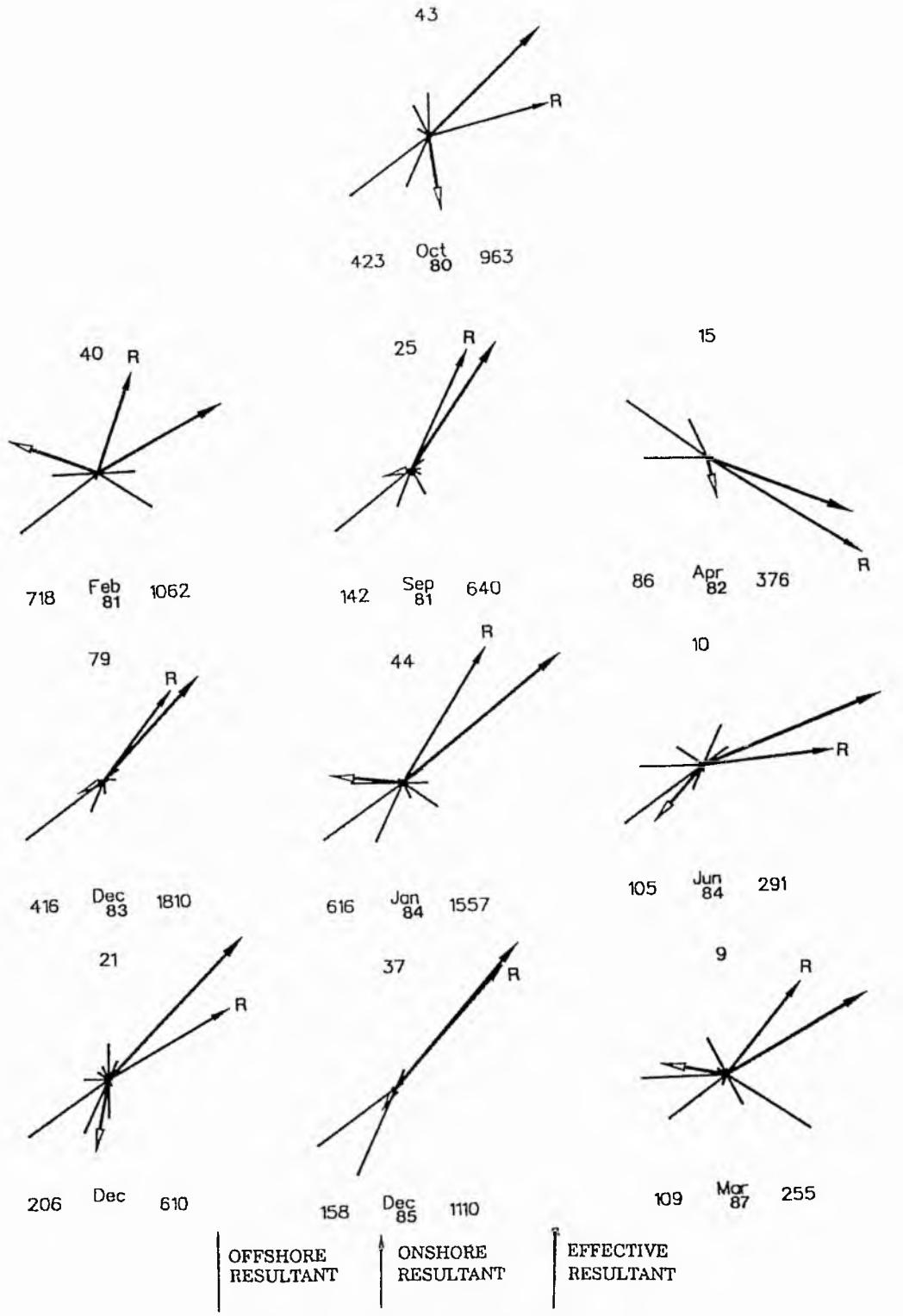

Fig. 4.13 Examples of monthly sand roses showing bimodal offshore wind regimes. Lines represent the sand drift potential from that particular azimuth and arrows point in the direction of the resultant drift potential. Numbers on the left, right and top centre of each sand rose are the onshore drift potential, offshore drift potential and reduction factor respectively.

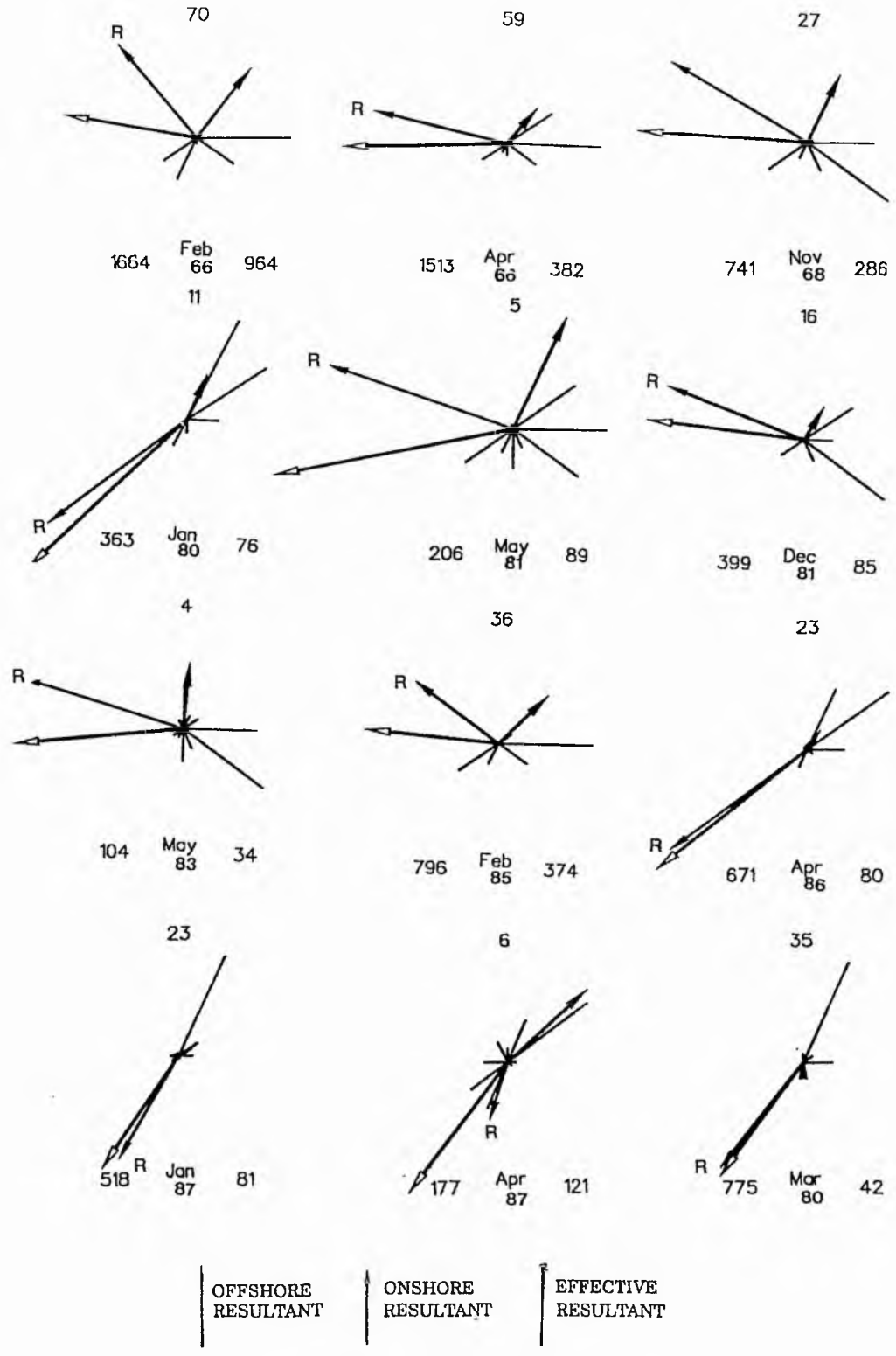

Fig. 4.14 Examples of monthly sand roses showing bimodal onshore wind regimes. Lines represent the sand drift potential from that particular azimuth and arrows point in the direction of the resultant drift potential. Numbers on the left, right and top centre of each sand rose are the onshore drift potential, offshore drift potential and reduction factor respectively.

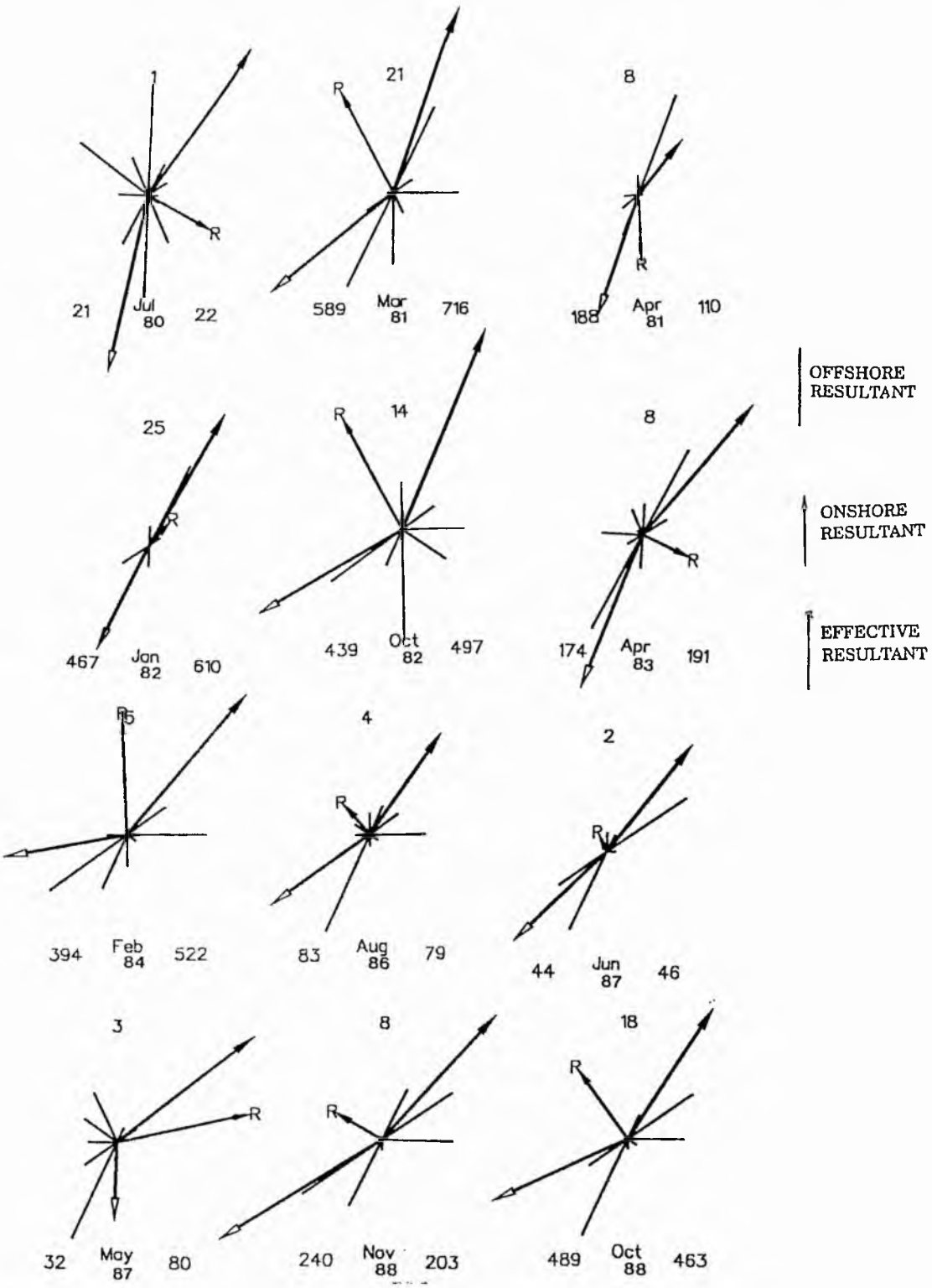

Fig. 4.15 Examples of monthly sand roses showing bimodal equal wind regimes. Lines represent the sand drift potential from that particular azimuth and arrows point in the direction of the resultant drift potential. Numbers on the left, right and top centre of each sand rose are the onshore drift potential, offshore drift potential and reduction factor respectively.

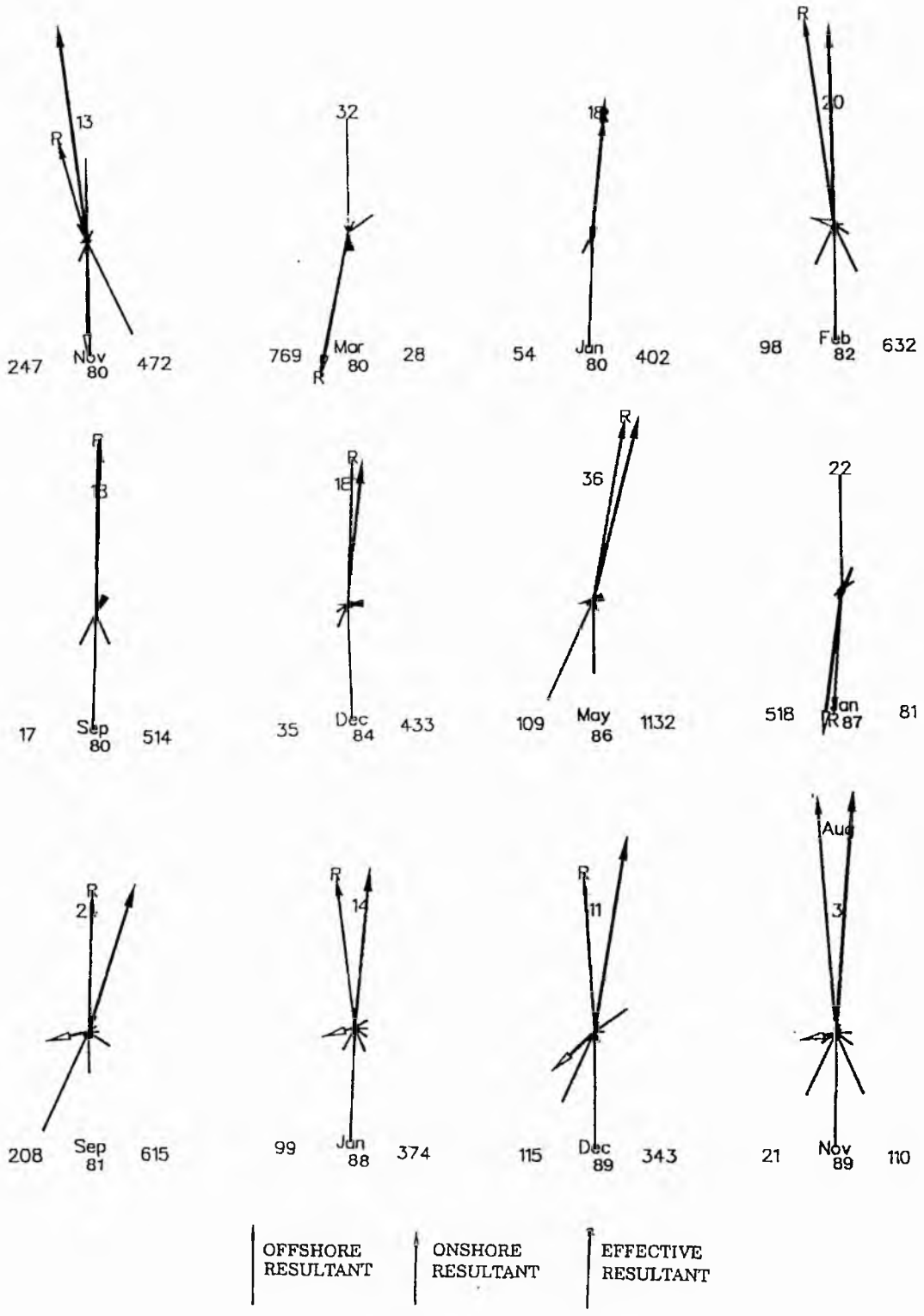

Fig. 4.16 Examples of monthly sand roses showing longshore wind regimes. Lines represent the sand drift potential from that particular azimuth and arrows point in the direction of the resultant drift potential. Numbers on the left, right and top centre of each sand rose are the onshore drift potential, offshore drift

Bimodal onshore wind regimes (Fig. 4.14) are prevalent during spring (April and May), late winter (January and February) and rarely in the months of November and December. The onshore sand drift potentials during the bimodal onshore winds ranges from 104 V.U. to 1664 V.U..

Bimodal equal wind regimes, characterized by nearly equal magnitudes of the onshore and offshore drift potential resultants (Fig. 4.15), operate during the summer months of June, July, August (Low RDP - 25 to 74 V.U.), occasionally in October and November (High RDP - 241 to 471 V.U.) and also in April (Intermediate RDP up to 188 V.U.).

Longshore winds are characteristic of the winter months (September to February) and blow towards north but rarely towards the south (Fig. 4.16). Bimodal longshore winds constitute significant magnitude of both northerly and southerly winds.

Monthly roses of sand drift potential for the entire 1980 - 1990 period are presented in Appendix III - D. A consolidated summary of the ten year monthly wind distribution is shown in Appendix III - E. Offshore winds dominate the distribution. However, both unimodal and bimodal onshore winds are also present.

From the above discussion it is evident that:

(i) Sand transport vector resultants are related to the seasonal component of the wind regime: strong offshore winds during the peak of winter; strong onshore winds during spring; bimodal dominantly onshore winds during late winter (January and February), autumn and spring (April and May); cyclic sea breeze and weak onshore winds during the summer months of June, July and August (Table 4.1).

(ii) Unimodal to bimodal wind regimes are prevalent at Tentsmuir. The magnitude of wind variability (ratio of the resultant drift potential and the drift potential) is between 0.55 to 0.85 indicating moderate to low variability of the prevalent winds. Both the intermediate (200-400 V.U.) and high drift potentials (>400 V.U.) recognised by Fryberger & Dean (1979) in the desert, are present in the area.

Table 4.1 Seasonal variation of wind regime along with drift potential and wind variability. Wind variability is the ratio of the resultant drift potential (resultant of all vectors) and the total drift potential (sum of all the vectors). Drift potentials-Low (<200 V.U.), Moderate (200-400 V.U.) and High (>400 V.U.). Wind variability- Low (0.85-1), Moderate (0.85-0.55), High(<0.55).

SEASON	WIND REGIME	DRIFT POTENTIAL	WIND VARIABILITY RDP/DP
WINTER	UNIMODAL OFFSHORE	HIGH	LOW
	LONGSHORE	MOD- HIGH	
AUTUMN	BIMODAL OFFSHORE	MOD-HIGH	MOD
SPRING	UNIMODAL ONSHORE	HIGH	MOD-HIGH
	BIMODAL ONSHORE	MOD	
SUMMER	BIMODAL EQUAL	MOD-LOW	HIGH

4.6 DISCUSSION AND CONCLUSIONS

The present chapter deals with the usage of long-term (ten year period 1980-90) wind data from a standard meteorological station for the evaluation of the aeolian activity in the Tentsmuir beach-dune complex. The analysis is a necessary precursor in an attempt to relate wind regime to known dune growth changes documented in sequential aerial photographs from the period 1978-1990.

Simple frequency analysis of the hourly wind data in terms of offshore and onshore components of the wind regime as a function of the total duration (number of hours) has been undertaken by Davidson-Arnott & Law (1990) while studying sediment supply to coastal foredunes at Long Point, Lake Erie, Canada. The methodology of using ambient wind velocity data from a proximal anemometer in order to study the prevalent wind regime and the resultant sand drift potential is widely applied to various continental and coastal dunefields (Fryberger & Dean, 1979; Fryberger & Ahlbrandt, 1979; Wasson & Hyde, 1983; Fryberger et al, 1984; Lancaster, 1983, 1985; Robertson-Rintoul, 1985; Havholm & Kocureck, 1988; Chapman, 1990)

The two-fold (frequency and vectorial) analysis of wind velocity data has resulted in the understanding of the prevalent wind regime in terms of the directional and magnitudinal variability within the temporal and spatial frames of reference.

While the frequency analysis gives a preliminary idea of the relative abundance of the different wind types operating in an area, the estimation of aeolian sand drift potentials and the construction of sand roses following the Fryberger & Dean method provides a fair estimation of the variability of the prevalent wind regimes and their concomitant sand entrainment capability (in terms of vector units). However, the drift potential of the winds calculated by this method are bound to be overestimations as the equation used to calculate the drift potential presupposes a dry, unvegetated sand surface. On a natural beach a whole host of factors such as vegetation, moisture, salt encrustations restrict the actual drift from the exposed surface.

The interpretation of the drift potential in terms of vector units does not provide a clear estimate of the potential sand input in realistic terms, since values of vector units are not straightforward numbers which can be used directly as a measure of sediment budget in any environment. More realistic values of long term potential sand transport rates and inputs in more understandable units as kg m^{-1} hr^{-1} and kg respectively have been estimated in Chapter 6. The Fryberger & Dean method provides a good visual interpretation of the variation in wind regime occurring at a site.

In general unimodal to bimodal winds of intermediate energy are the characteristic wind-types at Tentsmuir. The wind regime, as in many other locations, is composed of contrasting seasonal components (Glennie,1970, Havholm & Kocureck, 1988).

The analysis of the long-term wind velocity distribution in an area, the description of wind regimes and relating them to dune growth, is of great help in decision making for coastal landuse management (Chapman, 1990). Description of wind regimes and the accurate prediction of aeolian sedimentary processes are fundamental to the development of potential beach-dune sand transport models (Bauer *et al*, 1990).

Chapter 5

AEOLIAN SAND TRANSPORT: THE SHORT TERM EXPERIENCE

(with 12 figures and 3 plates)

Chapter 5

Aeolian sand transport: the short-term experience

5.1 INTRODUCTION

On beaches when a strong wind blows, aeolian sand transport is an important mechanism contributing to beach change. The determination of sand transport rate figures in projects to stabilise beaches in windy areas for protecting cultivated land from contamination by the intruding sand and for preventing river mouth closure. From the viewpoint of the dynamics of aeolian entrainment and deposition the measurement of sand transport rate is important as it provides the baseline against which theoretically computed or predicted values may be compared.

During the last fifty years, research on the rate of eolian sand transport within the beach and dune environments has not been very extensive. Most studies have been confined to wind tunnels in the laboratory except for a few sporadic field measurement contributions by Svasek & Terwindt (1974), Howard *et al,* (1978), Horikawa *et al,* (1985), Sarre, (1988), Illenberger & Rust, (1988), Gares (1987), Bauer *et al,* (1990), and Goldsmith *et al,* (1990). Most of the sand transport rate measurements on beaches have been aimed at the comparison of predicted models (e.g. Bagnold (1941), Kawamura, (1951), Kadib (1965) etc.) with measured transport rates (Sarre, 1988; Horikawa *et al,* 1985) with models corrected for slope dimensions of the dune (Howard *et al,* 1978), or in defining the limits (moisture, shear velocity) of the transport rate expressions (Svasek & Terwindt, 1974). Little has been achieved in the way of defining *detailed* aeolian sediment transfers and patterns of deposition along the coast for eg. the variability of transport rate within the beach (lower, middle and upper beach face) and dune (foredune and mature dune) sub-environments except for the recent works of Gares (1987), Bauer *et al,* (1990), and Goldsmith *et al,* (1990).

In consequence a programme of sand transport rate determination was undertaken on Tentsmuir beach. It was believed that the measurement of sand transport rates on the beach under the influence of winds from a range of directions would aid in defining sand flow paths and potential aeolian sand accumulation sites on

the coastline. By identifying the contributions of the different winds and the attendant sand transports which effect the beach-dune sediment budget an insight into the process-response relationships of the aeolian processes operative on the beach could hopefully be obtained. This form of information is of practical value for the management, control and conservation of the fragile beach-dune ecosystem.

The techniques employed in this exercise involved the use of sand traps to measure the transport rate and an anemometer array to enable calculation of the wind shear. As a broad range of sensors are available to carry out the sand transport rate observations a discussion of the techniques and apparatus used will be presented here.

5.2 TECHNIQUES

5.2.1 Anemometry

Many techniques are available for the measurement of wind speed and direction. The various types of anemometers used are propellors or cups (Goudie, 1981), hot wires or films (Shaw *et al,* 1973; Lang & Leuning, 1981) or acoustics (Shaw *et al,* 1973). The ultrasonic anemometer is the most sensitive although it suffers from a serious disadvantage in the present regard as data can be lost if a flying sand grain intersects an ultrasonic beam or hits an emitting probe. Hot wire anemometers have some problems of durability under the impact of blown sand grains and in stability for accuracy, especially in rain or sea breeze conditions. However, calibrated ultrasonic, cup, and propeller anemometers all give the same values of average wind speed for sampling time intervals longer than about ten minutes (Horikawa, 1987). Wind direction can be measured by a wind vane, by the strike of scour hollows downwind of obstructions or the crestal direction of ripples in the depositional pattern of wind blown sand. For field observations of wind speed Gill-type 3 cup anemometers are the most simple, reliable and accurate (±5% up to 50 m s^{-1}) devices with a life expectancy of 2 to 4 years (Sherman & Hotta, 1990). Gill anemometers require a recording device as they produce a signal either by directly generating a DC voltage, or by conditioning (using a photo chopper) an input AC supply. Hand held cup rotation anemometers are especially important for reconnaissance.

Wind speed measurements are interpreted as representing the mean horizontal flow of wind along a particular direction. Errors in wind speed measurement by rotation anemometers due to vertical, horizontal and longitudinal components of wind turbulence were analysed by Mac Cready (1966). The longitudinal error is due to the non-linearity of the rotation anemometers (Kaganov & Yaglom, 1976), which implies that the anemometer responds more quickly to the increase of wind speed than to the decrease. It is evident that the mean value of the rotation anemometer reading in a variable wind will be higher than the true mean value of the wind speed (overspeeding of about 10% at 2 m height). It is estimated that the total error both longitudinal and vertical can be of the order of 8 - 10 % (Kaganov & Yaglom, 1976; Izumi & Barad, 1970, Hogstrom, 1974).

5.2.2 Sand Traps

Sand traps aid in the measurement of the rate of sand movement. They help in the estimation of sand budget, taking into consideration the magnitudes and pathways of wind blown sand motion during a given time period. An efficient sand trap design should take into consideration both the mechanisms of transport and transport direction for the quantitative estimation of total aeolian load. There are two basic types of traps, vertical traps which stand erect on the sand surface to catch the sand which passes through a section, and horizontal traps which are buried with their tops flush with the sand surface and catch the sand which falls into them. Both the traps can be configured as total quantity type or distribution type. A more sophisticated technique being used at some unattended monitoring sites involves the use of automated electronic sand flux sensors (Breed & McCauley, 1991). A review on the subject of trap types and their efficiencies can be found in Horikawa (1987).

The main advantage of using the vertical trap lies in the fact that sand can be collected from any direction (Crofts, 1971; Larsen, 1971) the major disadvantage being that the presence of the vertical trap tends to modify the wind flow. Several vertical traps have been designed to collect sand at different heights (Sharp, 1964; Jensen, 1984; Bagnold 1938a), from different directions about an axial rod (Fryberger *et al,* 1984) or with a venturi vacuum generator in order to minimize stagnation

pressure within the trap and the problem of scour in front of the trap (Illenberger & Rust, 1986). A very simple and inexpensive trap was developed by Leatherman (1978). For the measurement of sand transport rates on the Tentsmuir beaches a modified version of the Leatherman (1978) vertical sand trap has been used.

5.2.2.1 Construction of the modified Leatherman (1978) trap

The trap consists of a 100cm long PVC tube, 3.5 cm. in diameter with two slits cut down on opposite sides for half the tube length (Fig. 5.1). The front slit is 1cm. wide whereas the wider rear slit, 2.5 cm in width is covered with a nylon mesh of 0.1 mm. aperture. In use the lower 30 cm of the trap is inserted into the ground and the base closed by a removable rubber bung. The original Leatherman (1978) trap differs from the modified version used here in the absence of an inner tube lining in the latter. The narrower slit which is 1cm in width is open for grains in motion to enter the trap. The screen over the slit allows the air to flow thereby reducing the problem of back pressure and also prevents the grains from exiting. The contents of the trap can be emptied by removing the lower detachable rubber bung. Since the main objective of the study was to monitor short term (15 minutes) aeolian transport activity across the coastal complex it was felt that the construction of the trap could be further modified. The length of the trap sunk into the ground was reduced from 25 cm to 15 cm in order to reduce the time which was spent in digging into the ground when it was important that the measurements be made simultaneously and quickly because in the area studied strong winds are generally followed or accompanied by precipitation which render the experiments futile.

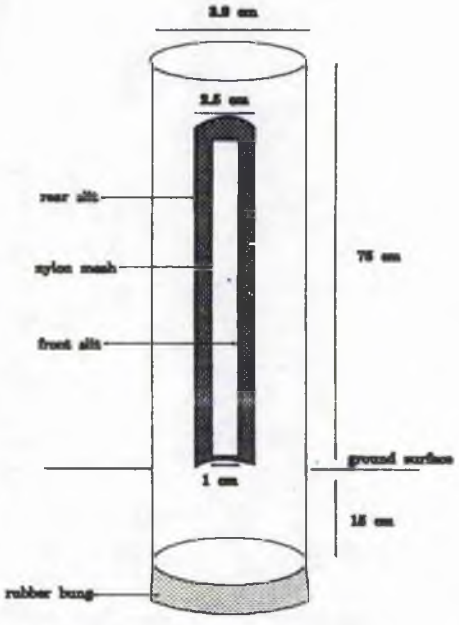

Fig 5.1 Diagram of modified version of Leatherman trap used in the experiments. Diagram not to scale.

5.2.2.2. Use of the trap

Field observations regarding the use of the trap in terms of efficiency, orientation, deployment and other problems that occur while using them (Wal & McManus, 1990) are given in the following paragraphs.

5.2.2.3 Efficiency of the trap

Trap efficiency can be defined as the ratio of trapped sand to the actual quantity of blown sand (Chepil & Milne, 1941). Efficiency determinations are usually carried out in wind tunnels. Whereas it is relatively easy to assess the relative efficiencies of different trap designs, absolute efficiencies are more difficult to establish (Pye & Tsoar, 1990). The efficiency of the Leatherman trap has been investigated by Marston (1986) and McCluskey (1987) who cite a figure of 70% which has been used in the present study to provide a correction factor for measured transport rates.

5.2.2.4 Reproducibility of the measurement

In order to test the reproducibility of data sets, obtained from traps under identical conditions, a series of four traps were installed along the beach during SW off-shore winds. The traps retained similar amounts of sand ranging from 10.3 - 10.8 gms (Fig. 5.2).

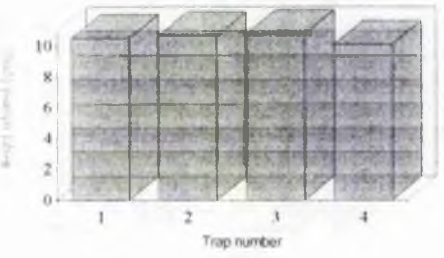

Fig. 5.2 Sediment yield of traps placed a meter apart on the beach to test reproducibility of results.

5.2.2.5 Slit orientation

Regarding slit orientation, care should be taken that the slit is flush with the ground surface if this is not done then some of the grains moving by surface creep may not be trapped thus limiting the efficiency of the trap The open slit should face the most prominent wind direction. If a situation arises in which the wind direction fluctuates rapidly during the period of time exposure, the traps may then be placed in a circular or arcuate array to take account of the varying directions of sediment transport. During the present investigation, which provides over 50 deployments this

5.2.2.6 Problems of scour and moisture

Intuitively one might expect that principally dry sand is transported in response to wind action, however observations reveal that sand grains having an appreciable amount of moisture (up to 1.5%) are also transported by the wind (especially high velocity winds >12 ms^{-1}). When such materials enter the trap slit there may be an accumulation of the sand at the mouth of the trap due to surface tension of water films on the moist grains (Fig. 5.3). This causes the trap entrance to close up although the lower end of the trap is still empty thereby limiting the trapping capacity of the instrument under such conditions. Although this problem has never been described by earlier workers, it is necessary to monitor the traps very carefully and expose them for shorter time periods (maximum period of 15 minute intervals) during experiments under very high wind velocity conditions in order to minimise the problem. On many occasions the field experiment had to be abandoned due to accompanying precipitation during strong winds, but it was interesting to observe that even under such conditions the sand movement occurred sporadically under the influence of an occasional strong gust.

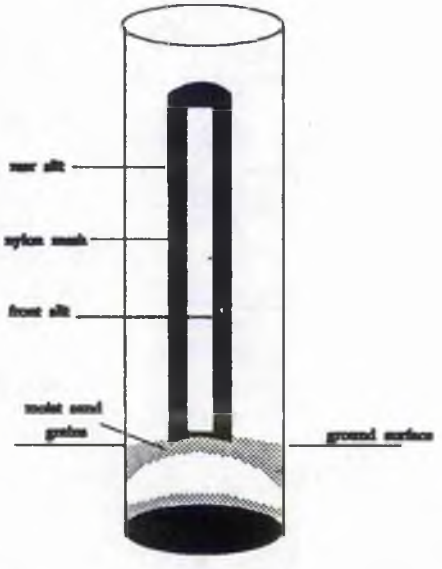

Fig. 5.3 Problem of trap entrance closure due to moist sand.

The problem of scour at the base of the trap was not encountered during this project. This may have been because the time for which the traps were exposed (15 minutes) was too short for such a problem to develop. Additionally the sand transport measured was generally over a fairly moist inter-tidal zone, whereas the development of a scour is normally associated with dry surface areas which are easily scoured by the wind.

5.2.2.7 Reasons for the trap choice

The low cost (£10 per trap) and ease of construction of the trap and good reproducibility of the data sets were among the other factors which led to the selection

of the Leatherman trap for this study. The traps were small enough to permit rapid deployment which enabled virtually simultaneous measurements at a range of adjacent sites for comparative purposes.

5.2.2.8 The experimental setup

Transects were established across the beach at several sites along the coastline, namely Tentsmuir, Kinshaldy and Earlshall for repeated trapping measurements to enable computation of aeolian sand transport rates. The traps were emplaced in an array of 5-8 installations in various beach-dune sub-environments during conditions of dominantly offshore, onshore or longshore winds (Fig. 5.4, Plate 5.1). Sub-environments examined were the primary dune, embryo dune, upper, middle and lower beach face areas, into which traps were inserted by digging a hole in the ground with a hand trowel and positioning the entry slit base flush with the ground surface. It was impracticable to place the units very close to the water's edge due to the problem of ground water seepage into the base of the trap. However, reduction of the length (length embedded into the ground surface) of the trap enabled the traps to be placed within 10 m of the water's edge in order to explain the limiting role of surface moisture on the sand transport rate. The traps were exposed to winds of 4 - 20 m s^{-1} for 15 minutes. Once exposed the traps were monitored very carefully to ensure that they were not clogged by the moist sand and that the slit faced the dominant wind direction. After the period of exposure the sand in the trap was emptied into air tight

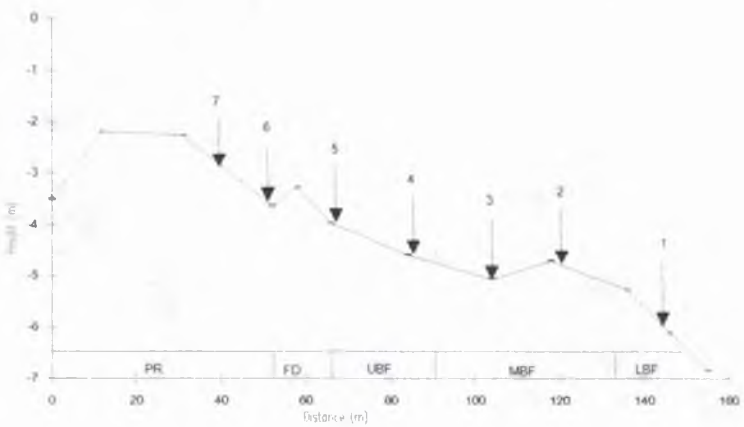

Fig. 5.4 Trap locations along beach-dune sub-environments. PR- primary dune ridge, FD-foredune, UBF- upper beach face, MBF- middle beach face, L.B.F- lower beach face.

polythene bags, brought to the laboratory and weighed immediately to ensure minimum moisture loss. The samples were then oven dried at 110^{0}C, reweighed and the moisture percentage determined. Sieving and grain size analysis of the samples was then carried out to establish the mean grain size of the trapped sand. The wind velocity was measured, at a series of heights adjacent to trap locations, using cup rotation anemometers to enable calculation of shear.

5.3. WIND VELOCITY MEASUREMENTS

For measuring velocity profiles (to derive u_*) it is necessary to deploy vertical arrays of anemometers and employ some form of recording device. At the inception of the measuring programme a single hand held cup anemometer was used to measure wind speed at a height of 2 m. However, one single reading was insufficient for the determination of wind shear, for which a profile of velocity measurements is required. For the bulk of the measuring work an array of three cup rotation Cassella anemometers (on loan from the Dept. of Civil Engineering, University of Aberdeen) was used. These were clamped to a 2.5 m long steel rod which was in turn screwed to a heavy metal plate which was inserted into the ground to give a secure vertical orientation (Fig. 5.5). The anemometer setup was emplaced in the middle of the beach and wind velocity determinations made at 50 cm, 100 cm and 200 cm above the ground surface. Each anemometer produces one output pulse per revolution which inputted into an integrated circuit pulse counter, the potential being supplied by a 5.6V d.c. dry cell battery. A precision timer gates the pulses to the counter for a preset period of 60 seconds and total count is displayed on an LCD screen. The wind

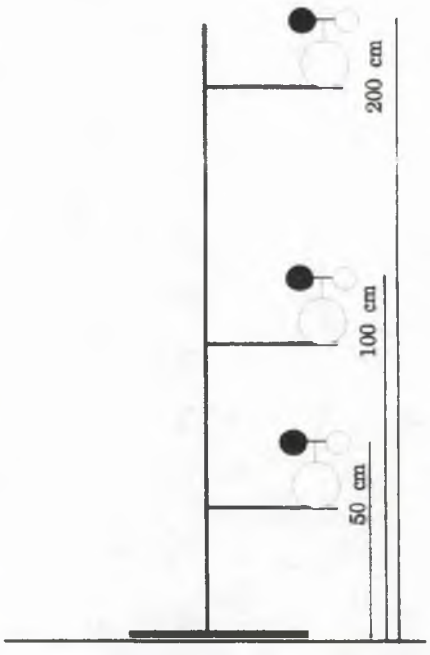

Fig. 5.5 Anemometer array used in the field experiments along the middle beach face.

direction was determined by the axes of the aeolian landforms produced on the beach. However for the taking of multiple simultaneous measurements the three anemometers are connected to a data logger which gives the number of revolutions of the cups during a minute. This number is then converted to the speed in m s^{-1} by a manufacturers calibration graph supplied with the anemometer. The wind speed measurements were then plotted as a wind velocity vs. logarithm of height plot. Lines were drawn across the points and the gradient or the slope of the line which is also a measure of the shear velocity was calculated using equation 3.3.

In all cases the direction of the wind was determined indirectly from measurement of the axes of aeolian landforms produced during sand migration across the beach surface.

5.3.1 Wind shear and bed roughness

Measurement of wind velocity in wind tunnels has been attempted by various researchers (Bagnold, 1941; Chepil, 1964; Chepil & Woodruff, 1963; Gerety & Slingerland, 1983; Horikawa *et al,* 1986; Belly, 1964) The measurement of shear velocities on natural beaches (O'Brien & Rindaulb, 1936; Deacon, 1949; Hsu, 1971, 1973; Svasek & Terwindt, 1974; Sarre, 1988; Bauer *et al,* 1990) enables the researcher to use this value in the various sand transport rate models (in most models the rate of transport is proportional to the cube of the shear velocity) to calculate the potential sand transport in kg s^{-1} m^{-1} width of the beach.

The wind speeds ranged from 4 m s^{-1} to 20 m s^{-1} at 2 m height. Wind velocity profiles during sand movement on the Tentsmuir beach, showed that the shear velocity ranged from 18.5 cm s^{-1} (at the threshold of sand movement) to 52 cms^{-1} (Fig. 5.6) during active sand transport. Since a single anemometer array was available the measurement of wind velocity profiles was restricted to the middle beach face sub-environment.

The projected focal point (u', z', $\pm$ 5% instrumental error) on the Tentsmuir beach corresponds to a wind speed of 1.75 ms^{-1} at a height of 0 .03 cm (Fig. 5.6). Numerous workers have reported their inability to successfully compute the empirical determination of the focal point (Zingg, 1953; Howard *et al,* 1978; Sarre, 1988) and

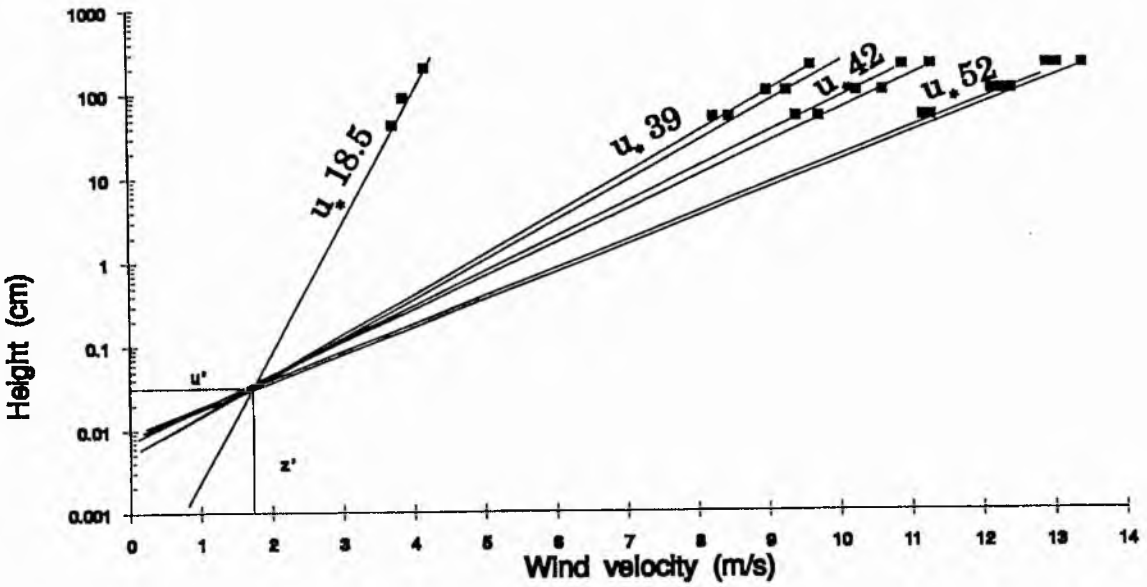

Fig. 5.6 Wind velocity profiles on Tentsmuir beach. Focal point is the intersection of u (velocity at z) and z (surface roughness height). u* is the shear velocity in cm s^{-1}.

have either resorted to the use of formulas for the determination of the z as a function of the grain diameter or have used the values determined empirically by other workers. A number of workers have given different values for the focal point u, z e.g. Bagnold (1941, p.60) (2.5 m s^{-1} at 0.3 cm), Belly (1964) (2.7 m s^{-1} at 0.3 cm), Horikawa *et al*, 1983 (2.5 m s^{-1} at 0.6 cm), Chepil & Woodruff, 1963 (2.14 m s^{-1} at 0.6 cm), Hsu (1973), (2.75 m s^{-1} at 1 cm). The importance of the focal point has been emphasized in chapter 3, as it links the shear velocity to the wind speed at any arbitrary height. This focal point determined in the field conditions on Tentsmuir beach has been linked to the mean wind speed at 10 m height, gathered from the long term monthly (10 years) wind data from the meteorological station located in the field area, to calculate the corresponding shear velocities. This will be used later in the thesis to estimate long-term sand input potentials for the 1980-1990 period.

The comparison of wind direction records from the adjacent Leuchars meteorological station with the simultaneous measurement of wind flows in the field, with the anemometers, indicate that the flow field was fairly constant in approach to the beaches. Any differences in the measured sediment transport cannot be attributed to a spatially varying directional flow field. Since, a single anemometer array was

available it was difficult to measure the *absolute* spatial variations of the magnitude of flow velocity across the beach-dune profile. While conducting wind velocity measurements across a beach and dune at Castroville, California Bauer *et al,* (1990) found that the temporal fluctuations in wind speed and direction across the beach and dune system were similar. However, they also observed the spatial variation of the absolute magnitude of the wind velocity noting that the fastest flow velocities occurred at the dune crests and smallest in the lee of the dunes.

5.4 SOURCE OF SAND & GRAIN SIZE ANALYSIS OF TRAPPED SEDIMENTS

Before embarking on the description of the rates of sand transport on the beach, it will be necessary to comment on the source of sand which is available for entrainment by the wind. Any wind (whether offshore, onshore or longshore) causes the drier exposed parts of the beach to become deflated. The offshore winds in particular deflate the exposed dune face and also both the upper and middle beach face areas (Plate 5.2). The longshore winds move the sand along the exposed dune face and along the drier upper beach face zone. The onshore winds on the other hand move the dry sand available in the middle beach face only (during rising tide) and also the lower beach face during low tide. Thus, at any one time the source of sand is compartmentalised and emanates from a well defined strand line beyond which the sand is relatively dry.

The sediments retained in the traps (Appendix IV-A) placed on beaches during onshore winds were unimodal in distribution peaking at 1.7 ϕ along the lower beach face, showing a bimodal distribution (peaking at 1.8 & 2.38 ϕ) along the middle beach face sub environment. The sediments showed a unimodal distribution this time peaking at 2.38 ϕ for the traps placed in the upper beach face and incipient foredune subenvironment. The grain size distribution of the trapped sediments is in many ways similar to that of the beach-dune sediment distribution discussed in section 2.3.1 (Fig. 2.11). Hence the sediments entrained by the wind are those that are surficially available in the various subenvironments. However, along the upper beach face and foredune the

wind entrains only the finer sediments, although the beach surface may contain coarser fractions.

SEM study of the trapped sediments showed that the bulk of the material was composed of sub-angular to sub-rounded quartz grains with conchoidal fractures. Coarser fractions of sub-angular shell fragments were also present. In places the quartz grains were seen to be armoured by a layer of halite crystals which were formed probably as a result of salt spray along the beach (Plate 5.3).

5.5 TYPES OF WIND FLOWS AND THE SAND MOVEMENT

While studying the rate of sand transport on the Tentsmuir beach, it was observed that the sand movement took place under the influence of varying wind velocities and it has been possible to identify the patterns or modes of transport associated with low, moderate and high velocity wind flows over very small time intervals for example 10 minutes. The 'threshold of sand movement' referred to in this section applies to visible sand transport across the beach under the influence of a threshold wind speed i.e. when the sand is first seen to move from an initial phase of no movement. This threshold wind speed determined from visual experimental observations was found to be approximately 4.3 ms^{-1} at 2 m height.

5.5.1 Constant very high wind velocity

Under favourable conditions of tide and weather winds blowing at velocities above 9 ms^{-1} moved the sediments *en masse* i.e. all portions of the beach and the exposed dune surface were subjected to sand movement simultaneously. This resulted in a considerable amount of sand transport in the form of horizontal eddies during the observation period. The wind velocity fluctuated without falling to zero i.e. the velocity ranged between 9.45 m s^{-1} and 15 m s^{-1}. The sediment was transported continually at greater or lesser rates, with the sediment transport never ceasing completely. However it is more common for sediment to respond to winds with occasional gusts in which the wind velocity may drop to zero after reaching a maximum value e.g. of about 15 m s^{-1} which results in a corresponding intermittent sand movement across the beach.

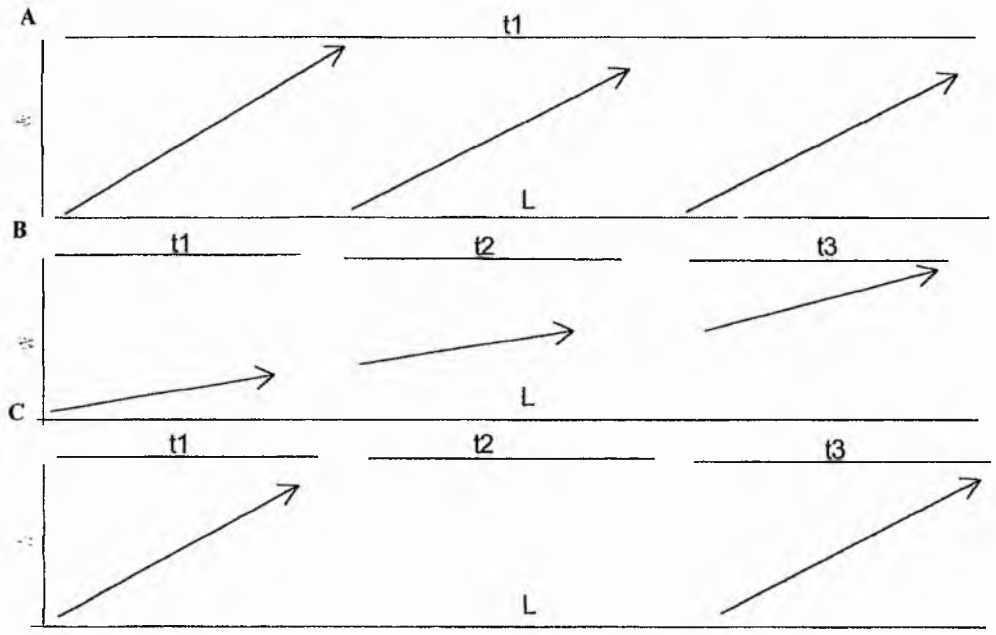

Fig. 5.7 Types of wind flows. A-high velocity flow (>9 ms^{-1}). B-moderate velocity flow (<9 ms^{-1}). C-low velocity (< 6 ms^{-1}) with occasional gusts. t1, t2 and t3 is the time interval (approximately a minute each). W-beach width. L-beach length. (Not to scale) The pattern of sediment movement is indicated by arrows.

5.5.2 Moderate velocity wind flows

Wind velocity ranging from 6 - 9 ms^{-1} results in small quantities of sand transport across the beach face. The sediment is moved in distinct fronts, apparently related to local turbulence. Locally ribbons of sand are set in motion . The sand moves across different parts of the beach dune face system at different times.

5.5.3 Low velocity wind flows

Low wind velocity ranging from 4.3 - 5.9 ms^{-1} results in very low sand transport rates as no sand transport takes place below 4.3 ms^{-1}. During low velocity wind flows just above the threshold, the sand movement appears to be intermittent in the form of occasional gusts. Sand transport under the influence low velocity wind flows is not always easily discernible by the eye but can be readily monitored by the sand traps. The sand movement is very similar in form to that recorded as 'burst and

sweep' phenomena in relatively quiet water flows with discontinuous motion of clouds of grains along the bed.

5.6 RATE OF SAND TRANSPORT

The aeolian sand transport rate experiments have been conducted during active sand transport conditions under the influence of winds of variable magnitude and direction. The traps were exposed for 15 minutes and several experimental runs were made during each experiment. Appendix IV-B shows results of field observations of aeolian sand transport on sixteen different days between March 1990 to September 1991. Experiments were conducted on occasions only when the wind velocity was above ~8 ms^{-1} at 2 m height.

Figure 5.8a shows a plot of measured transport rates of 56 trap results against the corresponding shear velocities measured during field observations. The sand transport rates vary from subenvironment to subenvironment and no clear relationship between sand transport rate and shear velocity is discernible. However, sand transport rate in the different subenvironments plot in distinct envelopes (Fig. 5.8b). Maximum sand transport rates are observed along the middle beach face subenvironment ranging from 0.01 to 0.3 kg s^{-1} m^{-1} x 10^{-1} for shear velocities ranging from 0.2 to 0.46 m s^{-1}. Lowest sand transport rates, for similar shear velocity spread, occur in the foredune (Fig. 5.8a & b). Lower beach face and upper beach face I envelopes fall in between the middle beach face and foredune envelopes. Sand transport rate envelope of the upper beach face subenvironment is very broad and envelops both dune and lower beach face envelopes (Fig. 5.8b).

5.6.1 Offshore sand transport

Strong offshore winds (>9 m s^{-1}) create deflation surfaces in the upper beach face area because all the sand is being transported towards the sea. Hence low sand transport rates 0.005 - 0.03 kg s^{-1} m^{-1} x 10^{-1} are observed along the upper beach face once this zone has been stripped of the mobile sand. The sand is moved from the upper beach face towards the middle beach face environment, and in consequence this zone is characterised by the presence of large volumes of mobile sand yielding

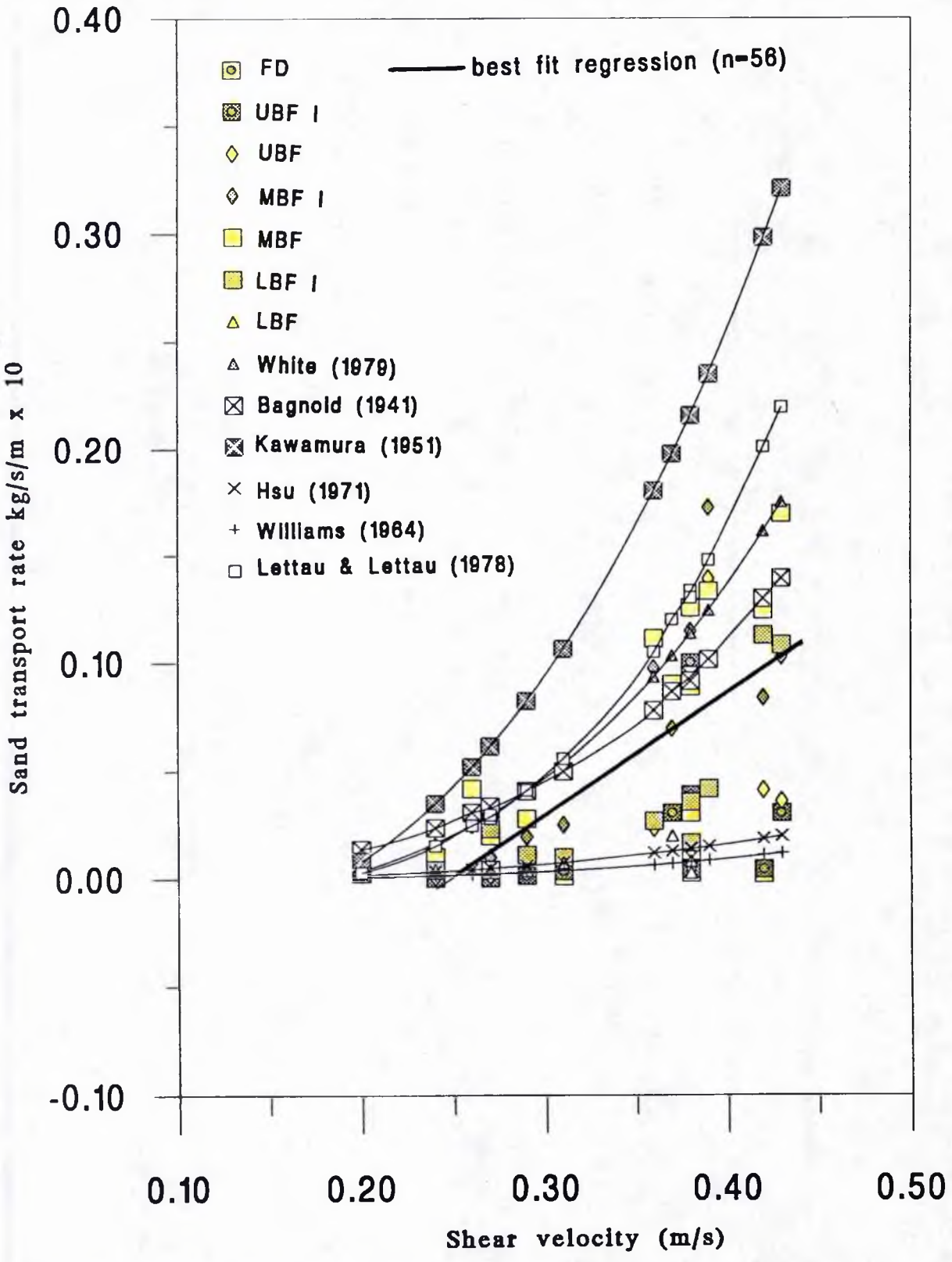

Fig. 5.8a Comparison between measured transport rates in various beach dune sub environments with those predicted by White (1979), Lettau & Lettau (1978), Kawamura (1951), Bagnold (1941) and Hsu (1971).

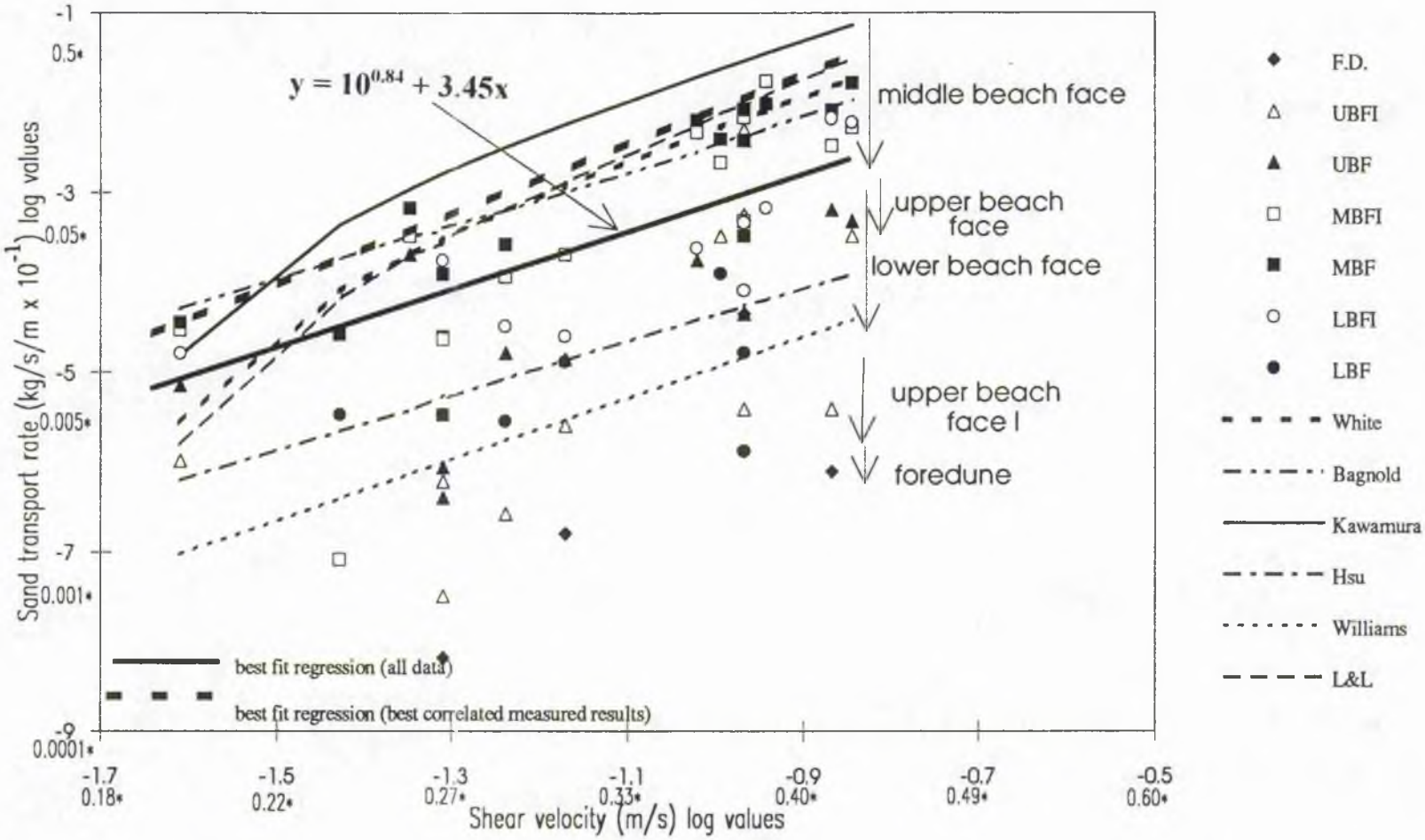

Fig 5.8b Comparison between the measured sand transport rates and those predicted by various workers. Logged values of shear velocity and sand transport rate have been used. Best fit regression for all the measuresd rates and middle beach face trap results are also shown. Envelopes of sand transport have also been marked. Middle beach face envelope refers to both M.B.F and M.B.F. I data. Similarly lower beach face refers to L.B.F and L.B.F I data. * - corresponding non log values.

high local sand transport rates ranging from 0.08 - 0.16 kg s^{-1} m^{-1} x 10^{-1}. As a result of the bonding effects near the water margin the rate of sand transport decreases (0.019 to 0.03 kg s^{-1} m^{-1} x 10^{-1}) across the lower beach face.

West sands - transect 12 (Fig. 5.9)

Due to the complete absence of a foredune apron along the backshore the sand transport rates in the upper beach face area ranged from 0.03 to 0.04 kg s^{-1} m^{-1} x 10^{-1} during wind speeds > 9 ms^{-1}. Under the same wind conditions very high sand transport rates were encountered along the middle beach face sub-environments (~0.08 to 0.16 kg s^{-1} m^{-1} x 10^{-1}). The bonding by water along the lower beach face reduced the transporting capacity of the winds to a value ranging from 0.019 to 0.03 kg s^{-1} m^{-1} x 10^{-1}.

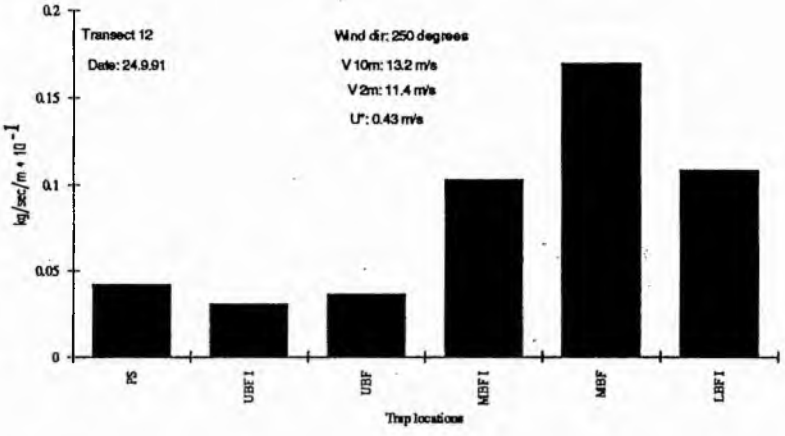

Fig. 5.9 Example of offshore sand transport at West Sands (transect 12). FD - foredune; UBF - upper beach face; MBF - middle beach face; LBF - lower beach face.

The transport rates determined during medium velocity winds < 9 m s^{-1} followed the same trend of maximum transport rates along the middle beach face (~ thrice that of the UBF and LBF values) with reductions along the upper and lower beach face, though the rates were smaller in magnitude. Across the landward face of the primary dune ridge offshore sand transport rates were very low as in comparison with those on the open beach. However the seaward facing dune face composed of unvegetated sand blowouts yielded transport rates (0.04 kg s^{-1} m^{-1} x 10^{-1}) comparable to those of the upper beach face area.

Kinshaldy - transect 7

At Kinshaldy the transport rates along the lower (0.019 to 0.038 kg s^{-1} m^{-1} x 10^{-1}) and middle beach face (0.083 to 0.16 kg s^{-1} m^{-1} x 10^{-1}) were comparable to West sands . However, the transport yield along the upper beach face (0.004 to 0.005 kg hr^{-1} m^{-1}), foredune (0.000002 to 0.002 kg s^{-1} m^{-1} x 10^{-1}) and the primary dune (0 to 0.00007 kg s^{-1} m^{-1} x 10^{-1}) area at Kinshaldy is much lower than the yield along the middle beach face (0.083 to 0.16 kg s^{-1} m^{-1} x 10^{-}).

Tentsmuir - transect 4

At Tentsmuir during low velocity winds (6-7 ms^{-1})the transport rates ranged from 0.004 - 0.005 kg s^{-1} m^{-1} x 10^{-1} along the lower beach face, 0.008 - 0.01 kg s^{-1} m^{-1} x 10^{-1} along the middle beach face and 0.001 - 0.002 kg s^{-1} m^{-1} x 10^{-1} along the upper beach face.

5.6.2 Onshore sand transport

Kinshaldy - transect 7 (Fig. 5.10)

Field measurements of sand transport rates during onshore winds (>9 ms^{-1}) on the beach showed increasing rates of sand transport landward of the low water mark and a subsequent decrease of sand transport beyond the potential foredune especially when the area is densely covered with the long dune grass (e.g. *Ammophila sp.*). An abrupt gradient in surface shear stress between the wind and vegetation causes sand to be deposited quickly in this zone. This results in the accumulation of large volumes of aeolian sand in the backshore and potential foredune area. Maximum sand

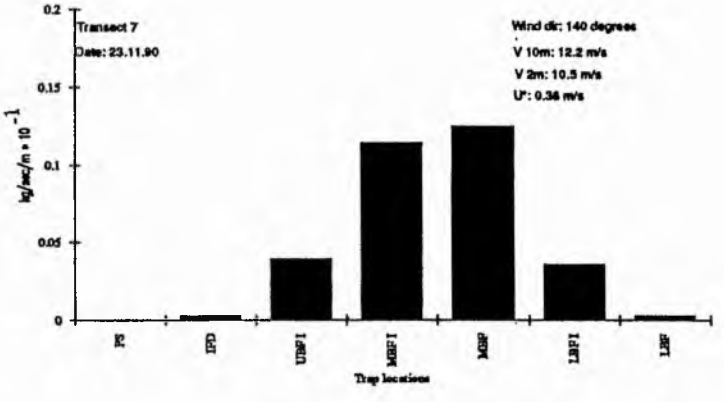

Fig. 5.10 Example of onshore sand transport at Kinshaldy (transect 7). PS - primary dune slope (seaward); FD - foredune; UBF - upper beach face; MBF - middle beach face; LBF - lower beach face.

transport rates are found in the middle beach face (0.12 to 0.13 kg s^{-1} m^{-1} x 10^{-1}), whereas net deposition occurs along the backshore and potential foredune areas (rates of approximately 0.01 kg s^{-1} m^{-1} x 10^{-1} are encountered in this zone) as no sediment is trapped in the primary dune area beyond the foredune zone. However, vertical accretion in the primary dune area (with dense *Ammophila* growth) appears to be primarily by grainfall deposition. Since, the Leatherman sand trap in this zone does not account for the sediment transported by grainfall, therefore, a sieve type trap must be deployed in the primary dune zone. The transport rates along the lower beach face range from 0.01 to 0.04 kg s^{-1} m^{-1} x 10^{-1}.

West Sands - transect 12

During moderate onshore winds (5-7 m s^{-1}) i.e. the daily sea breeze during summer significant transport rates (0.025 kg s^{-1} m^{-1} x 10^{-1}) have been across the unvegetated dune crest at West sands.

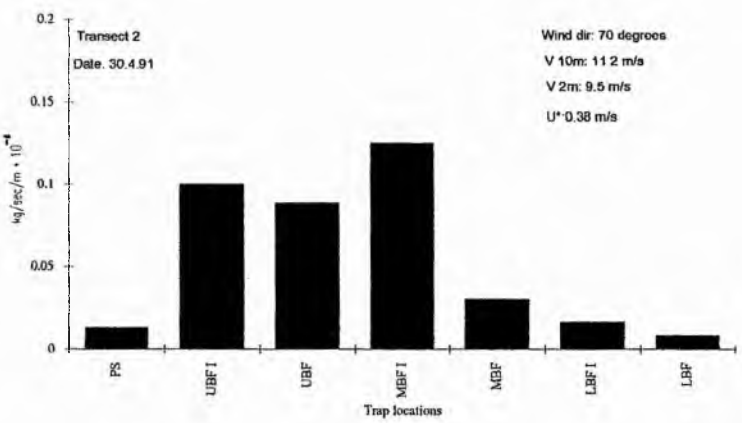

Fig. 5.11 Example of longshore sand transport at Tentsmuir Point (transect 2).PS - primary dune slope (seaward); FD - foredune; UBF - upper beach face; MBF - middle beach face; LBF - lower beach face.

5.6.3 Longshore sand transport

The longshore winds (>9ms^{-1}) are able to mobilise sand much more efficiently along the upper and middle beach face sub environments than the offshore winds (Fig. 5.11). However, their sand entrainment capability along the lower beach face is lesser than either the offshore or onshore winds. Very high upper and middle beach face longshore transport rates (0.1 to 0.13 kg s^{-1} m^{-1} x 10^{-1}) have been found at Tentsmuir point (Fig. 5.11).

5.7 RELATIONSHIP BETWEEN SHEAR VELOCITY AND SAND TRANSPORT RATE

As stated earlier the sand transport rate measured in various subenvironments along the Tentsmuir coast is not a function of shear velocity alone, since a wide scatter exists when the shear velocity is plotted against measured sand transport rates (Fig. 5.8a & b). However, a regression line for the fifty six trap results, on plotting the normal log values of the measured transport rates and shear velocity yields (Fig. 5.8b)

$$q = 0.84\ u_*^{3.45}$$

While elaborating on the results of the aeolian sand transport rate measurements along Saunton Sands, S.W. England, Sarre (1988) has described the transport rates to be a power function, of a similar order of magnitude, of shear velocity.

The trap results from various sub-environments indicated that the coefficient of determination (r^2) for the transport rates vs. shear velocity plots was most significant for the measurements made in the MBF, MBF I and LBF I sub-environment (r^2=0.69, 0.65 and 0.68 respectively) (Appendix IV-C). Since LBF I subenvironment is a zone bordering the middle and lower beach face zones, data from these environments will now be referred to as 'best correlated measured results'.

5.8 COMPARISON OF MEASURED WITH PREDICTED RATES

One of the questions to be answered in the context of aeolian sand transport across the beach-dune environment is 'How much sand is actually transported from a beach by comparison to the amount that can theoretically be moved on the basis of wind force and duration alone?' A close correspondence between the magnitude of predicted and measured transport rates is often used as the primary criterion for the judging the validity of predictive models. Such a comparison has been found to be inadequate (chapter 3, Fig. 5.8a&b) as the ideal conditions (unvegetated moisture free surface, uniform steady flow field) assumed in the models are rarely observed in the field conditions

The comparison of the measured transport rates on the beach with the various predictive models showed that the White (1979) expression is closest to the 'best correlated measured values of sand transport i.e. in areas far removed from the

influence of moisture or vegetation (Fig. 5.8a &b). Both the White (1979) and Lettau & Lettau (1978) expression are good fits for sand transport across a dry sand surface but largely overpredict the transport rate for sand blowing along the moist tidal margin (LBF) (Fig. 5.8a &b). A cubic fit of the 'best correlated measured results with those of White (1979) and Lettau & Lettau (1978) showed that the White (1979) expression plots quite closely to the measured values (Fig. 5.12) The drawback of the Lettau & Lettau (1978) expression is that it is not suitable (gross overpredictions) for predicting sand transport rates during high wind velocity shears > 40 ms^{-1} (Fig. 5.12).The interesting feature of the comparison is that both the expressions underpredict transport rates for shear velocities <0.22 m s^{-1} and over predict transport rates for shear velocities > 0.375 m s^{-1}. In between the two extremities the measured and predicted values fit closely. The probable explanation for the discrepancy between measured and predicted rates during shear velocities <0.22 m s^{-1} is the occurrence of local turbulence (gusts) during low wind shears. The overpredictions at high wind speeds has been related to a self limiting mechanism during such violent storms where increases in transport rates become proportionately smaller for increase in shear velocities (Sarre, 1988).

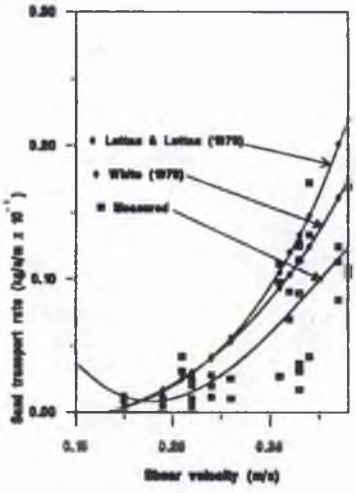

Fig. 5.12 Comparison of 'best correlated measured results' with White (1979) and Lettau & Lettau (1978) results Curves represent a polynomial regression line (cubic).

The Bagnold (1941) estimates are close to the average of the 'best correlated measured' results (Fig. 5.8b). The Kawamura (1951) expression grossly overpredicts (approximately double) sand transport rates during high wind shears (40 ms^{-1}). However, the predictability of the Kawamura formula is better during low wind shears e.g. 20 ms^{-1} (Fig. 5.8b). Interestingly, the Hsu (1971) formula gives results which are

quite close to the average values of the measured (n = 56) sand transport rates (Fig. 5.8b). The predictions made by Williams (1969) are totally incomparable (underpredictions) with the measured results.

Inclusion of a moisture parameter (Belly, 1964; Chepil & Woodruff, 1963 Ishihara & Iwagaki, 1952) a vegetation coefficient (Wasson & Nanninga, 1986) a parameter for the width of the exposed beach to the tide (Adriani & Terwindt, 1974) , water table level , precipitation and temperature factor (Sarre, 1988) in the sand transport models have met with varying success. The comparison between actual inputs of sand to potential inputs , calculated from the wind force and direction to provide a fair estimate of the sand movement from temperate beaches remains a serious problem and the inclusion of the various meteorological and limiting variables such as moisture and vegetation into the sand transport models is still a potential research thrust area and there remains much unexplained variance.

5.9 ROLE OF VEGETATION, MOISTURE AND BEACH WIDTH ON SAND TRANSPORT

5.9.1 Vegetation

The vegetation acts as a baffle, decreasing bed shear stress, increasing surface roughness and the thickness of the static layer of air, thereby increasing deposition, causing the dune to grow vertically in place rather than through slip face deposition and migration (Bagnold, 1954; Olson, 1959; Goldsmith, 1973). Attempts have been made to incorporate the effects of vegetation on the surface roughness into the Bagnold equation (e.g. Olson, 1958; Bressolier & Thomas, 1977). It is important to distinguish between vegetated coastal dunes and desert dunes which occur along the coastline (as in Sinai).

A 30% reduction in the measured sand transport is found between the transport on the open beach face and the first line of semi-vegetated dune surface at Tentsmuir point and Kinshaldy (Appendix IV-B). Landward of this semi - vegetated zone, in areas of long dune grasses the reduction is almost 100%. Similar observations have been made by Rosen (1979) on Tabusintac island where the landward transport has been reduced an average of 88% upon crossing the vegetation line of an accretional

dune. Along the Israeli coast, the effects of vegetation and beach slope appear to reduce theoretical aeolian transport by approximately 60% (Goldsmith *et al*, 1990). A 35% reduction of measured aeolian transport rates at the beach-dune transition at Island beach, New Jersey has been reported by Gares (1987).

5.9.2 Beach exposure

The tidal range on Tentsmuir sands (4-6 m) is the major factor controlling the beach area exposed to aeolian activity at a given time. The fetch (exposed surface length) of the sand available for transport by wind is as extensive as 250 m during low neap tides. During high tide the fetch is only 10-20 m at the same site, from the foot of the dune. Beach exposure limits the volume of sand transport significantly during lower wind velocities (< 7 m s^{-1}), due to the limited area available for transport. However, during high wind velocities (> 15 m s^{-1}) beach width exposure did not appear to have a limiting effect on the sand transport. As a consequence the potential of longshore winds for sand entrainment and transport is greatly enhanced with a fetch extending up to hundreds of metres. Experimental observations revealed that high velocity wind gusts were found capable of producing high sand transport even during limited beach exposures. This is in agreement with the findings of Borowka (1990).

5.9.3 Moisture

The trapping experiments have shown that sand movement by wind was not restricted to totally dry conditions and even moist sand (moisture content 1.2-1.5%) was moved on many occasions. The moisture content of the trapped sediments ranged from 0.5% to 0.75 % along the upper beach face zone. The sediments trapped along the lower beach face had a moisture content up to 2%. However, the surface moisture levels of the adhesion ripple area along the tidal margin was as high as 12%. The tidal range is the chief source of moisture in the inter-tidal zone throughout the year and is therefore one of the most important factors in limiting aeolian sand movement. The limiting effect of the surface moisture is important in the reducing the sand transport as the sand laden wind approaches the tidal limit on the beach. The sand transport

rate is reduced by about 30% along the tidal margin than the middle beach face due to the limiting effect of moisture. However, the effect of precipitation is interesting, as it was observed that the sand particles moved under the influence of a strong gust even while it was raining!

5.10 OFFSHORE/ONSHORE TRANSPORT AND THE SEDIMENT BUDGET

Sand transport rates are greatest in the middle beach face sub-environment during both offshore and onshore wind regimes. The offshore/onshore net sediment exchange results in a positive sediment budget along the potential foredune (semi-vegetated) area and the backshore, as there is a high sand transport/accumulation rate in this area during an onshore wind and very low sand transport rate during offshore winds. The middle beach face has a high sand transport rate during both onshore and offshore winds, denoting an excessive amount of mobile sand in this area and this zone is also the potential source of sand which is accumulated in the backshore/potential foredune area by onshore winds. An increase in the frequency of the onshore winds, with a consequent growth of the foredune causes the sediment budget of the beach to become increasingly negative.

However, the role of the offshore and longshore winds in creating a positive beach sediment budget, due to spatial compartmentalisation in response to the limiting effect of the tidal margin, should not be ignored. The general paradigm of relating dune development and growth to the *onshore wind frequency only* is seen to be inappropriate in the light of the present study. This work emphasises the importance of middle and upper beach face sediment budget spatial compartmentalisation by offshore and longshore winds. Such winds result in aeolian sand accumulation often in the form of small scale barchans and linear ridges on the foreshore. The chaotic assemblage of these structures often leads to the formation of dune ridge loci. A number of dunes round the globe (Cooper, 1967; Psuty, 1969; Leatherman, 1976; Rosen, 1979) have formed due to offshore and longshore aeolian sediment transport (Sherman & Hotta, 1990).

In general, variation in wind velocity, presence or absence of vegetation, ground surface moisture and the sand source limitation accounts for the variability of

the short-term aeolian sand transport rates on the Tentsmuir beach and dune sub-environments.

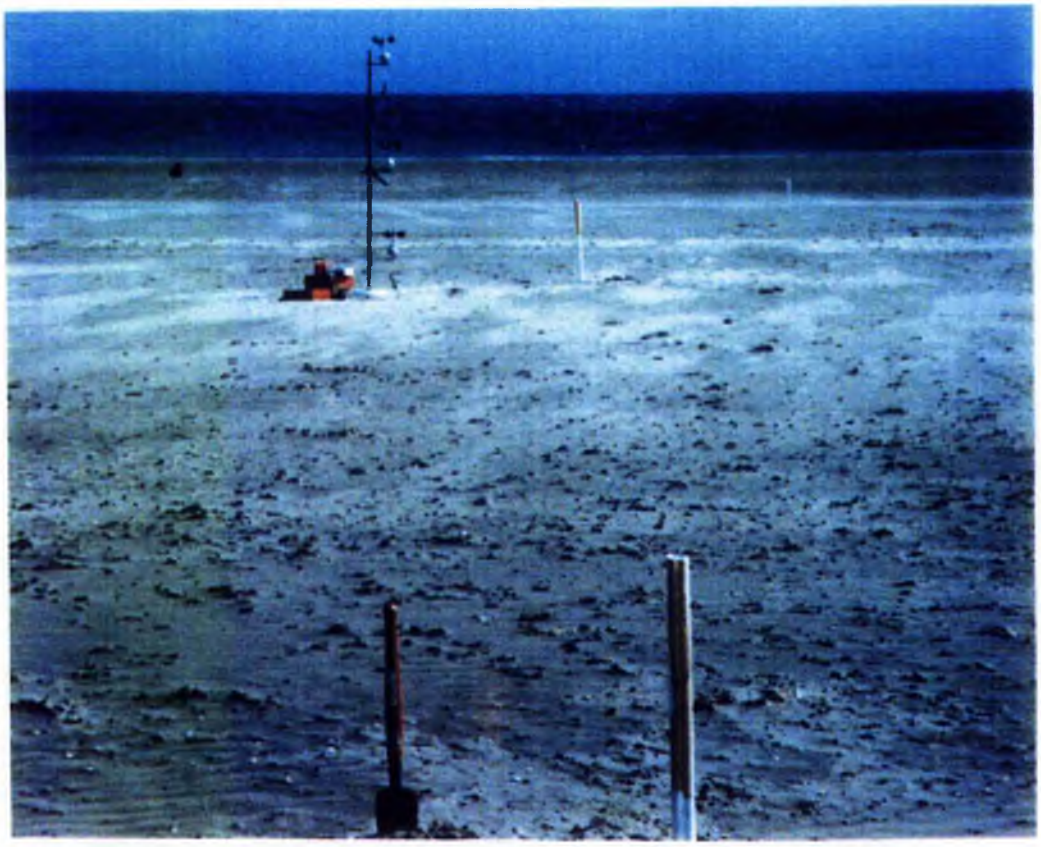

Plate 5.1 The experimental apparatus (anemometer array & traps) for measurement of sand transport rates on the beach.

Plate 5.2 The sand during an offshore wind is derived from a well defined strand line (arrow) landward of which sand is dry.

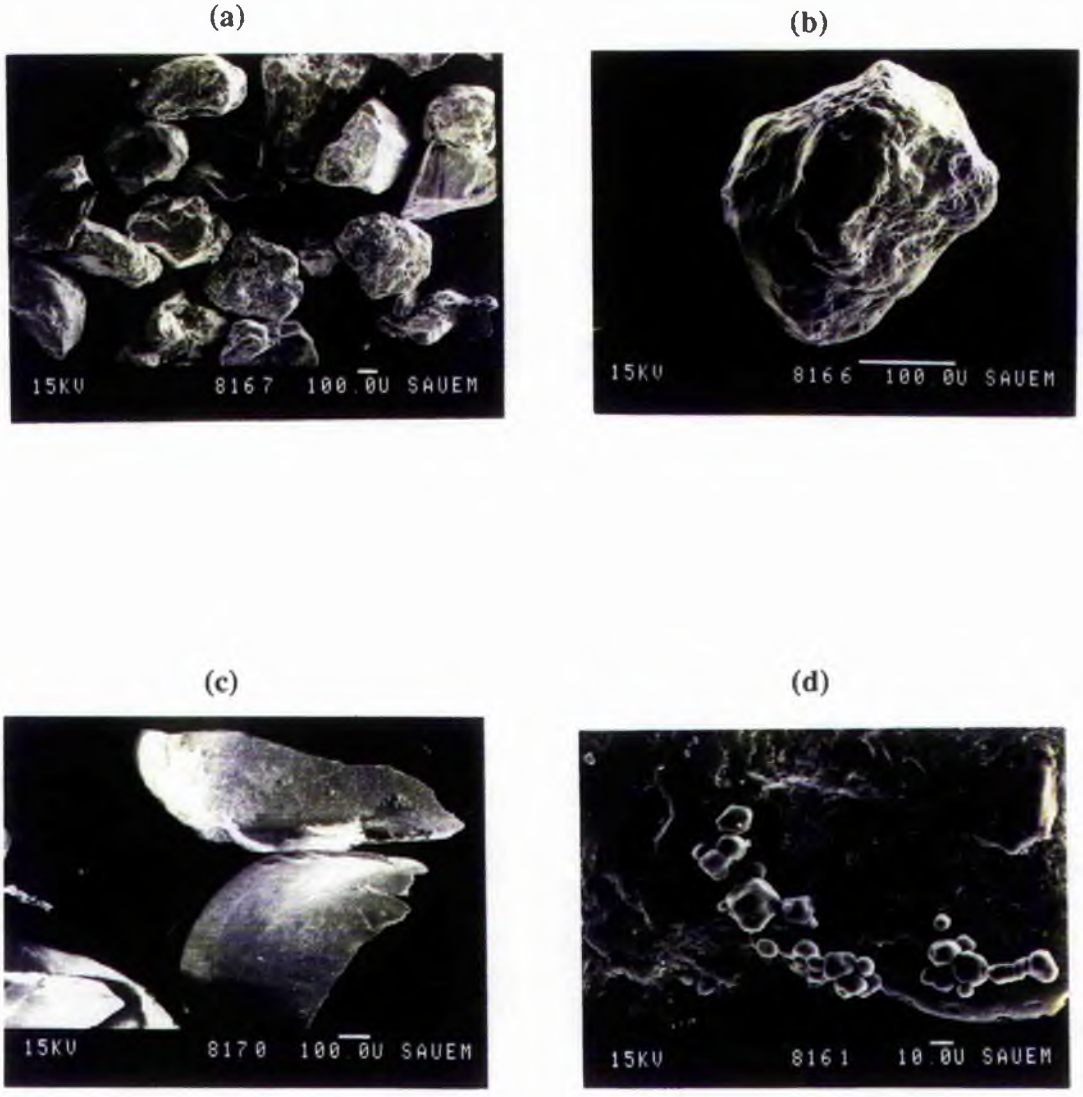

Plate 5.3 SEM photomicrographs of sediments retained in traps placed on beaches. (a) View of sub-angular-sub-rounded sediments (b) Quartz grain showing conchoidal fracture partly smoothed by abrasion, also showing upturned plates and irregular pits. (c) sub-angular shell fragments (d) halite crystals on a large quartz grain.

Chapter 6

LONG TERM SAND TRANSPORT RATES AND POTENTIAL INPUTS ACROSS THE INTER-TIDAL ZONE

(with 5 figures and 1 table)

Chapter 6

Long Term Sand Transport Rates And Potential Inputs Across The Inter-Tidal Zone

6.1 INTRODUCTION

Having measured the short term sand transport rates during field study across the various beach-dune sub-environments, attention can now be diverted to the prediction of long term sand input based on wind data for the last ten years. A comparison between the actual sediment inputs and the theoretically predicted values has also been made. The comparison provides an insight into the validity of using the potential transport approach for calculating actual transport rates across a beach located in a temperate region.

Estimation of potential sand input in the onshore, longshore and offshore direction has been accounted for in the light of the observations gathered during field measurements where, although the onshore transport leads to the formation of a positive foredune budget, the offshore and longshore transport resulted in a positive beach budget due to the limiting effect of sea water line.

6.2 METHODOLOGY

The procedure adopted is based on the on that used by Kadib (1964) and Sarre (1989). The wind data (1980 - 1990) at the Leuchars meteorological site have been grouped into 5 knots wind speed class intervals and divided into 12 compass directions, each covering 30°. Since sand transport is significant only above 5.9 ms^{-1} (at 10 m height), as stated earlier in chapter 4, the wind speed records below this value have been disregarded. Thus the four wind speed classes taken into consideration are shown in Table 6.1. The mid-point speed of each wind speed class was then linked to the mean shear velocity on the beach. This was done by linking the mid - point wind speed to the empirically determined focal point (u' z') (Fig. 5.6). The corresponding

Table 6.1 Shear velocities and corresponding sand transport rates on Tentsmuir Point for different wind speeds at R.A.F Leuchars. The contribution of each wind speed group to the total sand inputs is calculated from the number of hours the wind blew during 1980-1990 in each velocity class times the potential transport rate.

Leuchars wind speed class (ms^{-1})	Mid-point wind speed (ms^{-1})	Percentage hours (%)	Shear velocity (ms^{-1})	Transport rates ($kghr^{-1}m^{-1}$)	Total potential inputs ($m^3 \times 10^3$)	Percentage inputs (%)
5.6-8.1	6.8	65.2	0.19	0.5	4.2	3
8.6-10.5	9.6	22.3	0.29	14.5	44.6	31.5
11.2-13.7	12.2	10.2	0.39	44.8	60.8	43.1
14.3-16.8	15.5	2.3	0.49	98.1	31.8	22.4

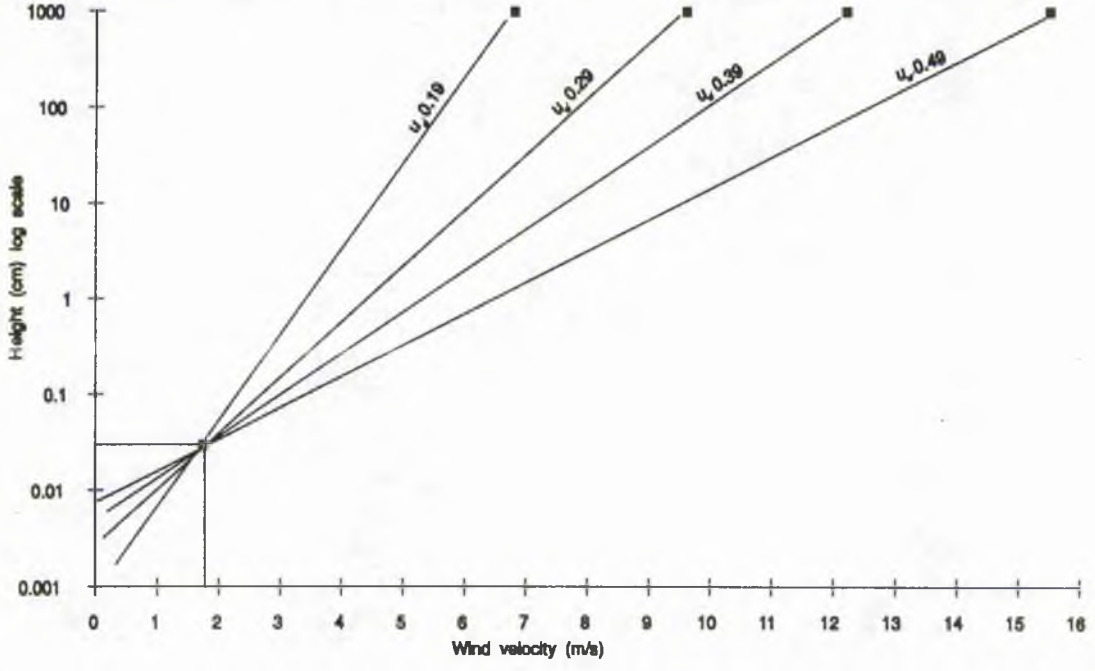

Fig. 6.1 Lines joining mid-point (6.8, 9.6, 12.2, 15.5) of wind speed classes to the empirically determined focal point u', z' (1.75, 0.03). Gradient of the line determined from equation is the shear velocity (u_*) for each of the wind speed classes.

shear velocities (u_*) were then calculated from the graph (Fig. 6.1) by means of equation 3.3. The use of the mid-point is a simplification, and also because the velocity classes are so narrow (2.6 ms^{-1}) that the difference does not significantly effect the calculation of the sand transport rate which is essentially the cube of the shear velocity value. The shear velocities have been taken to be constant for the hourly wind speed observations, however, it has been noticed that the shear velocity varies due to turbulence. Fluctuations in wind speed over an hour will also result in high sand transport rates during high wind speeds which may result in underestimations when compared with the actual rates. To some extent, the actual transport rates will be lower than the predicted rates during below average winds.

This technique has been applied to Zone 1 (Tentsmuir Point, Fig. 2.3) of the study area because net foredune accretion has been seen to occur in this area during the last ten years. It is thus an ideal site for comparison of potential sand inputs from theoretical expressions with measured values using ground survey and successive aerial photographs.

The calculation procedure used to estimate the potential sand transport rate is based on the capacity of wind force to transport sand using White (1979) expression (Table 6.1; eq. 3.34, p. 3.16).

$$q = 2.61\, u_*^3\, (1-u_{*t}/u_*)\, (1 + u_{*t}^2/u_*^2)\rho\ /g$$

This equation was chosen as it provided the best fit to the measured transport rates across the beach (chapter 5). An experimentally determined threshold shear velocity (u_{*t}) of 0.184 ms^{-1} (Fig. 5.6) has been used in the equation, ρ and g refer to the air density (1.22×10^{-6} kg m^{-3}) and acceleration due to gravity (9.8 ms^{-2}) respectively.

The potential movement directions are essentially onshore (positive dune and backshore budget), offshore (positive middle and lower beach face budget) and longshore (positive beach budget). Although earlier workers (Sarre, 1988) take only the potential onshore input into consideration, here the role of the longshore and offshore inputs are also analysed. The short term transport rate determinations have shown that both the longshore and offshore transport are instrumental in defining the net aeolian sediment budget.

The proportion of the sand inputs that winds from each of these directions contribute to the total inputs is dependent on the width of the reach exposed. The width of the reach exposed depends on the time for which the beach is covered or uncovered by the tide. Hence, the approximate time that the beach is influenced by the two tidal states in 24 hours is approximately half. If w_1 (50 m) and w_2 (250 m) are the widths of the beach exposed at Tentsmuir Point during high and low tide respectively. Actual reach widths 'R' for all the twelve directions are calculated by taking the sum of the modulus of the sine of the wind direction (o) multiplied by the 550 m length (L) of the Tentsmuir Point shoreline and the modulus of the cosine of the wind direction times the beach width (150 m) (Fig. 6.2). The reach width is given by,

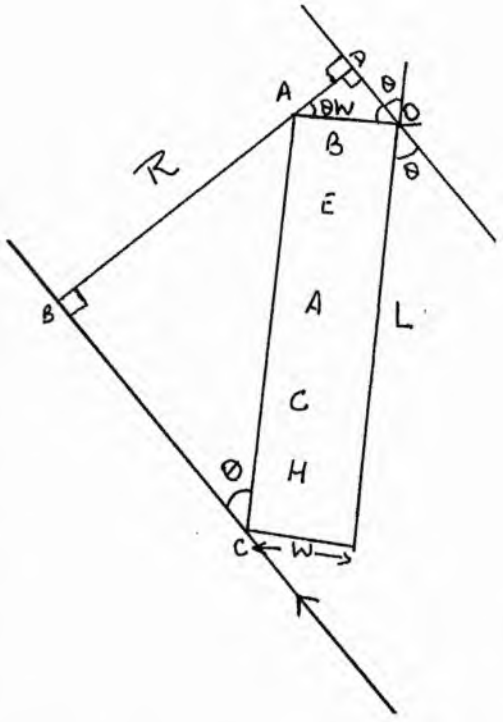

Fig. 6.2 Reach width, R, of a southeasterly wind at Tentsmuir Point is given by the length of the beach L (550 m) times the sine of the wind direction plus the average beach width W (150m - average of W_1 and W_2 where, W_1 = beach width at high tide, 50 m; W_2 = beach width at low tide, 250 m) times the cosine of the wind direction.

$$R = 1\,2\,(L \sin o \cdot w_1 coso) - 1\,2(L sino - w_2 coso) \qquad 6.1$$

finally the reach width is given by

$$R = L\,sino - coso(w_1+w_2)\,2 \qquad 6.2$$

The total mass of sand Q_p *moved* from a given direction is calculated as:

$$Q_p = q\,R\,t \qquad 6.3$$

where q is the rate of sand transport (kg hr-1m-1), R reach width (m) of a given wind and t is the number of hours the wind blew from a particular direction. The total sand input (m^3) is derived by dividing the total mass of sand Q_p by the bulk density of quartz sand (1500 kg m^{-3}) (Table 6.1).

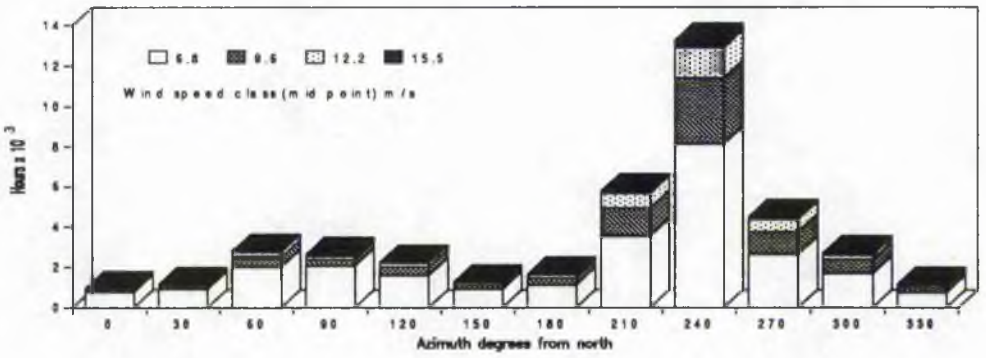

Fig. 6.3 Total hours of wind speed classes blowing from different azimuth directions - 1980 - 1990.

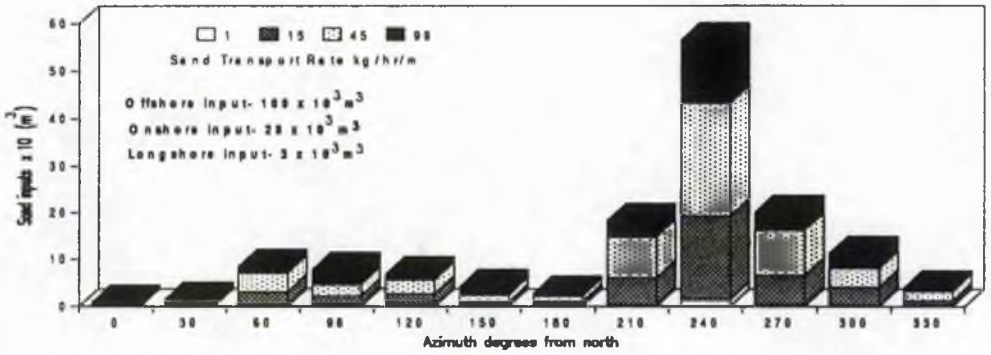

Fig. 6.4 Sand inputs along various azimuth directions 1980-1990.

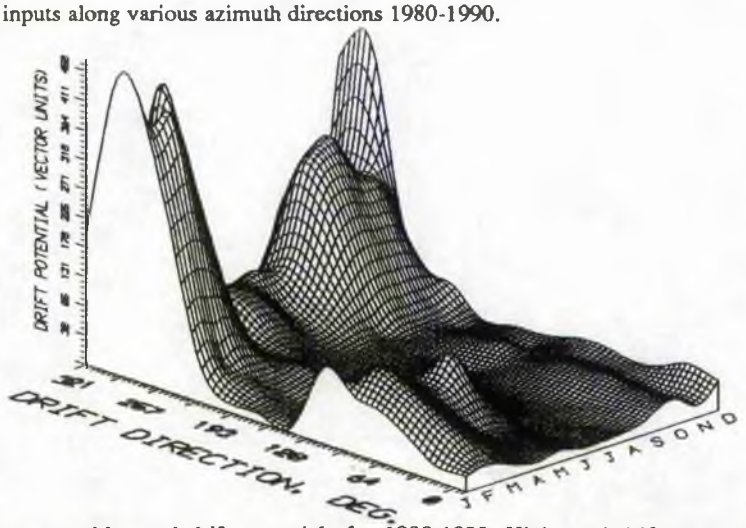

Fig. 6.5 Average monthly sand drift potentials for 1980-1990. High sand drifts occur during the winter months when the offshore winds predominate. Bimodal onshore sand drifts are characteristic of the spring season. The summer season is a low sand drift period. Onshore Bimodal offshore drifts (accompanied with weak onshore drifts) are prevalent during autumn.

6.3 WIND SPEEDS AND POTENTIAL SAND INPUTS -1980-1990

The total number of hours represented by the four wind speed classes from different azimuth directions over the last eleven years (1980-1990) are shown in Fig. 6.3. The 6.8 ms^{-1} wind speed class was by far the most prevalent speed class in various directions ranging in duration from $3x10^3$ hours in the onshore sector (0° to 180°) to as high as $8x10^3$ hours in the offshore direction (180° to 360°) (Fig. 6.3). It corresponded to 65% of the time but contributed to only 3% of the total sand input (Table 6.1). The 9.6 ms^{-1} and 12.2 ms^{-1} wind speed classes contributed 31.5 and 43.1 % of the total sand input respectively. Because of the method of computing the 12.2 ms^{-1} wind speed class is seen to have contributed more than the 9.6 ms^{-1} class although its share of the total time was less. The rarer high velocity winds (> 14.3 ms^{-1}) also contributed significant quantities of sediment transport in relation to their total ration. In general, wind speeds between 8.6 ms^{-1} and 13.7 ms^{-1} were the most substantial in defining the overall aeolian sediment budget.

The potential sand inputs estimated from equation 6.3 for the four wind speed classes are shown in Fig. 6.4. Comparison of Fig. 6.3 and Fig. 6.4, e.g. along the 240° azimuth, show that $8x10^3$ hours of 6.8 ms^{-1} wind speed contributed $2x10^3$ m^3 of sand input, whereas, $0.4x10^3$ hours of 15.5 ms^{-1} wind speed contributed $10x10^3$ m^3 of sand (Fig. 6.4). Thus low velocity winds of higher duration did not contribute significantly to the overall sediment budget. Conversely high velocity winds of shorter durations resulted in significant volumes of sand transport and inputs (Fig. 6.3).This trend is consistent along all the azimuths. The calculation of potential sand inputs in m^3 for winds originating from various azimuths is more comprehendible than the earlier method of estimating potential sand drifts in vector units (c.f. section 4.7). However, the latter provides a suitable graphical representation of the wind regimes and the attendant sand drift in an area (Fig. 6.5).

The onshore sand input is mainly derived from winds blowing between 60^0 to 120^0 i.e. from the east (Fig. 6.4). The offshore transport is brought about by winds originating from 210^0 to 240^0 i.e. from the south-west (Fig. 6.4). The total longshore transport over the eleven year period was 3 $x10^3$ m^3 whereas the onshore inputs and offshore transports totaled 28 $x10^3$ m^3 and 109 $x10^3$ m^3 respectively (Fig. 6.4).

6.4 MEASURED VS PREDICTED LONG TERM SAND INPUTS

The total amount of sand accumulated in the lee of the present day beach at Tentsmuir Point since 1980, based on successive aerial photographic and ground surveys is approximately 33 x 10^3 m^3 (c.f. section 2.1.1). The calculated total potential onshore sand input during the same period was 28 x 10^3 m^3. The discrepancy between the two figures (~15%), i.e. the underestimation of the predicted result, may have arisen from two factors (i) the inability of the present procedure to account for the short-term gusts which result in enhanced transport values above those from averaged hourly wind speeds, (ii) the contribution of the longshore and offshore winds in assimilating sediments close to and along the backshore and potential foredune areas. Hence one can safely use the White (1979) expression to measure and compare the aeolian sediment budget along the coast and make reasonable predictions. However, the overall coastal budget is not simply wind dominated but is controlled by the complex interplay of aeolian, wave and tidal processes.

6.5 DISCUSSION AND CONCLUSIONS

As discussed in chapter 4 the wind regimes in the study area are seasonal. However, it has been demonstrated that the mobility of the sand under the influence of a given wind speed is partly dependent on the state of the tide, and it is also influenced by several meteorological variables.

The tidal effect is by far the most important source of moisture on the beach and is also the most important factor for limiting sand transport (section 5.6.3). Thus, the effect of the tidal exposure time and extent have both been incorporated in calculating the reach width of a given wind.

The total erosional fetch of the sand available for aeolian transport, at Tentsmuir Point, during low tide is 200 m whereas during high tide the fetch may be limited to 50 m only. Similarly, the erosional fetch for the longshore winds in an area is very extensive and may exceed tens of kilometres (8 km along the coastline under observation). While calculating the reach width, the sine of 180^0 (southerly wind) and 0^0 (northerly wind) was taken to be zero. Hence, the transport potential of the

longshore winds has been underestimated. The reach width of the longshore winds will however be constrained by the width of the beach exposed, although the erosional fetch value is much more extensive than for either the offshore or onshore winds.

Since the variability of tidal exposure is a complicated phenomenon depending in turn on a number of variables such as seasonality and lunar cycles, the method outlined is a rough estimation of the effects it has in limiting aeolian transport on the beach.

The most important meteorological variable effecting sand transport is the wind duration and strength. Occasional strong gusts were found capable of moving sand even when it was raining.

The comparison between actual foredune accretion and potential sand inputs, calculated from the wind strength while incorporating the tidal effect, has provided a fair estimate of sand movement along the Tentsmuir beach. The inability of other workers (Sarre, 1989) to arrive at a similar conclusion was probably due to their dependency on the usage of predetermined shear velocity values (from equations of Howard *et. al.*(1978)) which lead to gross overestimations.

Chapter 7

COASTAL AEOLIAN SEDIMENTARY STRUCTURES AND FACIES ANALYSIS

(wth 13 figures, 22 plates and 1 table)

Chapter 7

Coastal Aeolian Sedimentary Structures & Facies Analysis

7.1 INTRODUCTION

During the study of sediment transport, the generation growth and migration of many bedforms have been observed in the many sub-environments of the beach-dune system. Excavation into many features permitted examination of the internal structures of the bedforms developed under known conditions with a view to establishing successions of allied structures and from there a framework of facies model analysis.

This unequivocal process-response relationship established between the landforms, aeolian sedimentary structures formed, and the dynamic conditions which caused them to come into existence, should help in concise paleoenvironmental reconstruction in the rock record. It will also aid in identifying coastal aeolian sequences in the older formations, conforming to one of the oldest paradigm in geology 'Present is the key to the past'.

7.2 AEOLIAN SEDIMENTARY STRUCTURES

7.2.1 Sand strips

Description

The sand strips along which mobile sand is seen to move have been observed on more than one occasion during a sand storm on the beach (Plate 7.1). Narrow longitudinal strips, hundreds of metres long, 2 - 2.5 m wide and approximately 1 to 2 mm thick are deposited parallel to each other (Plate 7.1). The heads of new strips begin in the spaces between the trails of the others. Plate 7.1 shows the development of sand strips across West Sands beach on 1.4.91 when the wind velocity (offshore, SW) was in excess of 15 m s^{-1} at 2 m height. The dry sand strips are formed across the damp inter-tidal zone and terminate along the water's edge. Sand strips are seen to

develop during both onshore and offshore strong winds. As the sand within the strips moves, sand particles are also seen to move vertically upwards in the form of dust spirals due to turbulence under very high velocity winds-the phenomenon known as 'bursting' and 'streaking'. The strips at all times are arranged in a regular manner across the beach with intervening deflation hollows containing coarser lag deposits such as shell layers (Plate 7.2). Observations of sands moving along such features reveals that high suspension concentration zones migrate discontinuously but along all adjacent sand strips the clouds of sand migrate together giving the appearance of wave crests advancing along the beach. The crest being seen only where they encountered the ridges.

Continuous strong winds for the next 28 hours resulted in the formation of sand lobes moving across the foreshore along where the sand strips had been seen to move the previous day (Plate 7.3 taken on 2.4.91). Whereas the vertical thickness of the sand strips on the first day had been about a couple of millimeters, on the second day the lobes attained thicknesses of a couple of centimetres. With a relative decrease in wind velocity ranging from 10-12 ms^{-1} (at 2 m height) the sand lobe surface developed into a surface carrying asymmetrically spaced ballistic (wind induced) ripples with wavelengths of approximately 16 cm and height of 1.5 cm. The ripples have highly sinuous long crests along the upstream which gradually straighten downstream. Buttress junctures (Allen, 1968) are common although some open junctures are also present.

During November 1968, when extremely high velocity (15-18 ms^{-1}) longshore (southerly-southeasterly) winds blew continuously between November 12 and 15, the formation of series of approximately a metre high barchans was observed (Plate 7.4) along the 800 m long stretch of the then Tentsmuir Point shoreline (in the backshore and middle beach face area). The distance between the horns of individual barchans being approximately 3 m. A barchan is a crescent shaped, bilaterally symmetrical structure, its lateral arms, horns or wings point downwind and enclose a steep slip face shaped by sand avalanching (Allen, 1984).

Interpretation

Sand strips formed on the beach when sediment laden, very high velocity winds develop transverse instability and sand is deposited in the form of longitudinal strips as suggested by Bagnold (1951). Carter (1988, p307-307) has attributed the development of these strips on the Irish coast to the interaction of sediment-air dynamics and the streaking and bursting of the near surface sediments in response to air turbulence.

The regularity and repetition of the strips strongly suggests some large scale rotary movement in the air stream. The spacing of these sand stripes and the formation of regularly spaced foreshore sand lobes (Plate 7.3) or mini barchans across the beach after a few days of storm, suggest that these zones of high sandflow may correspond to a conceptual model of Allen, (1984) (Fig. 7.1) who examined the sedimentological implications of secondary flow vortices in which there is insufficient sediment supply to cover the entire bed. The flow associated with neighbouring vortex cells reattaches with the bed (A) and diverges towards the point of its separation from the bed (S). Flow converges along the separation line and the maximum aerial concentration of sediments deposited as foreshore sand lobes (Plate 7.3) or barchans (Plate 7.4) occurs along the separation line of adjacent longitudinal vortex cells.

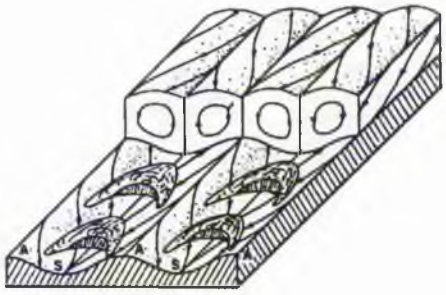

Fig. 7.1 Implications of secondary flow for sediment transport and transfer carrying a small amount of bed material over a cohesive deformable surface. Seconary circulation vortices are also shown (after Allen, 1984).

The stress along the sand stripes where the separation occurs (Fig. 7.2) is thought either to be equal (Bagnold, 1954) or larger than in the adjacent gravel lanes. In the present case A is represented by a coarse sand-shell deflation surface (Plate 7.2). Where reattachment occurs longitudinal, wind parallel secondary flow vortex cells provide a potential mechanism for the formation of the sand strips and foreshore sand lobes or barchans across a partly cohesive deformable beach surface.

The presence of a gravel layer on sand sheets which was considered of prime importance by Bagnold (1954) was denied by Glennie (1970) who pointed out the existence of vast areas of sand sheets in major deserts devoid of pebbles. A combination of rapid sedimentation, high wind velocities, and fairly uniform grain size of the sand is believed to cause the sand sheet to be deposited, with an evenly laminated sand bedding (Glennie, 1970).

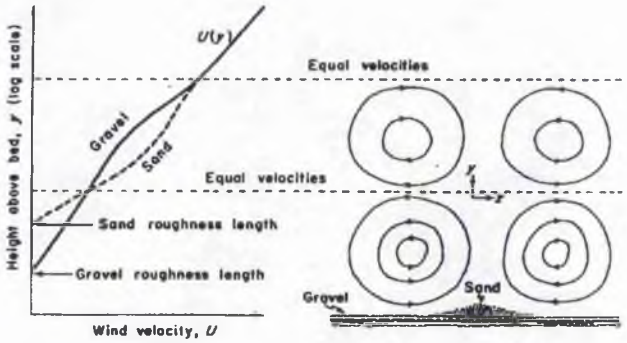

Fig. 7.2 Probable secondary currents associated with the transport by wind of sand in stripes, usually rippled over a gravel (coarse shell layer in the present case) surface, illustrated by schematic wind velocity profiles (left) and streamlines in the plane normal to flow (right) (after Bagnold, 1954).

Ballistic ripples are transverse (forming perpendicular to the wind direction) ridges of sand shaped by wind in deserts and along sandy coasts (Glennie, 1970). Recorded wavelengths range from 0.0005 m (Bagnold, 1937) to 22 m (King, 1916) increasing almost linearly with the coarseness of the sediment. Increase of wind speeds cause wavelength growth but make the ripples flatter (Bagnold 1954, Seppala & Linde, 1978). The stoss slope of aeolian ripples ranges from 8 to 100 whereas the lee slope ranges from 20 to 30° (Sharp, 1963). Aeolian ripples typically have ripple indices (R.I.: ratio of ripple wavelength (l) to height (h)) > 10-15, whereas for water ripples the R.I. is <10-15. A measure of the lateral continuity of ripples is provided by the horizontal form index of Allen (1963) which is the ratio of the mean crest length (c) to the mean wavelength (l). The vertical (R.I.) and horizontal form indices of the ripples developed on the Tentsmuir beach are 10.6 (l/h-16/1.5) and 11 (c/w-176/16) respectively (Plate 7.3). Aeolian ripples whose sinuous crest runs in a transverse direction to the local wind direction have horizontal form indices of 10-100.

The ballistic theory of ripple formation (relating ripple wavelength to a mean characteristic saltation path) suggested by Bagnold (1941) to explain the genesis of aeolian ripples has been a much debated topic (Sharp, 1963, Folk, 1977, Walker,

1981; Anderson & Hallet, (1987). Anderson (1987) has suggested while ripple wavelengths are affected by grain trajectory lengths, they do not correspond to the characteristic or mean saltation path of Bagnold (1941). However, he concluded that the ripple spacing is a function of the probability distribution of the total trajectory population, in which low-energy reptating grains outnumber high energy saltating grains by about nine to one and the ripple crest spacing should be approximately six times the mean reptation path length.

Barchans are believed to develop in areas where sand supply is low, indeed transition from transverse ridges to barchans may be observed due to a marked diminution in sand supply downwind (Summerfield, 1991, p.251). Once formed a barchan generates its own secondary airflows which maintain its equilibrium form while it migrates downwind (Warren, 1979). The elongation of the barchan arms is due to the higher rate of sand movement on the lower, outer parts of the dune due to the reduction in bed shear stress and a convergence of near-bed flow along and toward this trend (Allen, 1984).

7.2.2 Obstacle induced erosion and deposition

Topographic obstacles ranging in size from escarpments and hills to boulders and clumps of vegetation induce zones of airflow acceleration, deceleration, and enhanced turbulence (Gaylord & Dawson, 1987). Consequently there will be erosion or accumulation of sand, or both simultaneously in different places. There is no general classification of obstacle induced structures but three categories are identifiable 1) wind shadows 2) wind crescents and 3) scour remnant ridges (Allen, 1984, p185).

7.2.2.1 Wind shadows

Description

Ballistically rippled pyramidal sand accumulations form behind grass tussocks in the backshore and foredune area and in the lee of tidal debris along the strand line, during offshore or onshore winds (Plate 7.5). The tapering edge of the structure points downwind. Similar structures have been described in literature as 'sand shadows' (Fig. 7.3). If the sand surface is dry the sand shadow becomes characteristically ballistically

rippled during moderate to strong winds (Plate 7.5, width of scale 13cm). The ripple crests are almost rectilinear and strike more or less directly across the crest of the shadow. Their length/width (30/24, 27/21, 57/46) ratio (the shadow length is partly dependent on the width of the obstacle) ranges from 1.2 - 1.3; the wavelength of the ballistic ripples ranges from 3.5 - 4 cm. The observed maximum height of the tapering sand shadow in the upwind region ranges from 6 - 8 cm.

Fig. 7.3 A ballistically rippled sand deposit in the lee of a tussock of vegetation. Wind towards observer (diagram from Allen, 1984, after a photograph by Stone, 1967).

Interpretation

The term sand shadow was used by Bagnold (1954, pp189 -90) to describe a tapering accumulation of sand formed in the lee of an obstacle where the wind velocity is locally reduced. 'Current shadow' is a term used by Allen (1984) for such features in both aeolian and aqueous environments. The term sand drift was used by Reineck & Singh (1980, p221), as an alternative to Bagnold's (1954) sand shadow, for any kind of sand deposit associated with obstacles in the way of sand laden wind, which have well developed internal foreset laminae. The wind-flow over sand deposits is largely indicated by the patterns of superimposed ballistic ripples (Bradley, 1957; Gripp & Martens, 1963; Beheiry, 1967). Where the vegetation is more dense, the ripples mostly face inwards slightly towards the axis of the shadow, suggesting an inwards and upwards but still largely downstream flow of air in the mid - wake (Allen, 1984, p199).

While investigating the modification of airflow by a discrete, semi-circular roughness element (e.g. vegetation) in order to understand the formation of 'shadow dunes' Hesp (1988) concluded that these dunes are formed to the lee of discrete roughness elements by reverse flows that occur within a horizontally separated wake region. The height of the shadow dunes is determined by the roughness element width and the repose angle of the sand (Hesp, 1988).

7.2.2.2 Lee dunes/Current crescent

Description

Ridge shaped sand deposit tapering downwind in the lee of tree stumps, brought ashore by the spring tides along the backshore, are observed at Tentsmuir (Plate 7.6). The obstacle (tree stump) is partly embedded in an extensively deflated backshore environment. Small-scale deflation ridges on either side of the ridge are indicative of the scouring action of the wind in assimilating sediments from the side of the obstacle towards the centreline (Plate 7.6).

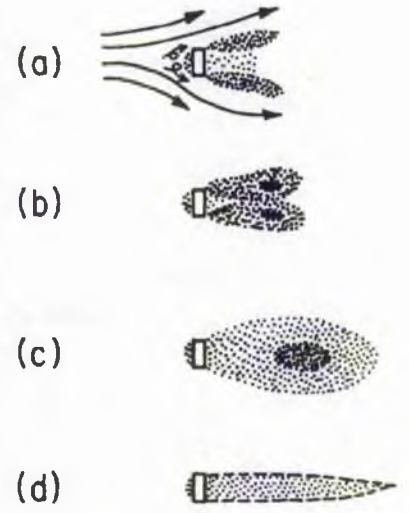

Fig. 7.4 Development of four types of lee dune downwind of an obstacle (after Bagnold, 1954).

Interpretation

As the airflow is deflected around and over an obstacle, a horseshoe shaped vortex is created and sand is initially deposited both in front of the obstacle and on either side as two tapering wings (Bagnold, 1954; Greeley *et al*, 1974 b) (Fig. 7.4a, 7.5). The two wings eventually coalesce (Fig. 7.4d) as the arms of the horseshoe vortex gradually transfers sand towards the centreline of the obstacle, and over time the lee dunes become higher, longer and narrower (Pye & Tsoar, 1990). Such structures originating from coalesced horseshoe shaped sand accumulations have been referred to as 'current crescents' by Allen (1984, p189-91).

Fig. 7.5 Schematic diagram showing the development of a horseshoe vortex around an obstacle (from Pye & Tsoar, 1990).

7.2.2.3 Scour remnant ridges

Description

The surface of the damp beach becomes deflated during strong winds leaving behind scattered ridges of sand, 5-10 millimetres high. (Plate 7.7, wind blowing from right to left). The surface of the beach then becomes irregular. The wind appears to

erode sand from behind and around the ridges. Some sand is accumulated behind the ridges in the downwind direction and the structure is a couple of centimetres long. Sand strips are seen to move across and over these remnant ridges.

Interpretation

Various hypotheses have been put forward for the development of these ridges. 'Scour remnant ridges' a term coined by Allen (1965a), and described as 'sand tails' by Reineck & Singh (1980, p79) and also described by Wunderlich (1972) are believed to be small simple ridges of either snow, sand or mud preserved to leeward of resistant objects such as shells, stones or the remnant crusts of hardened snow, or due to the breaching of the salt hardened crust (McKee, 1957; Gripp & Martens, 1963). The downstream slope of the ridge crests (5-12°) are thought to compare with the angle of impact of the saltation (Allen, 1984, p203). However, Berry (1973) observed the development of ridges, along the Baja California beach, which was devoid of resistant objects as shells or stones and has attributed the formation of these structures to the non-uniform compaction of sand grains.

In all cases the erosion is accomplished by saltating grains. The presence of resistant objects does not appear to be a prerequisite for the formation of the ridges. The abrasive action of a strong sediment laden wind on a moist beach surface will lead to the development of the ridges. The spacing and slope of the ridges is a function of the saltation trajectory.

7.2.2.4 Pyramidal wind shadow dunes

Strong offshore winds produce pyramidal sand accumulations 2-3 m high in the lee of the primary dune ridge (semi-vegetated by *Ammophila sp.*) along West sands. These pyramidal wind shadow dunes (Hesp, 1981) (Plate 7.8) ('echo' dunes of Tsoar, 1983) are formed by slip face accretion within a three dimensional flow structure, during offshore wind, in the lee of the primary dune ridge (>1.5m). Strong offshore winds (maximum speed 20 ms^{-1}) cause eddy currents in the lee of the pyramidal dunes to pick up sand from the surface downwind from the dune and transport it to the lee

slope. Massive aeolian sand accumulation in the lee of the an eroded dune cliff has also been observed. Often a scarp-fill sequence is observed on eroding dunes at Tentsmuir.

Interpretation

A pyramidal wind shadow dune is formed in the wake region by the eddies and vortices which flow from the edges of the plant cluster to the 'centreline' (Hesp, 1988). The centreline is the zone of maximum deposition where opposing vortices meet. Along the centreline a ridge is formed with linear slopes extending outwards from the ridge crest to the bed (Hesp, 1988).

This pyramidal sand shadow accumulation during high velocity offshore winds in the lee of a primary dune ridge, is a phase in the beach-dune recovery cycle (Carter, 1980; Carter *et al,* 1990) where sediments which have previously been lost from the dune by marine undercutting and scarping are returned to the dune slope (Fig. 7.6). Once the scarp slope becomes stable (below the angle of repose) it is stabilised by vegetation. As an agent of the recovery cycle, the offshore winds are conducive to the formation of a positive dune budget where net shoreline retreat is less than the gross retreat.

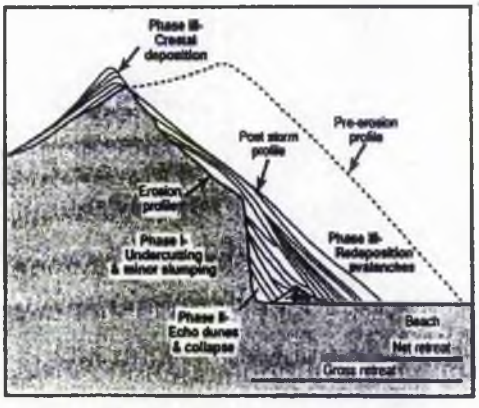

Fig. 7.6 Three phases of dune slope undercutting, slumping and recovery (after Carter, *et al,* 1990).

7.2.3 SCRATCH CIRCLES

The term scratch circles (*Scharrkreise* (in German)), introduced by R.Richter (1926), is applied to sets of concentric grooves cut generally in sand or mud by the action of sharp objects anchored at the centre of curvature of the set, but otherwise free to swing or rotate horizontally about the centre. Scratch circles are seen to form at Tentsmuir, along the backshore and foredune where the sharp blades of the *Elymus farctus* or *Ammophila sp.* cut grooves into the sparsely vegetated sand in the shape of circular arcs (Plate 7.9). The diameter of these arcs or circles ranges from 10-30 cm.

The prerequisite for the formation of scratch circles is the existence of sufficiently sparse vegetation, so that the wind can easily blow the plants around their axis (Langerfeldt, 1935, Seppala, 1972). However, fine examples of scratch circles have not only been reported on tidal muds formed by halophytes (Langerfeldt, 1935) but have also been illustrated to form at a water depth of 3800 m off Cape Horn! The scratch circles have been shown to have been formed either 1) during the deposition phase, when sand accretion causes the leaves of the grass growing within the sand to come into contact with the sand and etch circles on the surface or 2) during the deflation phase when the strong wind exposes the roots of the plants, which collapses and the wind blows the leaves around the roots in a circle (Seppala, 1972).

7.2.4 Adhesion structures

Classification

Adhesion structures form by the adhering of dry, wind-blown sand to a wet or damp surface. In plan view morphology and internal structure (given in brackets), three adhesion structures occur: adhesion ripples (climbing adhesion ripple structures), adhesion warts (adhesion warts) and adhesion plane bed (adhesion laminations). Experimental growth of adhesion structures (Kocureck and Fielder, 1982) shows that the three forms of structure result from subtly different environmental factors; this enhances the value of adhesion structures as tools for detailed paleoenvironmental interpretations. Lowering of water content of the surface produced adhesion laminations (Kocureck & Fielder, 1982). Thus, in nature a sequence of adhesion ripple structures overlain by adhesion laminations and finally wind ripple deposits indicates a drying upward sequence (Kocureck & Fielder, 1982). Their presence in ancient strata not only is a clear indicator of emergence with both a relatively dry sand source and a wet or damp depositional area but also may allow for some very specific paleoenvironmental reconstruction in terms of the moisture content, wind variability and the slope of the local depositional source (Kocureck & Fielder, 1982). Increasing wind directional variability produces adhesion warts instead of adhesion ripples which develop laterally upwind of a steady unidirectional wind. The adhesion warts experimentally developed by Reineck (1965) formed in strong winds with frequently

shifting directions thereby favouring upward domal rather than lateral accretion (Kocureck & Fielder, 1982).

7.2.4.1 Adhesion ripples

Description

Strong sediment laden unidirectional winds blowing across a plane surface of the beach having an appreciable amount of surface moisture (12 %>>) form adhesion ripples (Fig. 7.7, Plate 7.10). These are small sub-parallel ridges perpendicular to the windflow and migrate upwind (wind blowing away from the observer whereas ripples migrating towards the observer in Plate 7.10, length of scale 14cm). They show a systematic, rhythmic pattern with even spacing and typically have wavelengths of up to 2 cm and heights of 0.9-1.2 mm (Plate 7.10). The ripple crests are convex in the upwind direction. Very high accretion rates (0.05 cm min^{-1}) of the adhesion ripples have observed.

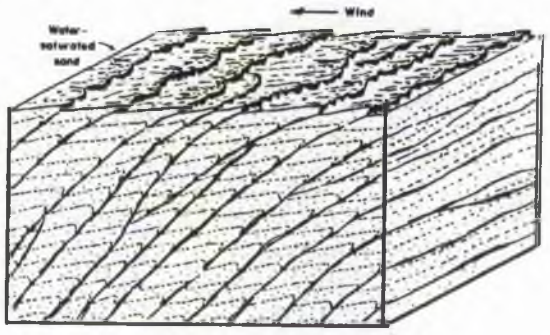

Fig. 7.7 Schematic 3-dimensional representation of bedding due to sand accretion on a wet adhesion - rippled sand surface (Allen, 1984).

Adhesion ripples also form on the St. Andrews bay beaches (Plate 7.11) occasionally as a coating on beds previously rippled or made plane by wave or tidal currents. Two dimensional ripples (as described above) may form on the plane portions of the beach or adhesion structures may develop varying systematically in dimension and scale with the slope and moistness of the surface, where the wind driven sand is plastered over the crest of former current ripples.

Interpretation

When the wind blows sand grains on to a sufficiently wet surface, deposition of sand takes place generally in the form of closely spaced transverse ridges to which the names anti ripplets (Van Straaten, 1953), Halftrippeln (Reineck, 1955), aeolian

microridges (Hunter, 1969), and adhesion ripples (Glennie, 1970) have been applied. The ridges are asymmetric with a gently sloping, bumpy downwind side and a steep, commonly overhanging upwind side (Plate 7.10, Fig. 7.7). This asymmetry is opposite that of 'normal' water or wind ripples. Accretion is accompanied by upwind ridge migration and adhesion ripples climb over the deposits left by their upwind neighbours to generate climbing adhesion ripple structures.

On beaches and inter-tidal flats adhesion ripples exhibiting an asymmetry of direction, which is opposite to that of ballistic and current ripples, climb into the wind with continuing deposition (Allen, 1984). Vertical internal sections parallel to the wind (Reineck, 1955; Bajard, 1966; Hunter, 1973), show irregular interconnected crinkly laminations (or foreset) inclined downwind at an angle of 20 - 60° (Fig. 7.7). Each forest is a pseudobed (McKee, 1965) or a translatent stratum (Hunter, 1977) and is produced by a single climbing adhesion ripple laminae. Climbing adhesion ripple structures are similar in appearance to the more common small-scale tabular cross stratification but can be distinguished by the crinkly appearance and thinness and the extremely tabular form of the foresets These evidently record the upwind climb of laterally adjacent ripples which as individuals varied in wavelength, height and crestal extent throughout life (Allen, 1984).

The adhesion ripples are believed to form when dry grains are trapped by a surface kept permanently moist by the capillary rise of water from below (Van Straaten, 1953). The development of the adhesion ripples, according to Allen (1984) as shown in Fig. 7.8, depends on the local slope of the wetted surface, the grain trajectory, and its capacity to retain particles blown over it. The steeper the approach angle, and the greater the intersection of a significant part of the surface tension film by the impacting grain, the higher is the restraining surface-tension force in contrast to the elastic rebound. Thus all grains arriving on trajectories as shallow as those of A and B are returned to the sand flow. However, the influence of the local slope on the rate of grain-capture is moderated by the ability of a wetting front to ascend, so that a limiting wavelength and height appear (Allen, 1984).

Ancient examples of adhesion ripples in the form of wavy laminations have been documented from the Permian Rotliegendes, NW Europe (Glennie, 1970),

Triassic aeolian dune and inter-dune sediments (Gradzinski *et al,* 1979), a Proterozoic lacustrine deposit (Clemmey, 1978), amongst current rippled sandstone of the Waterberg system, South Africa (De Vries, 1973), in a coastal dune - erg the Upper Cambrian Galesville sandstone (Fielder, 1982) and the Permian Toroweap formation, Arizona (Hunter, 1981). A number of reinterpretations have been made based on the recognition of adhesion structures in various formations. These formations earlier regarded as shallow marine or nearshore subaqueous deposits are now considered to be of aeolian origin (Fielder, 1982).

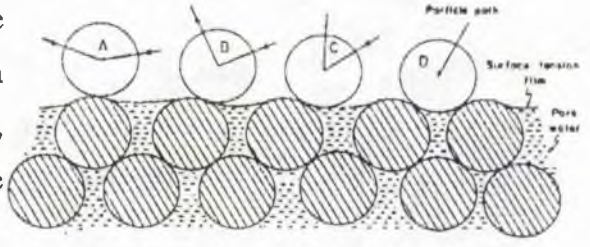

Fig. 7.8 The influence of approach angle on the ability of a surface of water - saturated sand to capture fresh wind blown sand grains (after Allen, 1984).

7.2.4.2 Adhesion plane bed

Description

An adhesion plane bed develops when saltating sand is seen to move over a damp surface, 1-1.5 m away from the tidal margin over a broad zone on the lower beach face approximately 3 m wide on the West Sands beach (Plate 7.12). It appears as a sand spray over a damp surface giving a 'sand paper' appearance (Fig. 7.9). The feature is a fraction of a millimeter in dimension and is structureless in form. However, along the wet tidal margin adhesion ripples have been seen to form simultaneously and the formation of the two structural types may be linked. A seaward sequence from adhesion plane bed (on an absolutely smooth damp surface) to adhesion ripples (plastered over a previously water ripple or a plane bed) at the tidal margin commonly develops under the influence of a moderately strong unidirectional offshore or longshore wind.

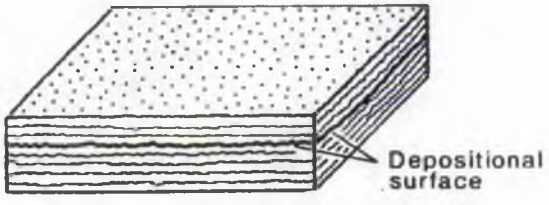

Fig. 7.9 Plan view shape and cross-sectional structure of an adhesion plane bed (after Kocurek & Fielder, 1982).

Interpretation

Adhesion laminations are faint crinkly layers of sand and only a single-grain to a few millimetres thick (Fig. 7.9). The extreme thinness, faintness and crinkly appearance of the adhesion laminae are the characteristic features of the adhesion laminations (Kocureck and Fielder, 1982). The bed is generally smooth with irregularities not much larger than grain roughness.

On a level depositional surface with the water content of the sands below that favourable for adhesion ripple development, adhesion plane bed forms (Kocureck & Fielder, 1982). While describing the formation of adhesion plane bed in interdune deposits at Padre Island Hunter (1981) believed that adhesion laminations underwent greatest accumulations during gusty winds, which blow dry sand on to the damp surface; slackening of the wind below threshold velocity for a few moments allows time for these grains to become damp and adhere to the surface.

The term 'adhesion plane bed' coined by Kocureck (1981) (Fig. 7.9), who independently identified Hunter's (1980) 'quasi planar adhesion stratification) is an adhesion structure which has been identified more recently than either - the adhesion ripples and the adhesion warts. Adhesion plane bed forms by a 'fly paper phenomenon'- grains adhere to a damp surface not marked by adhesion ripples or adhesion warts (Kocureck & Fielder, 1982).

7.2.4.3 Adhesion warts

Adhesion warts are small or oval bumps distinguished from adhesion ripples by their irregularity and open-arched nature (Reineck, 1955) (Fig. 7.10). They tend to have a random distribution due to frequently shifting wind directions of strong winds. The shifting directions prevent the adhesion structures from accreting in any one particular direction, favouring upward rather than lateral accretion. In the study area these structures were not seen to develop on the beach. The reason for their absence can be attributed to

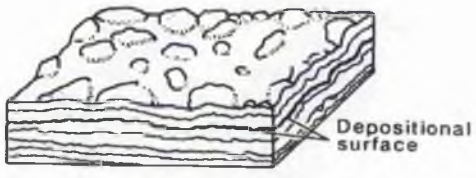

Fig. 7.10 Block diagram showing the plan view shape and cross-sectional structure of adhesion warts (after Kocurek & Fielder, 1982).

the fact that the winds in the area on a short-term basis (few hours- number of days) are seen to be unimodal, thus blowing consistently from a single direction, leading to the formation of adhesion ripples and not adhesion warts.

7.3 SUMMARY OF THE WIND CONDITIONS UNDER WHICH AEOLIAN BEDFORMS ARE GENERATED

On the basis of field observations of aeolian sand transport and the resultant bedforms produced under offshore, longshore and onshore winds on the beaches of Fife, a synthesis or model interlinking winds and the resultant structures is presented in Table 7.1. Each sub-environment is characterised by the presence of a particular sedimentary structure/structures formed under the influence of a particular wind regime. The variables in the model are wind speed, foredune height, and ground surface roughness (as a consequence of vegetation, moisture etc). Three wind velocity categorisations: <6 ms^{-1}, 6.1- 9 ms^{-1} and > 9.1 ms^{-1} (at 2 m height) have been made as a result of field observation.

Low wind velocities whether offshore or onshore, but slightly above the threshold (>4.3 ms^{-1}) when accompanied by occasional gusts, cause intermittent sand movement across the beach.

During very high wind velocities (>9 ms^{-1}, both offshore and onshore) sand strips move across the beach and the foreshore is an almost flat surface, as described by Bagnold (1941), Wilcoxon (1962) and Carter (1988).

7.3.1 Offshore wind induced structures

During high velocity (> 9 ms^{-1}) offshore winds the sand in the lee of the primary dune ridge (1.5-2 m high) is moulded into a pyramidal wind shadow structure pointing downwind. Seaward from the pyramidal dunes, an offshore wind creates a shelly deflation surface in the upper beach face zone. Beyond this deflation surface rippled foreshore sand lobes are formed in the zone of mobile sand in the middle beachface sub-environment. The rest of the sand flux is deposited in the form of sand shadows in the lee of tidal weeds, brought ashore by the tides along the high water mark. Adhesion ripples characteristically develop along the moist/wet tidal margin during

Table 7.1 Model of wind induced bedforms and structures during offshore/onshore sand transport. ' 1' refers to lee dunes formed downwind of tidal debris or any object found on the foreshore. ' * ' means the same as '2' and '3' but smaller volumes of sand will be entrained and deposited here. 'Rippled' refers to ballistically (wind induced) rippled deposits.'a' - Sand strips will transform into barchans if continued high velocity winds (in areas of abundant sediment supply and space) persist over a period of days (4-10). 'b' - Sand strips transform into foreshore sand lobes when high velocity winds blow for a couple of days (1-2). L.W.M. - low water mark (tide). H.W.M. -high water mark (tide). Due to fluctuations in wind flow the bedforms produced under the three velocity categories may be seen to coexist.

SAND TRANSPORT	4.3 - 6 m s^{-1}	6 - 9 m s^{-1}	> 9 m s^{-1}	
ONSHORE	INTERMITTENT SAND MOVEMENT ON THE DRIER PARTS OF THE FORESHORE	* LEE[1] DUNE (landward pointing) DEFLATION SURFACE	AEOLIAN SAND ACCUMULATION OVER & ACROSS THE CREST[3] AEOLIAN SAND ACCUMULATION[2] SAND STRIPS DEFLATION SURFACE	DUNE BACKSHORE H.W.M L.W.M
OFFSHORE	INTERMITTENT SAND MOVEMENT ON THE DRIER PARTS OF THE FORESHORE ADHESION STRUCTURES	RIPPLED DUNEFACE DEFLATION SURFACE RIPPLED SAND LOBES[b] LEE[1] DUNE ADHESION PLANE BED ADHESION RIPPLES	PYRAMIDAL DUNES DEFLATION SURFACE SAND STRIPS BARCHANS[a] ADHESION PLANE BED ADHESION RIPPLES	DUNE BACKSHORE H.W.M L.W.M

WIND VELOCITY

high velocity offshore and longshore winds. Away from the tidal margin an adhesion plane bed is formed.

7.3.2 Longshore wind induced structures

Longshore winds mobilise the sediments towards the northern and southern extremities of the beach, i.e. the mouths of the Eden and Tay estuaries. Along West Sands beach the Eden estuary outlet and the Swilken burn limit the longshore sand movement. The sediments in the drier backshore and middle beach face sub-environments are entrained by the longshore winds, leading to the formation of shore parallel sand accumulation (sand shadows, current crescents, barchans). The potential of the longshore winds to transport sediments is high as they have a much wider fetch than the onshore or offshore winds. Adhesion structures have also been observed at the land water interface.

7.3.3 Onshore wind induced structures

Onshore winds deposit sand on the windward dune slope and over the landward of crest of high foredunes (> 1.5m). Moderate to high wind velocities (6-15 m s^{-1}) result in the development of aeolian ripples on the dry foreshore sand, landward pointing shadow dunes in the lee of the tidal weeds and sand accumulation along the upper beach face or potential foredune area. A very high rate of sand accumulation is encountered in the backshore and the incipient foredune area during high velocity onshore winds.

The onshore winds deflate the lower beach face area and deposit sand along the middle and upper beach face. The area of the beach to be deflated will depend on the width of beach exposed to the wind at a given time.

7.4 AEOLIAN STRATIFICATION

The primary aeolian strata are arranged in various ways within modern aeolian deposits in response to wind regime, moisture levels, vegetation and resulting bedform development during deposition. During preservation complexity is increased by episodes of erosion between preserved sets of strata. These episodes of erosion

remove much of the original deposit, and produce the conspicuous bounding surfaces in ancient rocks (Fryberger, 1990).

The study of the internal structures of dunes has four wide ranging implications (Pye & Tsoar, 1990). First, they provide clues to the growth and dynamics of dune development and secondly, the internal structures of the dunes have been repeatedly used to distinguish between aeolian and subaqueous sands in modern and ancient deposits (e.g. Glennie, 1972; Hunter, 1977; Kocureck & Dott, 1981; Steele, 1983, 1985; Rubin & Hunter, 1985). Thirdly, internal structures in older dunes provide clues to the paleowind directions and permit testing of global circulation models for earlier periods in Earth history (Bigarella & Salamuni, 1961; Parrish & Peterson, 1988). Fourthly, sedimentary structures and associated textural variations exert an important influence on the porosity and permeability characteristics of the deposits, which may serve as hydrocarbon reservoirs and aquifers (Lupe & Ahlbranbt, 1979; Ahlbrandt & Fryberger, 1981; Weber, 1987; Chandler *et al,* 1989).

Most descriptions of aeolian stratification fall into one of the three types 1) Statistical- in terms of the strike and dip of the bedding planes; 2) Structural- description of stratification units in terms of crossbed sets, cosets or geometry of bounding surfaces e.g. McKee & Wier (1953) or 3) Geomorphic - description with reference to position on the dune e.g. slip face deposits or leeward slope deposits (Bagnold, 1956 pp. 241- 243).

Integration of the structural and geomorphic elements of aeolian stratification in the light of the depositional processes was attempted by Hunter (1977) and subsequently by Kocureck & Dott (1981). They recognised three groups of processes responsible for the formation of primary aeolian sedimentary structures (Fig. 7.11): (a) *grainflow deposition*, or avalanching, in which grains reach the brink of a dune then avalanche down the slip face (b) *grainfall deposition*, in which particles settle out of the air usually in zones of flow separation and (c) *tractional deposition* (Bagnold's accretion process), in which grains moving by saltation and impact creep come to rest in a sheltered position. Bagnold distinguished (b) from (c) in that during grainfall, the grains do not move forward when they reach the ground, whereas in tractional deposition they may bounce along until they find a stable position among other grains.

The different aeolian processes described above result in the formation of four kinds of primary aeolian strata (Fryberger *et al*, 1983, Fryberger 1990): (Fig. 7.11);

(a) *grainfall strata* formed by settling of the grains through still air in the lee of the dune,

(b) *avalanche strata* are formed when grainfall deposits at the top of the dune slipface steepens past the angle of repose (about 34° for dry sand) and slump or flow down the slipface,

(c) *ripple strata* which are of two types 1) layers left by the passage of single layers- each ripple leaving a small part of itself as a permanent deposit:

and 2) ripple foresets that form occasionally due to gusting,

(d) *adhesion strata,* which develop when drifting sand sticks to damp or wet surfaces.

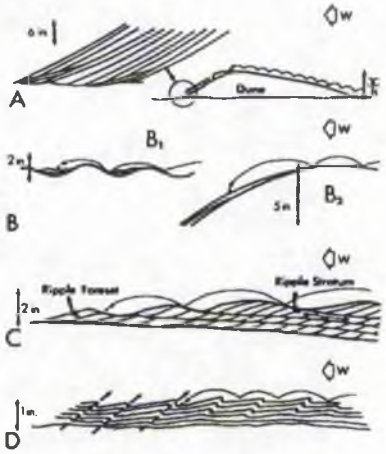

Fig. 7.11 Primary aeolian strata and origins. A: avalanche, B: grainfall, C: ripple, D: adhesion strata (after Fryberger *et al*, 1983).

7.4.1 Aeolian facies

The genetic description of a set of strata such as ripple produced, avalanche or grainfall produced in a particular depositional setting i.e. describing the sediments with respect to the aeolian facies group, has been proposed by Fryberger (1990) (Fig. 7.12). He identified four principal aeolian facies groups: dune, interdune, sand sheet and sabkha (Fig. 7.12). The description given by him is summarised below.

Dune facies consists of a mixture of avalanche, ripple and grainfall strata. The simplest crossbedding patterns develop in barchanoid dunes, which form in unimodal wind regimes, while more complex patterns occur in star dunes, which are formed in complex wind regimes.

Interdune facies generally contains horizontal strata in lenticular sets. The most common primary strata are ripple produced. Interdune areas may be erosional, dry, damp, wet or evaporitic resulting in the formation of fine even parallel layers in the dry interdune facies ranging to slumps, adhesion or bioturbated structures in the wetter interdune facies. Interdune deposits are thinnest in dunefields with rapidly moving

dunes, but are thicker among slow moving or immobile types as linear or star dunes. Some interdune sediments are of composite type representing the passage of multiple dunes but yet with no preservation of the dunes themselves (Simpson & Loope, 1985).

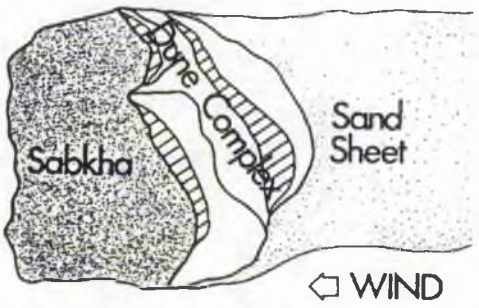

Fig. 7.12 The four aeolian facies. Interdunes are between dunes in the dune complex (after Fryberger, 1990).

The sedimentary features of sand sheets are similar to those of interdune areas, however the sand sheets are laterally extensive, and commonly thicker than those in interdunes. They consist of gently inclined ripple and grainfall strata.

The aeolian sabkha facies may be detrital dominant, in which sand predominates or it may be evaporitic dominant in which deposition of evaporites is faster than the deposition of sand. It is a group of mainly wind-laid sediments that develop in areas with high water tables and extremely saline water. Formation of irregular scour, contorted bedding, and slump structures are characteristic of sabkha deposits (Fryberger, Schenk and Krystinik, 1988).

Earliest descriptions of stratification types in coastal dunes were been made by Bigarella *et al,* (1969) and McKee & Bigarella (1979) while studying the dune ridges along the Brazilian coast. The internal structure of vegetated coastal dunes were studied by Goldsmith (1978), by measuring dip angles to deduce the paleowind direction. A preliminary facies model of the S.E Australian foredunes has been proposed by Hesp (1988). Recently McCann & Byrne (1989) have described the internal structure of the coastal dunes in Atlantic, Canada and have emphasised that vegetation characteristics (amount and type) play a major role in defining the total appearance of the strata.

7.5 INTERNAL STRUCTURES OF TENTSMUIR COASTAL DEPOSITS

The internal structures of the coastal deposits have been studied along a bulldozed excavation perpendicular to the shoreline and also by scraping the exposed dune face parallel to the shoreline. Since it is difficult to identify the stoss and lee side

of the coastal dunes as the dune shape is constantly modified due to the effect of vegetation growth, tidal activity etc., resulting in a hummocky appearance, the internal structure has to be related to the position of the shoreline.

In sections parallel to the shore the most common widespread bedding type encountered is the parallel laminated sands (Plate 7.13). Pinching out of the individual laminae is common. Sometimes the bedding has a very low dip and shows a slight variation in thickness laterally. The light and dark layers indicate heavy mineral segregation within the individual cross-bed. While studying the internal structures of the coastal dunes along the Brazilian coast, Goldsmith (1973) observed that structures transverse to the dominant wind are very low angle (< 5°) and straight to slightly undulating. While describing the internal structure of stage 1 foredune (along the Australian coast) (cf. Section 2.3, chapter 2). Hesp (1988) concluded that most transverse deposition (within stage 1 foredune) took place as a laterally continuous 'sheet' of laminae formed simultaneously along the dune, where few alongshore variations in vegetation existed, the potential for laterally even deposition was high.

Structureless sand lenses of varying magnitude are also present within the thinly laminated horizontally bedded sands (Plate 7.14). The structureless or faintly cross bedded sand lenses found within the thinly bedded strata are thought to be sand accumulations originally deposited around a grass tuft or some other obstacle by an onshore wind. The sand lenses are in effect the transverse sections of a sand shadow described earlier. The dimension of the lens varies proportionately with the size of the obstacle.

Occasionally, a shell layer is present within the laminated sands (Plate 7.15). The shell layers are indicative of phases of beach deflation by the winds, which deplete the beach surface of the fine sediments leaving behind the coarser shelly material (originally transported to the beach by tidal activity).

If vegetation is present, it is in the form of a structureless root bearing mound followed laterally by an unvegetated tail (Plate 7.16). This structure is interpreted as the widely spaced shadow dunes found along the backshore in the lee of pioneer dune grass, such as *Cakile maritima* or *Elymus farctus*. The unvegetated mound consists of grainfall deposits, whereas the unvegetated tail comprises of leeward dipping (~18°)

laminae produced by tractional deposition. In plate 7.16 the shadow structure appears to have been formed in response to alongshore or an obliquely onshore wind as the section is perpendicular to the shoreline.

Subaerial, predominantly wind-generated depositional processes operate in the backshore-dune environments (Walker, 1980). The incipient foredune facies consists of small-medium scale trough cross beds, sand lenses of shadow dunes amongst thinly laminated sands and scarce root debris.

It is suggested that the older dunes were initiated as shadow dunes in the lee of pioneer plants which later coalesced to form primary dunes as vegetation became more continuous and abundant. With increased sedimentation thick sequences of grainfall deposits with concomitant vegetation growth were formed.

As the dunes grow, complexity may develop as a result of increase in the density of vegetation cover. Scouring high velocity winds remove the unvegetated tail of the shadow dune, as soon as it develops, leaving a complicated sequence of beds and laminae. Plate 7.17 shows such successions of shadow dune formation indicating rapid foredune accretion as shadow dunes in the lee of the grass tufts and also faintly bedded or massive deposits formed by grainfall deposition amongst the dense dune grass canopy. Similar concave arching upward cross-strata found within the stage 3 Australian foredunes were interpreted as having been evolved as wind-eroded, saucer -shaped shallow troughs under conditions of a laterally variable vegetation cover (Hesp, 1988).

An exposed area perpendicular to the shore showed festoon cross - lamination, consisting of overlapping asymmetrically filled troughs 70 cm wide (Plate 7.18). The origin of the trough may have been in the form of a blowout or a depression which is a common feature in coastal dune settings. Subsequent deposition in the blowout may result in festoon cross-laminations. This type of cross strata is distinguished by 1) erosion surfaces that form plunging troughs and 2) thin concave upward laminae that fill the trough and conform largely to the shape of the trough floor (McKee and Bigarella, 1979). Thin parallel laminated inter-dune sands are seen to cap the festoon structure. The paleowind direction appears to be longshore (from north to south) since the section is perpendicular to the beach.

Festoon structure repeatedly described in fluvial environments, have not been described from modern aeolian deposits. The Pennsylvanian and Permian Casper formation, believed to be of aeolian origin abound in large trough cross - stratification (McKee & Bigarella, 1979). The greatest problem of assigning an aeolian origin has hitherto been largely conjectural, due to the absence of a modern aeolian analogue exhibiting all the Casper formation characteristics as trough - cross stratification, contorted bedding etc. (McKee & Bigarella, 1979). However, the example from Tentsmuir may provide the satisfactory solution to the mode of origin of these ancient deposits.

The sediments transported to the backshore and upper beach face by marine processes are redistributed over the area by winds and washover processes. Washover processes flooding the incipient foredune and backshore areas produces slumps, minor folds and bioturbation features within the wind rippled incipient foredune and slightly landward dipping backshore facies. The washover processes distort the original form of the aeolian deposit and a reduced version of the original deposit is preserved.

Contorted bedding, wavy laminations folds and slumps have been observed amongst the thinly laminated sands. Since precipitation and moisture due to tidal incursions are not uncommon at Tentsmuir the origin of the deformational structure can be attributed to the instability of the wet/damp sand. Examples of contorted bedding, slumps and folds are shown in plate 7.195. Experiments on contorted bedding by McKee *et al,* (1971), show that these structures are able to form only in wetted sand exposed to rainfall or some other form of moisture. The wetted material is relatively unstable on the steep flank of the dune, slips down over the underlying less-cohesive dry sand resulting in the formation of folds and faults (Glennie, 1970).

Aeolian movement of sand across the moist lower beach face produces faint crinkly laminations of adhesion plane bed, marking the presence of a damp surface, a couple of metres away from the tidal margin. Landward dipping adhesion ripple laminae, will mark the land-water interface, along the tidal margin. The genesis of these adhesion structures has been discussed earlier.

A vertical section of a beachface deposit, which has been deflated from time to time by strong winds, will reveal the presence of a thin shell lag layer, sand strips

preserved as parallel laminae, trough -cross bedded ridge-runnel deposits, landward dipping adhesion ripples, faint crinkly adhesion plane bed laminations amongst the low angle seaward dipping beach laminae. However, the preservation potential of the adhesion structures appears to be quite low. Nevertheless their recognition would be of paramount importance in making paleoenvironmental reconstructions.

Horizontal laminae and low angle accretion is also observed on the tops, wind ward slopes and rounded flanks of dunes (Glennie, 1970). He explained the formation of horizontal laminae in interdune areas, in accordance with Bagnold (1941), to a combination of rapid deposition, high wind velocities and fairly uniform grain size of the transported sand.

Description of various stratification types as observed in a vertical sequence and sedimentary structures in the various beach-dune environments interpreted in a temporal dimension can also be represented in a spatial context. An ideal prograding coastal beach- dune stratification and depositional model is shown in Fig. 7.13.

Unit A constitutes the beach facies consisting of adhesion ripple laminae followed by adhesion plane bed, seaward dipping horizontal laminae. The runnel constitutes trough cross-bed strata. Shell layers amongst parallel laminated sands are indicators of wind deflation.

Unit B comprises of thin cross-laminated beds of fine to medium sand dipping at low angles with sand lenses. There is occasional evidence of presence of vegetation during deposition. This unit is believed to be deposited as small shadow dunes around widely spaced pioneer plants ((Plate 2.20, 2.21)).

The shadow dunes described above eventually coalesce and a continuous foredune with abundant vegetation is developed (unit C) (Plate 7.22). In a vertical section this environment will be represented as bedded deposits attaining appreciable thicknesses formed mainly due to grainfall deposition or as precipitation structures due to occasional fresh sand inputs during gales. The bedding is distorted due to the presence of grainfall deposits with abundant plant remains.

During further growth of the dune it is succeeded seawards by a new incipient foredune, thereby limiting the fresh sand input and growth of the primary dune. Loss of

(a)

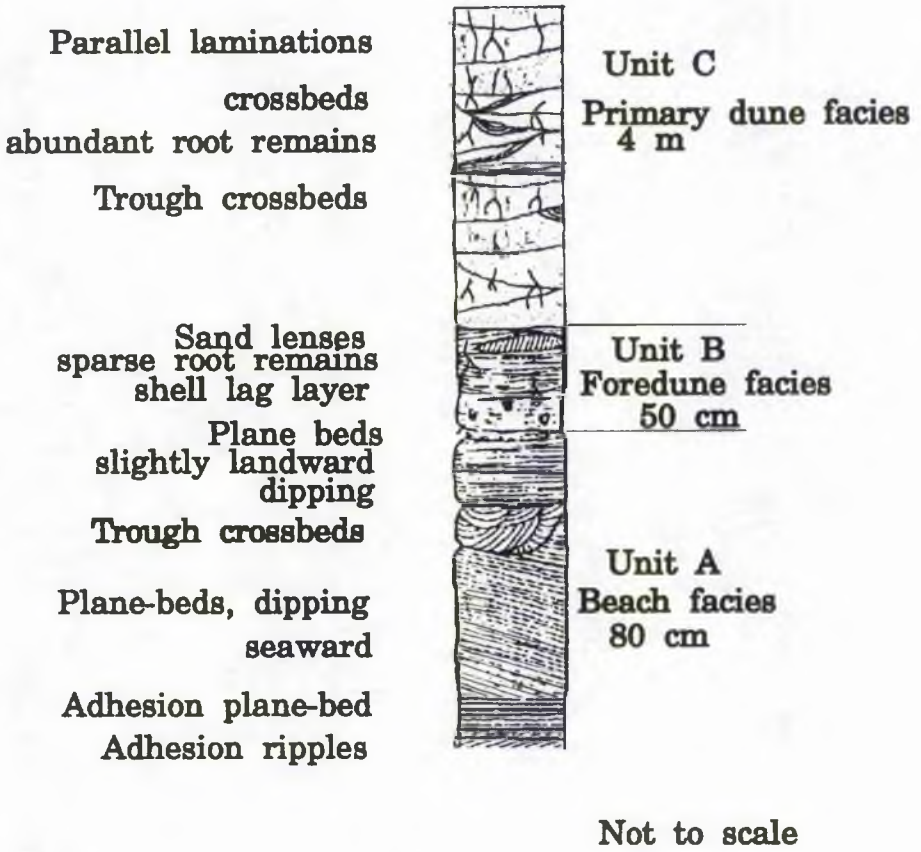

(b)

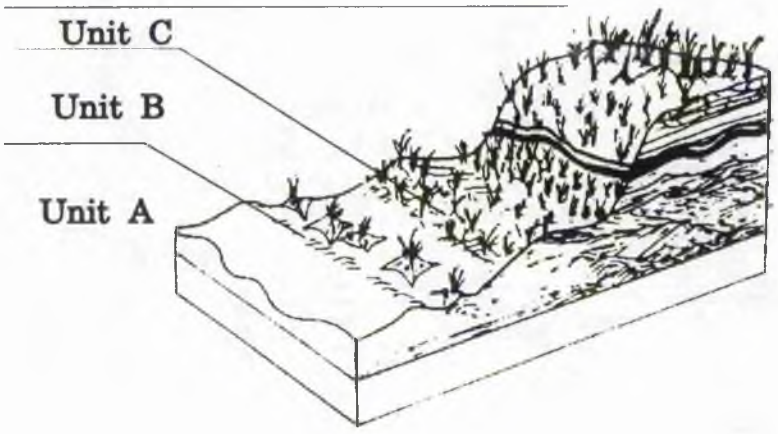

Fig. 7.13 (a) A conceptual facies model of a prograding coastal beach-dune complex (modified from Walker, 1980). (b) A depositional model of the coastal beach-dune complex showing the three depositional facies (modified from McCann & Brynne, 1989).

fresh sand input leads to a change in the dune vegetation habitat from dune grass into a moss and shrub dominant one, where in due course of time soil horizons develop.

7.6 CONCLUSIONS

Most of the structures seem to be developed in response to strong unidirectional winds. Parallel laminated sands, various cut and fill structures (trough-type deposits) and sand lenses are the usual forms seen in sections. The presence of contorted bedding, slumps and folds is indicative of the disturbance of moist/wet sand due to rainfall, water table levels or tidal incursions. The primary mode of foredune accretion at Tentsmuir is through the initial formation of a longitudinal sand body formed under the influence of unidirectional winds (tractional and grainfall deposition) and later vertical accretion in place (grainfall deposition) concomitant with vegetation growth, with little slip face migration and accretion. Thus the coastal dunes on this accreting system are not envisaged as having a significant migration phase during their development.

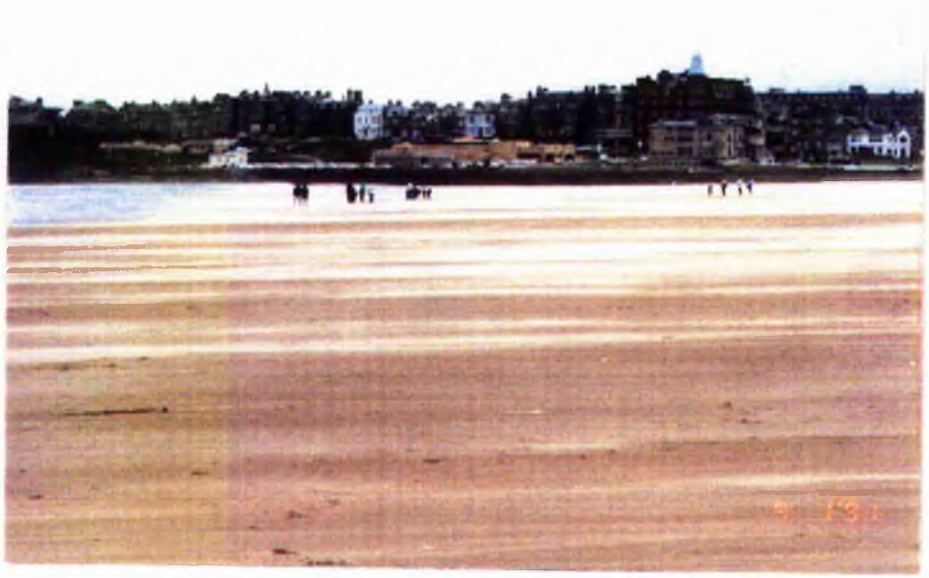

Plate 7.1 Sand strips moving offshore on West Sands beach, St Andrews during a high velocity offshore wind on April 1, 1991 (wind velocity > 15 ms^{-1} at 2 m height). Water edge seen in the background.

Plate 7.2 Regularly spaced sand strips and intervening shell deflation surfaces across West Sands beach, St Andrews during a high velocity offshore wind on April 1, 1991 (wind velocity > 15 ms^{-1} at 2 m height). The shell layer (arrow) corresponds to zone 'A' of Fig. 7.1.

Plate 7.3 Development of sand lobes during a period of 28 hours. The sand lobes are moving across the foreshore. Note the asymmetric sinuous ballistic ripples showing seaward transport. Photograph taken on April 2, 1991.b - buttress junctures and o - open junctures of the ripples are also observed.

Plate 7.4 Development of barchans at Tentsmuir Point during November 1968 during northerly longshore winds (from left to right). Distance between the horns of the individual barchans is ~ 3 m. The Tentsmuir forest cover is seen in the background. (Courtesy: Malcom Smith, Nature Conservancy Council, Cupar). Inset shows the windflow modification around an individual barchan. Diagram after Warren, 1979.

Plate 7.5 Ballistically rippled wind shadow formed in the lee of tufts of *Elymus farctus* along the backshore at Tentsmuir Point. Wind direction from left to right. Length of scale 13 cm.

Plate 7.6 Development of a lee accumulation formed in the lee of a tree stump (50 cm wide) along the backshore at Tentsmuir Point. The tree stump lies partly embeded in the deflated beach surface. Scouring action of the wind on either sides of the accumulation indicates that the wind scoured the sand from the sides of the obstacle and deposited it towards the centreline of the stump.

Plate 7.7 Scour remnant ridges formed on the St Andrews beach when a strong wind has deflated the beach surface leaving behind ridges of sand scattered across the surface. Sand strips are seen to move across in the background. Photograph taken on April 1, 1991.

Plate 7.8 Pyramidal wind shadow dunes formed in the lee of a primary dune ridge during very high velocity offshore winds on St Andrews beach. Inset shows a closeup of the pyramidal structure.

Plate 7.9 Scratch circles formed by the etching action of *Elymus farctus* blades leading to the devlopment of semi-cicular scratch marks on the sand surface.

Plate 7.10 Adhesion ripples developed on a moist beach surface at West Sands. The wind direction is away from the observer. Note the sub-parallel ridges perpendicular to wind flow migrating upwind. (Length of scale 14 cm).

Plate 7.11 Adhesion ripples (arrow) formed as a coating on the leeward side (wind direction is from right to left) of wave ripples. (Length of scale 14 cm).

Plate 7.12 Adhesion plane bed formation 1 to 1.5 m away from the tidal margin. Wind direction is from right to left. The sand paper appearance of the surface is very distinct. (Length of scale 14 cm).

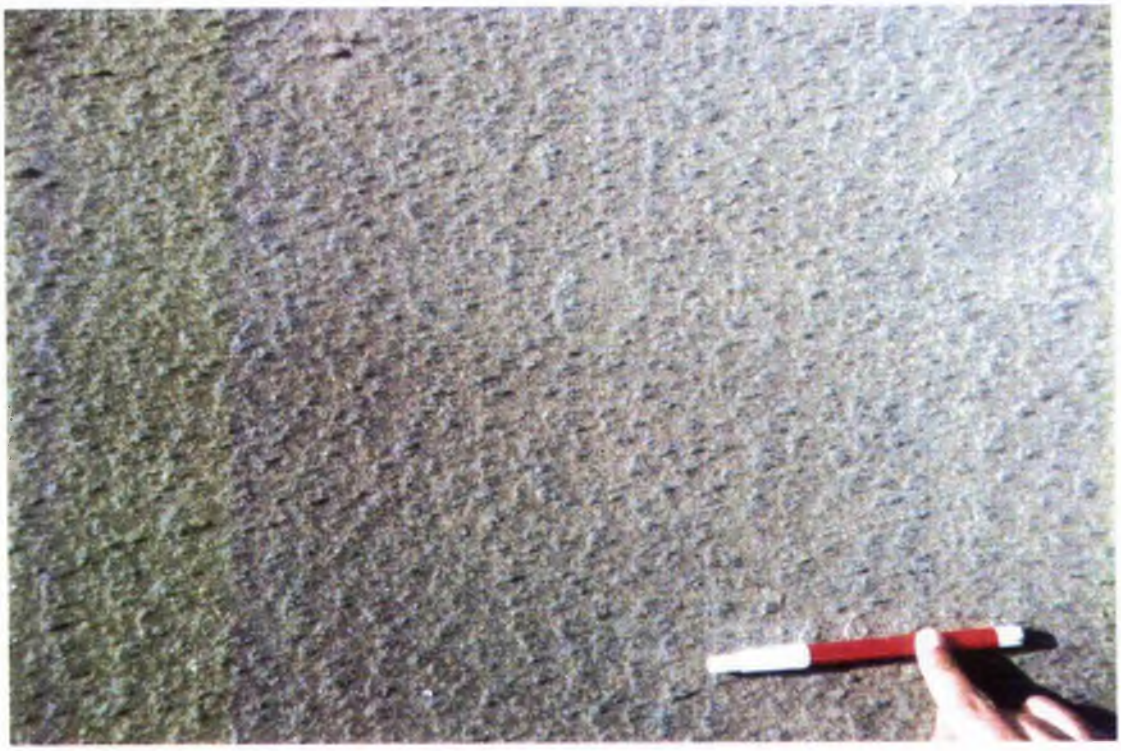

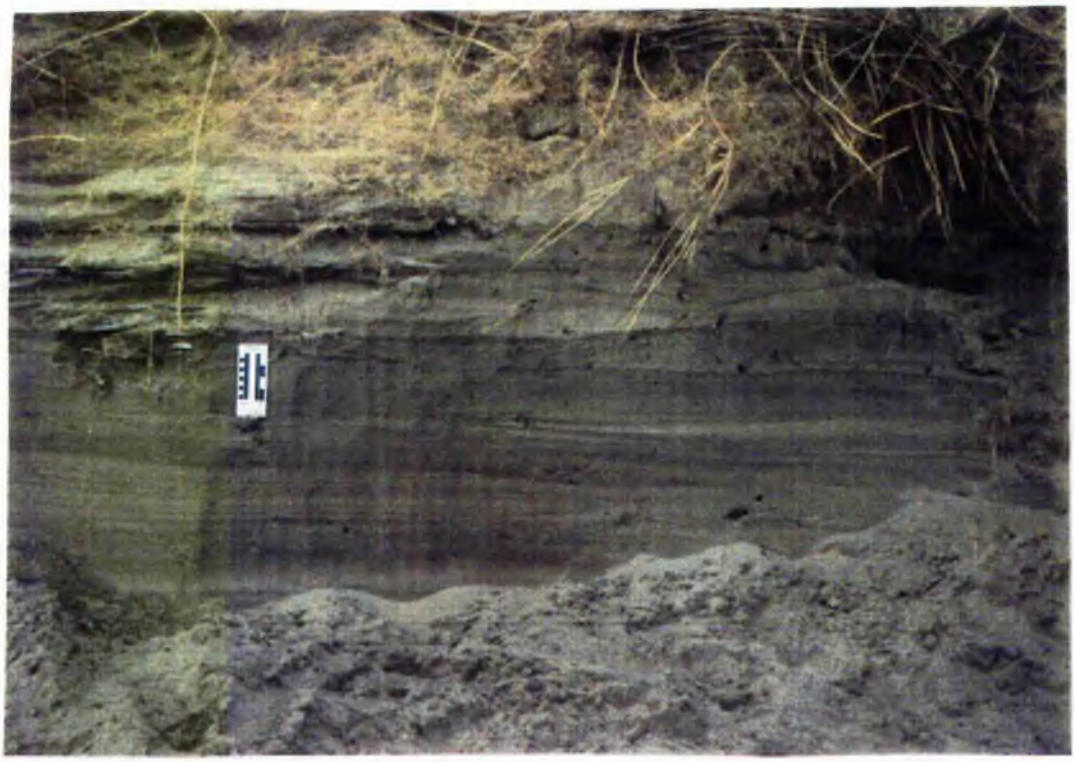

Plate 7.13 Parallel laminated sands exposed along the shoreline. Individual cross-bedded units thin out towards the midle of the photograph.

Plate 7.14 Closeup view of a sand lens 5.5 cm wide (centre arrow). The sand lens is structureless and there appears to be a stacking of lenses (left arrow) around the middle part of the photograph.

Plate 7.15 Shell layer deposited within a horizontally bedded sequence (arrow), signifying phases of beach deflation. The parallel laminated sand strips have been deposited by unidirectional strong winds. Overlying the parallel laminated beach deposits are present the cross-stratified dune sediments. The mottled surface towards the top is indicative of plant remains.

Plate 7.16 Cross section of a lee dune showing a structureless root bearing mound (solid arrow) followed laterally by an unvegetated tail (open arrow) with beds dipping at 18°. The vegetated mound consists of grainfall deposits whereas the leeward dipping laminae are beleived to have been produce by ?tractional deposits.

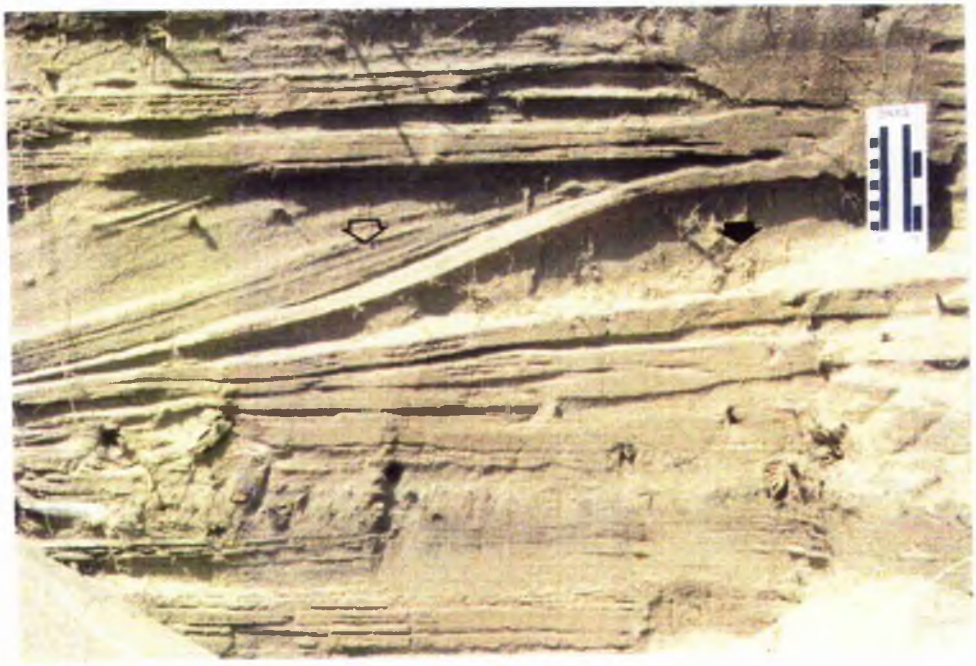

Plate 7.17 Densly vegetated dune succession showing vertical foredune accretion in the lower half of the photograph (zone a) where several lee or shadow dunes have coalesced and accreted very rapidly. Zone b is indicative of densely vegetated primary dune succession where the accretion has been slow - primarily by grain fall.

Plate 7.18 Trough type cross strata in coastal dunes (arrow) excavated in a trench perpendicular to the shore. The wind is in a direction perpendicular to the plane of the photograph. Scale length of exposed tape is 22.5 cm.

Plate 7.19 Contorted bedding (arrow) in excavation perpendicular to the shoreline.

Plate 7.20 Fore dune accretion around pioneer dune grass *Elymus farctus* (formerly known as *Agropyron sp.*) along the backshore.

Plate 7.21 Widely spaced small shadow dunes formed in the lee of *Cakile maritima* along the backshore.

Plate 7.22 Continuous dune accretion concommitent with dense *Ammophila sp.* growth at Tentsmuir Point.

Chapter 8
DISCUSSION AND CONCLUSIONS

(with 12 figures and 3 tables)

Chapter 8
DISCUSSION & CONCLUSIONS

8.1 INTRODUCTION

Throughout the work reported in this study attention has been directed almost exclusively to sand transport and dune formation in the Tentsmuir area. However, during preparation of the thesis visits have been made to other coastal sites in Scotland which have actively accreting dune systems. Most, but not all of these, are on the west coast of central Scotland where, onshore winds are dominant unlike the offshore dominated systems of Tentsmuir. Reference to existing accounts of the onshore dominated systems confirms that the landforms are often larger in scale and differ in the development of features such as barchanoid and parabolic dunes. In consequence, before entering a final discussion of the physical factors influencing sand transport at Tentsmuir a brief review will be made to draw attention to contrasts between features of coasts dominated by offshore and onshore wind systems. Such features are not confined to the Scottish coastlands for many have been reported from coasts of other continents. The morphological variation of the coastal dunes in relation to specific environmental setting envisages major differences between 'onshore' (west) and 'offshore' (east) dune systems of the U.K. and in other parts of the world. The 'offshore' system is exemplified by the Tentsmuir area and other locations represent 'onshore' systems.

Little has been achieved by way of geomorphological and process based studies on coastal dunes except for the study of Braunton Burrows (~1000 ha), southwestern England (Sarre, 1985), Formby Point (~1200 ha) (Pye 1990), Sands of Forvie (1277 ha), N.E. Scotland (Robertson-Rintoul, 1985) and Tentsmuir Point (1781 ha), eastern Scotland (Wal & McManus, 1992). Aeolian sand transport rate studies have been carried out only at Braunton Burrows (Sarre, 1985) and Tentsmuir (in this study). However, globally such studies have been attempted along the coastlines of Israel (Goldsmith *et al.*, 1990), Alexandria in South Africa (Illenbeger &

Rust, 1988), Oregon (Hunter *et al.*, 1983), Tabusintac Island, Canada (Rosen, 1979), Castroville, California (Bauer *et al.*, 1990) and Lake Erie (Davidson-Arnott & Law, 1990) and Magilligan Point (Carter & Wilson, 1990). Although more work is needed along the British coastline to warrant a comparison of the onshore and offshore systems, an attempt has been made to compare and contrast the west and east coast dunes with the aid of existing literature and field examination of the coastlands of the Kyle & Carrick and Cunninghame Districts in southwestern Scotland.

8.2 DUNE SYSTEMS OF THE U.K.

Sand dunes occur extensively around the coastline of Britain covering an area of 56, 000 ha which comprises 7.4% of the coastline (Doody, 1989) (Fig. 8.1). The Culbin sands are by far the most extensive single dunefield in the U.K. spanning over 4,000 ha. along the Moray Firth coastline. The prevailing wind and wave conditions, sand supply and beach profile determine the extent of dune development along the coasts (Doody, 1989). These factors may also be modified by the physical location of the dune. On analysing the distribution and area of the dune systems in the U.K. Doody (1989) found that major concentrations of dunes exist in the Western Islands (Outer Hebridean) and in North East Scotland (Fig. 8.1). Elsewhere they are smaller in area and more isolated. Five major types of dune systems have been identified in relation to the prevailing direction of sand movement by Ranwell & Boar (1986) (Fig. 8.2). These are (1) Bay dunes (both offshore and onshore sand movement), (2) Foreland dunes (offshore sand movement), (3) Spit dunes (longshore sand movement), (4) Offshore island/barrier dunes (longshore sand movement) and (5) Hindshore dunes (onshore sand movement). The dune development may be associated with specific environmental settings such as estuary or river mouth areas, or areas downdrift of eroding shorelines (Fig. 8.3). Present-day dune development has been recognised by Carter & Wilson (1991) in the first two environmental settings.

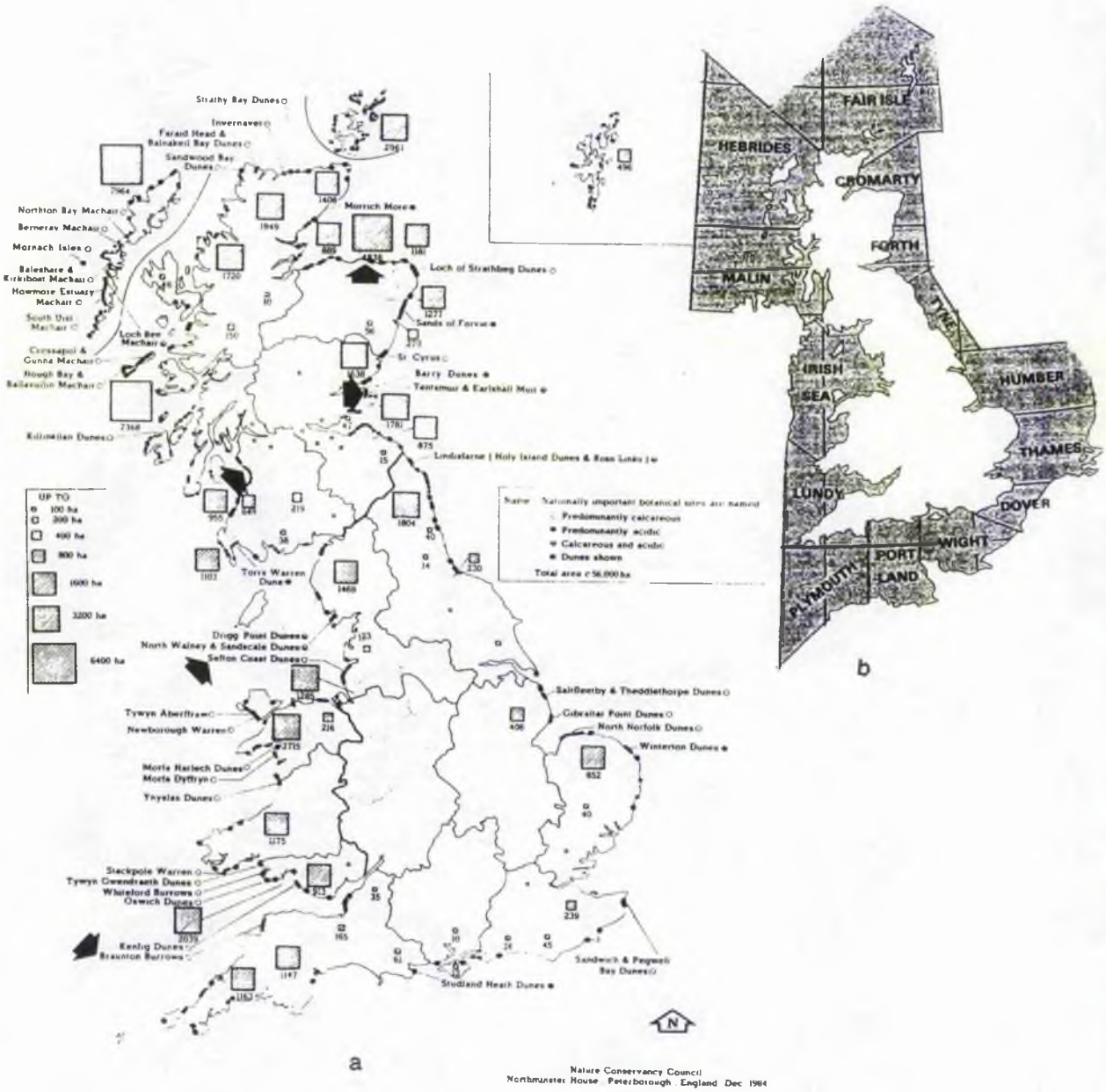

Fig 8.1(a) Distribution of sand dunes around the coastline of Britain (after Doody, 1989). Arrows show areas discussed in text.
b) Subdicvison of coiastline sectors.

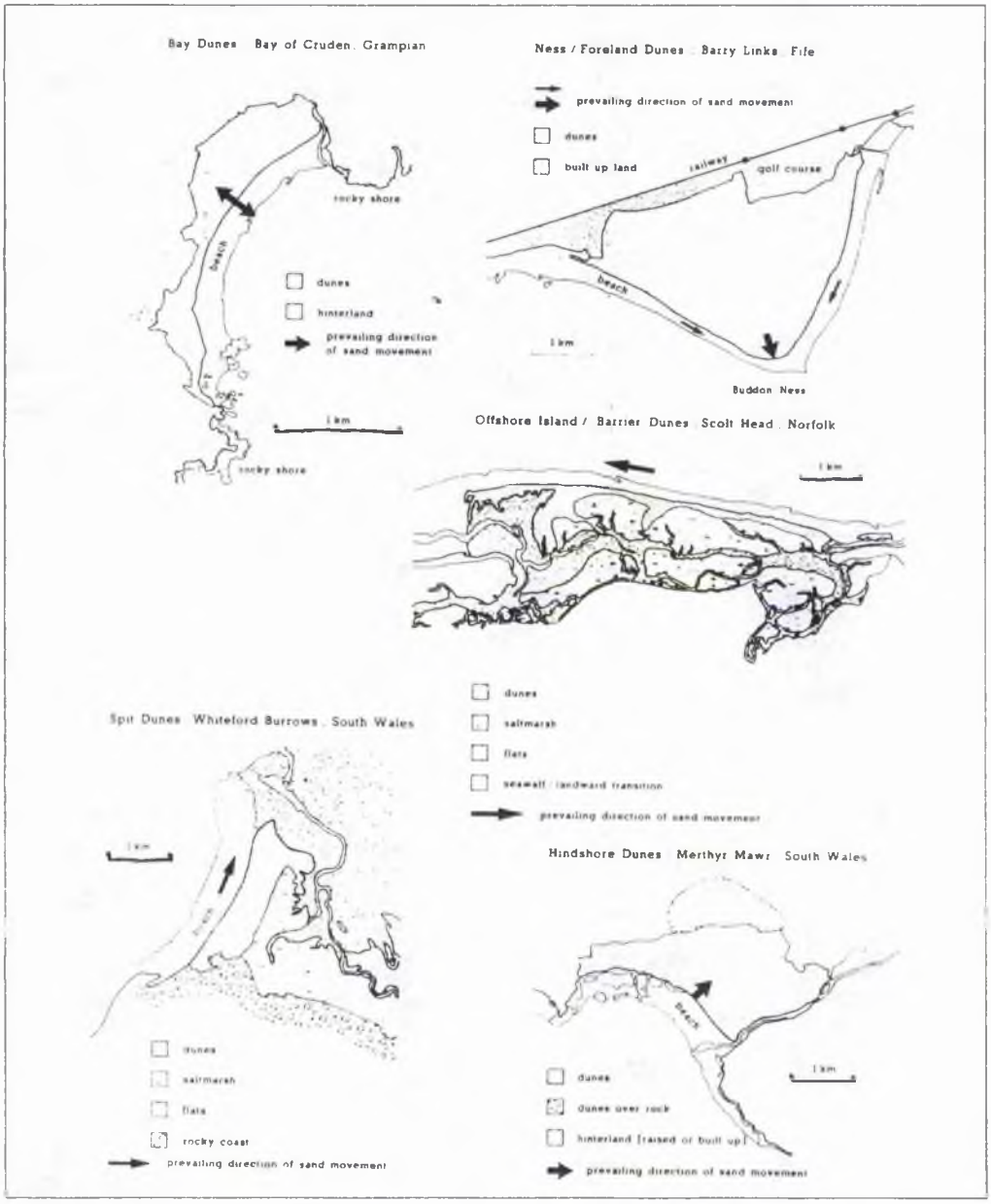

Fig. 8.2 Major types of dune systems in Britain in relation to the prevailing direction of sand movement (after Ranwell & Boar, 1986)

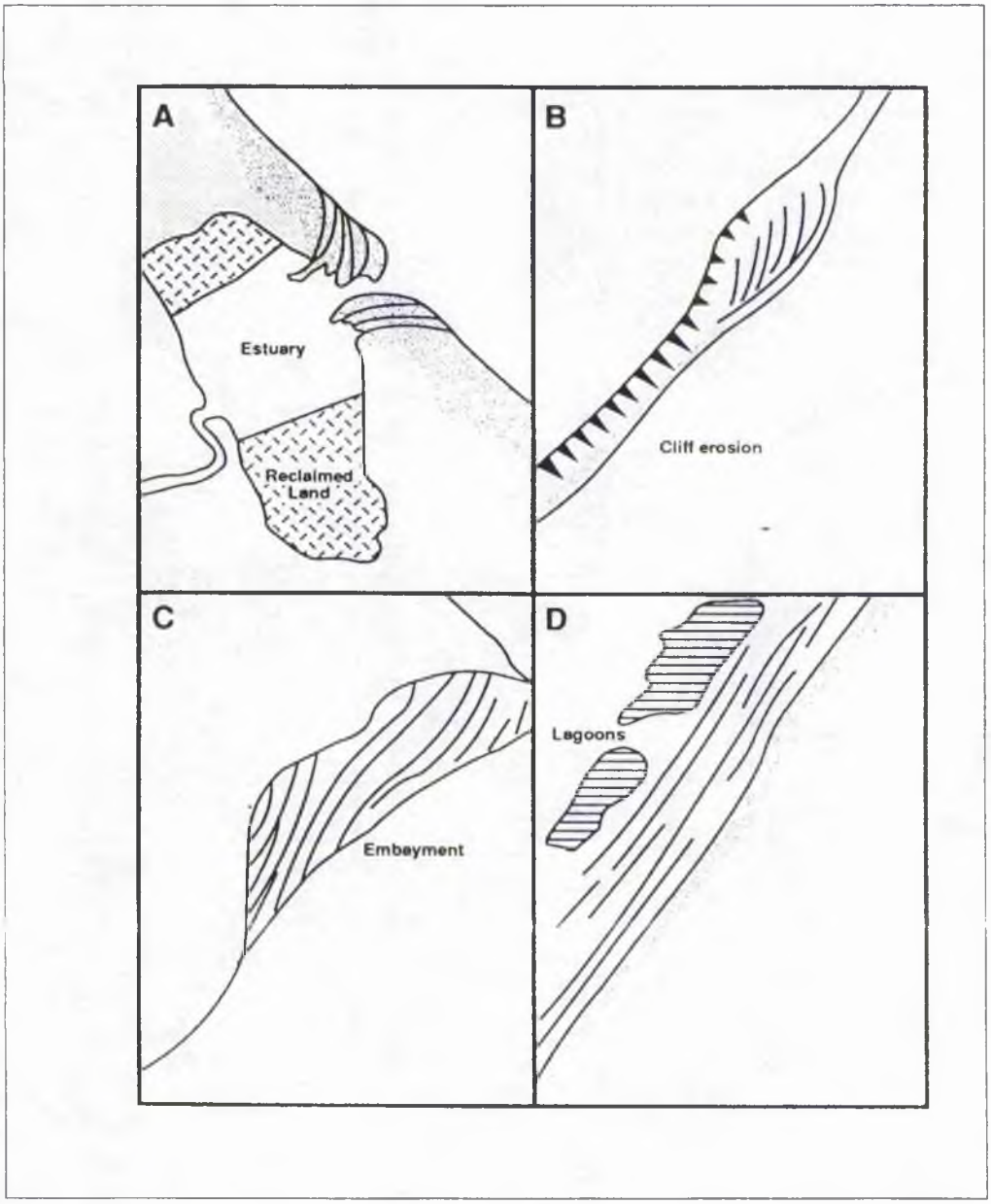

Fig. 8.3 Environmental settings of dune development in Ireland (after Carter & Wilson, 1991).

Table 8.1 Dune distribution indices of the British coastline ($D.D.I = \frac{Area\ of\ dune}{length\ of\ coast}$)

Basin	Dune system & area	D.D.I	Wind (dominant)	Estuary/River
Cromarty 300 km	Elgin 889 ha Culbin 4838 ha Strathbeg 1181 ha Forvie 1271 ha	27	Offshore Unimodal	Moray Firth
Forth 175 km	Barry 1638 ha Tentsmuir 1781 Lothian 875 ha	25	Offshore Unimodal	Firth oy Tay & Forth
Tyne 200 km	Nothumberland 2034 ha	10	Offshore	Tees estuary
Humber 275 km	Saltfleetby Gibraltar point 408 ha North Norfolk Winterton 852 ha	4.5	Offshore	Humber estuary The Wash
Thames to Portland 900 km	Sandwich & Pegwell 239 ha Studland 61 ha Total 433 ha	0.5	Longshore	Thames estuary Bays
Plymouth &Lundy 850 km	Cornwall 1163 ha Devon (Braunton) 1147 ha Kenfig 913 ha Glamorgan 2039 ha Pembroke 1175 ha	10	Onshore	Bristol channel Cardigan bay
Irish sea 850 km	Gwynedd 2715 ha Clwyd 216 ha Lancashire (Sefton) 1285 ha Cumberland 1469 ha Dumfries & Galloway (Tors Warren) 1141 ha	8	Onshore Complex	Liverpool bay Morecambe Bay Solway Firth
Malin 650 km	Strathclyde Ayr 1823 ha Argyll 7368 ha	20	Onshore Unimodal	Firth of Clyde Firth of Lorne Sound of Jura
Hebrides 450 km	Sutherland 1720 ha Highland (Ross & Cromarty) 1949 ha Outer Hebrides 7964 ha	8 26	Complex	Atlantic Ocean

The dune distribution and area on the U.K. mainland (Table 8.1) is governed by (1) the type of wind regime (offshore/onshore/longshore) and strength, (2) the type of landward (rocky shores, extreme marsh/saline areas, former and present river courses) and seaward (bay, estuary mouths, nearshore bathymetry (gentle/steep)) geomorphology, (3) temperature and rainfall variation, and (4) availability of

sediment. The simple ratio of dune area to coastal length is referred to as the Dune Distribution Index (D.D.I.)

$$Dunedistributionindex = \frac{Area}{length}\ \frac{of}{of}\ \frac{dune}{coast}$$

Very high D.D.I. values (in brackets) are obtained for the Moray Firth (27), Forth (25) and Malin sectors (20). The Outer Hebrides and Fair Isle group of islands also have very high values (ranging from 16-28). Since the overall environment and variables influencing dune development on the mainland of U.K. will be different from those of the islands (Outer Hebrides, Orkney & Shetlands) it is best to treat them as a separate grouping. Moderate dune distribution ratios are represented along the Tyne (10), Plymouth to Lundy (10) and Irish Sea sectors (8). The Humber (4.5) and Thames to Portland (0.4) sectors have lowest Dune Distribution indices. The regional dune development scenario shows high areas of dune proliferation along the northeastern, eastern and western coast of Scotland, moderate dune development along the northeastern, northwestern and southwestern England and low or sporadic dune occurrences along the southeastern and southern parts of the English coastline. The islands of Outer Hebrides, Orkney and Shetland abound in dune machair surfaces which are areas of grassed lowlands over dune flats used for grazing by crofters.

8.2.1 The wind regime

The winds from the west and southwestern sectors are the most dominant winds of the British Isles. They are onshore winds for the western coastline and offshore winds for the eastern coast. Sand roses (Fig. 8.4) and wind regimes (Fig. 8.5) of the Scottish coastline have been summarised by Robertson-Rintoul (1985). She indicated that winds with greatest directional variability and highest energy characterise the north and west coast (Dounreay, Machrihanish) whereas relatively lower wind energy coupled with greater constancy of wind direction are more normal along the east coast (Leuchars, Turnhouse). The wind strength decreases from north to south (compare Dounreay & Fraserburgh with Turnhouse and West Freugh). Complex wind regimes are observed at Wick, Dounreay, Machrihanish and West Freugh.

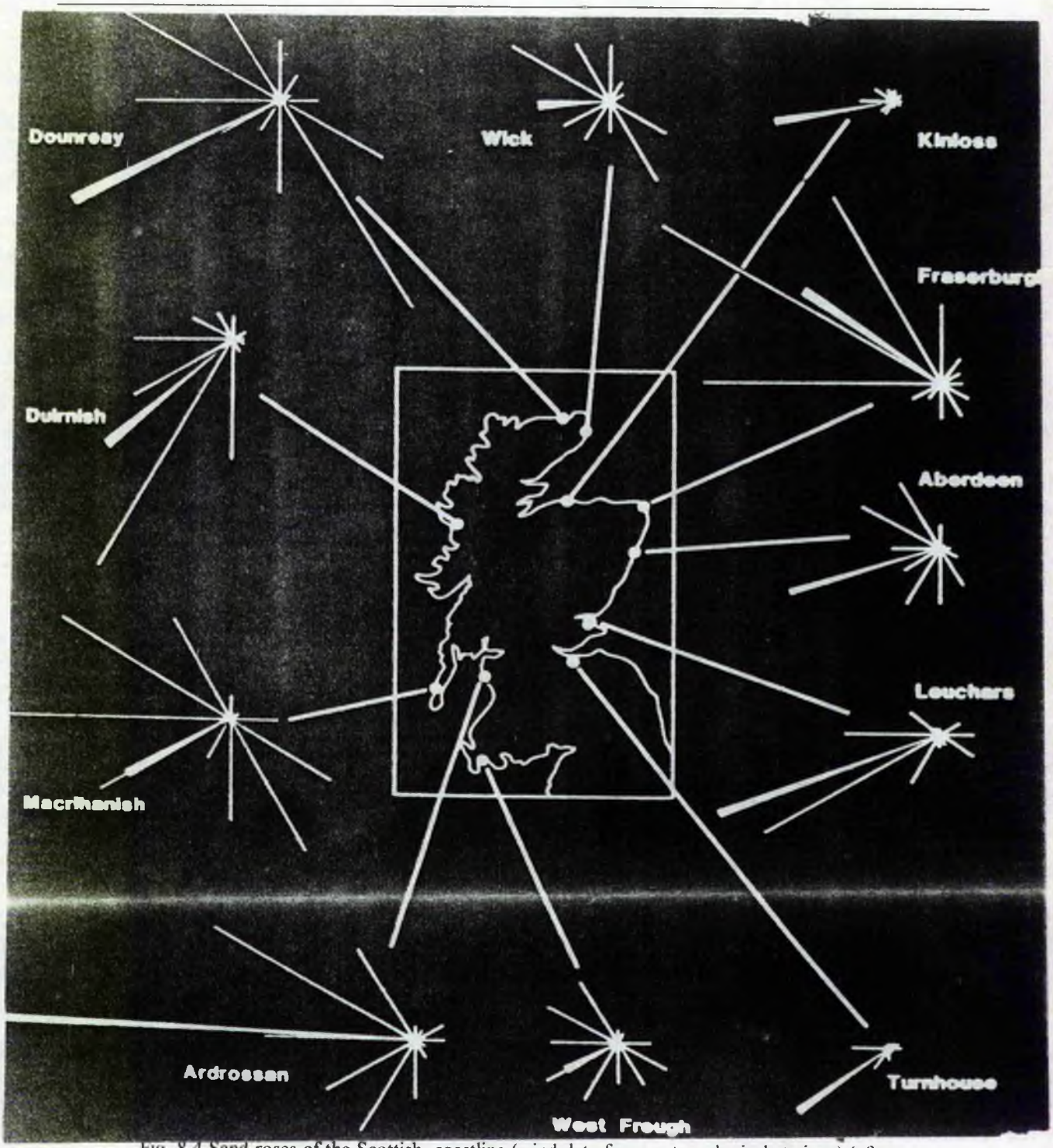

Fig. 8.4 Sand roses of the Scottish coastline (wind data from meteorological stations) (after Robertson-Rintoul, 1985)

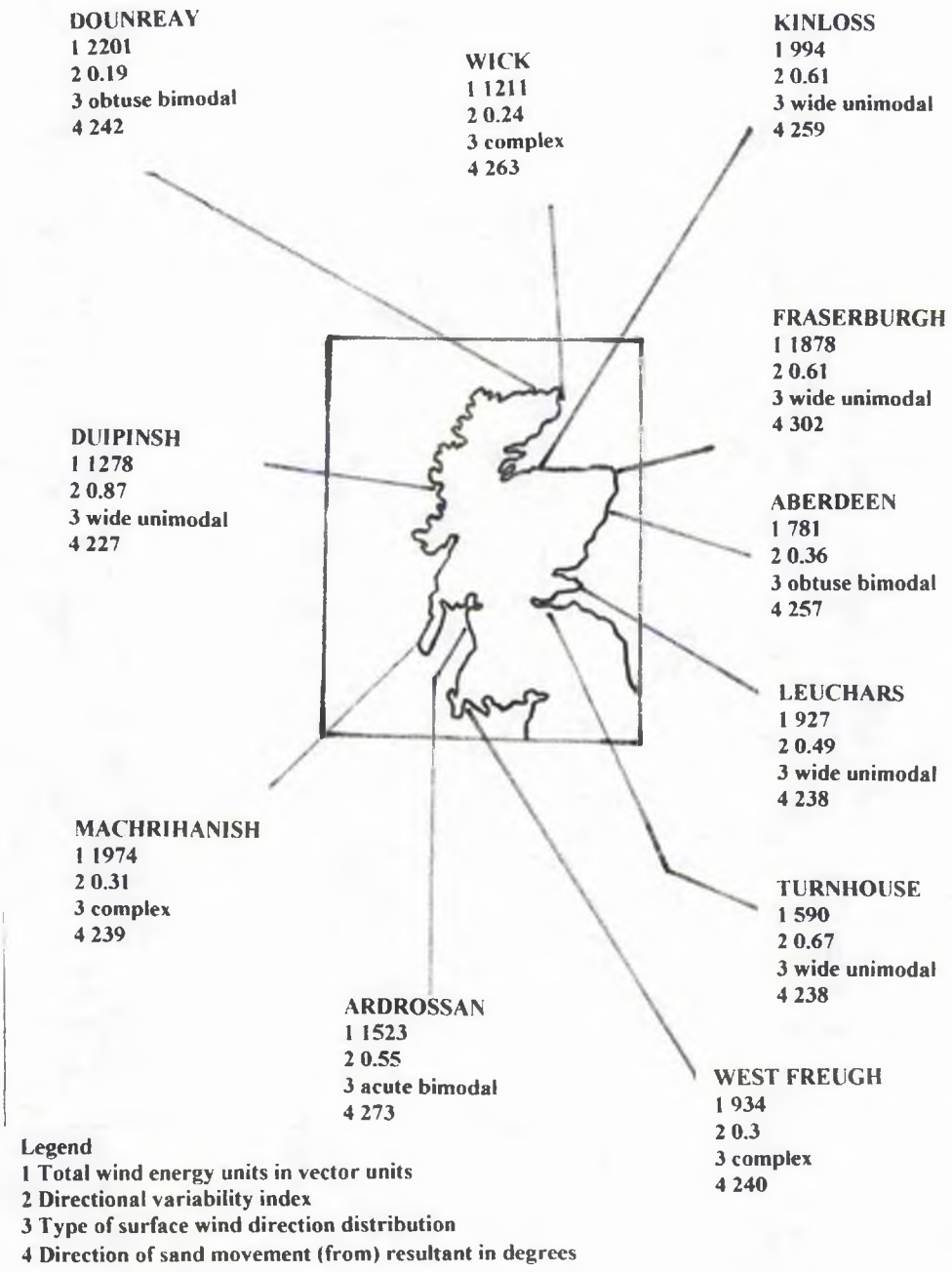

Fig. 8.5 Wind regimes of the Scottish coastline (wind data from meteorological stations) (after Robertson-Rintoul, 1985)

The dominant winds and waves, at Formby Point, Lancashire, originate from the west and west-northwest (onshore) and correspond with a maximum fetch of over 200 km in the Irish Sea (Pye, 1990). Wave energy is moderate and waves with significant heights above 2 m occur for not more than 3% of the year (Pye, 1990).

The winds at Braunton Burrows (Plymouth to Lundy sector) are also dominantly derived from the West and northwest with subordinate winds from the South and Southeast (Sarre, 1988) (Fig. 8.5). Elsewhere along the English coastline a similar trend is observed.

8.3 DUNE SYSTEMS DOMINATED BY ONSHORE WINDS

Although dune systems created by onshore winds exist in many places, observations of only a few typical sites are given.

8.3.1 Cunnighame and Kyle & Carrick District (Fig. 8.1, 8.6)

Pockets of dune development are observed along the south-western stretch of the Scottish coastline. Brief visits to this coast revealed that at Stevenston south of Saltcoats there are two dune ridges along with a row of incipient dune hummocks. The most inland dunes are approximately 10 m high and have abundant dune blowouts within them encircling areas up to 200 m^2. Podzolisation and carbonaceous horizons, abundant plant root remains and wavy bedding characterise the older dune ridge.

Seaward of this dune ridge is present a row of hummocky foredunes approximately 3-4 m high. The dunes do not occur as a continuous ridge but have numerous unvegetated gaps of mobile sand within them. These dunes represent stage 2 foredunes of the Short & Hesp (1980) (Fig. 2.10) classification. No podzolisation is evident among the foredunes. The 1-2 m high incipient dune forms along the berm are colonised by *Elymus farctus* and whereas the two discontinuous dune ridges are mainly *Ammophila arenaria* dominated.

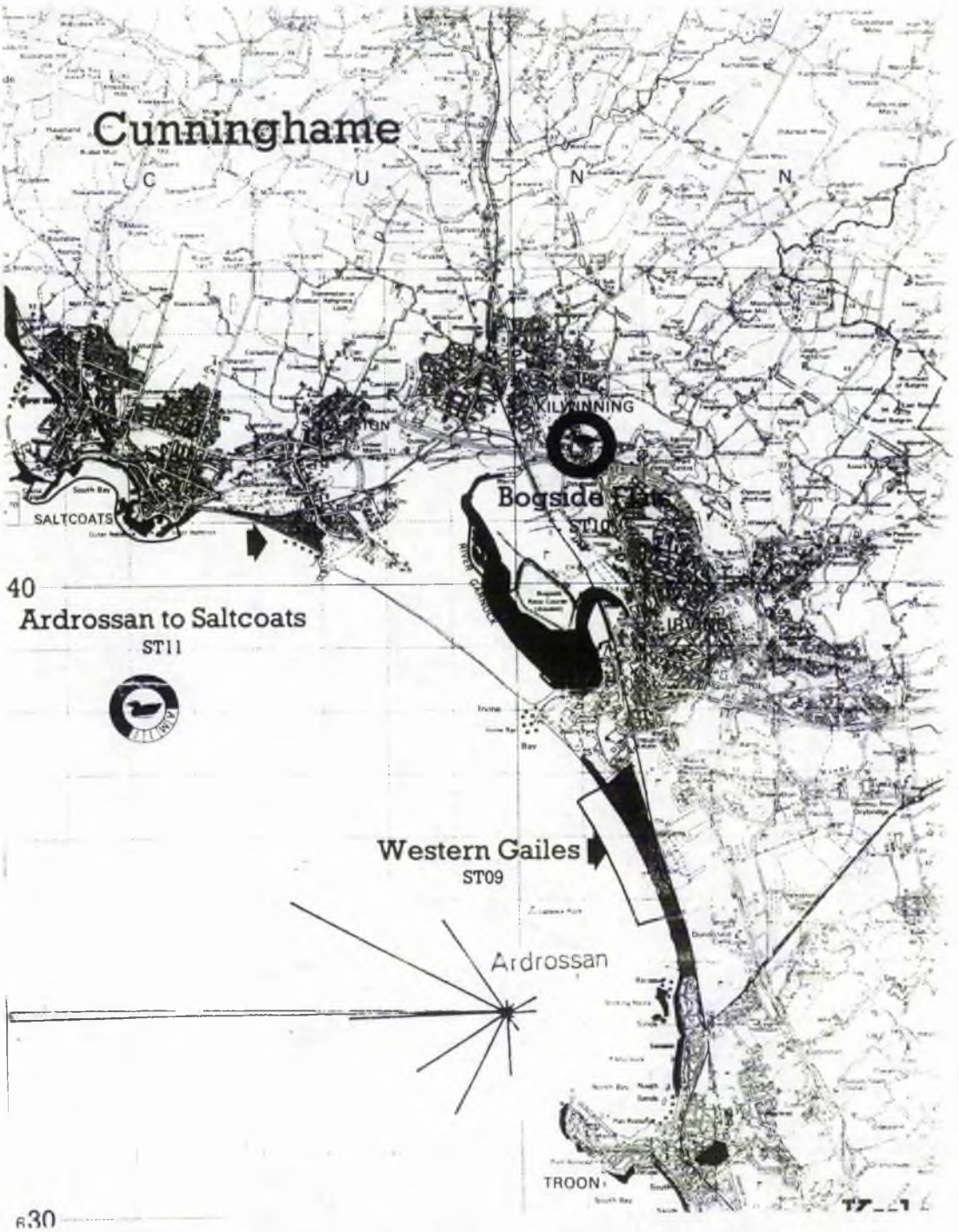

Fig 8.6 Location map of dunes of Cunnighame and Kyle and Carrick Districts of western Scotland and sand rose at Ardrossan. Arrows represent areas examined (courtsey Nature Conservancy Council).

Although the dunes have a dominantly hummocky or irregular appearance an aerial view of the current incipient foredune development stages suggests their formation initially in a row along the backshore, stabilised by primary dune grass the apices of the hummocks corresponding to areas of maximum pioneer vegetation concentration. Pedestrian pressure on these dunes may partly be responsible for the initiation of the broken ridge appearance and blowout initiation among the dune systems. Fragments of cherts, shales and cementstones (2-8 cm) form a pavement along the 20 m wide berm where incipient dune hummocks are forming parallel to the coast.

The beach is approximately 100 m wide and exhibits a ridge and runnel morphology. It is littered with abundant coal fragments.

The area of Western Gailes at Irvine (Fig. 8.6) has a 4 km long stretch of 6-8 m high *Ammophila arenaria* covered dunes. There is little or no foredune development. Sand fences have been used to conserve the seaward facing slope of the dune ridge which is composed of mobile sand and little vegetation in contrast to the densely vegetated landward dune face. Blowouts within the dunes are not common and erosion within the dunes is much less than in the dunes at Stevenston.

The dunes in northwestern Scotland consists of a single foredune parallel to the upper beach whereas the central west coast, except for Macrihanish, comprise of two foredune ridges parallel to the beach. At Macrihanish the dunes produced a well developed composite erosional and redepositional landscape (Robertson-Rintoul, 1985).

8.3.2 Lancashire coast - Formby Point

Blown sands extend over an area of about 30 km^2 along the coast between Crosby (Southport) and Southport (Pye, 1990). The maximum inland extent of the blown sand is 4 km at Formby Point. Aeolian sand transport along the coast has produced dunes which sometimes exceed 20 m in height. However, inland the sand forms a level sand sheet.

The older dune ridges have an average height of 10-12 m. The foredunes are 6-8 m high. Parabolic dunes are found inland whereas shore parallel sand ridges

dominate the present day foredunes. The older blown sands have been levelled down for agriculture. Map and documentary evidence show that the steep hummocky structure of these dunes owes its origin to marram planting practices introduced in the early eighteenth century. The morphology of the dune belt near the coast has been influenced by a range of human activities. Parallel ridges of sand seen on aerial photographs along the coast, approximately 200 m wide at Formby Point, are believed to have formed between 1880 and 1914 when systematic erection of brushwood fences and subsequent lining by *Ammophila* was in practice to encourage foredune growth. Between the sand ridges the depressions or slacks experience water logging during a rise in water table during winter and spring. The dunes formed prior to 1880 to 1914 period appear as isolated sand hummocks when only haphazard Ammophila planting was the conservation practice. Many of the irregularly shaped slacks appear as natural blowouts but true parabolic dunes are absent.

Transgressive sand sheets at Formby are an important feature of the dune landscape. The reason for their occurrence and development may either be related to periodic wave erosion which destroys any incipient foredune formation or to the ambient high wind regime. The *raison d' tre* for the formation of these transgressive dune sheets *in lieu* of parabolic dunes is a combination of the low resistance offered by marram grass to the mobile sand, large directional variability of the wind and extreme pedestrian pressure hindering natural dune form preservation.

Destructive storm waves (westerlies) coincident with high tides lead to significant dune erosion in the area.

8.3.3 Braunton Burrows

The 5.5 km long Braunton Burrows beach-dune system lies on the northern side of the Taw-Torridge estuary in southwestern England, and extends 1.5 km inland. The foredune heights range from 2-8 m; landward parabolic dunes are up to 30 m high. A wide intertidal zone, extending up to 1.5 km during spring tides, fronts the *Ammophila* dominated foredune (Sarre, 1988). Transgressive parabolic complexes (eg. Horsebreaker complex Fig. 8.7) exhibit significant landward migration.

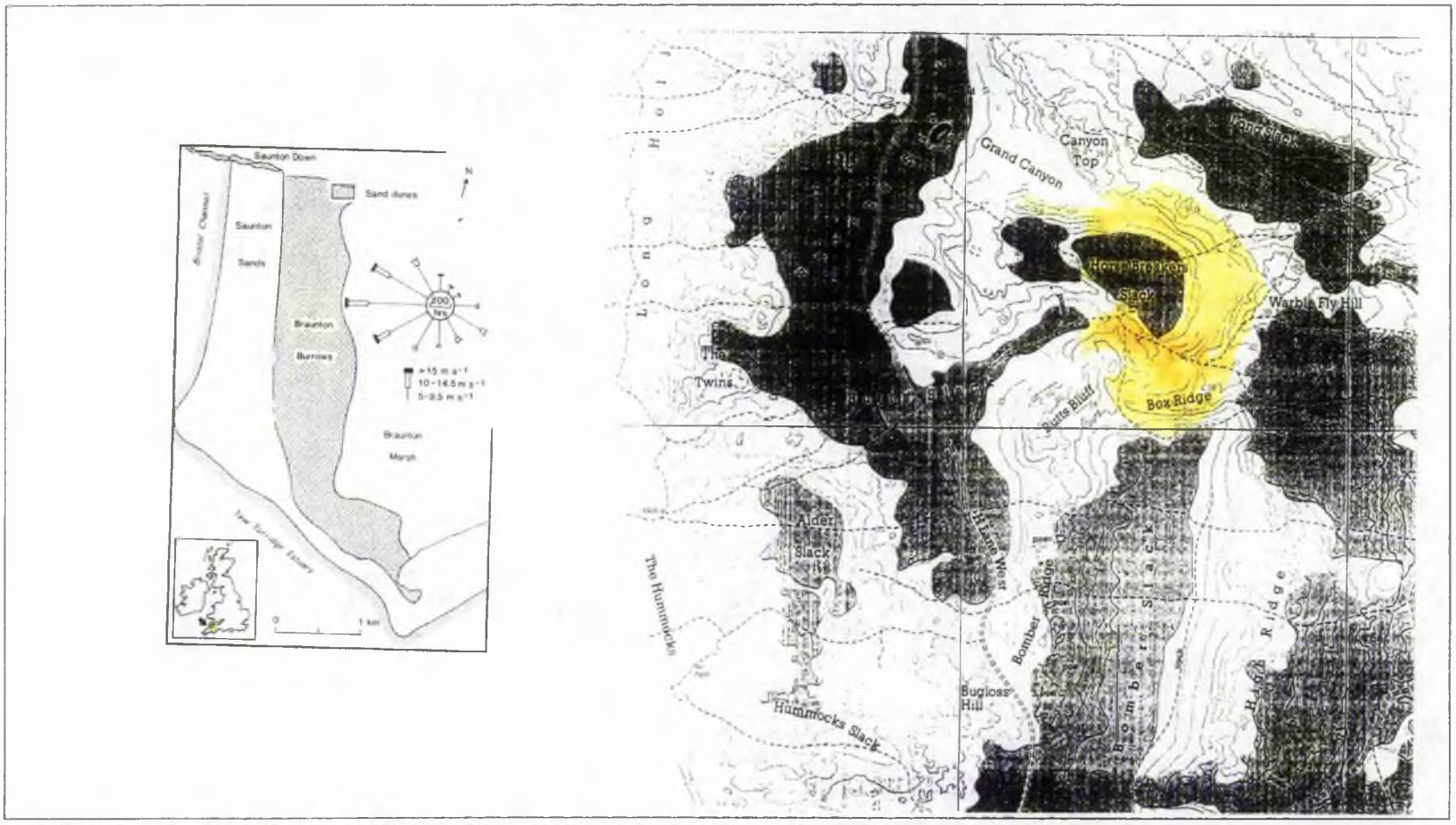

Fig. 8.7 Wind rose (data from RAF Chivenor, Sarre, 1988) and parabolic dunes (Horse Breakers complex) in Braunton Burrows, southwest England. Geomorphological map from Nature Conservancy Council.

8.3.4 Magilligan Point

Magilligan Point is a prograding beach-dune system at the mouth of Lough Foyle in Northern Ireland (Carter & Wilson, 1990). This triangular shaped beach ridge plain was formed during the Mid-Late Holocene. The foredunes at Magilligan Point are formed downdrift of eroding shorelines. The sediments are eroded from the adjacent cliffs and transported alongshore in nearshore sand bars which eventually weld onto the beach. Foredune accretion is episodic and largely associated with storm recovery beach ridge welding. The Magilligan foredunes (1-3 m high) are not the Darss (stage 1 Fig. 2.10) as they experience post-depositional mobility and fall in the stage 2 category of Hesp (1988) foredune classification (Fig. 2.10). The initial development of the dunes is controlled by the stranding of the litter lines and subsequent availability of fresh sand. The foredunes are fixed by the sand binding and stabilising vegetation comprising of *Ammophila arenaria*, *Elymus farctus* and *Elymus arenaria*. The average growth rate of the foredune varies from 6 and 9 $m^3 a^{-1} m^{-1}$.

Sediment is also transported inland through gaps or blowouts which are a prominent feature of the dune morphology. These gaps in the foredunes never seal and act as sediment transport corridors (Carter, 1990).

8.4 DUNE SYSTEMS DOMINATED BY OFFSHORE WINDS

8.4.1 Culbin Sands

The Culbin sands extend eastwards from the Maviston sandhills to the River Findhorn and are part of the aeolian sand deposits bordering the southern coast of Moray Firth (Fig. 8.8a). The evolution and changes at Culbin have been documented by Ogilivie (1923) and Steers (1937) (Fig. 8.8 b & c). The area at one time was part of a shallow bay into which the Findhorn flowed. The sand overwhelmed the area in 1694 coming from the west blocking the channel of Findhorn with the result the river opened a gap approximating the present mouth. Longshore sediment transport and accumulation along the southwest coast of the Moray Firth in response to the prevalent south westerly winds (Fig. 8.8d) and the present complex of the Culbin sands evolved.

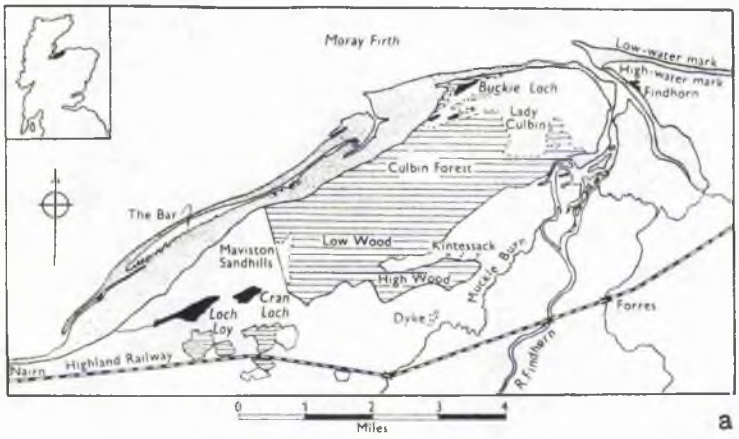

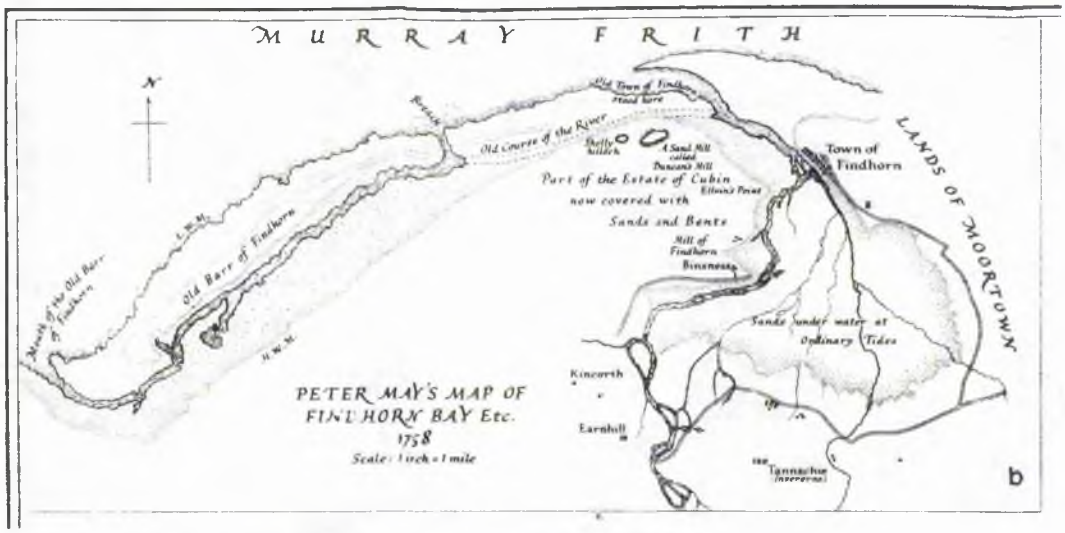

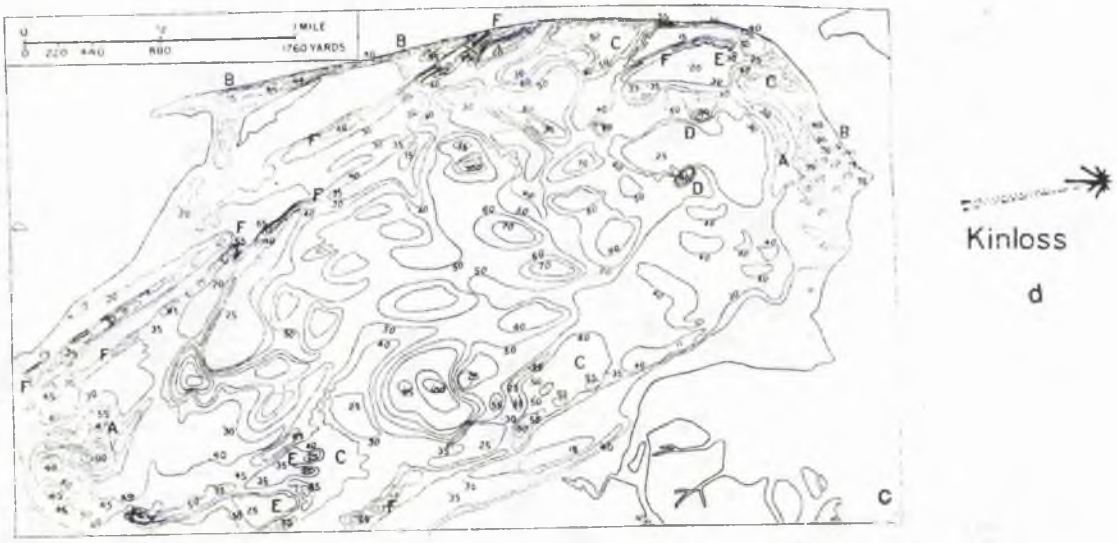

Fig. 8.8 (a) Location map of Culbin Sands, eastern Scotland (after Ovington, 1950). (b) Evolution of Culbin Sands showing old course of River Findhorn (Ogilivie, 1923). (c) Barchans of Culbin Sands (Ogilivie, 1923) (d) Sandrose at Kinloss (Robertson-Rintoul, 1985).

Barchan to megabarchanoid dunes are the dominant dune forms at Culbin forming transversely to the Southwesterly wind (Fig. 8.8c). The barchans at times attain heights up to 30 m. Occasionally, parabolic dune development takes place as a secondary blowout formation amongst the older dune surfaces. Parallel foredunes occur long the coast. Since the area was extensively planted in the 1920's any evidence of changes has been difficult to monitor.

8.4.2 Sands of Forvie

The Sands of Forvie, located approximately 19 km from Aberdeen, occupy a triangular area comprising North and South Forvie. North Forvie is a rocky, indented coastline whereas a wide sand beach marked by a partially eroded foredune, the landward boundary being the Ythan estuary, forms the coastline of South Forvie (Robertson-Rintoul, 1985). Early dunes and sandhills of Forvie are believed to have been in existence by at least 2000 B.C. Landsberg (1956) believes that excess sand from around the Ythan peninsula in the south (where the first dune ridge developed and stabilised) was transported as a sequential migration of seven sand waves advancing northwards onto the sloping platform of North Forvie. However, the inland parabolic dunes are aligned SW, parallel to the resultant wind vector which is offshore whereas the coastal edge dunes appear to grow in response to onshore sand movement (Robertson-Rintoul, 1985). The present day South Forvie dune complex is made up of various dynamic sand dune forms separated by bare sand deflation surfaces while North Forvie consists of largely stable parabolic dunes.

8.5 COMPARISON OF DUNE SYSTEMS FORMED UNDER THE INFLUENCE OF OFFSHORE AND ONSHORE WINDS

The comparison of the coastal dunes in east coast and west coast settings is presented in Table 8.2. The areas of comparisons are either self explanatory or have been derived from discussions in this chapter or earlier in the thesis. However, certain points will be addressed subsequently to make the comparison more explicit.

Table 8.2 Comparison of west and east coast dune systems

ONSHORE SYSTEMS	OFFSHORE SYSTEMS
Winds	
prevailing and dominant winds onshore	prevailing winds offshore, dominat winds onshore
Wind regime	
bimodal to complex	widely unimodal
Wind variability	
high	low to moderate
Dune coast	
Neutral or eroding coast, shingle ridge coast common	Neutral prograding and eroding coast, shingle ridge coasts unknown or absent
Dunes scattered along the entire coast, numerous isolated areas generaly associated with estuary-mouth circulation or downdrift pulses from eroding cliffs	Large dune systems in concentrated areas e.g. the Moray Firth , Tayside & Fife associated with river mouth closure, estuary mouths or downdrift pulses from eroding cliffs
Dune system	Dunes show seaward migration as accreting systems or static
Large expanses of dunes extending several kilometres inland	
	Seaward transition gradual marked by rapidly accreting foredunes on progradational coasts
Seaward transition marked by a narrow steep-faced dune behind which a flat plain (machair)	No such evidence
Expose rocky coasts show evidence of 'climbing' dunes forming a veneer of sand on rock e.g. SW England and North Scotland (hindshore coast)	Extensive rapid foredune accretion common
Extensive rapid foredune accretion rare	No clear evidence
Transgressive sand sheets (inland) common	Little or no blowout development
Large blowouts within the dunes	
Dune form	
Foredune	2-4 m high (stage 1 dunes)
4-6 m high (stage 2 dunes)	Crestal decoration & Washover dunes
Ramp dunes	Echo dunes
	Foredune densely covered by vegetation and maintains its original
High susceptibility to erosion by onshore storm waves leads to a relict eroded appearnce	
	6 m high (maximum)
Primary dune ridge	Slip face/precipitation/barchan
8-10 m high	
Large blowouts	
	Regular hairpin
Inland parabolic dunes	

8.5.1 General comparisons

Extensive single dune systems occur along the northeastern and eastern coast of Scotland whereas along the west coast (both England & Scotland) the dune

systems occur in small isolated pockets due to the rocky, high and indented nature of the coast. The Grampian east coast is characterised by long straight open coasts due to the low lying nature of the hinterland and is the most common physiographic setting for the extensive dune systems of Culbin, Forvie and Tentsmuir. In contrast, the high occurrence of bayhead and intersecting bays on the west and north coast do not provide a favourable receptacle for extensive sand accumulation. However, the isolated small dune pockets of the west coast are higher and exhibit transgressive dune development, extending several kilometres inland. The western coasts of central Scotland contain open dune beaches analogus to those of the east coast.

The west coast is characterised by bimodal to complex high energy winds, high rainfall and vegetation density in contrast to unimodal winds, low rainfall and vegetation density along the east coast.

The foredunes along the east coast generally evolve as beach ridge type stage 1 dunes (Fig. 2.10) classification) exhibiting *in situ* vertical accretion and little or no lateral movement. They evolve as linear continuous ridges in contrast to the west coast dunes occur as discontinuous ridges broken in places with gaps which never close representing stage 2 dunes (Fig. 2.10).

Blowouts are ubiquitous in the west coast sand accumulations and range in size to very large blowouts (~ 200 m^2). Blowouts are relatively rare on the east coast. High susceptibility to onshore storm waves along the west coasts creates a relict erosional dune morphology whereas the dunes along the east coast occur as well preserved undisturbed forms.

8.5.2 Parabolic/Transgressive dune systems along the east and west coast

The most frequently occurring dunes landward of most coasts in Britain are the V-plan compound parabolic dunes characterised by secondary blowout formation (Robertson-Rintoul, 1985). Parabolic dunes almost always develop from blowouts in a vegetated sand surface (Pye & Tsoar, 1990). All the parabolic dunes along the coast are secondary forms, the primary dunes being the barchans or shadow dunes (see also Orme, 1990). Present day barchans 35 to 50 m wide are developing along the northeastern end of the Iberian peninsula, at the St. Pere Pescador dune field, Spain

(Marques & Julia, 1988). Winds in excess of 90 m s^{-1}, blowing alongshore, from the north known as the Tramontanas, create these barchans which transgress landward to the south. In northwestern Spain mobile coastal dunes in areas of onshore winds reach over 30 m in height (pers. comm. McManus, 1992). Present day barchan development is reported from the Namibian coast where south and south-southeast winds in excess of 14 ms-1 produce 25-30 m high barchans migrating 30-60 m yr^{-1} (Corbett, 1989). In the Thar desert, India (Jaisalmer) west of stabilised hairpin parabolic dunes (Wasson *et al.*, 1983) are present active barchan dunes (2-8 m high) formed by the summer southwest winds (8.4 ms^{-1}) (Singhvi & Kar, 1992). Numerous parabolic dunes have been identified along the coastline of Britain and Denmark (Landsberg, 1956). The morphology of the parabolic dune form varies with the strength and directional variability of the wind, the source and amount of sand available, and on the nature of the vegetated surface (Pye & Tsoar, 1990). Seven variants of parabolic dune forms have been identified ranging from simple hairpin forms to complex transgressive linear ridges (Pye & Tsoar, 1990) (Fig. 8.9).

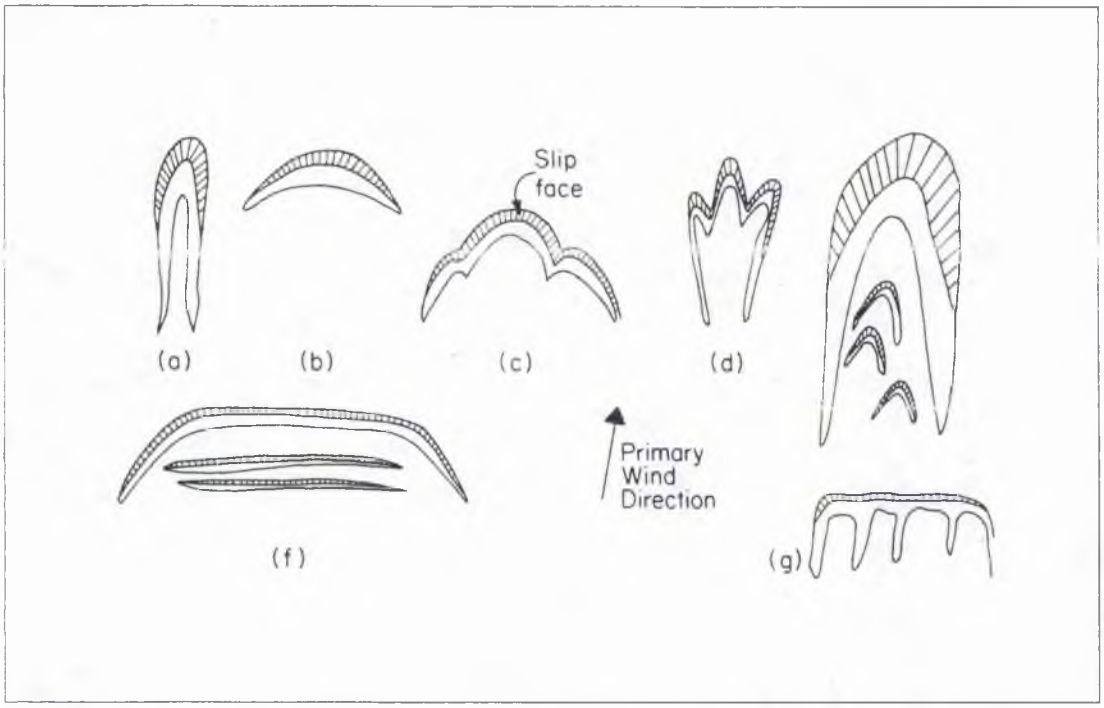

Fig 8.9 Variants of parabolic dune forms (a) Hairpin, (b) Lunate, (c) Hemicyclic, (d) Digitate, (e) Nested, (f) Transgressive and (g) Enechelon (after Pye & Tsoar, 1990).

In the present study the morphology of these inland parabolic dunes behind the coastline of the U.K. have been found to represent the ambient wind regime. Lunate to digitate parabolic dune forms abound on the west coast where the wind regime is bimodal to complex (e.g. Braunton Burrows, Newborough Warren) (Fig. 8.10). Hairpin dune forms are characteristic of the east coast parabolic dunes formed in response to unimodal winds (e.g. Sands of Barry, Morrich More) (Fig. 8.11). In general, the parabolic dunes along the west coast are broader than their east coast equivalents which are much longer than the west coast ones. The parabolas of the east coast are much more numerous, higher (40 m) and extensive than the east coast ones.

Although the wind regime is the most important factor in the dune forming process, a number of other factors as water table level and vegetation characteristics are equally important in the case of parabolic dunes. Analysis of the annual precipitation levels indicate 150-250 cm of rainfall along the west coast of central Scotland and 50-75 cm of rainfall along the east coast (Fig. 8.12). The symmetrical hairpin parabolic dunes of the east coast, in contrast to the irregular (hemicyclic or digitate) parabolic dunes of the west coast, are indication of the higher precipitation levels and vegetation spread of the west coast. The uneven downwind movement of the west coast parabolic dunes is caused due to dense vegetation spread, high precipitation levels and a more complex wind regime resulting in a more haphazard hemicyclic or digitate pattern.

In the northern part of the Cape York peninsula, Australia, the parabolic dunes are hairpin in shape, in contrast to the complex (digitate to hemicyclic) ones of the south. This variation in shape is due to a greater degree of directional variability of the wind regimes in the south (Pye, 1983c).

8.5.3 Global comparisons

Comparison of data on sand transport under a range of ambient wind regimes, determined by a range of techniques, and the resultant dune forms developed on the dune coasts worldwide are presented in Table 8.3.

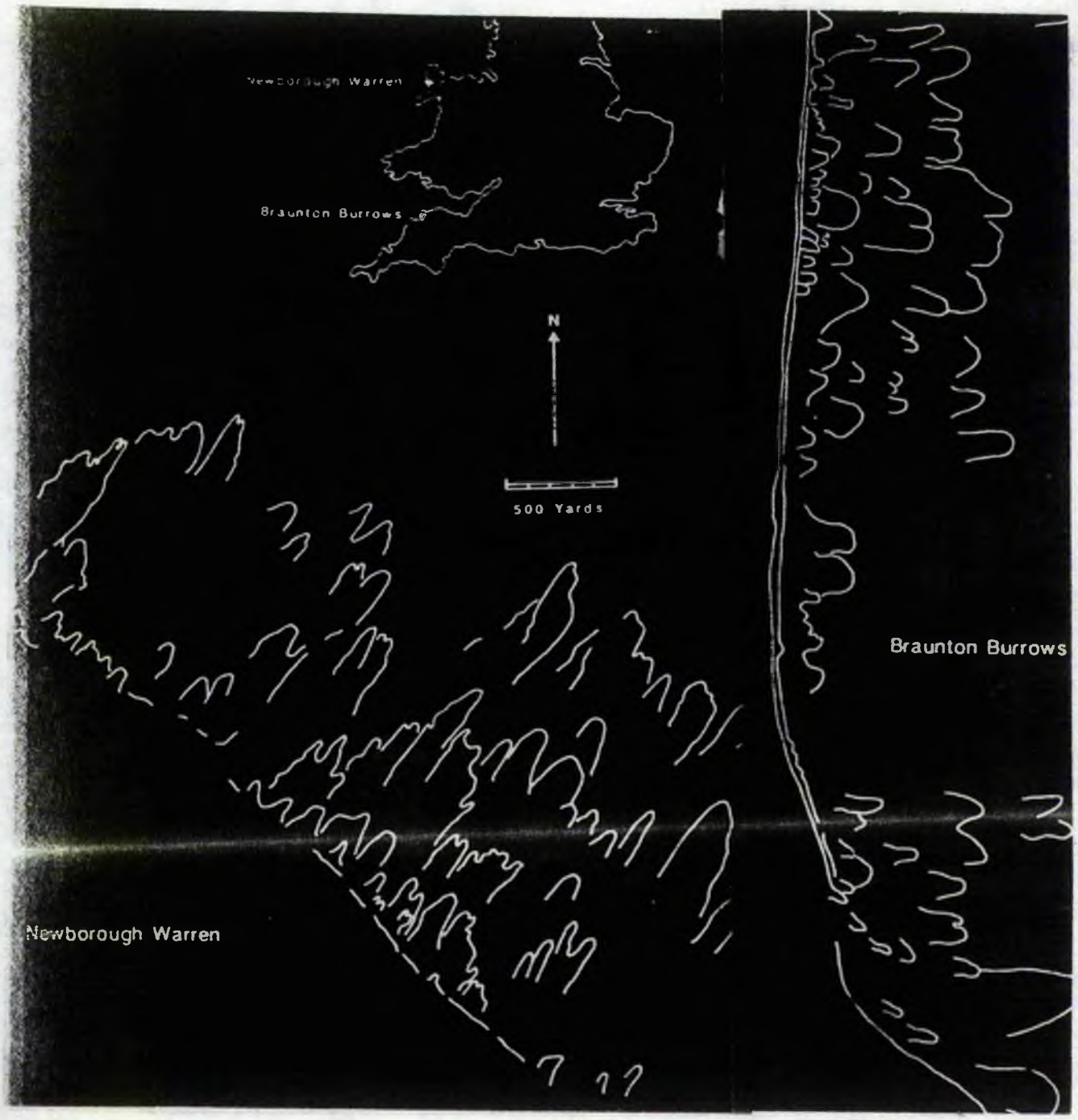

Fig. 8.10 Planimetric maps of parabolic dunes at Braunton Burrows and Newborough Warren (after Robertson-Rintoul, 1985).

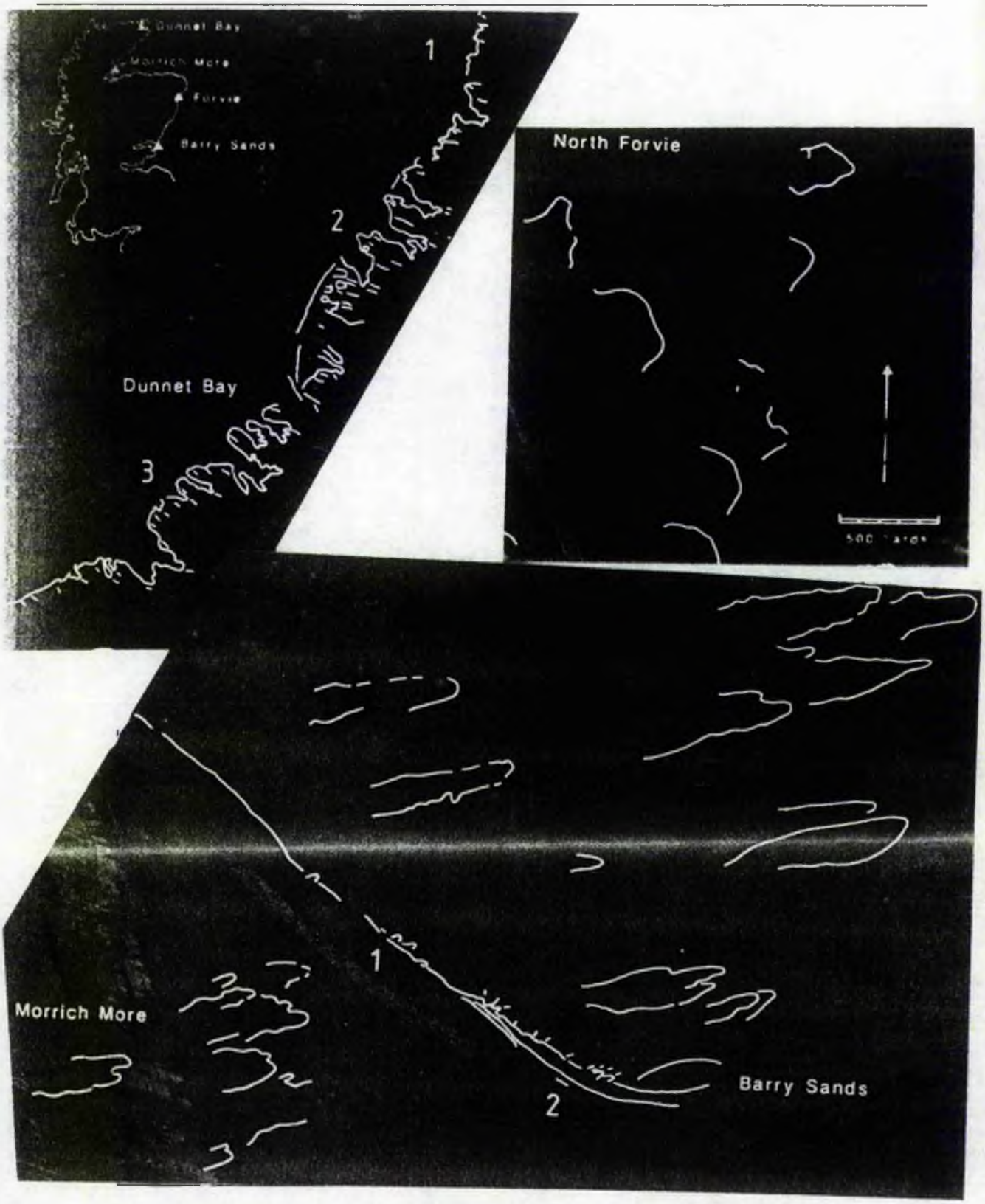

Fig. 8.11 Planimetric maps of parabolic dunes of Barry Sands, Morrich More and Forvie Sands. (after Robertson-Rintoul, 1985).

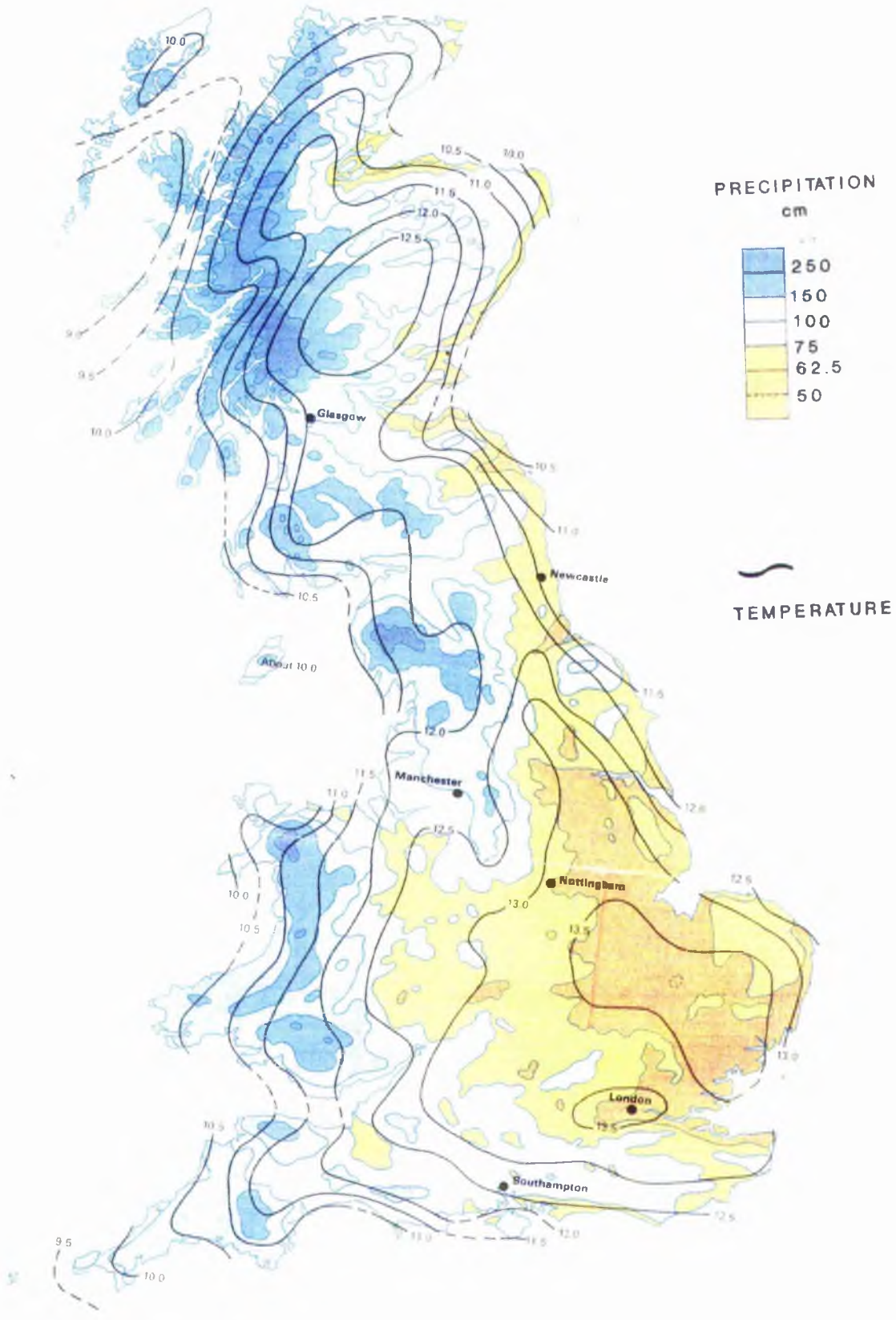

Fig. 8.12 Rainfall map of Britain (Bartholomew weather map, 1980)

TableTable 8.3 Wind regime and migration rates of dune systems of the world (**Kg s^{-1} m^{-1} (trap data); [1]major, [2] minor)

Location	Net transport rate direction	Winds	Wind/shear* velocity ms^{-1}	Grain size mm	Rainfall (cm)	Sand transport $m^3yr^{-1}m^{-1}$	Dune area & height (average)	Type of dune	Reference
Oregon dune, Coos Bay Newport, Michigan, USA	Onshore	[1]N (summer) Longshore [1]SW (winter) Oblique [2]E Offshore	5-13 5-22	0.25	163	34	120 km^2 25 m	Oblique	Hunter *et al*, 1983; Cooper, 1958
Alexandria dune field, South Africa	Onshore	[1]SW (year round) Oblique [1]E (summer) Onshore [2]NW (winter) Offshore	High energy (>400 VU)	0.2	40	21	150 km^2 25 m	Transverse	Illenburger & Rust, 1988
Israeli dunes	Onshore	[1]SE Offshore 2 - 8 ms^{-1} [2]NW Onshore 2 - 10 ms^{-1} [1]SW Onshore 2 - 12 ms^{-1} [2]NE Offshore 2 - 8 ms^{-1}	*0.24 - 0.28	0.024, 0.034	4 - 12	0.1 - 0.2	52 km^2 4 - 8 m	NE trending	Goldsmith *et al*, 1990
Tabusintac barrier dunes, Canada	Onshore	[1]NW Offshore [1]E & NE Onshore	5 - 12 5 - 7	-	50 - 85	0.9 (for May to September, rest covered in snow)	17.2 km^2 1 m	Single foredune ridge	Rosen, 1979
Castroville dunes, Monterey Bay, California, USA	Onshore	NW & N SW (winter)	5 - 15	0.3 - 0.5	193	**$1.6x10^{-3}$ - $2.2x10^{-3}$ (for upper beach face)	600 m^2 0.7 m	Hummocky dunes on barrier	Sherman *et al*, 1990; Cooper, 1967
Long Point (spit), Lake Erie, Canada	Oblique	[1]SW Oblique [1]W Oblique [2]S Longshore [2]NE Offshore	5 - 19 5.6 - 13 5.6 - 16 5.6 - 16	-	-	2.5	36 km^2 2 - 8 m	Shore parallel foredune ridge	Davidson-Arnot & Law, 1990
Braunton burrows, England	Onshore	[1]W, NW & SW Onshore [2]SE Offshore	5 - 15 5 - 10	0.17	100 - 150	**$0.5x10^{-3}$ - $20x10^{-3}$ (for all subenvironments)	8.25 km^2 4 - 8 m	Parallel foredune inland parabolics	Sarre, 1988
Magilligan Point, Ireland	Onshore	55% SW Offshore 45% Onshore	5 - 10	0.18	100 - 150	6 - 9	1200 ha 2 - 4 m	Foredune (stage 2)	Carter, 1990
Tentsmuir Point, U.K.	Offshore	[1]SW (winter) Offshore [2]E & NE (summer) Onshore	5 - 17 5 - 12	0.15 - 0.35	40 - 70	5.4 **$1.0x10^{-3}$ - $4x10^{-3}$ (for upper beach face) **$1.0x10^{-3}$ - $17x10^{-3}$ (for all subenvironments)	16 km^2 2 - 6 m	Foredune (stage 1)	

A paradigm, based on this worldwide evidence, for Holocene coastal dune development suggests that (1) onlapping sequences were succcessively emplaced and destroyed during the Flandrian transgression (12000 - 5000 BP.); (2) at the close of the transgression older parabolic dunes were formed from the destruction of earlier transverse or barchan dunes (3) most recent phase of dune activity occurred some 200-300 years ago. However, the reason for the activity of the parabolic dunes and recent activation (200-300 years) is uncertain and most probably may be attributed to human activity (clearing vegetation during grazing) or climatic changes associated with the Little Ice Age (300 years ago).

Simulation (Kutzbach & Wright, 1986) and outcrop studies of paleowinds of the aeolianites, of the Channel Islands, California (Johnson, 1977) for the period 20,000 - 7600 BP, show that the winds were dominantly westerlies as they are today. While wind strength has varied since the Pleistocene (higher wind energy earlier) there has not been a major shift in the prevailing wind direction.

Migration of dunefields along the Oregon, California, Alexandria, Israel, Lake Erie and Tentsmuir coasts is in the northeastern direction under the influence of strong westerlies. The rate of migration at Tentsmuir (4.7 $m^3 a^{-1} m^{-1}$) is much lower than those for the dunes of Oregon (31 $m^3 a^{-1} m^{-1}$) and Alexandria (21 $m^3 a^{-1} m^{-1}$) but is comparable to that obtained from Lake Erie (2.5 $m^3 a^{-1} m^{-1}$), Magilligan Point (6-9 $m^3 a^{-1} m^{-1}$), North Carolina (8-9 $m^3 a^{-1} m^{-1}$) (Savage & Woodhouse, 1968) and Padre Island, Texas (9-12 $m^3 a^{-1} m^{-1}$) (Dahl *et al.*, 1975). The results of trap measurements of sand transport rates at Tentsmuir are similar to those conducted along Braunton Burrows and Castroville dunes, California (Table 8.3).

The marine longshore sand transport plays an important role for the formation and growth of the present-day dunes at Alexandria (Illenberger & Rust, 1988), Tabusintac Island (Rosen, 1979), Magilligan Point (Carter, 1990) and in Israel (Goldsmith *et al.*, 1990) where 20-30% of the aeolian sediments are derived from the longshore transport system and foredune accretion occurs opposite sandwave development (as at Tentsmuir).

Sand transport rate measurements, along the Israeli beach dune profile during onshore winds, indicate maximum sand transport along the upper beach face and subsequent decrease in the landward direction. Similar observations have been

recorded at Tentsmuir. At Tabusintac Islands (from May to September) the wind carried 1556 m^3 of sand offshore, 2100 m^3 onshore and 1720 m^3 longshore. The longshore vector was the major contributor towards foredune accretion. The offshore transport along the Israeli coast ranges from 20-50% of the total transport although the net transport is generally onshore.

The aeolian processes active at Tentsmuir are similar to those recorded elsewhere. Although the Tentsmuir beach-dune system is dominated by an offshore wind regime, sand transport, foredune accretion and shoreline progradation rates are comparable to coastal dune systems having a predominant onshore vector. The dune migration rates at Tentsmuir are lower than those of the Oregon and Alexandria coasts where the winds are **directly onshore** but are similar to those locations where the winds are **oblique** and the net aeolian transport is longshore as at Long Point, Lake Erie, Israel and Tabusintac barrier dunes, Canada.

Thus, although there are superficial similarities between the two coastal dune systems, real differences appear to exist principally on the relative continuity of direction of sediment transport, the development of continuous linear coast parallel ridges, absence of large blowouts and extensive stretches of individual dune systems in straight open beach settings.

8.6 SUMMARY OF THE CHARACTERISTICS OF THE TENTSMUIR BEACHES

Study of successive aerial photographs taken during the last fifty years have shown that the area of Tentsmuir Point dunes has been one of rapid foredune accretion and shoreline change. The present day coastline is accretional at Tentsmuir Point, erosional at Tentsmuir south towards Kinshaldy, accretional at Kinshaldy and beyond to Earlshall. The Earlshall area is a wide beach containing much coarse shell material. No foredune development is evident at Earlshall. South of the Eden estuary, beyond the areas of estuarine silt are present the dunes and beaches of West Sands. St. Andrews.

8.6.1 Beach-dune topography

The present coastal dune topography is related to the local sediment supply. Rapidly extending foredunes are present at Tentsmuir Point and Kinshaldy, where sufficient sand supply is available due to the dynamic interplay of aeolian, wave and tidal processes coupled with substantial offshore resources. At Tentsmuir a low rate of sand supply and narrowing of the beach has resulted in an erosional dune face profile. Pyramidal wind shadow dunes are present in the lee of a primary dune ridge signifying a phase in the beach-dune recovery cycle, in which, after an initial stage of dune retreat by marine undercutting and erosion, sediments are returned from the beach to the dune during a subsequent recovery phase.

Foredune accumulation takes either the form of sand accumulations in the lee of obstacles and plants or that of barchan - like forms which later become colonised by dune grass. Subsequently both these forms of accumulation may become reduced to isolated sand hummocks surviving inundation during exceptional high tides.

The dune systems of the Tentsmuir coast do not fall within a single group of the Hesp (1988) classification and appear to span the intermediate to abundant supply grouping recognised by Carter (1988).

Fine to medium grained, moderate to well sorted beach sands are prevalent in the area. The dune sands are relatively fine grained, negatively skewed and better sorted than the beach sands.

Daily changes in the beach profile (vertical aggradation in swales and lateral migration of ridges) are related to the changes in the tidal cycle and the accompanying winds.

8.6.2 Wind regime

The wind regime in the area is seasonal (Wal & McManus, 1992). In winter the winds are unimodal offshore and longshore with moderate-high drift potentials and low wind variability. During spring, unimodal onshore winds have high drift potentials while the bimodal onshore winds have moderate drift potentials. Summer winds are bimodal equal with moderate to low drift potentials and high wind variability. Bimodal offshore winds with moderate to large drift potential and moderate wind variability characterise the autumn conditions.

8.6.3 Short-term sand transport

Sand transport rates are largest along the middle beach face sub-environments. The limiting effect of moisture reduces the aeolian transport rate along the lower beach face and moist tidal margin. This zone is also the limit of aeolian transport on the beach. Very low values of sand transport are encountered in this area. The foredune and backshore are areas of high sand accumulation during onshore winds, as the sand is unable to move beyond the foredune into the densely vegetated primary dune area.

8.6.3.1 Role of onshore winds

The onshore winds at Tentsmuir play a significant role in foredune development as they transport significant volumes of sand beyond the upper beach face sub-environment. Once the sand has been transported to the potential foredune zone by these winds it is stabilised by vegetation and there is little net transfer of the sediments from this area back to the beach during an offshore wind event. The onshore winds are responsible for the culmination of coastal dune development by transporting sediments landward onto the backshore area.

Examples of excessively high rates of foredune aeolian sand accumulation (during onshore winds) have been recorded in February 1966 and March 1981 during which the vertical growth of vegetation was unable to keep up with the high rate of sand transport (Warden reports, Nature Conservancy Council, *pers. comm.*). Oblique onshore winds (from E and ESE) during November 1968 led to the development of an approximately 1 m high, chain of barchan dunes along the uppermost parts of the beach.

8.6.3.2 Role of offshore winds

The frequency of offshore sand transport is much higher than the onshore transport. Onshore winds contribute to the development of a positive beach sediment budget due to the limiting effect of the sea water line. The winds may carry sand down the beach but the moist area inhibits further aeolian sand movement beyond this physical barrier.

The greater frequency of the offshore winds, results in the accumulation of large quantities of aeolian sand in the form of linear ridges across a major dune ridge, and also as barchans or foreshore sand lobes. If not destroyed by spring tides, these accumulations along the middle beach face and backshore, in the course of time, may act as loci for development of potential foredune ridges. The positive beach sediment budget is the much needed sand supply for the onshore winds which carry sand landwards. Hence, the offshore winds in the area act as potential coastal dune sediment source accumulators.

The offshore wind movement erodes the backshore and deposits the sediments on the beach face to be acted upon by the tides in the following few hours. At Tentsmuir Point, as a result of the presence of hummocky dune forms, the offshore winds are incapable of deflating the surface and transporting sediments from amongst the dunes so that it is the loose beach face sediments, material from the exposed seaward facing older dune cliff, or from a blowout, which are transported as far as the tidal limit during that period. Once the incipient foredune is stabilized by the extremely rapid growth of *Elymus farctus*, the offshore winds are rendered incapable of eroding sediments from the vegetational trap. The presence of a wet area (ranging from a few meters to tens of meters) along the seawater line acts as a seaward limit of aeolian deposition, thus emphasizing the swash zone sifting of sediments by off-shore winds.

During offshore winds the backshore area is deflated and after a while the wind creates a shell pavement having removed all the fines from the area. Low sand transport rates are encountered during offshore winds in the foredune zone due to the partially vegetated nature of this zone. The concept of zonality is very clear from the transport rate experiments. The beach-dune system can be divided systematically into zones based on varying transport rate indices. Maximum rates are encountered along the middle beach face zone and lower transport rates along the lower and upper beach face subenvironments due to the limiting effect of surface moisture and vegetation cover respectively.

Unlike sediment transport in a stream, where the flow is unidirectional, the total work performed in aeolian sand transport is not cumulative. The actual sand

movement, especially in the case of coastal dunes, is dependent partly on the degree of surface protection (vegetation) and the orientation of the shoreline.

The onshore aeolian sand transport vector results in long-term foredune accretion; the offshore and longshore components in a positive beach budget. However, the net beach sediment budget is a complex interplay of aeolian, wave and tidal processes.

8.7 RELATIONSHIP BETWEEN SHEAR VELOCITY AND SAND TRANSPORT RATES

Shear velocities measured along the middle beach face ranged from 18.5 cm s^{-1} (at the threshold of sand movement) to 52 cm s^{-1} (Wal & McManus, in press). Sand transport rates measured along the middle beach face showed the best correlation with shear velocity measurements. Low correlation values were obtained when relating shear velocities to sand transport rates measured along the lower beach face, upper beach face and foredune subenvironments. However, a power function line for the 56 trap results gives:

$$q \quad 0.85\, u^{*3.45}$$

Hence sand transport rates along the lower and upper beach face and foredune subenvironments cannot be related to shear velocity alone. The sand transport rates within the various subenvironments plot in distinct envelopes on a shear velocity-transport rate plot.

8.7.1 Comparison of measured with predicted rates

Comparisons of measured rates of sediment transport with those estimated from various transport rate expressions (which are essentially a function of grain size and shear velocity) provide mixed to poor correlations. The White (1979) expression provided the closest fit to the measured data of the transport rates along the dry unvegetated middle beach-face.

An extended programme of concomitant determination of shear velocity and transport rates values, using a more intricate network of anemometer arrays within the various beach-dune environments - is needed to identify the most appropriate prediction technique. In particular it should enable more precise definition and

exploration of the limiting effects of moisture and vegetation and their incorporation into the model equations to define more precisely the variability of the transport rates within the various coastal sub-environments.

8.7.2 Potential long-term sand inputs

The total volume of sand which was potentially moved offshore has been calculated using the shear velocity values for the wind speed categories of the meteorological data obtained from Leuchars meteorological site. Shear velocities on the beach {focal point u' (1.75 m s^{-1}) z' (0.03 cm)} were used to calculate the wind shears for the corresponding wind speed classes. The White (1979) expression has been used to calculate the long-term transport rates since it provided the closest fit to the short-term measured values (Wal & McManus, 1992). In order to calculate the total amount of sand moved the rates were multiplied by the reach width of the beach and the total number of hours that the wind of a particular speed class blew and the sum divided by the bulk density of sand to calculate the volume of sand moved.

At Tentsmuir Point, during the past eleven years $109x10^3$ m^3 of dry sand could have moved towards the sea. Areal and ground surveys estimate that $33x10^3$ m^3 of sand has accumulated in the lee of the present day beach for the same period. Predicted values of landward sand transport volumes for the area have been found to be $28x10^3$ m^3. Longshore transport rate estimates suggest that $3x10^3$ m^3 of sand has been transported alongshore.

8.8 WIND INDUCED AEOLIAN BEDFORMS

The aeolian sediment mobilisation produces distinctive sedimentary structures in response to offshore, onshore or longshore winds (Wal & McManus, 1992). Various wind induced sedimentary structures were seen to have been formed under a range of wind conditions and surface moisture. Very high velocity winds in excess of 9 m s^{-1} produced sediment laden sand strips on the beach. When the same wind conditions persisted for a considerable period barchans or foreshore sand lobes (crescent shaped forms with small height dimensions) developed. With a decrease in the wind velocity (below 9 m s^{-1}) the sand surface became rippled. The ripples disappeared as the wind became progressively stronger.

Obstacle induced aeolian depositional structures as wind shadows form locally in the area. Erosional structures as scour-remnant ridges were seen to occur across the foreshore during strongly deflating winds. Adhesion ripples and adhesion plane bed structures developed along the moist/wet tidal margin during offshore and longshore winds.

Thus during offshore winds a whole gradation of land forms are visible from shadow dunes, foreshore barchans/ lobes to adhesion ripples- a perfect representation of the factors which control the aeolian bedform development and migration, namely wind velocity characteristics (interaction of the velocity profile with surface roughness) and the availability of sediment.

As with the offshore winds the onshore winds also generate a range of aeolian, landward sand depositional loci across the beach face up to the dune edge in conjunction with tidal limits and the resulting beach face exposures. Sand strips, landward pointing shadow dunes and massive aeolian sediment deposition along the backshore and foredune area occurs during onshore transport.

The coastal beach-dune environment is made up a number of subenvironments: beach, foredune, primary dune and interdune/duneslack: each of which is characterised by a distinct lithofacies and sedimentary structures.

Along the exposed and trenched portions of the shoreline, parallel laminated sands have been observed. Invariably, most of the primary dune sequences were seen to abound in plant remains. Pinch out laminae and sand lenses are also present. Medium to small-scale trough cross-beds have been seen in a section cut across the dunes, where sand is believed to have been deposited in a preexisting hollow. Precipitation or lee dune structures were also seen. The angle of the foreset laminae of the precipitation structure is approximately 18°. The presence of a shell layer underlying the aeolian sequence is though to represent a deflated beach surface.

Thus, taking into account the sand transport mecahnisms and the associated sedimentary structures observed to develop in the various zones of the beach-dune environment, a prograding beach-dune facies model is envisaged.

The aeolian sand transport model can be universally applied to beaches subjected to varying wind conditions. However, variations may occur due to a whole

host of factors such as salt crusting, moisture content and, vegetation type, which have to be explained in future research work.

The facies model based on the presence of various sedimentary structures preserved in a vertical sequence will aid in the identification of a prograding coastal environment in ancient deposits.

8.9 COASTAL DUNE FORMATION

Foredune growth depends on the direction and strength of the wind, width of beach exposure, amount of sand available for entrainment, vegetation density and state of the tide. On an accreting shoreline such as Tentsmuir Point the following stages of foredune development can be envisaged:

1. Development of a berm seaward of the major dune ridge.
2. Sand accumulation along the landward limit or the dry backshore of the beach in the form of sand shadows formed in the lee of tidal debris or grass tussocks. The tussocks on being able to trap increasing quantity of sand may coalesce to generate a ridge like form.
3. Onshore/longshore winds (9-12 m s^{-1}), during favourable beach exposure (wide beach, neap tide conditions) result in the formation of massive sand accumulation in the form of sand strips and barchans, along the exposed areas, and sediment accumulations along the backshore and foredune area. In this case middle beach-face sediments serve as the primary source.
4. Spring tidal incursions may cover the accumulations on the foreshore with wave washed sediments resulting in the formation of a reduced and distorted remnant structure.
5. Colonisation of the backshore by pioneer dune vegetation (e.g. *Elymus farctus* and *Cakile maritima*) nourished by a continuous supply of fresh sand. Due to the stabilising affect of the vegetation species the foredune grows, the vegetation acts as a baffle for the sand.
6. Vertical accretion and lateral accretion continue until the formation of another berm seaward of the rising foredune ridge. Later sand supply is cut-off and a different vegetation succession thrives on the primary dune ridge. Sand supply is deficient but during gales occasionally some sediment replenishment may take place across the

primary dune ridge. In the long-term diminishing beach sediment budget and narrowing of the beach may eventually lead to dune collapse by storm-wave attack.

Potential dune building phases can be envisaged from October through June as the onshore winds are particularly important during that period. Furthermore dune development will be particularly significant from February to July as the offshore winds tend to be weaker during that period. The swash zone aeolian deposition will be concurrent with the onshore depositional events throughout the year but in a relatively smaller magnitude from April to August than during the remainder of the year.

As 80% of the dunes at Tentsmuir are vegetated (see map), aeolian sand transport from a bare (beach) to a vegetated surface (dune), a transport vector which may otherwise serve to return sand in the opposite direction (from the dune to the beach), is bound to be suppressed. This inability of the offshore transport vector to trigger sand transport will cause sand transport on the beach be strongly biased towards those components of the transport vector field which have onshore directions.

This leads one to estimate NW-SE trending foredune accumulation in the more exposed parts of the shoreline, such as a shoreline abutment, and N-S transverse aeolian sand ridges in the more restricted linear part of the shoreline. This theory is substantiated while examining the trend of foredune development in at Tentsmuir. Comparison of the 1945 areal photographs with the 1990 cover shows NW-SE trending successive foredune ridge development in the northernmost part of the exposed shoreline and the development of shore parallel foredune ridges (N-S trending) in the central part of the restricted shoreline.

The NW-SE alignment of the foredune in the northernmost sector of the shoreline is believed to have been formed under the cumulative effect of the winds moving from the onshore quadrant (0°-180°)

It is difficult to classify the Tentsmuir dunes as 'barchan' or 'parabolic' because they certainly appear to have been formed under the influence of the onshore vector resultant of the wind regime, as successive lee side accumulations stabilized by the pioneer vegetation such as *Ammophila* and *Elymus*, the vegetation growth keeping pace with the rapid vertical and lateral foredune accretion.

However, the strong offshore wind resultant is instrumental in the redistribution of the sediments from the partly vegetated areas and the swash zone, providing a good source of loose sediments to be transported to the foredune by the offshore winds.

The island-type morphology of the dunes is due to the overwash processes breaching the foredune from time to time and encroachment of sea-water during the spring tides and storm surges through the tidal channels, which are relicts of former shorelines within the dunes resulting in a hummocky island appearance.

8.10 CONCLUSIONS

In conclusion the following points can be listed as contributions to the understanding of the sedimentological effects of aeolian processes active in the Tentsmuir area

1. Study of successive aerial photographs of the study area indicates that foredune accretion is related to the nearshore sediment supply and shoreline progradation occurs where the dune budget is positive and the beach budget is negative.

2. Analysis of meteorological wind data for the last eleven years indicates that the wind regimes are seasonal.

3. The Leatherman trap can be used for the monitoring short term sand transport rates where the exposure of the trap is limited to 15 minutes.

4. Shear velocities on the Tentsmuir beaches ranged from 18.5 cm s^{-1} to 52 cm s^{-1} and the focal point, u' and z' values were 1.75 m s^{-1} and 0.03 cm respectively.

5. A good correlation (r^2=0.65) exists between shear velocity and sand transport rates for transport rate measurements made along the middle beach face subenvironment. The White(1979) transport rate expression gave results closest to the middle beach face transport rate measurements.

6. The variability of the short-term aeolian sand transport rates of the fine to medium grained beaches appears to be a function of (i) variation in wind velocity, (ii) presence or absence of vegetation, (iii) ground surface moisture (iv) sand source size and limitation.

7. Estimation of long term (1980-1990) potential aeolian sand inputs indicate that 109 x 103 m3 of sand was blown offshore, $28x10^3$ m^3 was moved onshore and $3x10^3$ m^3 of sand was transported alongshore. During the same period $33x10^3$ m^3 of sand accumulated in the lee of the beach in the form of hummocky dune accumulations.

8. Whereas the onshore winds lead to a positive foredune sediment budget the offshore and longshore winds result in a positive beach sediment budget. The positive beach budget is the much needed sediment supply for the onshore winds to carry sand landward for subsequent foredune build-up.

9. Ballistic ripples, wind shadow structures, barchans, scour-remnant ridges and adhesion structures form in response to winds moving across the beach.

8.11 FUTURE RESEARCH

There exists a real need to define the position of the focal point (u',z' coordinates) through repetitive determinations of shear velocity at the inception of particle entrainment and motion. An intricate network of anemometer arrays in the various beach-dune subenvironments will help to account for the spatial variability in shear velocity determinations during simultaneous trapping observations. The limiting effect of moisture and vegetation on sand transport has to be elucidated further. Detailed observation of coastal dune change (accretion, erosion) with particular reference to blowout dynamics is an interesting strategy for coastal management studies.

BIBLIOGRAPHY

References

Adriani, M.J. & J.H.J Terwindt 1974. Sand stabilization and dune building. Rijkswaterstaat Communications, No. 19 The Hague: Government Publishing Office.

Ahlbrandt, T.S. & S.G. Fryberger 1981. Sedimentary features and significance of interdune deposits. In: *Recent and ancient non-marine depositional environments. models for ex.ploration, F. G. Etheridge & R. M. Flores (eds),* Soc Econ. Palaeontol. Mineral. Spec. Publ. No. 31, 293-314.

Aibulatov, N.A. 1961 In: *Dynamics & morphology of sea coasts,* Rept. 48, Trudy Inst. Oceanogr., Moscow

Al-Mansi, Ahmed M.A., 1986 Sediment transport and beach erosion in Monifieth Bay, Tay Estuary, Scotland, *University of Dundee*, unpublished Ph.D. thesis.

Allen, J.R.L. 1963. Asymmetrical ripple marks and the origin of water-laid co-sets of cross-strata. *Geol. J.* **3**, 187-236.

Allen, J.R.L. 1965b. A review of the origin and characteristics of Recent alluvial sediments*Sedimentology*, **5**, 89-191

Allen, J.R.L. 1968 Current ripples. *North Holland*, Amsterdam.

Allen, J.R.L. 1984. Sedimentary structures. *Elsevier*, Amsterdam

Ancker, Van der, J., P. Jungerius & L. Mur. 1985. The role of algae in the stabilization of coastal dune blowouts. *Earth Surf. Proc. Landf.* **10**, 189-192.

Anderson, R.S. 1987 A theoretical model for aeolian impact ripples. *Sedimentology* **34**, 943-956

Anderson, R.S. and B. Hallet 1986. Sediment transport by wind: toward a general model. *Bull. Geol. Soc. Am.* **97**, 523-35

Arnott, R.G.D. & M.N. Law 1990. Seasonal patterns and controls on sediment supply to coastal foredunes, Long Point, Lake Erie. In: *Coastal Dunes: Form and Process, Nordstrom, K.F., Psuty, N.P. & Carter, R.W.G. (eds),* John Wiley & Sons Ltd., 177-199.

Aubrey, D.G. 1979. Seasonal patterns of onshore or offshore sediment movement. *Jour. Geophy. Res.* **84**, 6347-6354.

Bagnold, R.A. 1936. The movement of desert sand. *Proc. R.. Soc. A.*, **157**, 594.

Bagnold, R.A. 1937. The transport of sand by wind. *Geogr. J.* **89**, 409-438.

Bagnold, R.A. 1938. The measurement of sand storms. *Proc. R. Soc. London*, Ser. A **167**, 282-291.

Bagnold, R.A. 1941. The physics of Blown sand and desert dunes. *Methuen*, London.

Bagnold, R.A. 1951. Sand formation in southern Arabia. *Geogr. J.* **117**, 78-86.

Bagnold, R.A. 1954. Experiments on a gravity-free dispersion of large solid spheres in a Newtonian fluid under shear. *Proc. R. Soc. London.* Ser. A 225, 49-63.

Bagnold, R.A. 1956. Flow of cohesionless grains in fluids. *Philos. Trans. R. Soc. London*, Ser. A 249, 235-97.

Bajaard, J. 1966. Figures et structures sedimentaries dans la zone intertidale de la partie orientale de la Baie du Mont-Saint-Michel. *Rev. Geogr. Phys. Geol. Dyn.*, **2** (8), 39-111.

Bauer, B.O., D.J. Sherman, K.F. Nordstrom, & P.A. Gares 1990. Aeolian transport measurement and prediction across a beach and dune at Castroville, California. In: *Coastal Dunes: Form and Process, Nordstrom, K.F., Psuty, N.P. & Carter, R.W.G. (eds),* John Wiley & Sons Ltd., 39-56.

Beheiry, S.A. 1967. Sand forms in the Coachella Valley, Southern California. *Ann. Am. Assoc. Geogr.* **57**, 25-48.

Belly, P.Y. 1962. Sand movement by wind. Technical report, Hydraulic Engineering Laboratory, Wave Research Projects, *University of California*, Berkley.

Belly, P.Y. 1964. Sand movement by wind. US Army Corps of Engineers, Coastal Engineering Research Center, Technical Memorandum, No. 1.

Berg, N. H. 1983. Field evaluation of some sand transport models. *Earth Surf Proc. Landf.* **8**. 101-14.

Bigarella, J. J., R. D. Becker & G. M. Duarte, 1969. Coastal dune structures from Paran, Brazil. *Mar. Geol.* 7, 5 55.

Bigarella, J. J. & L. Salamuni, 1961. Early Mesozoic wind patterns as suggested by dune bedding in the Botucatu Sandstone of Brazil and Uruguay. *Geol. Soc. Am. Bull.* **72**. 1089-105.

Bird, E.C.F. & M.L. Schwartz, (eds.) 1985. The World's Coastlines. *Van Nostrand Rheinhold*, New York.

Bisal, F. & J. Hsieh, 1966. Influence of moisture on erodibility of soil by wind. *Soil Sci.* **102**, 143-6.

Bisal, F. & K. F. Nielsen, 1962. Movement of soil particles in saltation. *Can. J. Soil Sci.* **42**, 81 6.

Boalch, Christopher R 1988, Wave-shore zone interactions and the potential for beach nourishment in coastal protection at the head of St Andrews Bay. *University of Dundee*, unpublished Ph.D thesis.

Borowka, R.K. 1990 The Holocene developement and present morphology of the Leba Dunes, Baltic coast of Poland. In: *Coastal Dunes: Form and Process, Nordstrom, K.F., Psuty, N.P. & Carter, R.W.G. (eds)*, John Wiley & Sons Ltd., 289-311.

Boughey, A.S. 1957 Ecological studies of tropical coast lines. *Jour. Ecol.* **45**, 673-4.

Bradley, J.S. 1957. Differentiation of marine and sub-aerial sedimentary environments by volume percentage of heavy minerals, Mustang Island, Texas. *J. Sedim. Petrol.*, **27**, 116-125.

Breed, C.S. & J.F. McCauley, 1991. The climatic environment of modern aeolian processes in Arizona (USA) deserts *(Abs.). The dynamics and environmental context of Aeolian sedimentary systems.*

Bressolier, C. & Y.F. Thomas, 1977. Studies on wind and plant interactions on the French Atlantic coastal dunes. *J. Sedim. Petrol*, **47**, 331-338.

Brookfield, M. 1970. Dune trends and wind regimes in Central Australia. *Z. Geomorph Suppl. Bd.* **10**, 121-153.

Buckley, R. 1987. The effect of sparse vegetation on the transport of dune sand by wind. *Nature* **325**, 426-28.

Buller, A.T. & J. McManus, 1972 Simple metric sedimentary statistics used to recognise different environments. *Sedimentology*, **18**, 1-21.

Campbell. E. M. 1968. Lunettes in southern South Australia. *Trans. R. Soc. . Austr.* **5**, 92-109.

Campbell, S. 1979. Soil stabilization by a prokaryotic desert crust: implications on Pre-Cambrian land biota. in: *Origins of life*, Reidel, Holland, 335-348.

Capot-Rey, R. 1945. Dry and humid morphology in the Western Erg. *Geogr. Rev.* **35**, 391 407.

Carr, A.P., M.W.L Blackley, & H.L. King, 1982 *Earth Surf. Proc. Landf.* 7, 267-282.

Carter, R. W. G. 1976. Formation, maintenance and geomorphological significance of an eolian shell pavement. *J. Sedim. Petrol.* **46**, 418-29.

Carter, R.W.G. 1988. Coastal environments. *Academic Press.* 617p.

Carter, R.W.G. 1989. Mechanisms associated with the erosion of sand dune cliffs, Magilligan, Northern Ireland. *Earth Surf. Proc. Landf.* **14**, 1-10.

Carter, R.W.G. 1990. The geomorhphology of coastal dunes in Ireland. *Catena supplement*, **18**, 31-40.

Carter, R.W.G. & Wilson, P 1990. The geomorphological, ecological and pedological development of coastal foredunes at Magilligan Point, Northern Ireland. In: *Coastal Dunes: Form and Process, Nordstrom, K.F., Psuty, N.P. &*

Carter, R.W.G. (eds), John Wiley & Sons Ltd., 130-157.

Carter, R.W.G. & Wilson, P 1991. Chronology and geomorphology of the Irish dunes. In: *A guide to the coastal sand dunes of Ireland. Quigley, M.B. (ed.)*., 18-41.

Chambers (1843) Existence of raised beaches. *Edin. Phil. J.* **34**, 298-306.

Chandler, M.A., G. Kocureck, D.J. Goggin, & L.W. Lake, 1989. Effects of stratigraphic heterogeneity on permeability in eolian sandstone sequence, Page sandstone, Northern Arizona, *Bull. Amer. Assoc. Petroleum Geologists*, 73, 658-68.

Chapman, D.M. 1990. Aeolian sand transport- an optimised model. *Earth Surf. Proc. Landf.* **15**, 751-760.

Chepil, W. S. 1941. Relation of wind to the dry aggregate structure of a soil. *Sci. Agric.* **21**, 488-507.

Chepil, W. S. 1945a. Dynamics of wind erosion: I. Nature of movement of soil by wind. *Soil Sci.* **60**, 305-20.

Chepil, W. S. 1945b. Dynamics of wind erosion: II. Initiation of soil movement. *Soil Sci.* **60**, 397-411.

Chepil, W S 1951. Properties of soil which influence wind erosion. IV State of dry aggregate structure *Soil Sci.* **72**, 387-401.

Chepil, W S. 1956 Influence of moisture on erodibility of soil by wind. Proc. *Soil Sci. Soc. Am.* **20**. 288-92.

Chepil, W.S. 1957. Sedimentary characterstics of dust storms: III. Composition of suspended dust. *Am. J. Sci.* **255**, 206-213.

Chepil, W. S. 1959. Equilibnum of soil grains at the threshold movement by wind. *Proc. Soil Sci. Soc. Am.* **23**, 422-8.

Chepil, W. S. & R. A. Milne 1941. Wind erosion of soils in relation to size and nature of the exposed area. *Sci. Agric.* **21**, 479 87.

Chepil, W.S. & Woodruff, N.P. 1963. The physics of wind erosion and its control. *Advances in Agronomy*, **15**, 211-302.

Chisholm, J.I. 1966. An association of raised beaches with glacial deposits near Leuchars, Fife. *Bull. Geol. Surv. GB.* **24**, 163-174.

Chisholm, J.I. 1971. The stratigraphy of the post-galcial marine transgressions in N.E. Fife. *Bull. Geol. Surv. GB.*, **37**, 91-107.

Clemmey, H. 1978. *Spec. Publ. Int. Assoc. Sedimentology.*, **2**, 259-78.

Cooper, W.S. 1958. Coastal sand dunes of Oregon and Washington. *Memoir of the Geological Society of America* 72, 169p.

Cooper, W.S. 1967. Coastal dunes of California. *Memoir of the Geological Society of America* 104.

Corbett, I.B. 1989 The sedimentology of diamondiferous deflation deposits within the Sperrgebiet, Namibia. Unpublished PhD. thesis, *University of Cape town.*

Cracknell, A.P., N. McFarlane, K. McMillan, J.A. Charlton, J. McManus, & K.A. Ulbright, 1982. Remote sensing in Scotland using data received from satellites. A study of the Tay Estuary region using Landsat MSS imagery. *Jour. of Remote Sensing*, **3**, 113-137.

Crawford, R.M.M & D Wishart. 1966 A multivariate analysis of the development of dune slack vegetation in relation to coastal accretion at Tentsmuir. *J. Ecol.*, **54**, 729-744.

Crofts, R. 1971. Sand movement in the Emlyberg dunes, Mayo. *Irish Naturalists Jour.* **17**, 132-6.

Cullingford, R.A. 1972. Late-glacial and post-glacial shoreline displacement in the Earn-Tay area and eastern Fife. *University of Edinburgh*, unpublished Ph.D. thesis.

Cullingford, R.A. & D.E Smith, 1966. Late glacial shorelines in eastern Fife. *Trans. Inst. Brit. Geogr.*, **39**, 31-51.

Dahl, B.E., Fall, B.A. & Otteni, L.C. 1975. Vegetation for creation and stabilisation of foredunes, Texas coast. In: *Cronin, L.E.*

Estuarinre Research: Volume II. Geology & Engineering. Academic Press. New York, 457-470.

Daniel, H.A. 1936. Jour. Am. Soc. Agron. **28**, 570-80.

Davidson-Arnott, R.G.D. & M.N. Law, 1990. Seasonal patterns and controls on sediment supply to coastal foredunes, Long Point, Lake Erie. In: *Coastal Dunes: Form and Process, Nordstrom, K.F., Psuty, N.P. & Carter, R.W.G. (eds),* John Wiley & Sons Ltd., 177-200.

Davies, J.L. 1980. Geographical variation on coastal development. 2nd Ed., *Longman,* London.

De Ploey, J. 1980 Some field measurements and experimental data on wind blown sands In: *Assessment of erosion, M. de Boodt & D. Gabrieli (eds),* Chichester Wiley, 541-52.

Deacon, E.C. 1949 Vertical diffisuion in the lowest layers of the atmosphere. *Quart. Jour. Roy. Met. Soc.* **75**, 89-103.

Deshmukh, I.J. 1974. Fixation, accummulation and release of energy by *Ammophila arenaria,* Tentsmuir. *University of Dundee,* unpublished PhD thesis .

De Vries, W.C.P 1973. *Geol. Mijnbouw.*, **52**, 133-140.

Doody, J. P. 1989. Conservation and development of the coastal dunes in Great Britain In: *Perspectives in coastal dune management, F. van der Meulen, P. D. Jungerius & J. Visser (eds),* The Hague: SPB Academic Publishing, 53 68.

Draga, M. 1983. Eolian activity as a consequence of beach nourishment - observations at Westerland (Sylt), German North Sea coast. *Z. Geomorph. Suppl.* Bd. 45, 303-19.

Du Bois, R. 1988. Seasonal changes in beach topography and volume. *Mar. Geol.*, **81**, 79-96.

Ellwood, J. M., P. D. Evans & I. G. Wilson 1975. Small-scale aeolian bedforms. *J. Sedim. Petrol.* **45**, 554 -61.

Ferentinos, G. & J. McManus, 1981. Nearshore processes and shoreline development in St Andrews Bay, Scotland, U.K.. *Special Publication International Association of Sedimentologists,* 161-174.

Fielder, G. 1982. Lateral and vertical relationships of the Cambrian Galesville sandstone, Wisconsin Dells, *Madison University, Winsconsin,* unpublished Master's thesis.

Fletcher, J. & W. Martin. 1948. Some effects of algae and moulds in the rain crusts of desert soils. *Ecol.*, **29**, 95.

Folk, R.L. 1974 Petrology of sedimentary rocks. *Hemphill,* Austin

Folk, R.L. 1977. Folk's bedform theory - reply. *Sedimentology*, **24**, 864-874.

Folk, R.L. & W.C. Ward. 1957. Brazos River bar: a study in the significance of grain size parameters. *J. Sedim. Petrol.*, **27**, 3-26.

Forster, S. & T. Nicholson, 1981. Microbial aggregation of sand in a maritime dune succession. *Soil. Biol. Biochem.*, **13**, 205-208.

Fryberger, S. G., C. J. Shenk & L. F. Krystinik, 1988. Stokes surfaces and the effects of near-surface groundwater table on aeolian deposition. *Sedimentology*, **35**, 21 41.

Fryberger, S.G. 1990. Eolian stratification. In: *Modern & ancient eolian deposits: Petroleum exploration & production.* Rocky mountain section, SEPM, Denver, Colarado, 7.1-7.15.

Fryberger, S.G. 1990a. Bounding surfaces in eolian sediments. In: *Modern & ancient eolian deposits: Petroleum exploration & production.* Rocky mountain section, SEPM, Denver,

Fryberger, S. G. & G. Dean 1979. Dune forms and wind regime. In: *A study of global sand seas, E. D. McKee (ed.).* Prof. Pap. US Geol. Surv. No. 1052, 137-169.

Fryberger, S. G., A. M. Al-Sari, T. J. Clisham, A. R. Rizvi & K. G. Al-Hinai, 1984. Wind sedimentation in the Jafurah Sand Sea. Saudi Arabia. *Sedimentology*, **31**, 413-31.

Garcia Novo, F. 1976 Ecophysiological aspects of the distribution of *Elymus areneria* and Cakile Maritima on the dunes at Tentsmuir. *Ecol. Plant.*, **11** (1), 13-24.

Gares, P. 1987 Eolian sediment transport and dune formation on undeveloped and developed shorelines. *The State University of New Jersey, Rutgers*, unpublished Ph.D. thesis.

Gary, M., R. McAfee, Jr & C.L. Wolf (eds.) 1972. *Glossary of Geology*, American Geological Institute, Washington. DC, 805p.

Gaylord, D. R. & P. J. Dawson, 1987. Airflow terrain interactions through a mountain gap, with an example of eolian activity beneath an atmosphenc hydraulic jump. *Geology*, **15**, 789-92.

Gerety, K. M. & R. Slingerland, 1983. Nature of the saltating population in wind tunnel experiments with heterogeneous size-density sands. *In: Eolian sediments and processes, M. E. Brookfield & T. S. Ahlbrandt (eds)*, Amsterdam: Elsevier, 115-31.

Gimmingham, C.H. 1964. Maritime and submaritime communities. In: *The vegetation of Scotland, J.H. Burnett (ed.)*, Oliver & Boyd, Edinburgh, 67-142.

Glennie, K. W. 1972. Permian Rotliegendes of Northwest Europe interpreted in light of modern desert sedimentation studies. *Bull. Am. Assoc. Petrol. Geol.* **56**, 1048-71.

Glennie, K.W. 1970. Desert Sedimentary Environments. *Development in Sedimentology* 14. Amsterdam, Elsevier.

Goldsmith, V. 1973. Internal geometry and origin of vegetated coastal sand dunes. *J. Sedim. Petrol.* **43** (4), 1128-1142.

Goldsmith, V. 1985. Coastal dunes. In: *Coastal Sedimentary Environments, Davis, R.A. Jr. (Ed.)*, Springer Verlag, New York.

Goldsmith, V. 1989. Coastal dunes as geomorphological systems. *Proceedings of the Royal Society of Edinburgh*, 96B, 3-15.

Goldsmith, V., P. Rosen, & Y. Gertner, 1990. Eolian transport measurements, winds, and comparison with theoretical transport in Israeli coastal dunes. In: *Coastal Dunes: Form and Process, Nodstrom, K.F., Psuty, N.P. & Carter, R.W.G. (eds.)*, John Wiley & sons, 79-102.

Goudie, A. (ed.) 1981. Geomorphological techniques. *Allen & Udwin*, London.

Gradzinski, R., Gagol, J. & Slaczka, A. 1979. *Acta Geol. Pol.*, **29**, 151-175.

Greeley, R. & J. D. Iversen 1985. Wind as a geological process. *Cambridge Univ. Press*, Cambridge.

Greeley, R., J. D. Iversen, J. B. Pollack, N. Udovich & B. White 1974a. Wind tunnel studies of Martian aeolian processes. *Proc. R. Soc. London*, Ser. A 341, 331-60.

Greeley, R., J. D. Iversen, J. B. Pollack, N. Udovich & B. White 1974b. Wind tunnel simulations of light and dark streaks on Mars. *Science* **183**, 847-9.

Green, C.D. 1974a Sedimentary and morphological dynamics between St Andrews Bay and Tayport, Tay estuary, Scotland, *University of Dundee*, unpublished PhD. thesis.

Green, C.D. 1974b A study of hydraulics and bedforms at the mouth of the Tay Estuary, Scotland. *Proc. 2nd. Int. Est. Res. Conf. Myrtle Beach*, S. Carolina.

Gripp, K. & L. Martens, 1963. Wenn die Natur im Sande Spielt. Verlag der Gesellschaft der freunde des vaterlandischen Schul- und Erziehungswesens, Hamburg.

Grove A.T. 1950. Tentsmuir-Fife Soil blowing and coastal changes. Unpublished manuscript held by the N.C.C., Edinburgh, 24 pp.

Haggart, B. Andrew, 1978, A pollen and stratigraphical investigation into a peat deposit in St. Michael's wood, near Leuchars, Fife, *University of Dundee*, unpublished M.A. thesis,

Havholm, K.J. & Kocureck, G. 1988. A preliminary study of the dynamics of a modern draa, Algodones, southeastern California, USA. *Sedimentology*, **35**, 649-669.

Hesp, H. 1979. Sand trapping ability of culms of marram grass (Ammophila arenaria). *J. Soil Conserv. Serv. N.S.W.* 35. 156-160.

Hesp, P. 1981. The formation of shadow dunes. *Jour. Sedim. Perol.* **51**, 101-111.

Hesp, P. A. 1988. Morphology, dynamics and internal stratification of some established foredunes in southeast Australia. *Sediment Geol.* **55**, 17 41.

Hesp, P. A. 1988a. Surfzone, beach, and foredune interactions on the Australian south east coast. *Jour. Coast. Res.*, Spec. Iss. No. 3, 15-25.

Horikawa, K. 1987. Nearshore dynamics & coastal processes. 469 pp.

Horikawa, K. & H. W. Shen 1960. Sand movement by wind acrion US Army, Corps of Engineers, Beach Erosion Board, Tech. Memo. 119.

Horikawa. K., S. Hotta & N. C. Krauss 1986. Literature review of sand transport by wind on a dry sand surface. *Coastal Eng.* **9**, 503-26.

Hotta. S. S. Kubota, S. Katori & K. Horikawa 1985. Sand transport by wind on a wet sand surface. Proc. *19th Coastal Eng. Conf. Houston*, 1265-1281.

Howard, A. D., J. B. Morton, M. Gad-el-Hak & D. B. Pierce 1978. Sand transport model of barchan dune equilibrium *Sedimentology*, **25**, 307-38.

Hoyt, J.H. 1966. Air and sand movements to the lee of dunes. *Sedimentology*, **7**, 137-143.

Hsu, S. A. 1971. Measurement of shear stress and roughness length on a beach *Jour. Geophys. Res.* **76**, 2880-2885.

Hsu, S. A. 1973. Computing eolian sand transport from shear velocity measurements. *J. Geol.* **81**, 739-743.

Hunter, R. E. 1969. Eolian microridges on modern beaches and a possible ancient example. *J. Sedim. Petrol.* **39**, 1573-1578.

Hunter, R.E. 1973. Pseudo-crosslamination formed by climbing adhesion ripples. *J. Sedim. Petrol.* **43** (4), 1125-1127.

Hunter, R. E. 1977. Basic types of stratification in small eolian dunes. *Sedimentology*, **24**, 361-87.

Hunter, R.E. 1980. Quasi-planar adhesion stratification- An aeolian structure formed in wet sand. *J.Sedim. Petrol.*, **50**, 263-266.

Hunter, R.E. 1981. Stratification styles in aeolian sandstones, some Pennsylvian to Jurassic examples from the Western Interior USA. In: *Recent and ancient nonmarine depositional environment models for exploration, F.G. Ethridge & R.M. Florence (eds.)*, Soc. Econ. Paleontologists & Mineralogists Spec. Pub. 31, 315-329.

Hunter, R. E. & B. M. Richmond, 1988. Daily cycles in coastal dunes. *Sediment. Geol.* **55**, 43-67.

Hunter, R.E., B.M. Richmond, & T.R. Alpha 1985. Storm controlled oblique dunes of the Oregon coast. *Bull. Geol. Soc. Am.*, **96**, 1451-1465.

Illenberger, W. K. & I. C. Rust 1986. Venturi-compensated eolian sand trap for field use. *J. Sedim.. Petrol.* **56**, 541-3.

Illenberger, W. K. & I. C. Rust, 1988. A sand budget for the Alexandria coastal dunefield, South Africa *Sedimentology* **35**, 513-21.

Ingle. J. C. 1966. The movement of beach sand. *Developments in Sedimentology* 5. Amsterdam: Elsevier.

Ishihara, T. & Y. Iwagaki 1952. On the effect of sandstorm in controlling the mouth of the Kiku river. *Bull. Disaster Prevention Res. Inst.*, Kyoto Univ.

Iversen, J. D., J. B. Pollack, R. Greeley & B. R. White 1976. Saltation threshold on Mars: the effect of interparticle force surface roughness and low atmospheric density. *Icarus* **29**, 381-93.

Jackson, P. S. 1977. Aspects of surface wind behaviour. *Wind Eng.* **1**, 1-14.

Jackson, P. 1981. On the displacement height in the logarithmic velocity profile. *J. Fluid Mech.*, **111**, 15-25.

Jarvis, J. & C.A.R. Riley, 1987. Sediment transport in the mouth of the Eden estuary, *Est. Coastal & Shelf Sci.*, **24**, 463-481.

Jeffreys, H. 1929. On the transport of sediment by streams. Proc. Camb. *Philos. Soc.* **25**, 272-276.

Jennings, J.N. 1957. On the orientation of parabolic or U-dunes. *Geographical Journal*, **123**, 474-480

Jennings, J.N. 1957. On the orientation of parabolic or U-dunes. *Geogr. J.* **123**, 474-480.

Jensen, N. O. & O. Zeman 1985. Perturbation in mean wind and turbulence in flow over topographic forms. In: *Proceedings of the international workshop of the physics of blown sand, O. E. Barndorff-Nielsen, J. T. Moller, K. R. Rasmussen & B. B. Willetts (eds)*, Dept. Theoretical Statistics, Institute of Mathematics, Univ. Aarhus, Mem. 8. **2**, 351-68.

Johnson, J.W. 1965. Sand movement on coastal dunes. Proceedings of the federal inter-agency sedimentation conference, *United States Department of Agriculture Miscellaneous Publication*, Number 970, 747-755.

Johnson, D.L. 1977. Late Quaternary climate of coastal California: evidence for an Ice age refugium. *Quat. Res.***8**, 154-179.

Kadib, A.A. 1964. Calculation procedure for sand transport by wind on natural beaches. *Misc. Paper no. 2-64*, US Army CERC.

Kadib, A.A. 1965. A function of sand movement by wind. *Hydraulic Eng. Lab. Tech. Rep. HEL-2-12. Berkeley: Univ. California*

Kaganov, E.I. & A.M. Yaglom, 1976. Errors in wind speed measurements by rotation anemometers. *Boundary layer Meteorol.* **10**, 229-244.

Kawamura, R. 1951. Study of sand movement by wind. Rep*t. Inst. Sci. & Techn. Univ. Tokyo 5.*

Kawamura, R. 1964. Study of sand movement by wind. *Hydraulic Eng. Lab. Tech. Rep. HEL-2-8, 99-108. Berkeley: Univ. California.*

King, W.H.J. 1916. The nature and formation of sand ripples and dunes. *Geogr. J.* **47**, 189-209.

Kocurek, G. 1981 Significance of interdune deposits and bounding surfaces in aeolian dune sands. *Sedimentology* **28**, 753-80.

Kocureck, G & G. Fielder, 1982. Adhesion structures. *J. Sedim. Petrol*, **52**, 1229-1241.

Kocurek, G. & R. H. Dott, Jr 1981. Distinctions and uses of stratification types in the interpretation of eolian sand. *J. Sedim. Petrol.* **51**, 579-95.

Komar, P.D. 1976. Beach processes and sedimentation. *Prentics Hall* Englewood Cliffs, N.J.

Kutzbach, J.E. & Wright, H.E. (1986) Simulation of the climate of 18,000 yrs B.P.: Results from North American/ North Atlantic/ European sector and comparison with the geologic record of North America. *Quat. Sci Rev.*, **4**, 147-187.

Lancaster, N. 1983. Controls of dune morphology in the Namib sand sea. In: *Eolian sediments and processes, M. E. Brookfield & T. S. Ahlbrandt (eds)*, Amsterdam: Elsevier, 261-89.

Lancaster, N. 1985. Wind and sand movements in the Namib Sand Sea. *Earth Surf. Proc. Landf.* **10**, 607-610.

Landsberg, S.Y. 1956. The orientation of dunes in Britain & Denmark in relation to the wind. *Geog. J.* **122**, 176-189.

Lang, A. & R. Leuning. 1981. New omnidirectional anemometer with no moving parts. *Bound. Layer Meteorol.*, **20**, 445-457.

Langerfeldt, F. 1935 Untermeerische Scharrkeise im Schilck. *Natur und Volk* **65**, 458-61.

Larsen, F.D. 1971 Eolian sand transport on Plum Island, Massachussets. *Coastal Environ.*, 356-67.

Leatherman, S.P. 1978. A new aeolian sand trap design. *Sedimentology*, **25**, 303-306.

Leatherman, S.P. 1976. Barrier island dynamics: overwash processes and aeolian transport. *Proc. 15th Coastal Eng. Conf.*, ASCE, New York, 1958-1974.

Lettau, K. & H. Lettau, 1978. Experimental and micrometeorological field studies of dune migration. In: *Exploring the world's driest climate. H. H. Lettau & K. Lettau (eds.)*, Madison: Center for Climatic Research, Univ. Wisconsin, 110-147.

Lupe, R. & T. S. Ahlbrandt, 1979. Sediments in ancient eolian environments - reservoir inhomogeniety. In: *A study of global sand seas. E. D. McKee (ed.).* Prof. Pap. US Geol. Surv. No. 1052, 2-51.

Lyles. L. & R. K. Krauss, 1971. Threshold velocities and initial particle motion as influenced by air turbulence. *Trans. Am. Soc. Agric. Eng. Abs.* 14, 563-66.

Mac Cready, P.B. 1966. Mean wind speed measurements in turbulence. *Jour. Appl. Meteorol.* **5**, 219-25.

Mainguet, M. & Callot, Y. 1978. L'erg de Fachi-Bilma. *Memoires et Documents* 18. Paris: Centre National de la Recherche Scientifique.

Mainguet, M. & M.C. Chemin, 1983. Sand seas of the Sahara and Sahel: An explanation of their thickness and sand dune type by the sand budget principle. In: *Eolian sediments and processes, M.E. Brookfield & T.S. ahlbrandt (eds),* Amsterdam: Elsevier, 353-363.

Mainguet, M. 1986. The wind and desertification processes in the Saharo-Sahelian and Sahelian regions. In: *Physics of desertification. F. El-Baz & M.H.A. Hassan (eds),* Dordrecht: Martinus Nijhoff, 210-240.

Malina, F.J. 1941. Recent developments in the dynamics of wind erosion *Trans. Am. Geophys. Union* **22**, 62-84.

Marston, R.A. 1986. Maneuver-caused wind erosion impacts, South Central New Mexico. In: *Aeolian Geomorphology, W.G. Nickling (ed.),* Allen & Udwin, Boston, 273-290.

Mather, A.S. & Ritchie, W. 1977. The beaches of the highlands and islands of Scotland. *Countryside Commission for Scotland.*

Mather, A.S. & W. Ritchie, 1984. The beaches of Scotland. *Countryside Commission for Scotland.*

McCann, S.B. & M.L. Byrne, 1989. Stratification models for vegetated coastal dunes in Atlantic, Canada. *Proceedings of the Royal Society of Edinburgh,* 96B, 203-218.

McCluskey, R.M. 1987. The role and magnitude of aeolian processes in the barrier island environments. *Rutgers the State University,* New Brunswick.

McEwan, I. & B.B. Willets, 1991 Numerical model of the saltation cloud. *Acta Mech.* **1**, 53-66.

McGill, J.T. 1958. Map of coastal landforms of the world. *Geogr. Rev.*, **48**, 402-405.

McKee, E.D. 1957. Primary structures in some recent sediments. *Am. Assoc. Petrol. Geologists. Bull.* **41**, 1704-1747.

McKee, E.D. 1966. Structures of dunes at White Sands National Monument. New Mexico. *Sedimentology* 7, 3 69.

McKee, E.D. & J.J. Bigarella, 1979. Sedimentary structures in dunes, with two sections on the Lagoa dunefield. ed. McKee, E.D. *United States Geological Survey. Professional Paper* 1052, 83-136

McKee, E.D. & G.W. Wier, 1953 Terminology for stratification and cross stratification in sedimentary rocks. *Geol. Soc. Am. Bull.*, **64**, 359-378.

McKee, E. D. & J. J. Bigarella, 1979. Sedimentary structures in dunes. In: *A study of global sand seas E. D. McKee (ed.), 83-134. Prof. Pap. US Geol. Surv. No. 1052.*

McKee. E. D., J. R. Douglass & S. Rittenhouse 1971. Deformation of lee side laminae in eolian dunes. *Bull. Geol. Soc. Am.* **82**, 359-78.

McLaren, P. 1981 An interpretation of trends in grain size measures. *J. Sedim. Petrol,* **51**, 2, 611-24.

McManus, J. 1989. Grain size determination & interpretation. In: *Techniques in sedimentology. ed. Maurice Tucker.* 63-85.

McManus, J., A.T. Buller, & C.D. Green, 1980. Sediments of the Tay Estuary: VI. Sediments of the lower and outer reaches. *Proc. Roy. Soc. Edin.* 78B, 133-153.

Mitha, S., M. Q. Tran, B. T. Werner & P. K. Haff, 1986. The grain-bed impact process in aeolian saltation. *Acta Mech.* **63**, 267-78.

Monteith, J.H. 1973. Principles of environmental physics. *Edward Arnold*, London.

Morgan, R.P.C. 1978. Field studies of rain splash erosion. *Earth Surf. Proc. & Landf.*, **3**, 295-299.

Morton, J.K. 1957. Sand dune formation on a tropical dune. *Jour. Ecol.* 504-505.

Nalpanis, P. 1985. Saltating and suspended particles over flat and sloping surfaces. II. Experiments and numencal simulations. In: *Proceedings of the international workshop on the physics of blown sand, O. E. Barndorff-Nielsen, J. T. Mo11er. K. R. Rasmussen & B. B. Willetts (eds)*, Dept. Theoretical Statistics, Institute of Mathematics, Univ. Aarhus, Mem. 8. 37-66.

Nickling, W. G. & M. Ecclestone, 1981. The effects of soluble salts on the threshold shear velocity of fine sand. *Sedimenology* **28**, 505-10.

O Brien, M. P. & B. D. Rindlaub, 1936. The transportation of sand by wind. *Civil Eng.*, **6**. 325 7.

Ogilivie, A.G. 1923. Physiography of the Moray Firth coast. *Trans. Roy. Soc. Edin.*,LIII Part II, **19**, 377-404.

Oke, T. 1978. Boundary Layer Climates, *Meuthen*, New York.

Olson, J. S. 1958. Lake Michigan dune development 1. Wind velocity profiles. *J. Geol.* **66**, 254 63.

Olson, J.S. & E. Van Der Maarel, 1989. Coastal dunes in Europe: A global view. In: *Perspectives in coastal dune management, Van der Meulen, F, Jungerius, P.D. & Visser, J.H. (eds.)*, SPB Academic Publishing, The Hague, The Netherlands, 3-32.

Parrish, J. T & F. Peterson, 1988. Wind directions predicted from global circulation models and wind directions determined from eolian sandstones of the western United States-a comparison. *Sediment. Geol.* **56**, 261-82.

Passega, R. 1957. Textures as charcteristics of clastic deposition. *Bull. Amer. Assoc. Petrol. Geologists*, **41**, 1952-1984.

Passega, R. 1964 Grain size representation by C M patterns as a geological tool. *Jour. Sed. Petrol.* **34**, 840-847.

Psuty, N.P. 1969. Beach nourishment by aeolian processes, Paracas, Peru. Proc. 10th Meeting, New York-New Jersey Division, *Association of American Geographers*, **3**, 117-123.

Psuty, N.P. 1986. Principles of dune beach interaction related to coastal management. *Thalassas*, **4**, 11-15.

Psuty, N.P. 1988. Sediment budget and beach/dune interaction. *Journal of Coastal Research*, Special Issue No. 3,1-4.

Psuty, N.P. & S.W.S. Millar, 1989. Coastal Dunes: A concept of zonality. *Essener Geogr. Arbeiten*, **18**, 149-169.

Pye, K. 1980. Beach salcrete and eolian sand transport: evidence from North Queensland. *J. Sedim.. Petrol.* **50,** 257-261.

Pye, K. 1983. Coastal dunes. *Progress in Physical Geography*, 7, 531-557.

Pye , K. & Tsoar, H. 1990. Aeolian sand and sand dunes. *Unwin Hyman*, London, 396p.

Pye, K. 1990. Physical and human influences on coastal dune development between the Ribble & Mersey estuaries, northwest England. In: *Coastal Dunes: Form and Process, Nodstrom, K.F., Psuty, N.P. & Carter, R.W.G. (eds.)*. John Wiley & sons, 339-355.

Ranwell, D.S. 1972. Ecology of salt marshes and sand dunes. *Chapman & Hall*, London.

Ranwell, D.S. & Boar, R. 1986. Coast dune management guide. *Institute of Terrestrial Ecology*, Monkswood, Huntingdon.

Reineck, H.E. & I.B. Singh, 1980. Depositional sedimentary environments. *Springer Verlag.*

Reineck, H. E. 1955. Haftrippeln und haftwarzen. ablagerungsformen von flugsand. *Senckenbergiana Lelhaea* **38**, 347-57.

Rempel, P. 1936. The crescentic dunes of the Salton Sea and their relation to vegetation. *Ecology* **17**. 347-58.

Rice, M.A. 1991. Grain shape effects on aeolian sediment transport. *Acta Mechanica*, **1**, 159-66.

Rice, R.J. 1962. The morphology of the Angus coastal lowlands. *Scott. geogr. Mag.* **78**, 5-14.

Richard, W.B. 1973. A note on asymmetrical structures caused by differential wind erosion of a damp sandy forebeach. *Jour. Sedim. Petrol.* **43**, 1, 205-6.

Richards, L.A. 1947. Pressure membrane apparatus- construction & use. *Agric. Engg.*, **28**, 451-4.

Richter, R. 1926. *Natur Mus.*, **56**, 389-407.

Rintoul- Robertson, M.J. 1985. The morphology & dynamics of parabolic dunes within the context of the coastal dune systems of mainland Scotland, *Hertford college, Oxford*, Unpublished Ph.D thesis.

Ritchie, W. 1979. The beaches of Fife. *Countryside Commission for Scotland.*

Rosen, P. 1979. Aeolian dynamics of a barrier island system. In: *Barrier Islands, Leatherman S.P. (ed.)*, Academic Press, New York, 81-98.

Rubin, D. M. & R. E. Hunter, 1985. Why deposits of longitudinal dunes are rarely recognized in the rock record. *Sedimentology* **32**. 147-57

Rumpel, D. A. 1985 Successive aeolian saltation studies of idealized collisions. *Sedimentology*, **32**, 267-80.

Sarre, R.D 1984 Sand movement from the inter-tidal zone and within coastal dune systems by aeolian processes. Jesus College, Oxford Unpublished Ph.D. thesis.

Sarre R. D 1987 Aeolian sand transport. *Progress in Physical Geography*, **11**, 157-82.

Sarre R. D. 1988. Evaluation of aeolian sand transport equations using intertidal zone measurements, Saunton Sands, England. *Sedimentology* **35**, 671-679.

Sarre, R. D. 1989. Aeolian sand drift from the intertidal zone on a temperate beach: potential and actual rates *Earth Surf. Proc. Landf.* **14**, 247-58.

Sarrikostis, E.C, 1986. Potential longshore sediment transport patterns between Montrose and Fife Ness, Scotland. *University of Dundee*, unpublished PhD. thesis.

Savage, R.P. & W.W. Woodhouse, 1968. Creation and stabilisation of coastal barrier dunes. *Proc. 11th Conf. Coastal Engg. ASCE*, 671-700.

Schwartz, Maurice, L. (1982) *eds.* The encyclopedia of beaches and coastal environments.

Seppala, M. 1972. Location morphology and orientation of inland dunes in northern Sweden. *Geogr. Ann.* **54A**. 85-104.

Seppala, M. & K. Linde 1978. Wind tunnel studies of ripple formation. *Geogr. Ann.* **60A**. 292.

Sharp, R. P. 1963. Wind ripples. *J. Geol.* **71**, 617-36.

Sharp, R. P. 1964. Wind-driven sand in Coachella Valley, California. *Bull. Geol. Soc. Am.* **75**, 785-804.

Shaw, R., G. Kidd, & G. Thurtell, 1973. A miniature three-dimensional anemometer for use within and above plant canopies. *Bound. Layer Meteorol.*, **3**, 359-380.

Shepard, F.P. 1963. Submarine geology. 2nd. Ed., *Harper & Row*, New York.

Sherman, D.J. & S Hotta, S. 1990. Aeolian sediment transport. theory and measurement. In. *Coastal Dunes: Form and Process, Nordstorm, K.F., Psuty, N.P. & Carter, R.W.G. (eds.), John Wiley & Sons Ltd.*, 17-39.

Shields, A. 1936. Application of similarity principles and turbulence research to bed-load movement. Translation of Mitteilungen der preussischen Versuchsansta/tfur Wasserbau und Schiffbau W. P.

Short, A.D. & P.A. Hesp, 1982. Wave, beach and dune interactions in southeastern Australia. *Mar. Geol*, **48**, 259-284.

Short, A.D. 1987. Modes, timing and volume of Holocene cross-shore and aeolian sediment transport, South Australia. *Coastal Sediments 1987*, ASCE, New Orleans, 1925-1937.

Short, A.D. 1988. Holocene coastal dune formation in southern Australia: A case study. *Sedim. Geol.* **55**, 259-284.

Simpson, E.L. & D.B. Loope, 1985 Amalgamated interdune deposits, White Sands, New Mexico. *Jour. Sedim. Petrol.* **55**, 361-65.

Singhvi, A.K. & Kar, A. 1992. Thar desrt in Rajasthan , Land, Man and Environment. *Geological Society of India.* Bangalore, 191 pp.

Sissons, J.B., D.E. Smith & R.A. Cullingford. 1966. Late-glacial and post-glacial shorelines in the southeast of Scotland. *Trans. Inst. British. Geogr.* **39**, 9-18.

Sly, P.G. 1977. Sedimentary environments in the Great Lakes In: *Proceedings of the SIL-UNESCO Symposium on interactions between sediments and freshwater, H.L. Golterman, (eds.)*, pp. 76-82. Amsterdam

Sly, P.G. 1978 Sedimentary processes. In: Lakes-Chemistry, Geology, Physics (Ed. A. Lerman), pp.65-89. *Springer Verlag*, Berlin

Smalley, I.J. 1970. Cohesion of soil particles and the intrinsic resistance of simple soil systems to wind erosion,. *Jour. Soil Sc.*, **21**, 154-61.

Smith, H.T.U. & C. Messenger, 1959. Geomorphic studies of the Provincetown Dunes, Cape Cod, Massachusetts Technical Report No. 1, Office of Naval Research Geography Branch University of Massachusetts, Amherst.

Snead, R.E. 1982. Coastal landforms & surface features: A photographic atlas & glossary. Hutchinson Ross, Stroudsburg, Pennsylvania.

Sonu, C.J. 1973 Three-dimensional beach changes. *Jour. Geol.* **81**, 42-46.

Steele, R. P. 1983. Longitudinal draa in the Permian Yellow Sands of northeast England. In: *Eolian sediments and processes, M. E. Brookfield & T. S. Ahlbrandt (eds)*. Amsterdam: Elsevier, 543-50

Steele, R. P. 1985. Early Permian (Rotliegendes) palaeowinds of the North Sea-comment. *Sediment. Geol.* **45**. 93-7

Steers, J.A. 19 The Culbin sands and burghead bay. *Geogr. Jour.* **90**, 498-528.

Stewart, H.B. 1958 Sedimentary reflections on depositional environments in San Migue Lagoon, Baja, California, Mexico. *Bull. Am. Assoc. Petrol. Geol.* **42**, 2567-2618.

Stone, R.O. 1967. *Earth-Sci. Rev.*, **3**, 211-268.

Summerfield, M.A. 1971. Global geomorphology. *Longman Scientific & Technical.*

Svasek, J. N. & J. H. J. Terwindt 1974. Measurements of sand transport by wind on a natural beach. *Sedimentology* **21**, 311-22.

Thomas, D. S. G. 1986 Dune pattern statistics applied to the Kalahari dune desert, Southern Africa. *Z. Geomorph.* **30**, 231-42.

Thomas, D.S.G. 1987. Discrimination of depositional environments using sedimentary characteristics in the mega-Kalahari, Central southern Africa. In: *Desert sediments: ancient & modern, L. Frostick & I.Reid (eds.)*. Oxford, Blackwell., 293-306.

Trask, P.D. (ed.) 1939. Recent marine sediments, *Am. Assoc. Petroleum Geologists*, 736p.

Tsoar, H. 1983. Wind tunnel modelling of echo and climibing dunes. *In: Eolian sediments and processes, M.E. Brookfield & T.S. Ahlbrandt (eds.)*, Elsevier, Amsterdam, 247-259

Tsoar, H. & D. Blumberg, 1991. The effects of sea cliffs on inland encroachment of aeolian sand. *Acta Mechanica Suppl.* 2, 131-146.

Ungar J. E. & P. K. Haff 1987. Steady state saltation in air. *Sedimentology* **34**, 289-99.

Van Straaten, L. M. J. U. 1953. Rhythmic patterns on Dutch North Sea beaches. *Geol. Mijn.* **15**, 31-43.

Wal, A. & J. McManus. 1990. Aeolian sand trap reliability (*Abs.*). *BSRG*, Reading.

Wal, A. & J. McManus. 1992. Aeolian sand transport in a Scottish coastal environment (*Abs.*). *Intl. Symposium on the Evolution of Deserts, Ahmedabad, India.*

Wal, A. & J. McManus. 1992. Wind regimes and sand transport on a coastal beach-dune complex in eastern Scotland, U.K. *Geol. Soc. London Spec Publ.* 159-171.

Walker, R.J. 1980. Barrier island systems. In: *Facies Models (1st edition). R.G.Walker (ed.),* Geoscience, Canada.

Walker, J.D. 1981. An experimental study of wind. ripples. *Mass. Inst. Technol.*, unpublished M.Sc. thesis.

Warren,A. 1979. Aeolian processes. In: *Geomorphology, C. Embleton & J. Thornes (eds.),* Edward Arnold, London, 325-351.

Wasson R. J. and R. Hyde 1983a. Factors determining desert dune type. *Nature* **304**, 337-339.

Wasson R. J. & R. Hyde 1983b. A test of granulometric control of desert dune geometry. *Earth Surf. Proc. Landf.* **8**, 301-12.

Wasson, R.J. Rajaguru, S.N. Misra, V.N., Agarwal, D.P. Dhir, R.P., Singhvi, A.K. and Rao, K.K. 1983. Geomorphology, late Quaternary stratigraphy and palaeoclimatology of the Thar dune field. *Z. geomorph. Suppl.* **45**, 117-151.

Wasson, R.J. & P.M. Nanninga 1986. Estimating wind transport of sand on vegetated surfaces. *Earth. Surf. Proc. Landf.* **11**, 505-514.

Weber, K J. 1987. Computation of initial well productivities in aeolian sandstone on the basis of geologic model. Leman gas field. UK. In: *Reservoir sedimentology, R. W. Tillman & K. J. Weber (eds),* Spec Publ. No 40. Soc. Econ. Paleontol. Mineral. 333-354.

White. B. R. 1979. Soil transport by winds on Mars. *Jour. Geophys. Res.* **84**, 4643-4651.

White, B. R. 1982. Two-phase measurements of saltating turbulent boundary-layer flow. *Int. J. Multiphase Flow*, **8**, 459-73.

White, B. R. 1985. The dynamics of particle motion in saltation. In: *Proceedings of the international workshop on the physics of blown sand. O. E. Barndorff-Nielsen, J. T. Moller, K. R. Rasmussen & B. B. Willetts, (eds),* Dept. Theoretical Statistics, Institute of Mathematics, Univ. Aarhus, 101-140.

White, B. R., R. G. Greeley, J. D. Iversen & J. B. Pollack 1976. Estimated grain saltation in a Martian atmosphere. *Jour. Geophys. Res.* **81**, 5643-50.

White, B. R. & J. C. Schulz 1977. Magnus effect in saltation. *J. Fluid Mech.* **81**, 497-512.

Wilcoxon, J.A. 1962. Relationship between sand ripples and wind velocity in a dune area. *Compass*, **39**, 65-76.

Willets, B.B., M.A. Rice, M.A. & S.E. Swaine, 1982. Shape effects in aeolian grain transport. *Sedimentology*, **29**, 409-17.

Willets, B.B., I.K. Mc Ewan, & M.A. Rice, 1991. Initiation of motion of quartz grains. *Acta Mechanica* **1**, 123-134.

Willetts, B. B. & M. A. Rice, 1985. Inter-saltation collisions. In: *Proceedings of the international workshop on the physics of blown sand O. E. Barndorff-Nielsen, J. T. Moller, K. R. Rasmussen & B. B. Willetts (eds),* Dept. Theoretical Statistics, Institute of Mathematics. Univ. Aarhus. Mem. 8,83-100.

Willetts, B.B. & M.A. Rice, 1986. Collision in aeolian saltation. *Acta Mech.* **63**, 255-265.

Williams, G. 1964. Some aspects of the eolian saltation load. *Sedimentology* 3, 257-87.
Williams, G. P 1966. Particle roundness and surface texture effects on fall velocity. *J. Sediment. Petrol.* **36**, 255-9.

Wilson, I.G. 1973. Ergs. *Sediment. Geol.* **10**, 77-106.

Woodhouse, W.W. 1978. Dune building and stabilisation with vegetation. SR-3, CERC, US Army Corps of Engineers, Fort Belvoir, VA.

Wunderlich, F. 1972. *Senckenbergiana Marit.*, **4**, 47-79.

Yasso, W.E. 1966. Heavy mineral concentration and sastrugi-like deflation furrows in a beach salcrete at Rockaway Point, New York. *J. Sedim. Petrol.* **36**, 836-838.

Zeigler, J.M. & S.D.Tuttle, 1961. Beach changes based on daily measurements of four Cape Cod beaches. *J. Geol.* **69**, 583-599.

Zingg, A. W. 1953 Wind tunnel studies of the movement of sedimentary material. *Proceedings of the 5th Hydraulics Conf. Bull.* 34, 111-35. Iowa City: Inst. of Hydraulics.

APPENDICES

Appendix I - A Daily tide data from Tay estuary tidal chart for the survey period (June 29 - July 31, 1990)

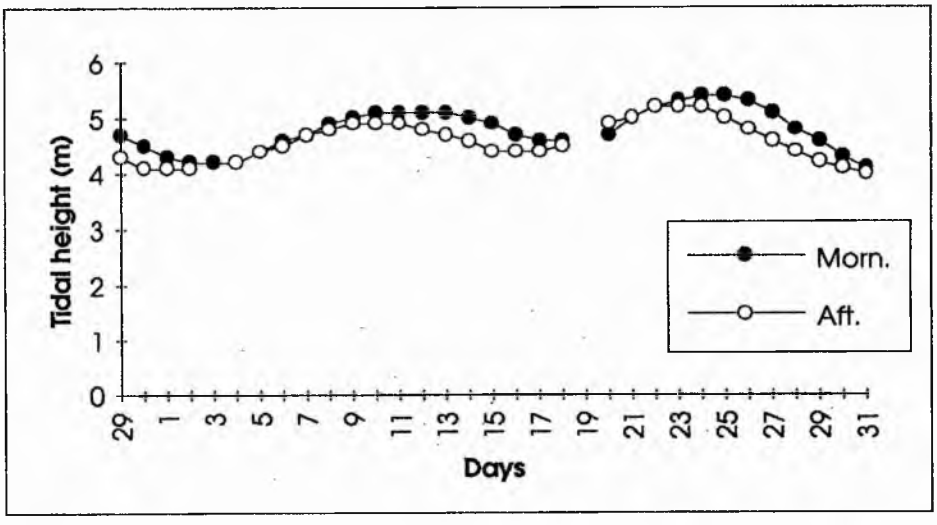

Appendix I - B Daily Wind Data From 29, June To 25, July 1990

SPEED (m/sec) (Data from Leuchars Meteorological Station)

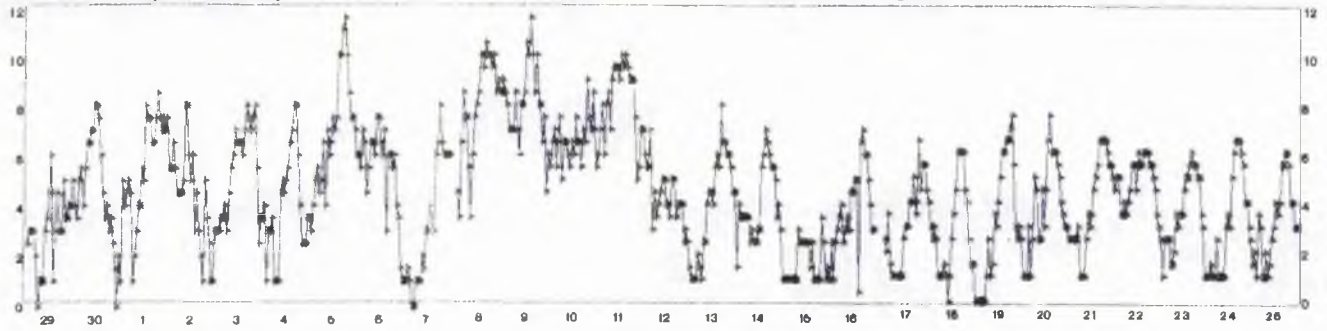

AZIMUTH (Degrees)

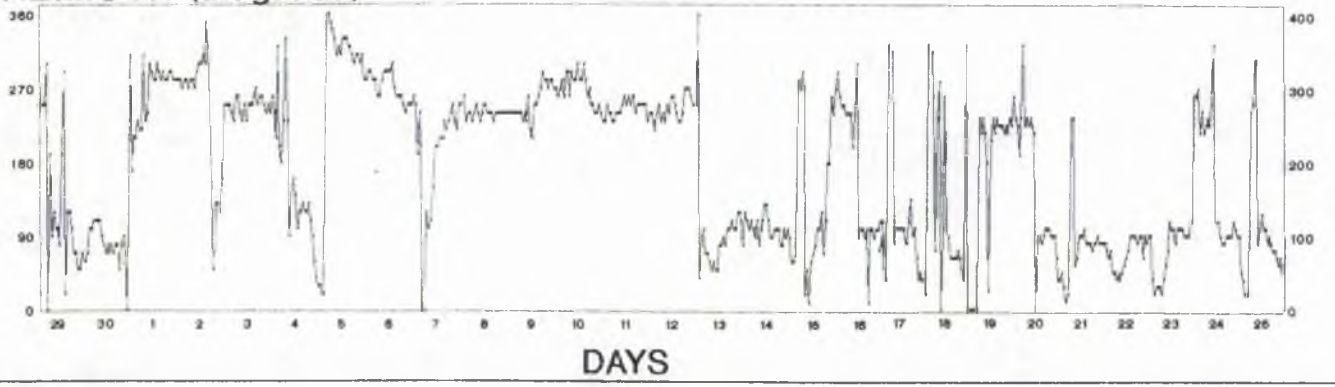

Appendix I - C Example of Grain Size Data Sheet

SAMPLE NO:	E1A - L.B.F
SAMPLE LOCATION:	Leuchars
DATE OF COLLECTION:	October 14, 1989
DATE OF EXPERIMENT:	October 20, 1989
DATE OF ANALYSIS:	January 10,1990
TOTAL ORIGINAL WEIGHT:	150
TOTAL EXPERIMENTAL WEIGHT:	150.36
DIFFERENCE:	0.356
CORRECTION FACTOR (CF):	0.9976

S.No.	BS Sieve Mesh	Grain Size (phi)	Mid phi	Exp Wt (gms)	Wt.*CF (gms)	Wt. %	Cum. Wt. %
1	8	-1.75 - -1.04	-1.40	0.082	0.08	0.05	0.05
2	16	-1.04 - 0	-0.52	0.55	0.55	0.37	0.42
3	25	0 - 0.74	0.37	1.295	1.29	0.86	1.28
4	36	0.74 - 1.24	0.99	2.632	2.63	1.75	3.03
5	44	1.24 - 1.5	1.37	4.367	4.36	2.90	5.94
6	52	1.5 - 1.76	1.63	8.75	8.73	5.82	11.76
7	60	1.76 - 1.99	1.88	22.123	22.07	14.71	26.47
8	72	1.99 - 2.24	2.12	40.127	40.03	26.69	53.16
9	85	2.24 - 2.49	2.37	51.164	51.04	34.03	87.19
10	100	2.49 - 2.72	2.61	15.364	15.33	10.22	97.40
11	120	2.72 - 3.01	2.87	3.576	3.57	2.38	99.78
12	150	3.01 - 3.26	3.14	0.121	0.12	0.08	99.86
13	170	3.26 - 3.49	3.38	0.168	0.17	0.11	99.98
14	200	3.49 - 3.71	3.60	0.028	0.03	0.02	99.99
15	240	3.71 - 3.91	3.81	0.009	0.01	0.01	100.00

FOLK & WARD

Mz= 1.96
Isd= 0.35
Isk= -0.28
Kg= 1.33

Percentile Derivatives(phi)

P5 = 1.1
P10 = 1.5
P16 = 1.64
P25 = 1.8
P50 = 2.15
P75 = 2.2
P84 = 2.25
P90 = 2.3
P95 = 2.4

TRASK

Md= 0.275
So= 1.04
Sk= 0.825
QDa= 0.01

Quartile Derivatives (mm)

Q25 = 0.24
Q50 = 0.275
Q75 = 0.26

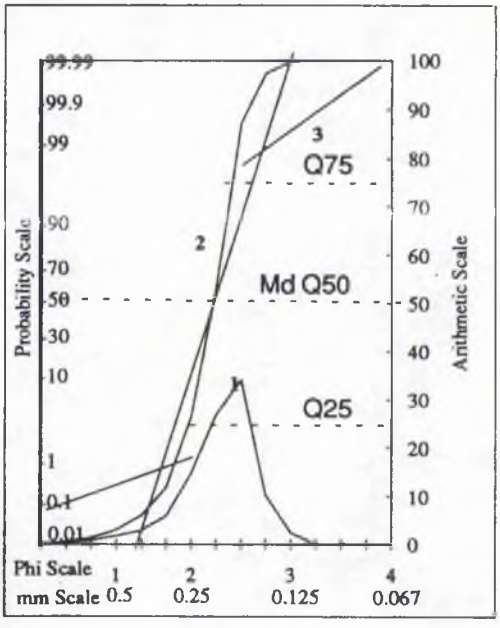

Data sheet of sieve analysis of sediment samples along various transects in the study area. Right hand corner shows examples of types of sediment distribution curves plotted using results of sieve analysis. (1) Frequency curve; (2) Cumulative curve; (3) Log-probability curve. Curves 1 & 2 are plotted on an arithmetic scale; curve 3 is plotted on a log-probability scale. Q25, Q50 & Q75 are read from the cumulative curve.

Appendix I - D Grain-size Analysis

Histograms, Normal frequency curve and Cumulative frequency curve (on normal and probability scale) were plotted for each of the samples.

The graphical parameters are calculated using the Folk and Ward's, and Trask's methods.

The parameters calculated by Folk and Ward's formula are;

1. Graphic Mean (M_z) : $(P_{16} + P_{50} + P_{84})/3$
2. Inclusive Graphic Standard Deviation (I_{sd}) : $(P_{84} - P_{16})/4 + (P_{95} - P_5)/6.6$
3. Inclusive Graphic Skewness (I_{sk}) :

$$\{(P_{84} + P_{16} - 2P_{50})/2(P_{84} - P_{16})\} + \{(P_{95} + P_5 - 2P_{50})/2(P_{95} - P_5)\}$$

4. Graphic Kurtosis (K_g) : $(P_{95} - P_5)/2.44(P_{75} - P_{25})$

Trask's parameters were calculated using the following formulae;

1. Median Grain Size (M_d) : Q_{50}
2. Sorting Coefficient (S_o) : $(Q_{75}/Q_{25})^{1/2}$
3. Skewness (S_k) : $(Q_{25}.Q_{75})/(Q_{50}^2)$
4. Quartile Deviation (QDa) : $(Q_{75} - Q_{25})/2$

where, 'P_x' and 'Q_x' are percentile values in phi and metric units, respectively.

Appendix I - E Statistical Parameters of Sediment Subsamples

Location	Median	Mean	Dispersion		Skewness		Kurtosis		% CO3
Transect 11									
L.B.F.	2.20	1.96	0.35	WS	-0.28	NS	1.33	L	4.60
L.B.F.1	2.00	1.98	0.29	VWS	-0.15	NS	1.02	M	5.60
M.B.F.	2.00	1.98	0.88	MS	-0.39	VNS	4.68	EL	15.30
M.B.F.1	2.00	1.98	0.34	VWS	-0.12	NS	1.14	L	10.10
U.B.F.	2.00	2.34	0.26	VWS	-0.54	VNS	1.53	VL	6.20
U.B.F.1	2.10	2.10	0.25	VWS	0.03	SYM	1.56	VL	2.60
Average	2.05	2.06	0.40		-0.24		1.94		7.40
Transect 10									
L.B.F.	2.10	2.09	0.26	VWS	-0.10	SYM	1.16	L	4.20
M.B.F.	2.10	2.09	0.26	VWS	-0.11	NS	1.15	L	8.70
M.B.F.1	2.10	2.09	0.25	VWS	-0.08	SYM	1.06	L	5.03
U.B.F.	2.10	2.08	0.24	VWS	-0.13	NS	1.00	M	3.30
U.B.F1	2.10	2.09	0.26	VWS	-0.10	NS	1.16	L	3.20
Average	2.10	2.09	0.25		-0.10		1.11		4.89
Transect 9									
L.B.F.	2.00	1.96	0.34	WS	-0.18	NS	0.92	M	2.00
M.B.F.	2.05	2.04	0.26	VWS	0.04	SYM	1.22	L	7.40
F.D.	2.15	2.13	0.26	VWS	0.02	SYM	0.94	M	8.40
Average	2.07	2.04	0.29		-0.04		1.03		5.93
Transect 8									
L.B.F.	2.14	2.15	0.29	VWS	-0.05	SYM	1.48	L	3.90
L.B.F.1	2.10	2.05	0.30	VWS	-0.26	NS	2.03	VL	5.30
M.B.F.	2.05	1.99	0.39	WS	-0.32	VNS	1.48	L	10.30
M.B.F1	2.00	1.99	0.39	WS	-0.32	VNS	1.49	L	0.60
U.B.F.	2.00	2.03	0.30	VWS	-0.14	NS	1.28	L	0.80
F.D.	2.00	1.97	0.53	MWS	-0.32	VNS	1.49	L	29.20
Average	2.05	2.03	0.37		-0.24		1.54		8.35
Transect 7									
L.B.F.	2.00	1.95	0.37	WS	-0.23	NS	1.10	M	2.10
L.B.F.1	2.00	1.96	0.40	WS	-0.14	NS	1.01	M	1.30
M.B.F.	2.05	1.93	0.66	MWS	-0.37	VNS	1.07	M	4.30
M.B.F.1	2.05	2.07	0.60	MWS	-0.46	VNS	1.05	M	3.40
U.B.F.	2.00	1.90	0.46	WS	-0.44	VNS	1.43	L	14.30
F.D.	2.00	1.94	0.54	MWS	-0.36	VNS	1.80	VL	11.80
Average	2.02	1.96	0.51		-0.33		1.24		6.20
Transect 6									
L.B.F.	2.00	1.97	0.34	VWS	-0.11	NS	1.00	M	2.10
L.B.F.1	1.85	1.85	0.37	WS	-0.08	SYM	1.06	M	3.90
M.B.F.1	1.75	1.62	0.61	MWS	-0.43	VNS	1.29	L	12.60
U.B.F.	1.90	1.72	0.83	MS	-0.57	VNS	2.14	VL	22.90
F.D.	1.90	1.87	0.36	WS	-0.13	NS	0.94	L	4.40
Average	1.88	1.81	0.50		-0.26		1.29		9.18

Location	Median	Mean	Dispersion		Skewness		Kurtosis		% CO3
Transect 5									
L.B.F.	1.80	1.77	0.44	WS	-0.09	SYM	1.00	M	3.10
L.B.F.1	1.80	1.77	0.43	WS	-0.19	NS	93.00	M	3.50
M.B.F.	1.00	1.00	0.81	MS	-0.10	NS	1.23	L	10.80
M.B.F.1	1.60	2.16	0.40	WS	-0.13	NS	1.82	VL	7.40
U.B.F.	2.25	1.92	0.79	MS	-0.56	VNS	0.83	P	26.10
F.D.	2.40	2.29	0.53	MWS	-0.35	VNS	0.99	M	17.60
Average	1.81	1.82	0.57		-0.24		16.48		11.42
Transect 4									
L.T. 1	1.89	1.84	0.34	VWS	-0.18	NS	0.99	M	14.40
I.T. 1	1.89	1.80	0.43	WS	-0.28	NS	0.89	P	7.90
H.T. 1	2.80	2.10	0.40	WS	0.10	SYM	1.46	L	2.60
Dune	2.00	1.97	0.36	WS	-0.12	NS	1.05	M	0.90
Average	2.15	1.93	0.38		-0.12		1.10		6.45
Transect 3									
L.T. 1	1.68	1.61	0.52	MWS	-0.28	VNS	1.05	M	6.60
I.T. 1	1.92	1.91	0.31	VWS	-0.05	SYM	1.05	M	1.84
H.T. 1	2.05	2.03	0.27	VWS	0.01	SYM	1.12	L	1.40
Dune	2.00	1.97	0.36	WS	-0.15	NS	1.09	M	1.90
Average	1.91	1.88	0.37		-0.12		1.08		2.94
Transect 1									
L.B.F.	2.25	2.27	0.28	VWS	-0.09	SYM	1.50	VL	11.84
L.B.F.1	1.75	1.69	0.63	MWS	-0.19	NS	0.87	P	6.40
M.B.F.	2.10	2.06	0.31	VWS	-0.23	NS	1.06	M	3.90
M.B.F.1	2.10	2.07	0.31	VWS	-0.20	NS	1.49	L	8.20
U.B.F.	1.24	1.23	0.39	WS	0.32	VPS	1.19	L	2.90
U.B.F.1	1.20	1.31	0.40	WS	0.39	VPS	0.90	M	3.10
Average	1.77	1.77	0.39		0.00		1.17		6.06

L.B.F. - Lower beach face
M.B.F. - Middle beach face
U.B.F. - Upper beach face
F.D. - Foredune

VWS-Very Well sorted
WS-Well Sorted
MS-Moderately Sorted

VNS-Very -vely Skewed
NS--vely Skewed
PS-Positively Skewed
SYM-Symmetrical

L-Leptokurtic
M-Mesokurtic
P-Platykurtic

Appendix II List of symbols used in the text

g	-	acceleration due to gravity (9.81 ms^{-2})
A^*	-	Kadib's (1965) constant (value 43.5)
a'	-	William's (1964) constant 0.1702
A	-	Bagnold's (1941) constant (value 0.1 to 0.118)
ρ'_s	-	density of sand grain
ρ	-	density of air (1.22 x 10^{-6} kg m^{-3}),
b'	-	William's (1964) constant 3.4222
B'	-	function of the plant cover percentage C_p (Buckley, 1987)
B^*	-	Kadib's (1965) constant (value 0.143)
B	-	impact coefficient (value of 0.8 for uniform sand of 0.25 mm)
$c_{(z)}$	-	concentration of particles given by:
C_c	-	Chepil's (1945) constant (value 1.0 to 3.1)
C_L	-	Lettau & Lettau (1978) constant 4.2
C_B	-	constant related to B with values of 1.5 for nearly uniform sand, 1.8 for naturally graded sand, 2.8 for poorly sorted sand, and 3.5 for a pebbly surface
C_z	-	Zingg's (1953) constant (value 0.83)
d	-	mean grain diameter of sand (mm)
D	-	standard grain diameter of a quartz grain (0.25 mm)
F_r	-	particle Froude number
$F_{(x)}$	-	normal distribution integral between the limits of infinity and (u^*B^*-1/n_o)
G_o	-	mass of sand falling in unit time per unit area
h	-	displacement height (the aerodynamic boundary, usually assumed to be at the sand surface, h = 0 m)
I	-	measure of the disturbance to the bed caused by impacting grains
k_p	-	constant dependent on plant shape (Buckley, 1987)
K_k	-	Kawamura's constant (value 2.78)
k	-	Von Karman universal constant for turbulent flow (0.33 to 0.41)
K	-	Hsu (1971) dimensional sand transport coefficient with same dimensions as q, where K = -0.47 + 4.97 D, for D = 0.25mm
l	-	average grain path length
m	-	mass of a sand grain
M_e	-	equivalent moisture at 15 atm pressure
η_o	-	normalised standard deviation of the turbulent lift force (value 0.5)
ξ	-	degree of sheltering in the laminar sublayer
ψ^*	-	flow intensity
ϕ	-	intensity of sediment transport
O	-	is the free fall velocity of the grains
q_{st}	-	rate of sand transport on a sloping surface
s	-	salt content in mg/g of soil
τ_w	-	shear stress caused by the wind directly
τ	-	shear stress
τ_s	-	shear stress exerted due to the impact of the sand grains
τ_t	-	threshold shear stress during equilibrium conditions
τ_o	-	total shear stress exerted by the wind
u_z'	-	threshold wind velocity at heightz'

ψ	-	Kadib's (1965) dimensionless parameter
u_1	-	initial horizontal velocity of sand grain
u_2	-	horizontal velocity of sand grain after travelling a distance l
q	-	rate of sand transport
q_s	-	sand in saltation per unit width in unit time
u_2	-	initial horizontal velocity of sand grain lifted from the surface
u_*'		shear velocities for saltating flows
u_*	-	shear velocity
u_z'		wind velocity at height z'
u_t	-	threshold velocity
$u_{*_{tw}}$	-	fluid threshold velocity for wet sand
u	-	average wind velocity
$u_{(z)}$	-	horizontal velocity of the grains as a function of height
w_2	-	final velocity of rise
w_1	-	initial velocity of rise
w	-	moisture content (%)
x	-	angle of repose of sand and
z	-	distance above the surface
z_o	-	surface roughness height during no sand movement
z'	-	surface roughness height during sand movement
θ	-	slope of the surface in the direction of transport

Appendix III - A Meteorological table containing surface wind data from which estimates of relative sand drift are made.

FREQUENCY ANALYSIS OF WIND DIRECTION AND SPEED (NUMBER OF HOURS)

SC

LEUCHARS JANUARY 1987 | DCNN 1577 | SITE NO. 1 | LAT. 56.0N LONG. 2.0W | N.G.R. NO (37) 457 202 | HEIGHT OF VANE AMSL. 25 METRES | TIME ZONE (GMT+ 0) HOURS | BLOCK NO. 27 | C.G. NO. 11 | QCSTATE 5

MEAN SPEED KNOTS	TOTAL NUMBER OF HOURS FROM(DEGREES TRUE) 350 -010	020 -040	050 -070	080 -100	110 -130	140 -160	170 -190	200 -220	230 -250	260 -280	290 -310	320 -340	VARIABLE	TOTAL	DIRECTION ONLY MISSING
CALM	-	-	-	-	-	-	-	-	-	-	-	-	-	0	
1 - 3	7	3	7	6	14	12	6	5	38	16	11	18	0	143	0
4 - 6	5	1	0	5	18	1	3	4	122	30	17	12	0	218	0
7 - 10	0	0	5	5	13	8	19	5	86	5	4	5	0	155	0
11 - 16	1	5	34	11	16	10	1	2	33	7	4	2	0	126	0
17 - 21	0	2	39	7	6	0	0	0	2	6	4	0	0	66	0
22 - 27	0	0	23	6	3	0	0	0	0	1	2	0	0	35	0
28 - 33	0	0	1	0	0	0	0	0	0	0	0	0	0	1	0
34 - 40	0	0	0	0	0	0	0	0	0	0	0	0	0	0	0
41 - 47	0	0	0	0	0	0	0	0	0	0	0	0	0	0	0
48 - 55	0	0	0	0	0	0	0	0	0	0	0	0	0	0	0
56 - 63	0	0	0	0	0	0	0	0	0	0	0	0	0	0	0
OVER 63	0	0	0	0	0	0	0	0	0	0	0	0	0	0	0
TOTAL 0- 3	7	3	7	6	14	12	6	5	38	16	11	18	0	143	0
TOTAL 4-10	5	1	5	10	31	9	22	9	208	35	21	17	0	373	0
TOTAL 11-21	1	7	73	18	22	10	1	2	35	13	8	2	0	192	0
TOTAL 22-33	0	0	24	6	3	0	0	0	0	1	2	0	0	36	0
TOTAL 34KT OR OVER	0	0	0	0	0	0	0	0	0	0	0	0	0	0	0
SPEED ONLY MISSING	0	0	0	0	0	0	0	0	0	0	0	0	0	0	

NUMBER OF HOURS SPEED AND DIRECTION BOTH MISSING 0

NUMBER OF HOURS DIRECTION ONLY MISSING 0

GRAND TOTAL 744

PRODUCED BY ADVISORY SERVICES BRANCH, METEOROLOGICAL OFFICE, BRACKNELL, BERKS. RG12 2SZ

Appendix III - B Example of worksheet showing calculation of monthly sand drift potential for the twelve azimuth directions.

DEC '89

Azimuth	Speed Class(knots	1-3	4-6	7-10	11-16	17-21	22-27	28-33	34-40	Total	Azimuth	Drift potential
groupings	weighting factor				2.7	25.3	75	172.1	342.3	743	groupings	V.U.
350-010	Raw Data	1	3	0	0	0	0	0	0	4	350-010	0
degrees	%occr	0.13	0.4	0	0	0	0	0	0	0.5384	020-040	0
	Vector Units				0	0	0	0	0	0	050-070	0
020-040	Raw Data	0	0	0	0	0	0	0	0	0	080-100	0
degrees	%occr	0	0	0	0	0	0	0	0	0	110-130	0
	Vector Units				0	0	0	0	0	0	140-160	4
050-070	Raw Data	2	0	0	0	0	0	0	0	2	170-190	33
degrees	%occr	0.27	0	0	0	0	0	0	0	0.2692	200-220	514
	Vector Units				0	0	0	0	0	0	230-250	1676
080-100	Raw Data	1	0	0	0	0	0	0	0	1	260-280	32
degrees	%occr	0.13	0	0	0	0	0	0	0	0.1346	290-310	0
	Vector Units				0	0	0	0	0	0	320-340	0
110-130	Raw Data	1	3	3	0	0	0	0	0	7	Total (V.U.)	2259
degrees	%occr	0.13	0.4	0.404	0	0	0	0	0	0.9421		
	Vector Units				0	0	0	0	0	0		
140-160	Raw Data	2	2	1	2	1	0	0	0	8		
degrees	%occr	0.27	0.27	0.135	0.269	0.135	0	0	0	1.0767		
	Vector Units				0.727	3.405	0	0	0	4.1319		
170-190	Raw Data	3	6	15	15	8	0	0	0	47		
degrees	%occr	0.4	0.81	2.019	2.019	1.077	0	0	0	6.3257		
	Vector Units				5.451	27.24	0	0	0	32.692		
200-220	Raw Data	1	13	32	46	35	26	5	0	158		
degrees	%occr	0.13	1.75	4.307	6.191	4.711	3.499	0.673	0	21.265		
	Vector Units				16.72	119.2	262.4	115.8	0	514.16		
230-250	Raw Data	15	37	91	161	89	48	6	15	462		
degrees	%occr	2.02	4.98	12.25	21.67	11.98	6.46	0.808	2.019	62.18		
	Vector Units				58.51	303.1	484.5	139	691	1676.1		
260-280	Raw Data	7	9	8	13	5	1	0	0	43		
	%occr	0.94	1.21	1.077	1.75	0.673	0.135	0	0	5.7873		
	Vector Units				4.724	17.03	10.09	0	0	31.844		
290-310	Raw Data	1	3	0	0	0	0	0	0	4		
degrees	%occr	0.13	0.4	0	0	0	0	0	0	0.5384		
	Vector Units				0	0	0	0	0	0		
320-340	Raw Data	3	4	0	0	0	0	0	0	7		
degrees	%occr	0.4	0.54	0	0	0	0	0	0	0.9421		
	Vector Units				0	0	0	0	0	0		

Raw Data - is the number of hours the wind blew from a particular direction

Note: No winds in excess of 40 knots were recorded during 1980-90.

Appendix III - C Listing of FORTRAN program used to plot 12 sand roses, one per month and also to calculate the offshore, onshore and effective resultant drift potential for each month.

```
c*************************************************************************
******
c       program to plot 12 sand roses, one per month; program takes data from st
andard
c       input and produces graphical output as well as output to standard output
;
c       to redirect use the form:
c       newplot < infile > outfile
c       the last line of the infile is an integer which can take the values 1 or
 2
c       1       :       output to screen
c       2       :       output as PostScript to file POST
c
c
c
c
c
c*************************************************************************
********
        real azimuth(12), vector(12,12), amax, x,y,a,b,c,d
        real actlen,mmlen,rdd1t6,rdd7t12,rdd1t12
        real rdp1t6,rdp7t12,rdp1t12
        integer row, col, n,itype
        character*18 title1
        character*31 title2
        character*3 month(12)
        character*6 xmonth(12)
        character*1 letter1
        character*1 letters
        character*1 letter
        n=12
        data azimuth/330.0,0.0,30.0,60.0,90.0,120.0,150.0,180.0,210.0,240.0,
     &  270.0,300.0/
        data month/'Jan','Feb','Mar','Apr','May','Jun','Jul','Aug',
     &  'Sep','Oct','Nov','Dec'/
        data letter/'R'/
        data letter1/'L'/
        data letters/'S'/
        PI=4.0*ATAN(1.0)

        write(6,*) ' RDD1-6  RDP1-6  RDD7-12  RDP7-12  RDD1-12  RDP1-12'

        read(5,*) k
c reads data from standard input
        do i=1,k
                read(5,*) xmonth(i)
                read(5,*)(vector(i,j),j=1,n)
        end do
c
c prepare for UNIRAS
c user selects device
      read(5,*) itype
      if (itype.eq.1) then
         call groute('select mx11;exit')
      else if (itype.eq.2) then
         call groute('select mpost;exit')
      else
         call groute(' ')
      end if
c
      call gopen
```

```
c set portrait mode for hardcopy
      if (itype.eq.2) call rorien(2)

c returns size of work area in
      call grpsiz(xsizmm, ysizmm)

c works out positioning for each small diagram
        m=0
        do 20 row=1,4
        c=0.9-0.2*(row)
        d=c+0.2

        do 10 col=1,3
        a=0.05+0.25*(col-1)
        b=a+0.2
        m=m+1

c must shift everything up and to the right (needed for portrait)
c so add a constant to xo,yo

      if (itype.eq.2) then
        xo=a*xsizmm +0.17*xsizmm
        yo=c*ysizmm +0.01*ysizmm
      else
        xo=a*xsizmm
        yo=c*ysizmm
      endif

        xl=(b-a)*xsizmm
        yl=(d-c)*ysizmm


c find centre  and top of middle diagram for use later when centring label
        if (m.eq.2) then
                xcen=xo+xl/2.0
                ycen=yo+yl
        end if



        amax=vector(i,m)
        do i=2,n
                if(vector(i,m).gt.amax) amax=vector(i,m)
        end do
        amax=amax*1.4

c amax=amax*1.4; should allow enough space round diagram for text

c define plot size of each small graph in mm
        call bgraf(xo,yo,xl,yl)
        call glimit(-amax,+amax,-amax,+amax,0.0,0.0)
        call gscale

c calculate the end co-ords (x,y) of each vector and plot;
        call gwicol(0.3,1)
        do i=1,n
                y=vector(i,m)*cosd(azimuth(i))
                x=vector(i,m)*sind(azimuth(i))

        call gvect(0.0,0.0,0)

        call gvect(x,y,1)
```

```
        end do

c add names of months
        call rtxfon('simp',1)
        call rtxhei(2.0)
        call rtxjus(1,2)
        call rtx(-1,month(m),0.0,-amax/1.4)

c calculate resultant vector (RDP) and resultant azim (RDD) of first 6 vectors
C initialise first; then find the i and j components of RDP
      vi=0.0
      vj=0.0
      do l=1,6
          vi =vi+vector(l,m)*cosd(azimuth(l))
          vj =vj+vector(l,m)*sind(azimuth(l))
      end do

c calculate RDP
      rdp1t6=sqrt(vi*vi+vj*vj)

c calculate RDD
        if (vi.gt.0.0 .and. vj.gt.0.0) then
          rdd1t6 = atan(abs(vj/vi))*180.0/pi
        else if (vi .lt.0.0 .and. vj .gt. 0.0) then
          rdd1t6 = 180.0-(atan(abs(vj/vi))*180.0/pi)
        else if (vi .gt.0.0 .and. vj .lt. 0.0) then
          rdd1t6 = 360.0-(atan(abs(vj/vi))*180.0/pi)
        else if (vi .lt.0.0 .and. vj .lt. 0.0) then
          rdd1t6 = 180.0+(atan(abs(vj/vi))*180.0/pi)
        else if (vi .eq.0.0 .and. vj .gt. 0.0) then
           rdd1t6=90.0
        else if (vi .eq.0.0 .and. vj .lt. 0.0) then
           rdd1t6=180.0
        else
      end if

c add 180.0 to rdd1t6
      rdd1t6=rdd1t6+180.0

c calculate the end coords
        y=rdp1t6*cosd(rdd1t6)
        x=rdp1t6*sind(rdd1t6)

c plot line as an arrow
        call garrow(0.0,0.0,0,x,y,4,1,1,0.5)
        call rtx(1,letterl,x*1.05,y*1.05)


c calculate resultant vector (RDP) and resultant azim (RDD) of remaining
C initialise first; then find the i and j components of RDP
      vi=0.0
      vj=0.0
      do l=7,n
          vi =vi+vector(l,m)*cosd(azimuth(l))
          vj =vj+vector(l,m)*sind(azimuth(l))
      end do

c calculate RDP
      rdp7t12=sqrt(vi*vi+vj*vj)
```

```
c calculate RDD
        if (vi.gt.0.0 .and. vj.gt.0.0) then
          rdd7t12 = atan(abs(vj/vi))*180.0/pi
        else if (vi .lt.0.0 .and. vj .gt. 0.0) then
          rdd7t12 = 180.0-(atan(abs(vj/vi))*180.0/pi)
        else if (vi .gt.0.0 .and. vj .lt. 0.0) then
          rdd7t12 = 360.0-(atan(abs(vj/vi))*180.0/pi)
        else if (vi .lt.0.0 .and. vj .lt. 0.0) then
          rdd7t12 = 180.0+(atan(abs(vj/vi))*180.0/pi)
        else if (vi .eq.0.0 .and. vj .gt. 0.0) then
           rdd7t12=90.0
        else if (vi .eq.0.0 .and. vj .lt. 0.0) then
           rdd7t12=180.0
        else
       end if

c add 180.0 to rdd7t12
      rdd7t12=rdd7t12+180.0

c calculate the end coords
        y=rdp7t12*cosd(rdd7t12)
        x=rdp7t12*sind(rdd7t12)

c plot line as an arrow
        call garrow(0.0,0.0,0,x,y,1,1,1,0.5)
        call rtx(1,letters,x*1.05,y*1.05)

c calculate resultant vector (RDP) and resultant azim (RDD)
c should really use the two resultants I've found, but no
c time to use an elegant method!
C initialise first; then find the i and j components of RDP
      vi=0.0
      vj=0.0
      do l=1,n
          vi =vi+vector(l,m)*cosd(azimuth(l))
          vj =vj+vector(l,m)*sind(azimuth(l))
      end do

c calculate RDP1t12
      rdp1t12=sqrt(vi*vi+vj*vj)

c calculate RDD
        if (vi.gt.0.0 .and. vj.gt.0.0) then
          rdd1t12 = atan(abs(vj/vi))*180.0/pi
        else if (vi .lt.0.0 .and. vj .gt. 0.0) then
          rdd1t12 = 180.0-(atan(abs(vj/vi))*180.0/pi)
        else if (vi .gt.0.0 .and. vj .lt. 0.0) then
          rdd1t12 = 360.0-(atan(abs(vj/vi))*180.0/pi)
        else if (vi .lt.0.0 .and. vj .lt. 0.0) then
          rdd1t12 = 180.0+(atan(abs(vj/vi))*180.0/pi)
        else if (vi .eq.0.0 .and. vj .gt. 0.0) then
           rdd1t12=90.0
        else if (vi .eq.0.0 .and. vj .lt. 0.0) then
           rdd1t12=180.0
        else
       end if

c add 180.0 to rdd1t12
      rdd1t12=rdd1t12+180.0

c output rdd and rdp to standard output
        write(6,*) rdd1t6,rdp1t6,rdd7t12,rdp7t12,rdd1t12,rdp1t12
```

```
c calculate the end coords
        y=rdp1t12*cosd(rdd1t12)
        x=rdp1t12*sind(rdd1t12)

c plot line as an arrow
        call garrow(0.0,0.0,0,x,y,1,1,1,0.4)

c calculate scale factor sf
        sx=2.0*amax/xl
        sy=2.0*amax/yl
        actlen=sqrt(x*x+y*y)
        mmlen=sqrt(x*x/(sx*sx)+y*y/(sy*sy))
        sf=actlen/mmlen

c add scale factor, sf to each small diagram
        call rtxhei(2.0)
        call rtxn(sf,0,0.0,+amax/1.3)
c       add rdp1t6 and rdp7t12 values to plot
        call rtxhei(2.0)
        call rtxn(rdp1t6,0,-amax/2.0,-amax/1.3)
        call rtxn(rdp7t12,0,amax/2.0,-amax/1.3)


  10    continue
  20    continue

 200    continue


c plot both titles centred
        open(3,file='title',status='unknown')
         read(3,30) title1
         read(3,40) title2
         close(3)
        call rtxjus(1,2)
        call gvport(0.0,0.0,xsizmm,ysizmm)
        call glimit(-1.0,+1.0,-1.0,+1.0,0.0,0.0)
        call rtxhei(3.0)
        call gscamm
        call rtx(-1,title1,xcen,-ycen*1.08)
        call rtx(-1,title2,xcen,-ycen*1.04)

        call gclose
30      format(a18)
40      format(a50)
        stop
        end
```

Appendix III - D Monthly sand roses from January 1980 to December 1990.

Monthly Sand Roses and Sand Drift Potential –1980

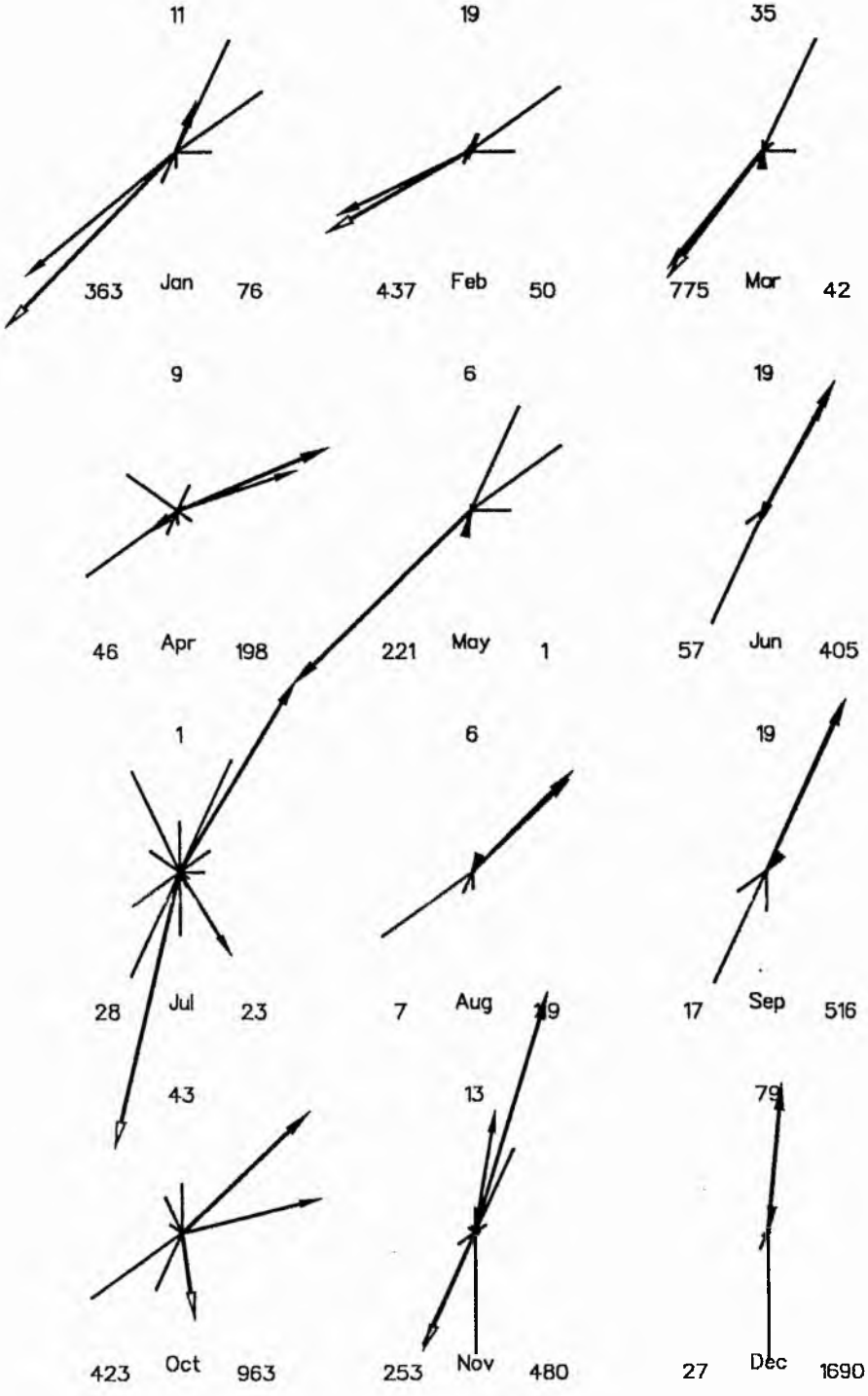

Monthly Sand Roses and Sand Drift Potential —1981

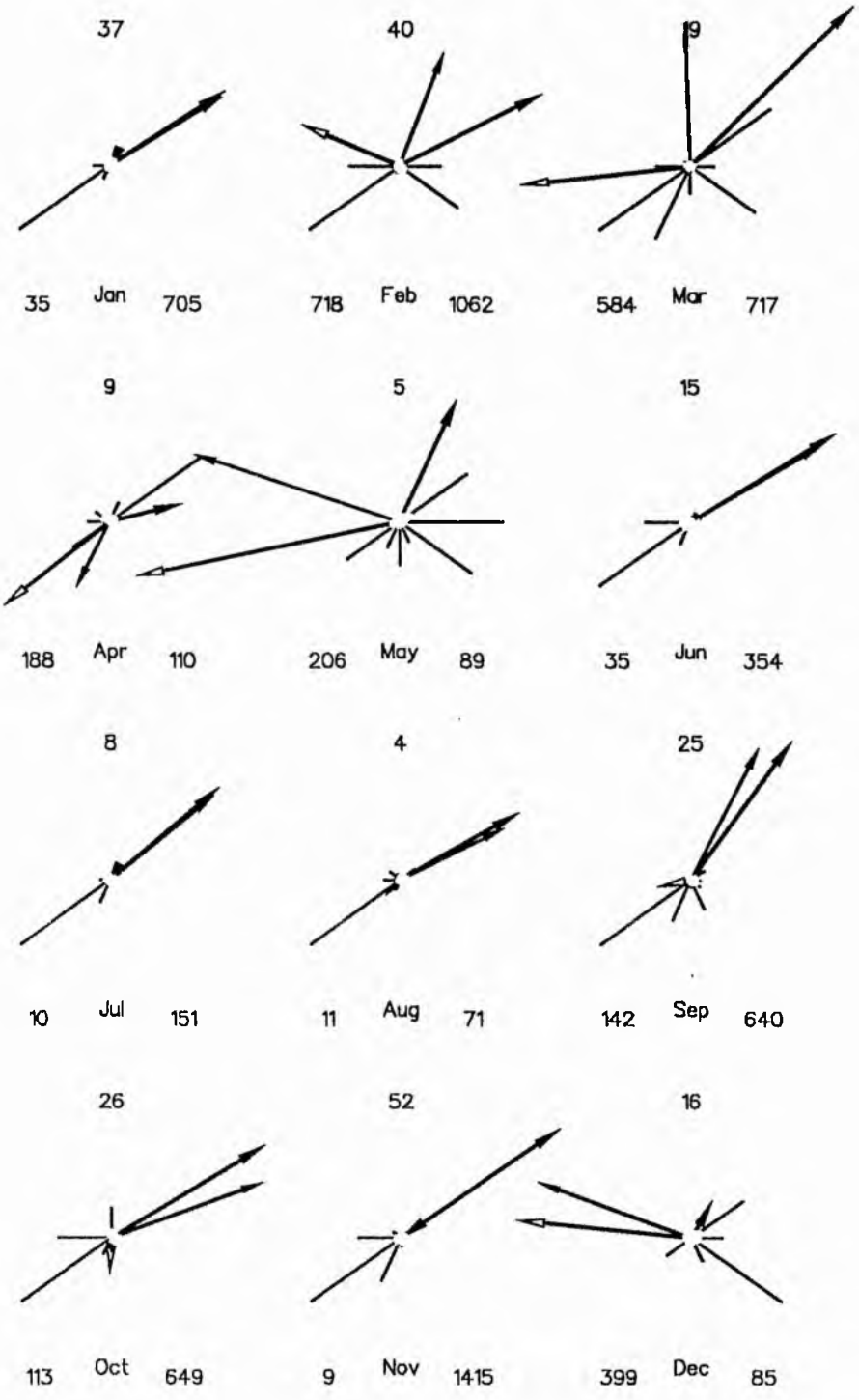

Monthly Sand Roses and Sand Drift Potential –1982

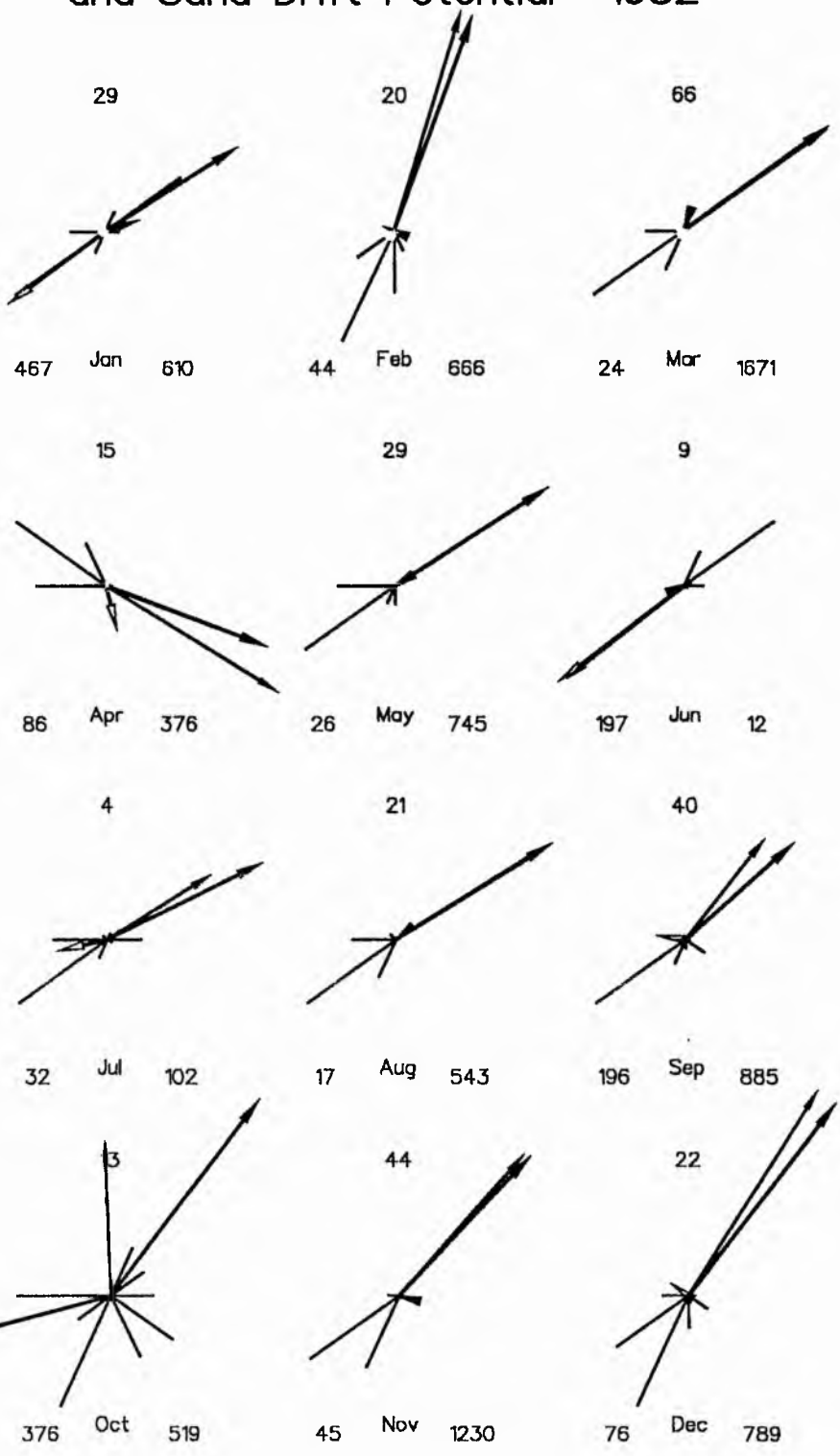

Monthly Sand Roses and Sand Drift Potential —1983

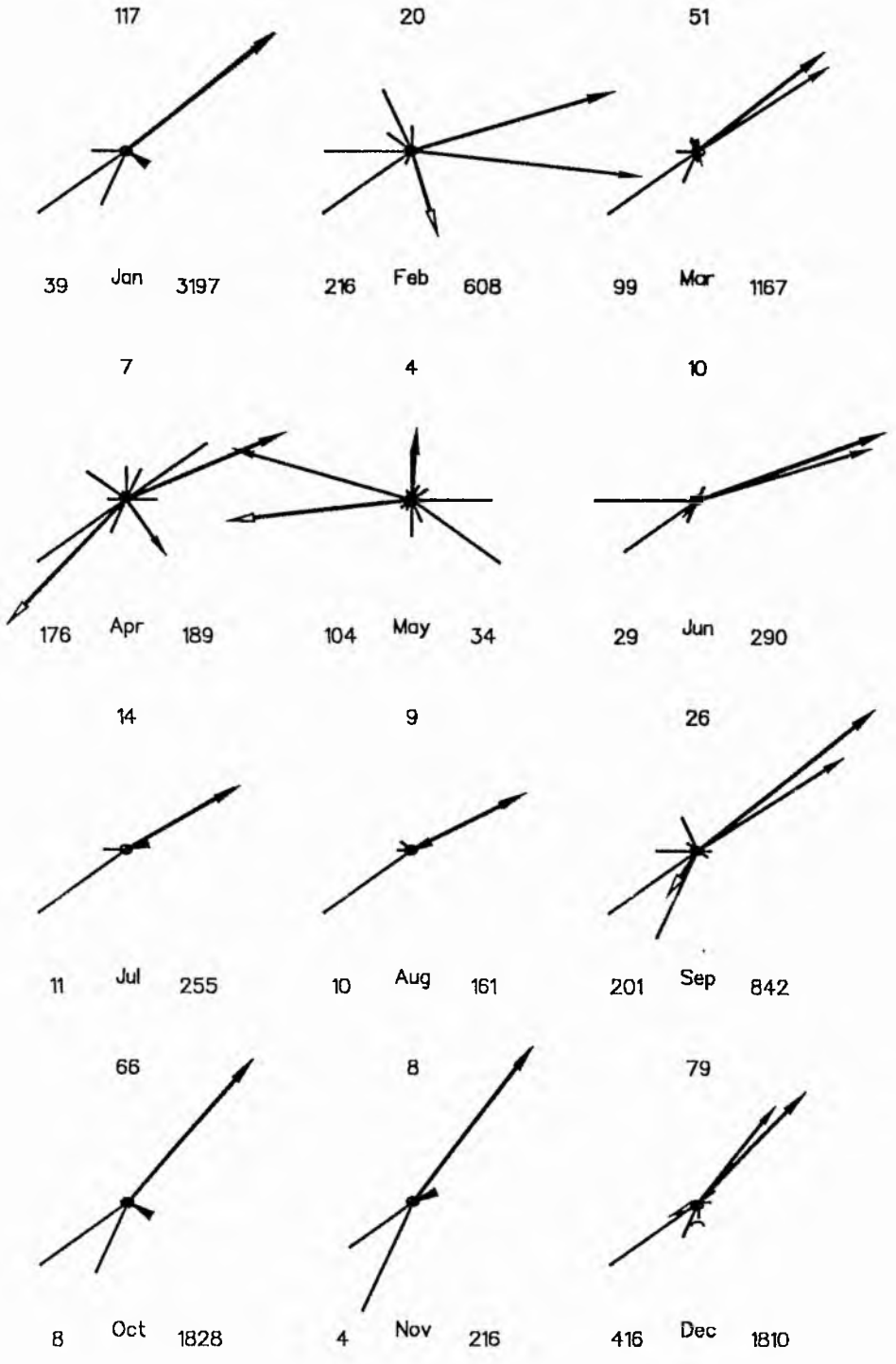

Monthly Sand Roses and Sand Drift Potential –1984

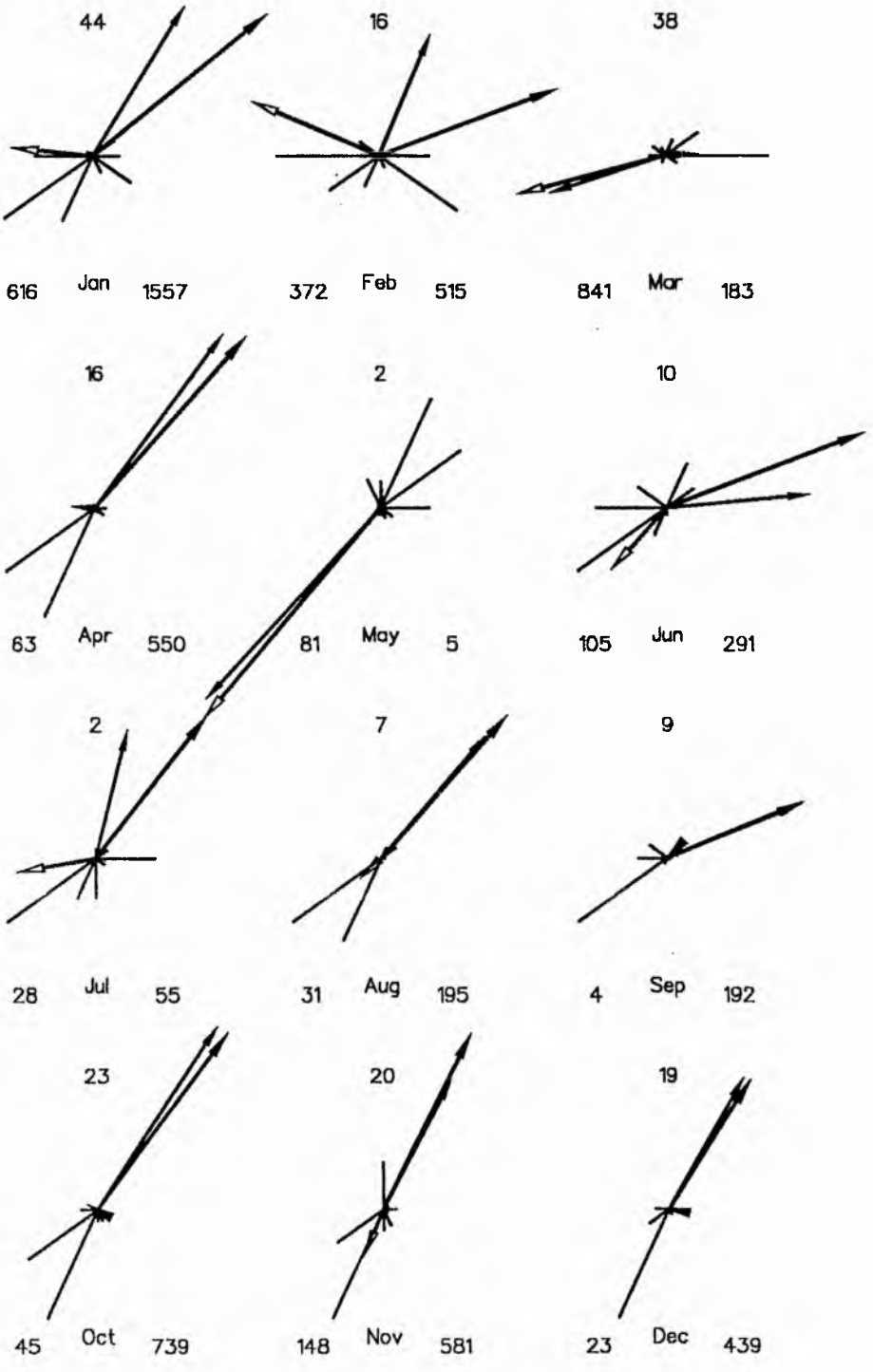

Monthly Sand Roses and Sand Drift Potential –1985

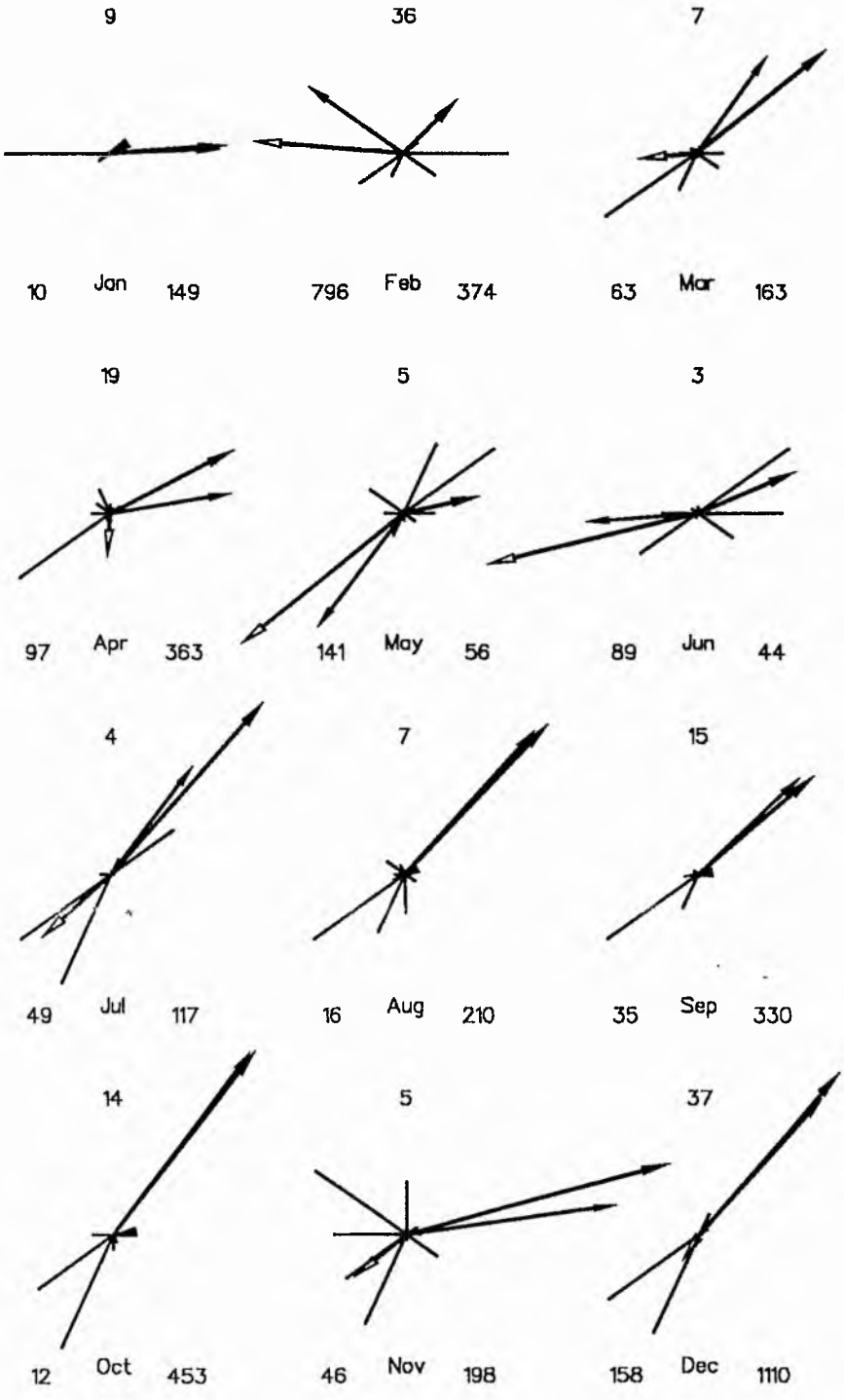

Monthly Sand Roses and Sand Drift Potential —1986

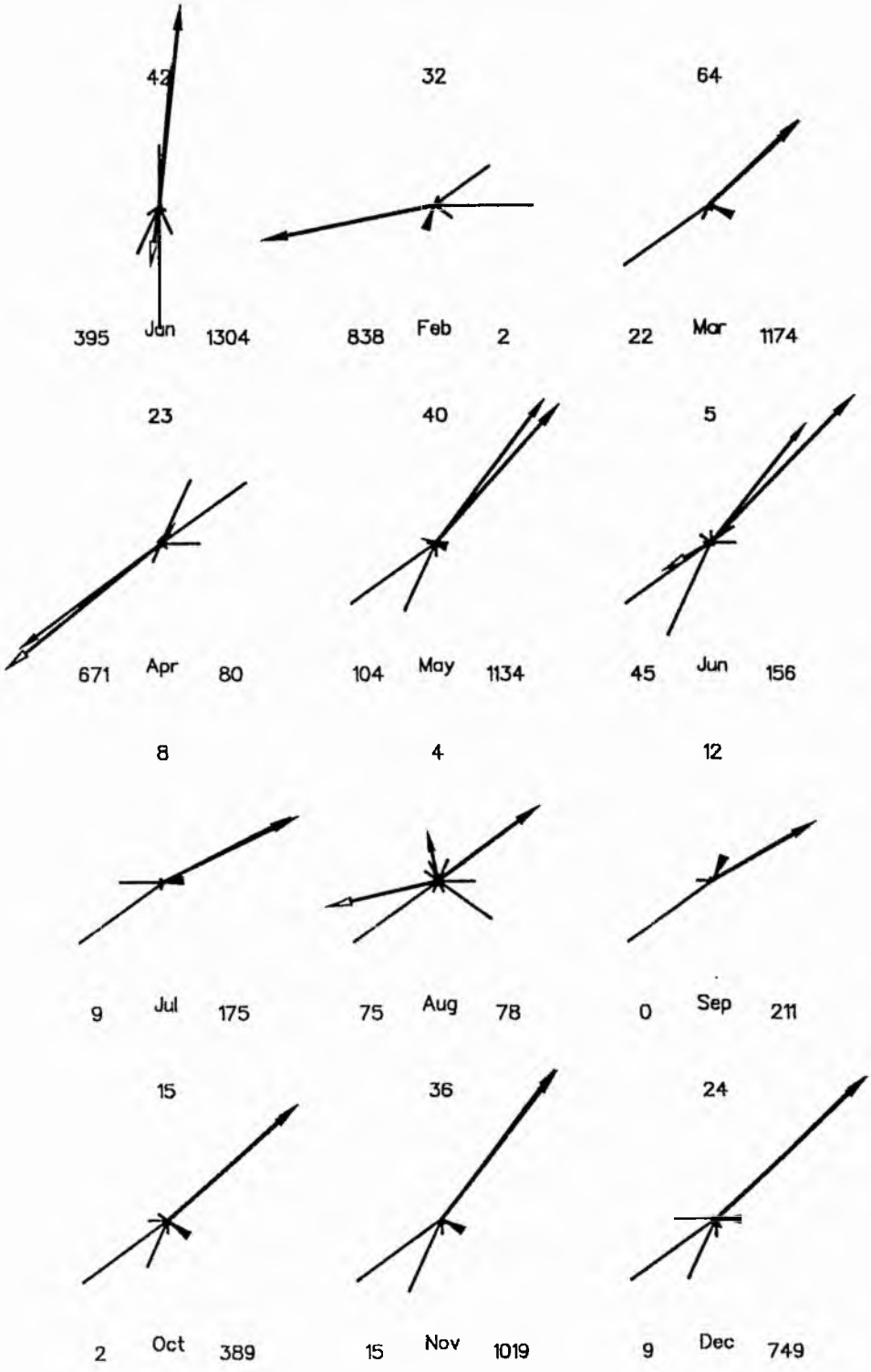

Monthly Sand Roses and Sand Drift Potential—1987

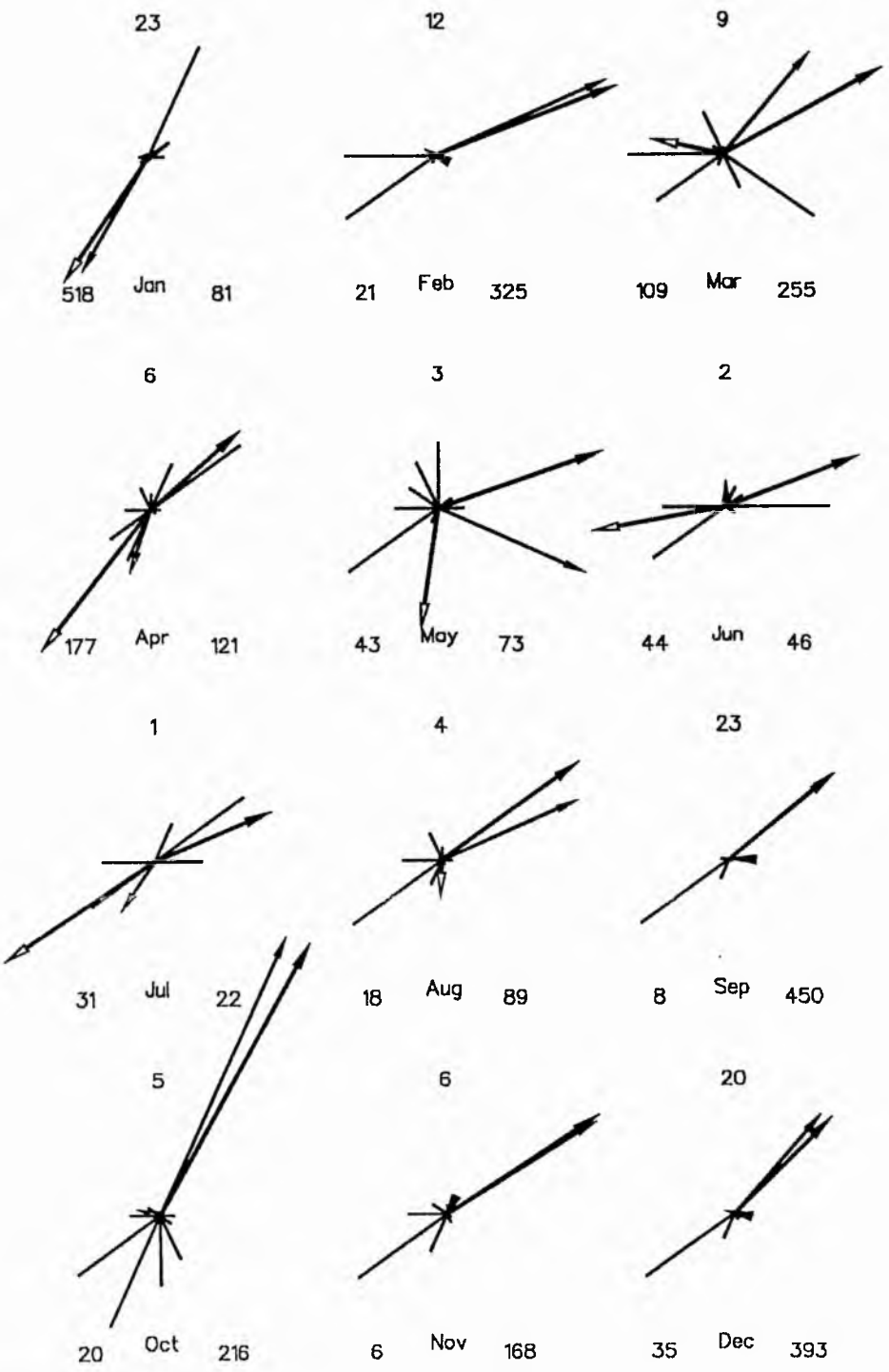

Monthly Sand Roses and Sand Drift Potential –1988

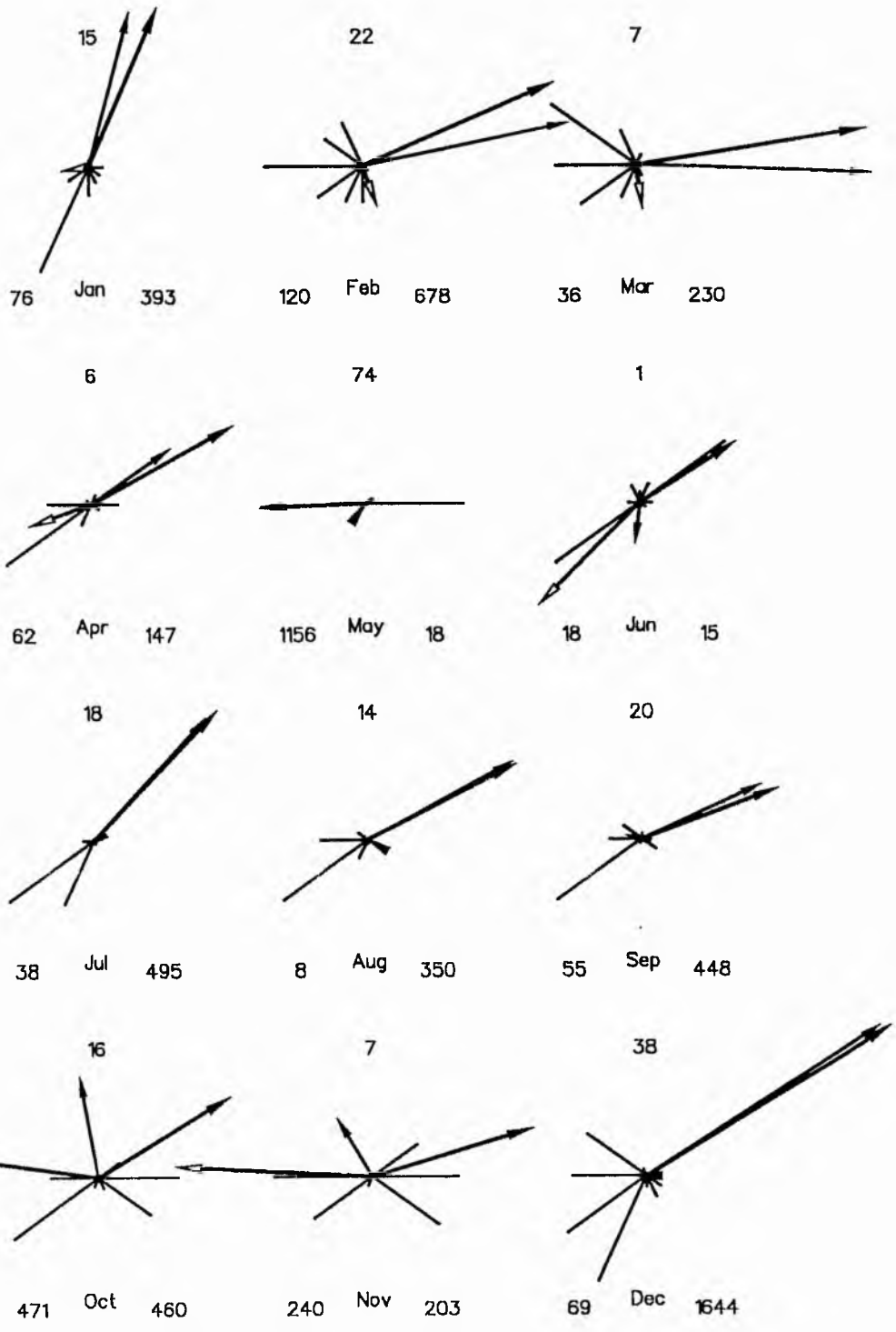

Monthly Sand Roses and Sand Drift Potential –1989

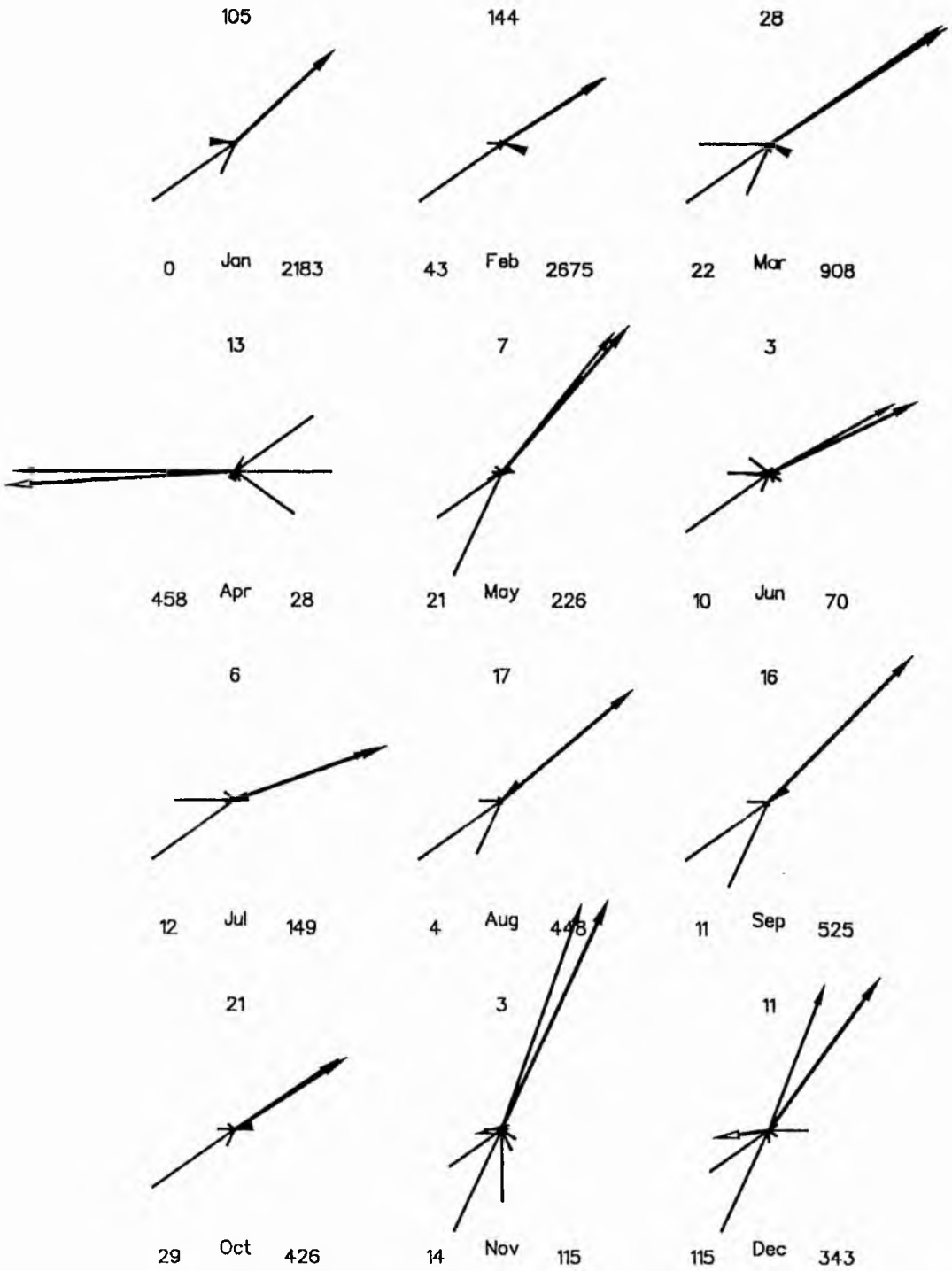

Monthly Sand Roses
and Sand Drift Potential —1990

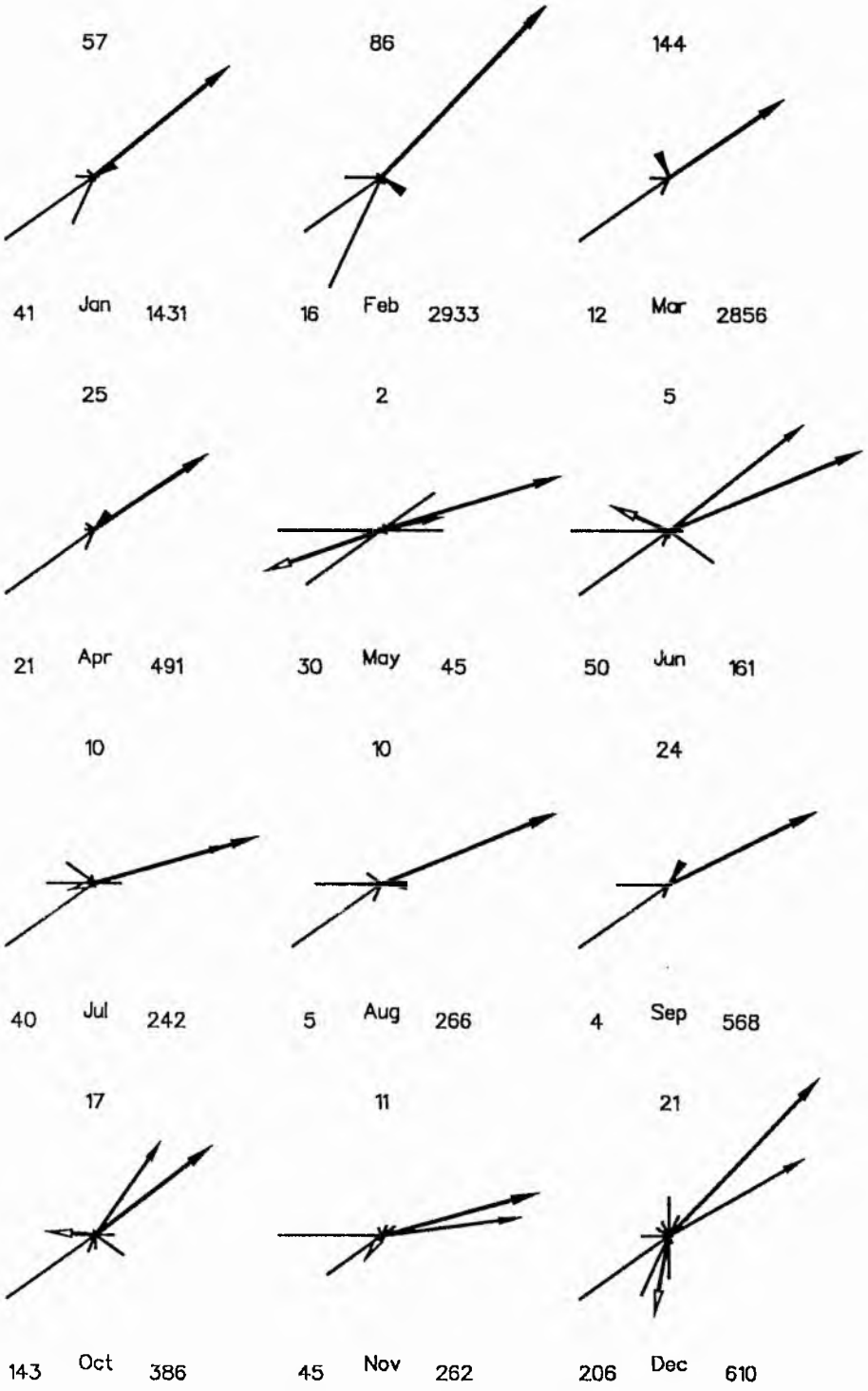

Appendix III - E Summary of drift potentials from January 1980 to December 1990.

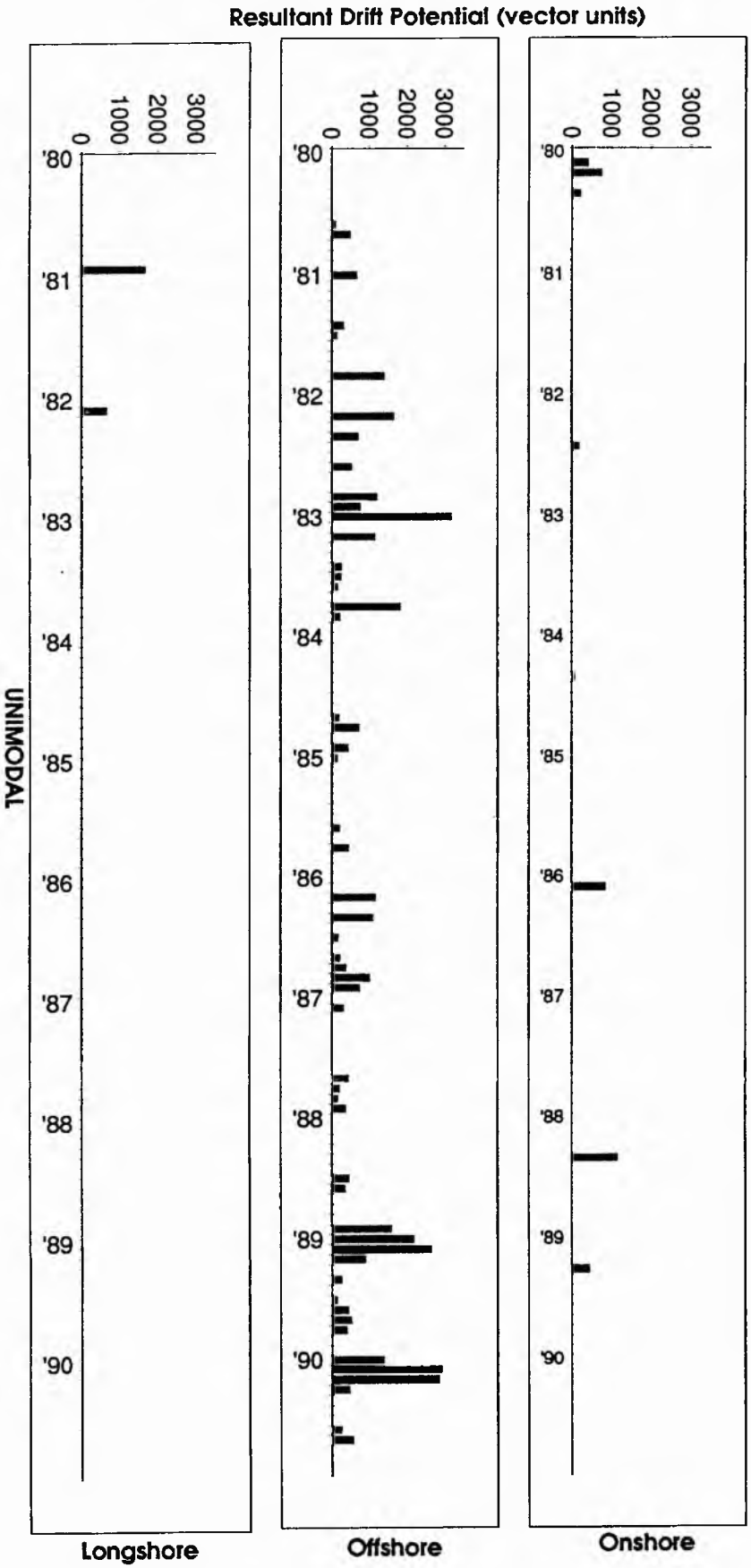
Resultant Drift Potential (vector units)
0
1000
2000
3000
'80
'81
'82
'83
'84
'85
'86
'87
'88
'89
'90
UNIMODAL
Longshore
Offshore
Onshore

Resultant Drift Potential (vector units)
BIMODAL
0
1000
2000
3000
'80
'81
'82
'83
'84
'85
'86
'87
'88
'89
'90
Equal
Longshore
Offshore
Onshore

Appendix IV Examples of grain size distribution of sediments retained in the trap during sand transport rate measurements.

(a) Tentsmuir Point - transect 2

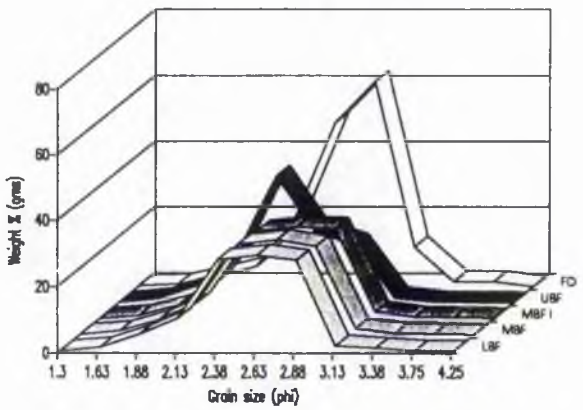

(b) Tentsmuir - transect 4

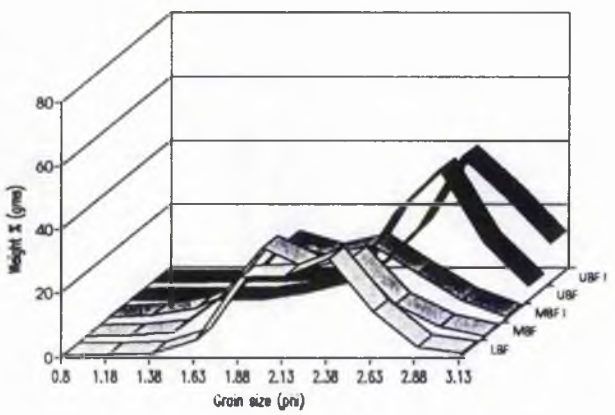

(c) Kinshaldy - transect 7

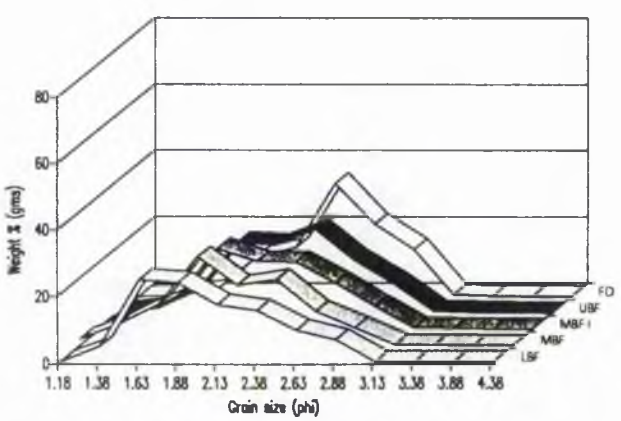

Appendix IV - B Examples of Sand Transport Along Various Transects

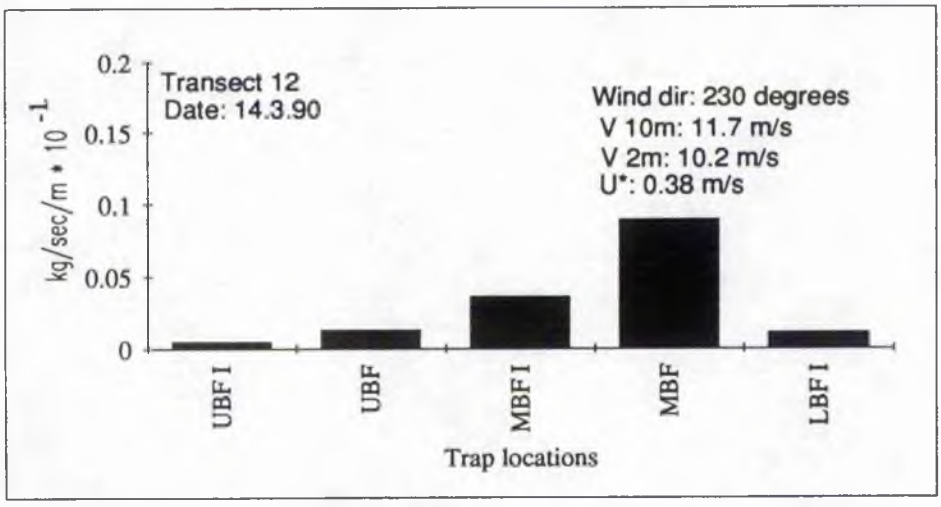
Transect 12
Date: 14.3.90
Wind dir: 230 degrees
V 10m: 11.7 m/s
V 2m: 10.2 m/s
U*: 0.38 m/s
kg/sec/m * 10 -1
0.2
0.15
0.1
0.05
0
UBF I
UBF
MBF I
MBF
LBF I
Trap locations

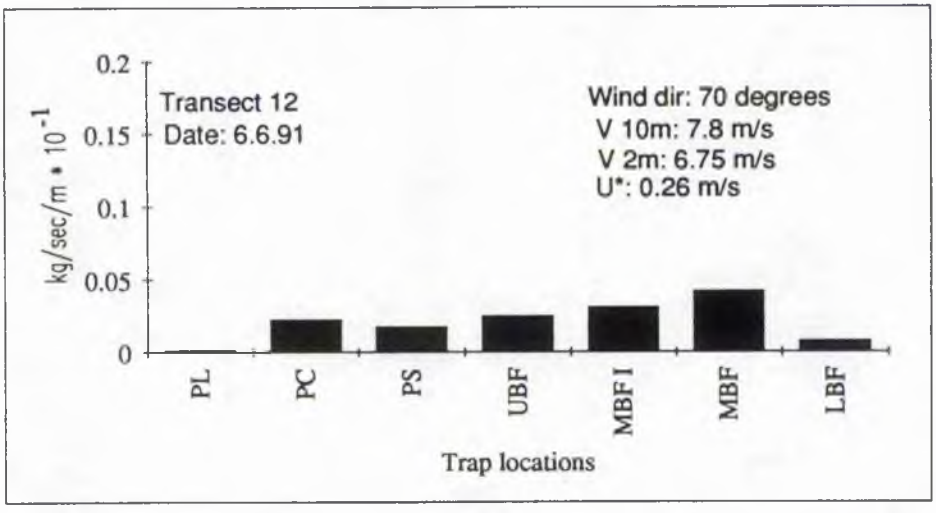
Transect 12
Date: 6.6.91
Wind dir: 70 degrees
V 10m: 7.8 m/s
V 2m: 6.75 m/s
U*: 0.26 m/s
kg/sec/m * 10 -1
0.2
0.15
0.1
0.05
0
PL
PC
PS
UBF
MBF I
MBF
LBF
Trap locations

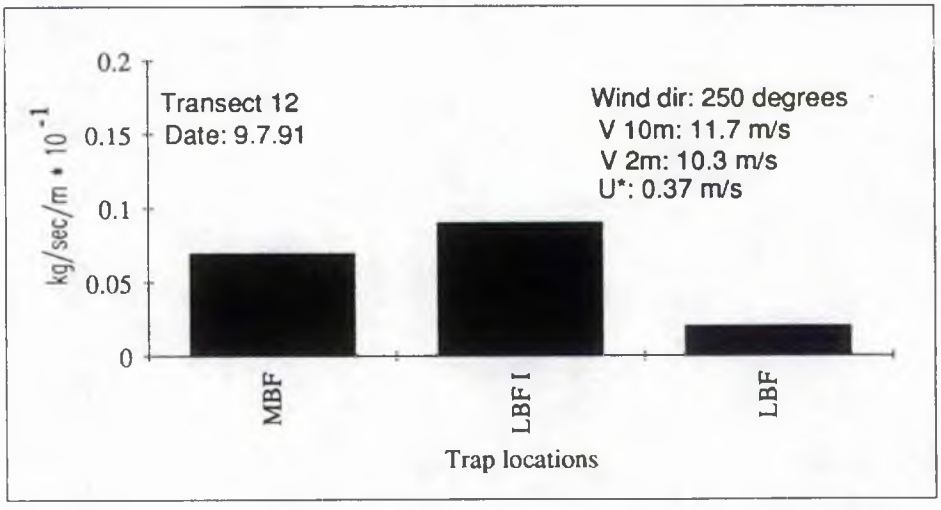
Transect 12
Date: 9.7.91
Wind dir: 250 degrees
V 10m: 11.7 m/s
V 2m: 10.3 m/s
U*: 0.37 m/s
kg/sec/m * 10 -1
0.2
0.15
0.1
0.05
0
MBF
LBF I
LBF
Trap locations

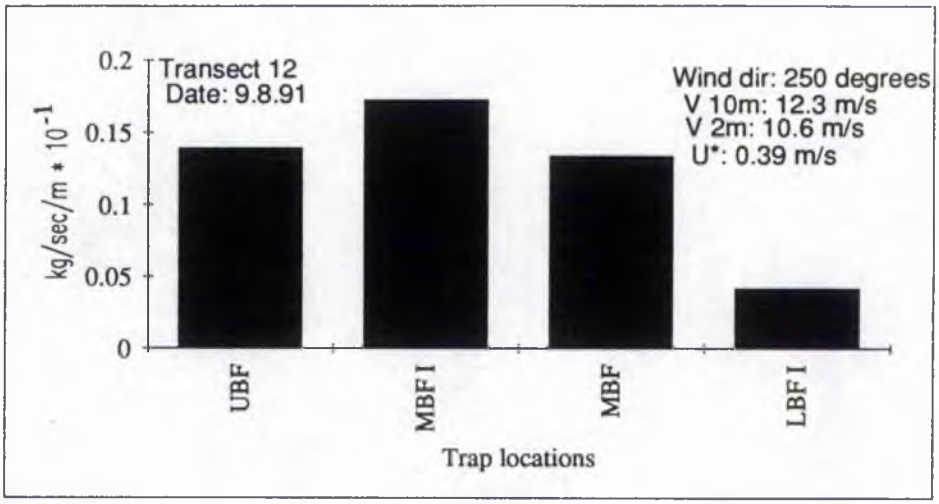
Transect 12
Date: 9.8.91
Wind dir: 250 degrees
V 10m: 12.3 m/s
V 2m: 10.6 m/s
U*: 0.39 m/s
kg/sec/m * 10-1
0.2
0.15
0.1
0.05
0
UBF
MBF I
MBF
LBF I
Trap locations

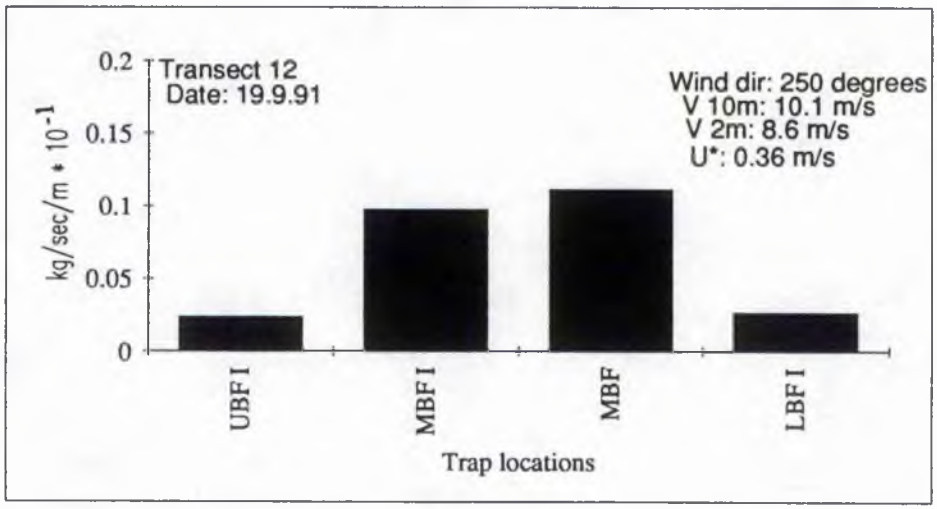
Transect 12
Date: 19.9.91
Wind dir: 250 degrees
V 10m: 10.1 m/s
V 2m: 8.6 m/s
U*: 0.36 m/s
kg/sec/m * 10-1
0.2
0.15
0.1
0.05
0
UBF I
MBF I
MBF
LBF I
Trap locations

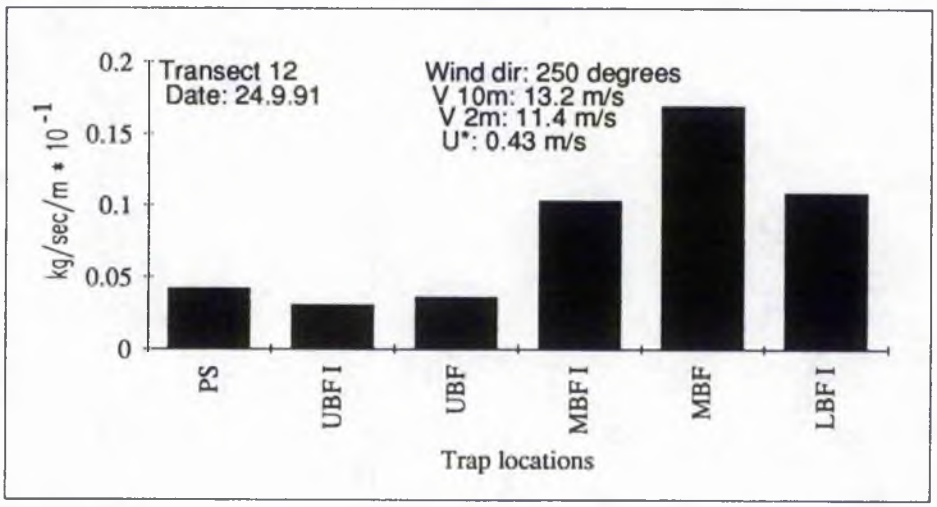
Transect 12
Date: 24.9.91
Wind dir: 250 degrees
V 10m: 13.2 m/s
V 2m: 11.4 m/s
U*: 0.43 m/s
kg/sec/m * 10-1
0.2
0.15
0.1
0.05
0
PS
UBF I
UBF
MBF I
MBF
LBF I
Trap locations

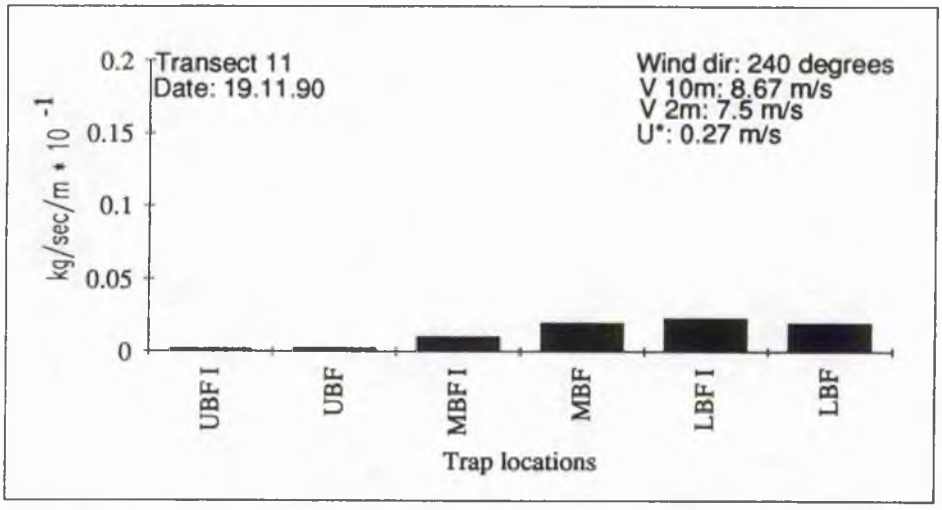
Transect 11
Date: 19.11.90
Wind dir: 240 degrees
V 10m: 8.67 m/s
V 2m: 7.5 m/s
U*: 0.27 m/s
kg/sec/m * 10 -1
0.2
0.15
0.1
0.05
0
UBF I
UBF
MBF I
MBF
LBF I
LBF
Trap locations

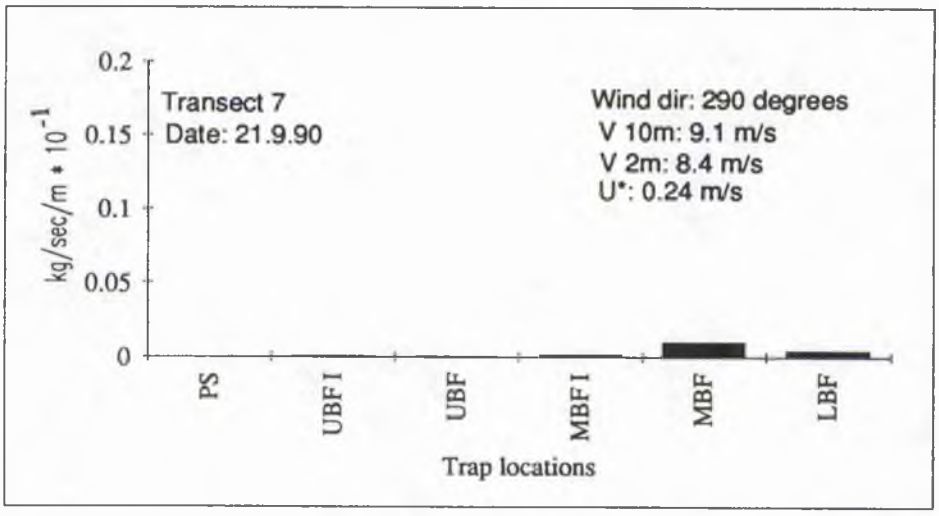
Transect 7
Date: 21.9.90
Wind dir: 290 degrees
V 10m: 9.1 m/s
V 2m: 8.4 m/s
U*: 0.24 m/s
kg/sec/m * 10 -1
0.2
0.15
0.1
0.05
0
PS
UBF I
UBF
MBF I
MBF
LBF
Trap locations

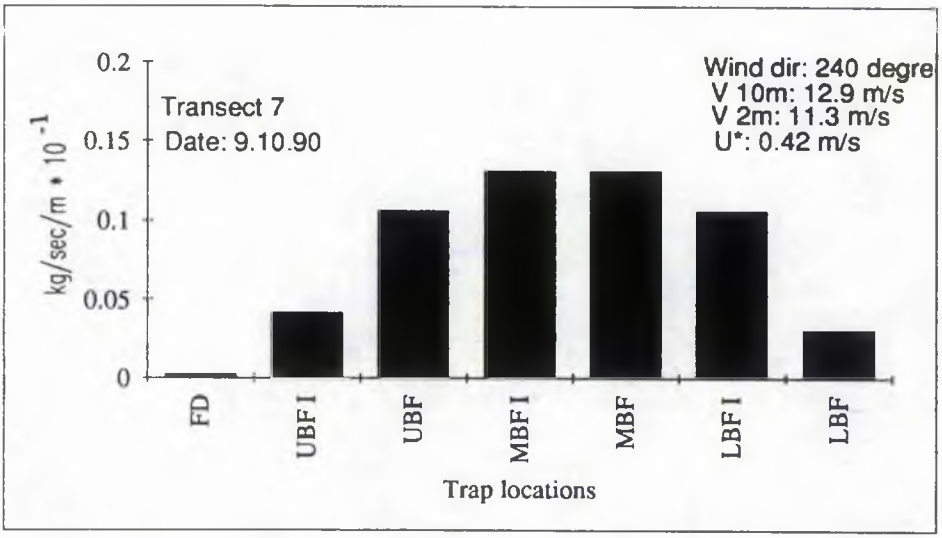
Transect 7
Date: 9.10.90
Wind dir: 240 degre
V 10m: 12.9 m/s
V 2m: 11.3 m/s
U*: 0.42 m/s
kg/sec/m * 10 -1
0.2
0.15
0.1
0.05
0
FD
UBF I
UBF
MBF I
MBF
LBF I
LBF
Trap locations

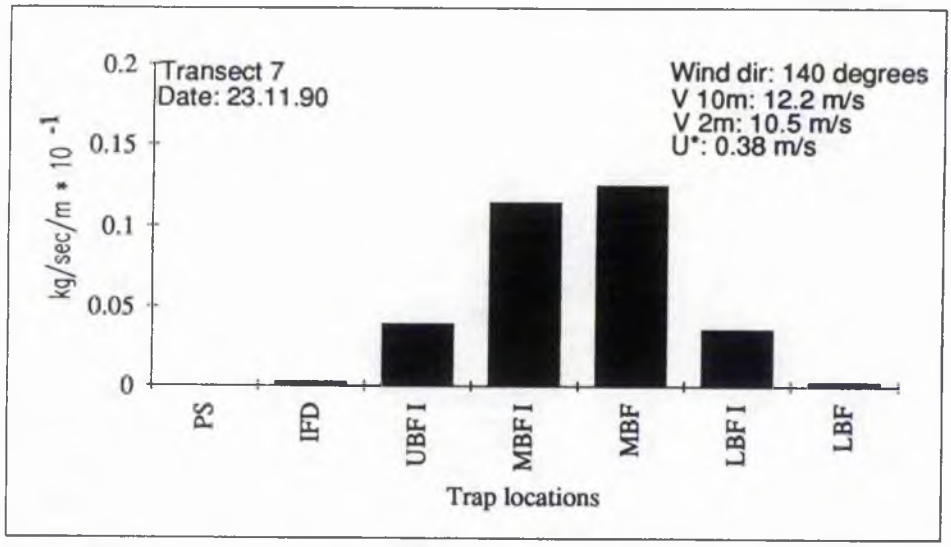
Transect 7
Date: 23.11.90
Wind dir: 140 degrees
V 10m: 12.2 m/s
V 2m: 10.5 m/s
U*: 0.38 m/s
kg/sec/m * 10 -1
0.2
0.15
0.1
0.05
0
PS
IFD
UBF I
MBF I
MBF
LBF I
LBF
Trap locations

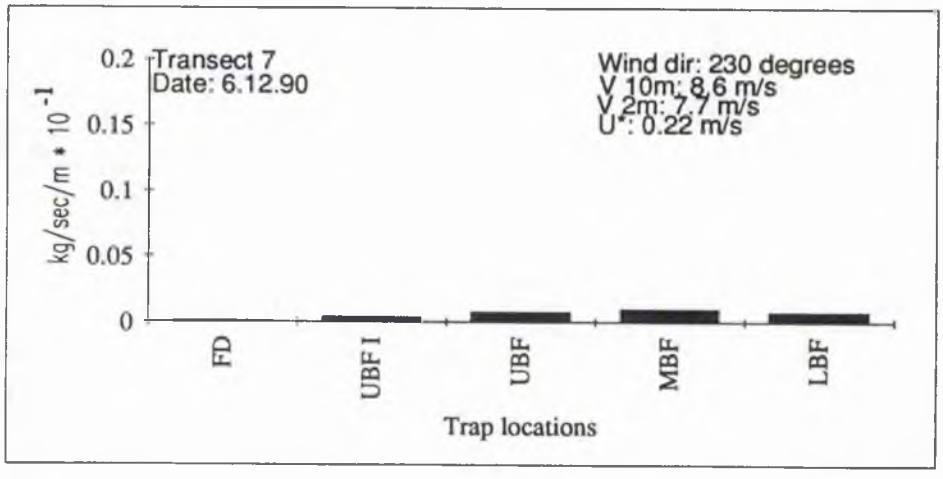
Transect 7
Date: 6.12.90
Wind dir: 230 degrees
V 10m: 8.6 m/s
V 2m: 7.7 m/s
U*: 0.22 m/s
kg/sec/m * 10 -1
0.2
0.15
0.1
0.05
0
FD
UBF I
UBF
MBF
LBF
Trap locations

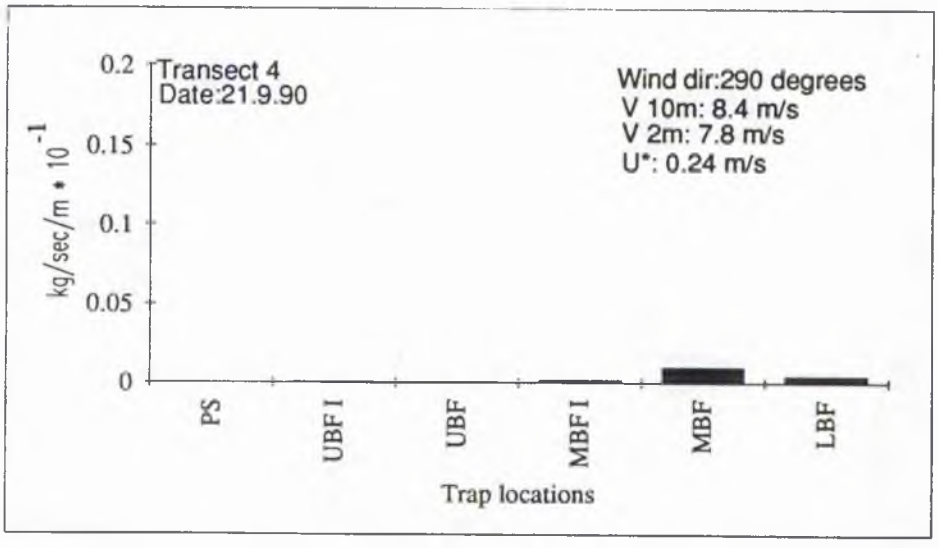
Transect 4
Date:21.9.90
Wind dir:290 degrees
V 10m: 8.4 m/s
V 2m: 7.8 m/s
U*: 0.24 m/s
kg/sec/m * 10 -1
0.2
0.15
0.1
0.05
0
PS
UBF I
UBF
MBF I
MBF
LBF
Trap locations

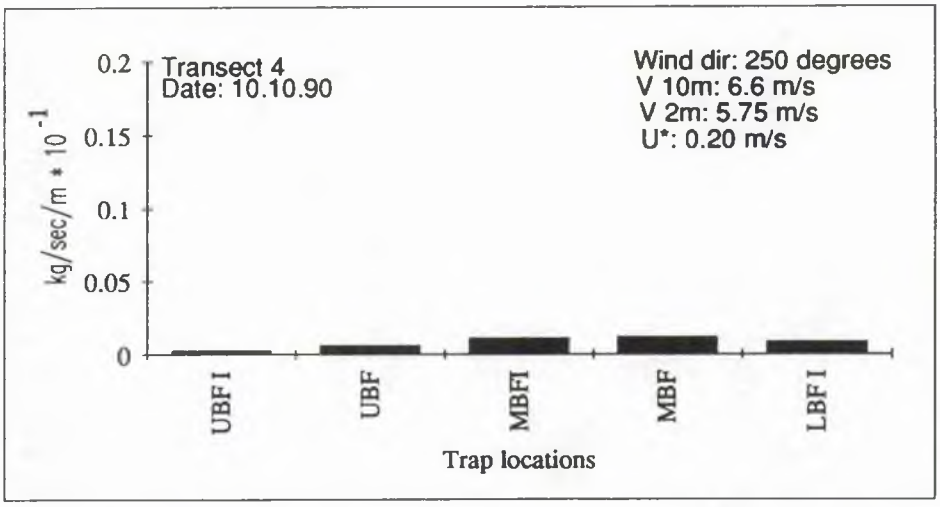
Transect 4
Date: 10.10.90
Wind dir: 250 degrees
V 10m: 6.6 m/s
V 2m: 5.75 m/s
U*: 0.20 m/s
kg/sec/m * 10 -1
0.2
0.15
0.1
0.05
0
UBF I
UBF
MBFI
MBF
LBF I
Trap locations

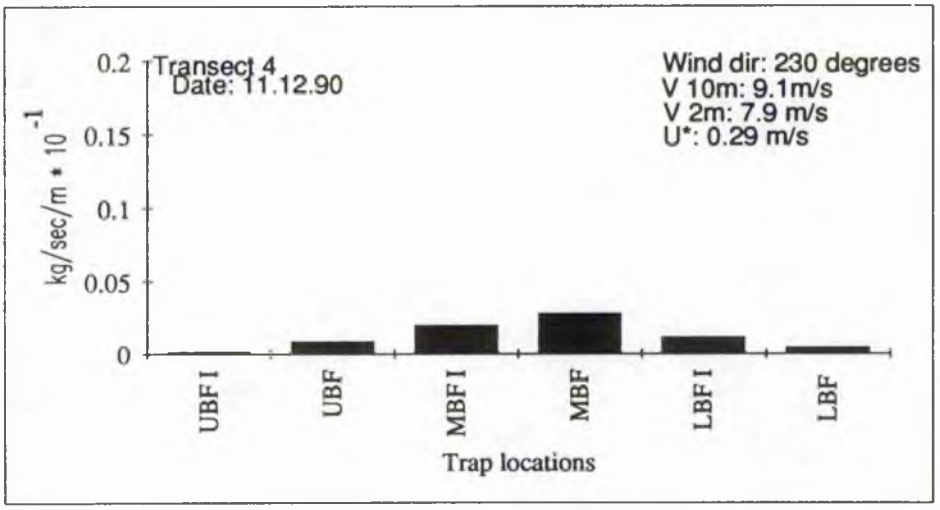
Transect 4
Date: 11.12.90
Wind dir: 230 degrees
V 10m: 9.1m/s
V 2m: 7.9 m/s
U*: 0.29 m/s
kg/sec/m * 10 -1
0.2
0.15
0.1
0.05
0
UBF I
UBF
MBF I
MBF
LBF I
LBF
Trap locations

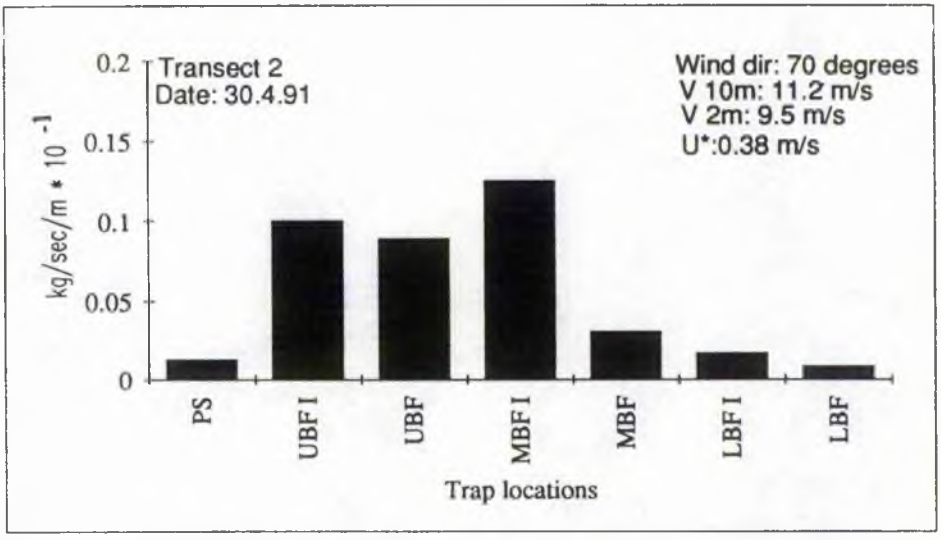
Transect 2
Date: 30.4.91
Wind dir: 70 degrees
V 10m: 11.2 m/s
V 2m: 9.5 m/s
U*:0.38 m/s
kg/sec/m * 10 -1
0.2
0.15
0.1
0.05
0
PS
UBF I
UBF
MBF I
MBF
LBF I
LBF
Trap locations

Appendix IV - C

Measured Sand Transport Rates (log values) vs Shear Velocity (log values) Plots In Various Beach-Dune Subenvironments.

Legend

L.B.F.- lower beach face

U.B.F.- upper beach face

M.B.F.- middle beach face

F.D.- Foredune

Note:Last diagram has all the measured data points from which the equation on page 5.19 has been derived.

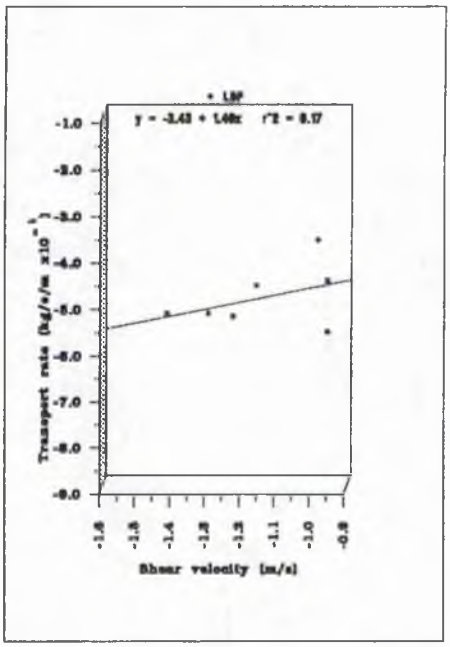
Transport rate (kg/s/m x10⁻³)
-1.0
-2.0
-3.0
-4.0
-5.0
-6.0
-7.0
-8.0
-9.0
-1.6
-1.5
-1.4
-1.3
-1.2
-1.1
-1.0
-0.9
Shear velocity (m/s)

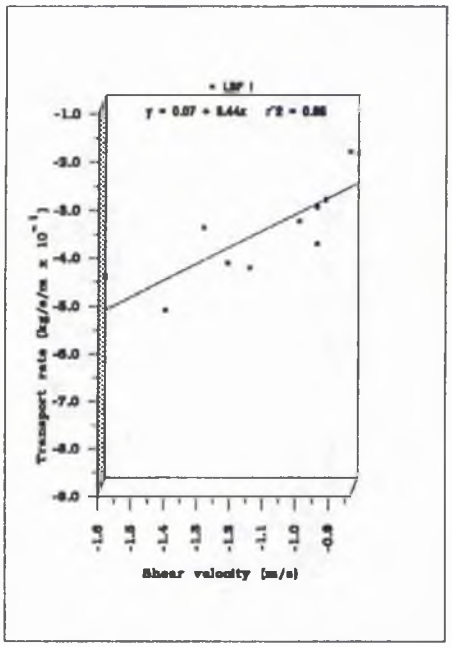
Transport rate (kg/s/m x 10⁻³)
-1.0
-2.0
-3.0
-4.0
-5.0
-6.0
-7.0
-8.0
-9.0
-1.6
-1.5
-1.4
-1.3
-1.2
-1.1
-1.0
-0.9
Shear velocity (m/s)

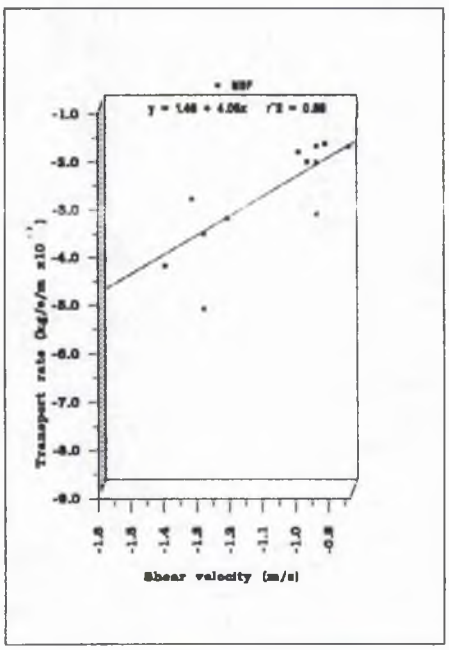
Transport rate (kg/s/m x10⁻³)
-1.0
-2.0
-3.0
-4.0
-5.0
-6.0
-7.0
-8.0
-9.0
-1.6
-1.5
-1.4
-1.3
-1.2
-1.1
-1.0
-0.9
Shear velocity (m/s)

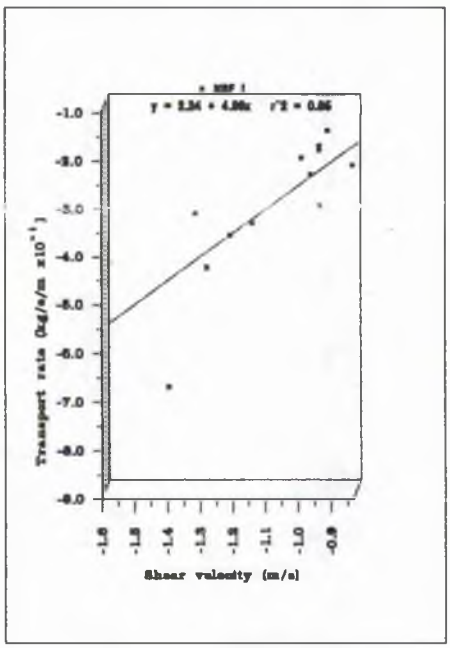
Transport rate (kg/s/m x10⁻³)
-1.0
-2.0
-3.0
-4.0
-5.0
-6.0
-7.0
-8.0
-9.0
-1.6
-1.5
-1.4
-1.3
-1.2
-1.1
-1.0
-0.9
Shear velocity (m/s)

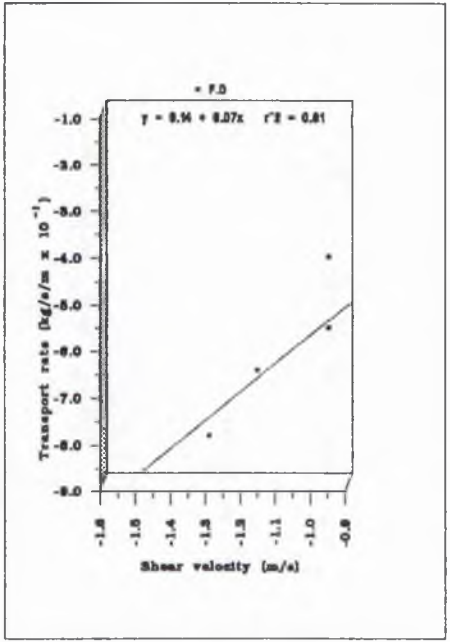
y = 8.14 + 0.07x r^2 = 0.81
Transport rate (kg/s/m x 10^-1)
-1.0
-3.0
-5.0
-4.0
-5.0
-6.0
-7.0
-8.0
-9.0
-1.6
-1.5
-1.4
-1.3
-1.2
-1.1
-1.0
-0.9
Shear velocity (m/s)

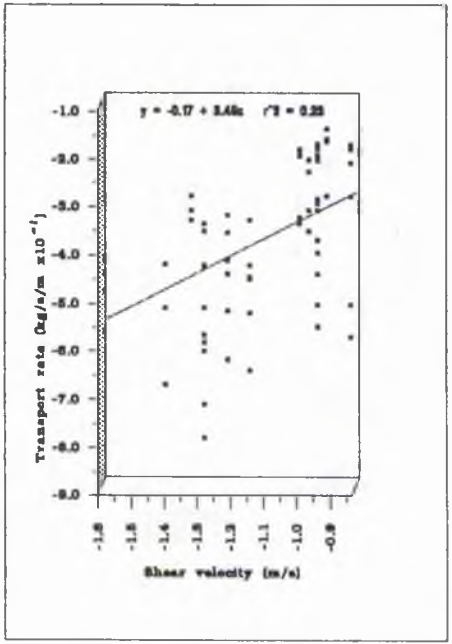
y = -0.17 + 3.48x r^2 = 0.25
Transport rate (kg/s/m x10^-1)
-1.0
-2.0
-3.0
-4.0
-5.0
-6.0
-7.0
-8.0
-9.0
-1.6
-1.5
-1.4
-1.3
-1.2
-1.1
-1.0
-0.9
Shear velocity (m/s)

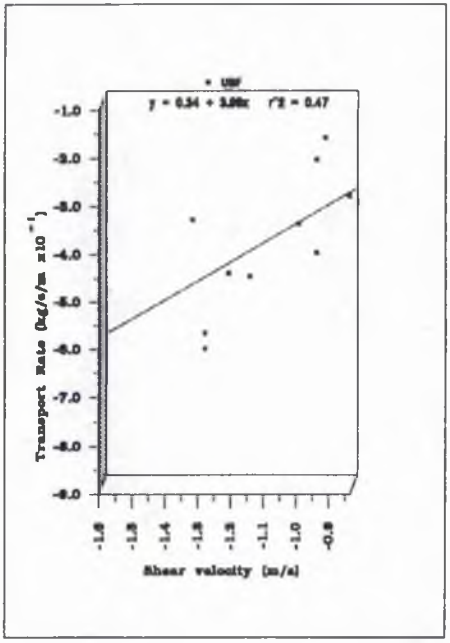
Transport Rate (kg/s/m x10⁻⁴)
Shear velocity (m/s)

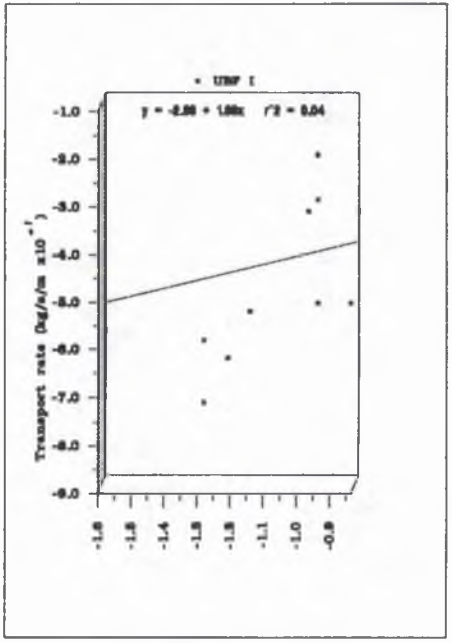
Transport rate (kg/s/m x10⁻⁴)

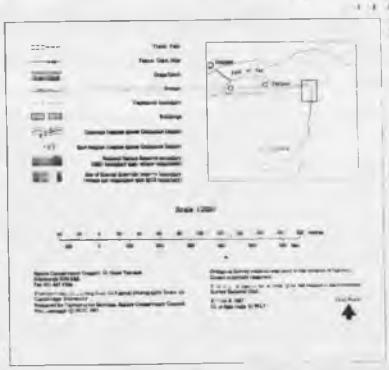

NATURE CONSERVANCY COUNCIL

Tentsmuir Point
National Nature Reserve

ENCLOSURE 1